Vascular Disease in Multiple Sclerosis:

Impact on Pathology and Radiologic Outcomes

Ruth Geraldes

Wolfson College, University of Oxford



Department of Clinical Neurosciences
Medical Sciences Division
University of Oxford

A thesis submitted for the degree of Doctor of Philosophy
Trinity Term, 2019

Vascular Disease in Multiple Sclerosis: Impact on Pathology and Radiologic Outcomes

Ruth Geraldes, Wolfson College, Oxford University

A thesis submitted for the degree of Doctor of Philosophy, Trinity Term, 2019

Abstract

Shared risk factors, immobility, and inflammation may predispose to systemic- and cerebro-vascular disease in Multiple Sclerosis (MS). On the other hand, vascular risk factors (VRF) and comorbidities may have a direct impact on MS pathology. A *post mortem* and an *in vivo* magnetic resonance imaging (MRI) study were set up as complementary approaches to test these hypotheses. In the first, objective measures of systemic and cerebro-vascular disease were obtained from a unique cohort of MS and non-MS cases in whom whole body autopsy reports and brain tissue were available for study. This work revealed that cardiovascular disease is less common, but has a stronger impact on cerebral small vessel disease (cSVD) in MS compared with non-MS, and associates with a lower burden of active plaques. Histological analysis showed an increased cSVD burden in those who die young with highly active MS and that periarteriolar hemosiderin deposition, enlarged spaces and inflammation are key features of MS pathology. In the *in vivo* brain MRI study imaging markers were compared between MS cases with and without VRF and non-MS cases with VRF. By doing so, imaging discriminators between MS and cSVD were identified. While MS does not seem to influence cSVD imaging markers, the different VRF have distinct effects on MS imaging markers: smoking and dyslipidaemia associating with a higher burden of these markers and diabetes having the opposite effect. Using this combined approach, this thesis advanced the knowledge of the contribution of vascular disease/VRF into MS radiological and pathological heterogeneity, identified markers that can be useful on MS differential diagnosis, and has evidenced that the cerebral microvasculature is structurally abnormal in MS and may be an important therapeutic target.

Publications related to thesis

Papers:

Geraldes R, Esiri MM, DeLuca GC, Palace J. Age-related small vessel disease: A potential contributor to neurodegeneration in multiple sclerosis. Brain Pathol. 2017; 27(6):702-722

Geraldes R, Ciccarelli O, Barkhof F, De Stefano N, Enzinger C, Fillipi M, Hofer M, Friedemann P, Preziosa P, Rovira A, DeLuca CG, Kappos L, Yousry T, Fazekas F, Frederiksen J, Gasperini C, Satre-Garriga J, Evangelou N, Palace J. The current role of MRI in differentiating multiple sclerosis from its imaging mimics. Nat Rev Neurol. 2018; 14(4):199-213

Geraldes R, Juryńczyk M, dos Passos G, Pichler A, Chung K, Hagens M, Ruggieri S, Huerga E, Jorda M, Enzhinger C, Chard D, Barkhof F, Gasperini C, Rovira A, DeLuca GC, Palace J. Distinct influence of different vascular risk factors on WM brain lesions in multiple sclerosis (*in preparation*)

Published abstracts:

Geraldes R, Esiri M, Palace J, DeLuca GC. Systemic vascular disease burden in multiple sclerosis: a post-mortem case-control study. Neuropathology and Applied Neurobiology. 2016; 42(1):24

Geraldes R, Esiri M, Palace J, DeLuca GC. Systemic Vascular Disease Burden in Multiple Sclerosis: a post mortem case-control study. European Committee for treatment and research in Multiple Sclerosis (ECTRIMS) meeting, London 2016 (ECTRIMS online library 146224)

Geraldes R, Esiri M, Palace J, DeLuca G. Does global systemic vascular disease burden and atheroma burden affect total plaque area in multiple sclerosis? Neuropathology and Applied Neurobiology. 2017; 43 (1):54

Geraldes R, Esiri M, Palace J, DeLuca G. Systemic vascular disease burden and multiple sclerosis pathology: a post mortem study (ECTRIMS online library October 2017, 200601)

Geraldes R, Esiri M, Palace J, DeLuca GC. Large artery atheromatous disease and cerebral small vessel disease: a post mortem study. Neuropathology and Applied Neurobiology. 2018; 44(1):44

Geraldes R, Esiri M, Palace J, DeLuca G. Pathological correlated of age at death in multiple sclerosis. JNNP. 2018;89(10):e8

Geraldes R, Esiri M, Palace J, DeLuca G. Correlates of pontine small vessel disease: a post-mortem study. Eur J Neurol. 2018; 25 (2): 60

Geraldes R, Esiri M, Palace J, DeLuca G. Cerebral small vessel disease in multiple sclerosis. Neuropathology and Applied Neurobiology. 2018 (*in press*)

Relevant publications indirectly related to thesis

Papers:

Compston A, Geraldes R, Schmierer K, Cerqueira JJ, Palace J, Thompson A, Tinelli M, Rosa MM. Time matters in multiple sclerosis: can early treatment and long-term follow-up ensure everyone benefits from the latest advances in multiple sclerosis? JNNP. 2018; 89(8):844-850

Ahmed O, Geraldes R, DeLuca G, Palace J. Multiple Sclerosis and the risk of systematic venous thrombosis: a systematic review. Multiple Sclerosis and Related Dis. 2019;27:424-430

Juryńczyk M, Tackley G, Kong Y, Geraldes R, Matthews L, Woodhall M, Waters P, Kuker W, Craner M, Weir A, DeLuca GC, Kremer S, Leite MI, Vincent A, Jacob A, de Sèze J, Palace J. Brain lesion distribution criteria distinguish MS from AQP4-antibody NMOSD and MOG-antibody disease. J Neurol Neurosurg Psychiatry. 2017; 88(2):132-136

Juryńczyk M, Geraldes R, Probert F, Woodhall MR, Waters P, Tackley G, DeLuca G, Chandrate S, Leite MI, Vincent A, Palace J. Distinct brain Imaging characteristics of autoantibody-mediated CNS conditions and multiple sclerosis. Brain. 2017; 140 (3): 617-627

Published abstracts:

Messina S, Geraldes R, Chua Y, Taylor J, Cavey A, Rubio Diaz A, Everett R, Reeve S, Mariano R, DeLuca GC, Leite M I, Palace J. Smoking on disability accumulation in Neuromyelitis Optica and Multiple Sclerosis. (ECTRIMS online library October 2017, 200154)

Ahmed O, Geraldes R, Ahmed A, DeLuca G, Palace J. Multiple sclerosis and the risk of venous thrombosis: a systematic review (ECTRIMS online library October 2017, 199458)

Acknowledgements

This thesis would not have been possible without the nurturing environment that surrounded me throughout its development.

I am grateful to my joint DPhil supervisors, Dr Jacqueline Palace and Professor Gabriele DeLuca who guided me through my doctoral studies with all their energy, enthusiasm and love for research. I would like to thank Dr Palace for contributing her immense clinical research experience and for giving me the opportunity to join a team of extraordinary fellows and an international research community. I wish to express my gratitude to Professor DeLuca for sharing his clinical and scientific rigour, his passion for teaching and for making me a part of his stimulating lab team.

I was fortunate to count on the generous support of Professor Margaret Esiri, who was present at every step of my pathology work and who patiently proof read my thesis. Most of all I am deeply grateful for her quiet presence, which helped me through the turbulent days.

I wish to acknowledge the support I received from my lab colleagues: Richard Yates, who patiently guided me through lab techniques; Dr Damian Jenkins, for all his support and help with the pathology scoring, and Bryan Adriaanse for the intense lab meeting discussions. I also extend thanks to the Oxford Brain Bank team: Marie Hamard, for aiding with brain tissue sampling and processing; Ana Xambre, for paraffin block cutting; Connor Scott, for imaging analysis training; and Carolyn Sloan, for general technical support. I am also grateful to the Oxford University Hospitals (OUH) Neuropathology team, especially the lab manager Hannah Kayser, who provided me with access to the lab facilities.

My imaging project was the result of a multicentre collaboration within the MAGNIMS consortium. I am indebted to colleagues from all participating centres: Professor Christian Enzinger & Dr Alexander Pichler (University of Graz), Professor Declan Chard & Dr Karen Chun (University College, London), Professor Frederik Barkhof & Dr Marloes Hagens (VU Medical University, Amsterdam), Professor Claudio Gasperini & Dr Serena Ruggieri (San Camillo-

Forlanini Hospital, Rome), and Dr Alex Rovira, Dr Manuel Jorda & Elena Huerga (Universitat Autonoma de Barcelona).

I would also like to thank Dr Maciej Juryńczyk and Dr Giordani dos Passos for their meticulous imaging scoring and for their critical advice and to Professor Yazhuo Kong, Professor Mark Jenkinson's FMRIB team (Ludovica Griffanti, Hannah Nowicka) and Dr George Tackley for their support with imaging analysis. I am also grateful to Dr Wim van Hecke, Annemie Ribbens and Ruben Houberts from Icometrix for their assistance with lesion segmentation.

Most of all, I would like to acknowledge my friends and research fellows Dr Romina Mariano and Dr Silvia Messina, for their continuous encouragement throughout the challenges of imaging analysis and their thorough thesis proof reading.

I am indebted to Professor Rafael Perera from the Nuffield Department of Primary Care Health Sciences for his feedback on the pathology work statistical analysis as well to my friend Professor João Branco (Técnico, Lisbon) for his *ad hoc* statistical input.

I am deeply grateful to Professor Isabel Leite who challenged me to undertake this project and to my colleagues Dr Ester Coutinho, Dr Pedro Cruz and Adriana Roca who advised and encouraged me along the way. I would also like to thank the OUH MS team members, especially the MS nurses Pete Monaghan and Chris Rigozzi, as well as the OUH MS trials team members: Dr Matt Craner, Ana Cavey, Helen Birmingham, Christina Abarno, Daniel Cullen, Joy Hodder and Sadia Ahmad, for their understanding, encouragement and for allowing for me to balance my clinical work with my research during my final months. Most importantly, I would like thank my MS patients, who are my constant source of inspiration.

Finally, I wish to thank my family: my father, for teaching me through example to be curious and hardworking; my mother, for sharing with me her immense joy of living and motivation; and most especially my husband and my two sons, who have embarked on this adventure with me, leaving many things behind. I am forever grateful for their enormous generosity and love.

Contents

List of Figures **12**

List of Tables **14**

Abbreviations **16**

1 Introduction **17**

1.1. Multiple Sclerosis (MS) and vascular disease: key reasons to study an interaction 17

1.2. Brief overview on the cerebral microcirculation 19

1.3. MS overview 22

1.3.1. Clinical summary and natural history 22

1.3.2. Epidemiology and risk factors 24

1.3.3. Immunology, inflammation and neurodegeneration 28

1.3.4. Classical MS features detected by imaging and its pathological correlates 31

1.4. Age- VRF- related cSVD 36

1.4.1. The aging brain 36

1.4.2. Cardiovascular disease and VRF 37

1.4.3. cSVD overview 40

1.5. Differentiating MS from cSVD with MRI 43

1.6. MS and vascular disease: evidence for a possible interaction 45

1.6.1. MS associates with worse vascular disease 45

1.6.2. VRF and vascular comorbidities lead to worse MS outcomes 52

1.7. Thesis Overview 55

1.7.1. Research hypotheses 55

1.7.2. Study design 58

2 The influence of MS on systemic atherosclerosis and vascular end-organ damage **65**

2.1.Introduction 65

2.2. Material and Methods 66

2.2.1. Study population 66

2.2.2. Assessment of Clinical data and SysVasc using autopsy reports 66

2.2.3. Statistical analysis 69

2.3. Results 71

2.3.1. Cohort characteristics 71

2.3.2. Construction of a SysVasc score from autopsy reports ... 74
2.3.3. SysVasc score validity ... 76
2.3.4. SysVasc in MS and non-MS ... 77
2.4. Summary of main findings ... 82
2.5. Discussion ... 82

3 The influence of MS on type 1 cSVD ... 88

3.1. Introduction ... 88
3.2. Materials and Methods ... 89
3.2.1. Study population ... 89
3.2.2. Tissue sampling ... 89
3.2.3. Neuropathological Evaluation ... 92
3.2.4. Statistical Analysis ... 100
3.3. Results ... 101
3.3.1. Cohort characteristics ... 101
3.3.2. Scoring cSVD pathologies and Global cSVD Index construction ... 104
3.3.3. Global cSVD Index, SysVasc Score and cervical/intracranial atheroma in MS and non-MS ... 108
3.3.4. The influence of MS on Global cSVD Index considering age at death and SysVasc Score ... 110
3.3.5. The influence of MS on individual cSVD pathologies ... 114
3.3.6. The influence of MS on cSVD considering age at death cervical/intracranial large artery atheroma. ... 117
3.3.7. Inside plaque cSVD and its relationship with outside plaque cSVD and SysVasc ... 117
3.4. Summary of main findings ... 120
3.5. Discussion ... 120

4 The influence of MS on cerebral periarteriolar/perivenular inflammation and venous collagenosis ... 124

4.1. Introduction ... 124
4.2. Materials and Methods ... 125
4.2.1. Study population and tissue sampling ... 125
4.2.2. Neuropathological assessment ... 126
4.2.3. Statistical Analysis ... 129
4.3. Results ... 130
4.3.1. Cohort characteristics ... 130

4.3.2. Periarteriolar and perivenular inflammation 130
4.3.3. FWM periventricular cSVD in non-MS and MS 134
4.3.4. Venous collagenosis 135
4.3.5. Description of peri-arteriolar changes in MS 137
4.4. Summary of the main findings 140
4.5. Discussion 141

5 The influence of systemic and cerebral vascular disease on MS pathological outcomes: a post mortem study 145

5.1. Introduction 145
5.2. Materials and Methods 147
5.2.1. Study population 147
5.2.2. Macroscopic global WML burden assessment 147
5.2.3. Tissue sampling and neuropathological evaluation 148
5.2.4. Assessment of demyelination 148
5.2.5. SysVasc and cerebrovascular disease assessment 151
5.2.6. Statistical analysis 152
5.3. Results 153
5.3.1. Cohort characteristics 153
5.3.2. Demyelination and plaque activity outcomes 153
5.3.3. The relationship between MS pathology outcomes and age at death and disease duration 155
5.3.4. The relationship between MS pathology outcomes and SysVasc 157
5.3.5. The relationship between MS pathology outcomes and cSVD 160
5.3.6. MS pathology outcomes and individual cSVD pathologies 165
5.3.7. The relationship between MS pathology outcomes and intracranial artery atheroma burden 168
5.4. Summary of the main findings 168
5.5. Discussion 169

6 Specificity of imaging surrogate markers in differentiating MS from cSVD 176

6.1 Introduction 176
6.2. Materials and Methods 178
6.2.1. Study design and cohorts 178
6.2.2. Imaging Analysis 178
6.2.3. Statistical analysis 184
6.3. Results 185

6.3.1. Clinical features of the cohorts used for lesion visual scoring and volumetric analysis....185
6.3.2. Inter-rater agreement for the visual scoring....186
6.3.3. MS and cSVD imaging surrogate markers specificity....186
6.3.4. Clinical features and WML volumes of the cohorts included on probabilistic mapping analysis....192
6.3.5. Lesion distribution....193
6.4. Summary of the main findings....197
6.5. Discussion....198

7 The influence of VRF on MS imaging surrogate markers....204

7.1 Introduction....204
7.2. Materials and Methods....205
7.2.1. Study design and cohorts....205
7.2.2. Imaging Analysis....205
7.2.3. Statistical analysis....206
7.3. Results....206
7.3.1. Clinical features of the cohorts used for MS imaging markers visual scoring....206
7.3.2. The relationship between MS imaging markers and age and disease duration....208
7.3.3. MS imaging markers visual scoring results: comparisons between MS with and without VRF....208
7.3.4. Clinical features and WML volumes of the cohorts use for probabilistic mapping analysis....217
7.3.5. Lesion distribution....218
7.4. Summary of the main findings....221
7.5. Discussion....221

8 The influence of MS on cSVD imaging markers....226

8.1. Introduction....226
8.2. Materials and Methods....227
8.2.1. Study design and study cohorts....227
8.2.2. Imaging Analysis....227
8.2.3. Statistical analysis....228
8.3. Results....228
8.3.1. Clinical features of the cohorts used in Chapter 8....228

8.3.2. Relationship of cSVD markers with age 230
8.3.3. cSVD imaging surrogate markers in MS with VRF compared with non-MS with VRF 230
8.3.4. Lesion distribution 232
8.4. Summary of main findings 234
8.5. Discussion 234
9 Key findings, implications for clinical practice and for future research 237
10 Bibliography 243

List of Figures

Figure 1.1. Aging with MS 18
Figure 1.2. Cerebral microcirculation 20
Figure 1.3. Typical imaging features of MS with conventional MRI 36
Figure 1.4. Post mortem study design 59
Figure 1.5. In vivo brain imaging study design 61
Figure 1.6. Cohorts included in the in vivo brain imaging study 62
Figure 2.1. SysVasc score construction. 69
Figure 2.2. Cohort Selection for autopsy reports scoring 71
Figure 2.3. SysVasc Scores in vascular and non-vascular causes of death in the whole cohort. 76
Figure 2.4. Heart weight variation with age at death in MS and non-MS cases 78
Figure 2.5. Regression plots of SysVasc and atheroma on age, for MS and non-MS cases 80
Figure 3.1. Sampled brain areas for cSVD scoring 91
Figure 3.2. Differentiation between damaged small veins and arterioles in MS. 93
Figure 3.3. WM rarefaction scoring in PLP immunostained sections. 99
Figure 3.4. Cohort selection for histology analysis. 102
Figure 3.5. Global cSVD and Age at death in non-MS and MS 107
Figure 3.6. Global cSVD Index and cSVD per brain region in non-MS and MS (outside plaque) 109
Figure 3.7. Relationship between SysVasc score and Global cSVD Index in all non-MS and MS and segregated by age at death 111
Figure 3.8. Individual cSVD pathologies per brain region in non-MS and MS (outside plaque). 115

Figure 3.9. Inside and outside plaque cSVD per brain area....119
Figure 4.1. Scoring of cSVD in FWM....129
Figure 4.2. Periarteriolar (a) and perivenular (b) inflammation per brain region in non-MS and MS (outside plaque)....132
Figure 4.3. Periarteriolar and perivenular inflammation inside and outside plaque per brain area....134
Figure 4.4. cSVD per FWM periventricular layer in non-MS and MS cases without periventricular plaques....135
Figure 4.5. Venous collagenosis per FWM periventricular layer and outside PV area in non-MS and MS cases without periventricular plaques....137
Figure 4.6. Periarteriolar veils....139
Figure 4.7. Peri-arteriolar veils in MS (inside and outside plaque) and non-MS....140
Figure 5.1. Macroscopic global WML assessment....147
Figure 5.2. Assessment of MS demyelination. 149
Figure 5.3. Plaque activity classification. 151
Figure 5.4. Relationship between total number of plaques (a), percentage of overall plaque area (b). 156
Figure 5.5. Percentage of cortical demyelination area and age at death.....156
Figure 5.6. The relationship between disease duration and MS pathology outcomes, SysVasc and cSVD segregated by age at death 157
Figure 5.7. Relationship between MS pathology outcomes and SysVasc segregated by age at death 159
Figure 5.8. Percentage of cortical demyelination area and SysVasc segregated by age at death 160
Figure 5.9. Relationship between MS pathology outcomes and Global cSVD Index segregated by age at death....163
Figure 5.10. Percentage of cortical demyelination area and Global cSVD Index for all cases (a) and segregated by age at death (b).....165
Figure 6.1. Basal ganglia lacuna example....181
Figure 6.2 Example of basal ganglia and thalamus segmentation using FSL FIRST....182
Figure 6.3. MS imaging surrogate marker visual scoring results in MS without VRF and non-MS with VRF.....190
Figure 6.4. cSVD imaging surrogate markers visual scoring results in MS without VRF and non-MS with VRF.....192
Figure 6.5. Lesion probability distribution analysis 196
Figure 7.1. Comparisons of MS imaging markers between MS with and without VRF.....210

Figure 7.2. Dawson fingers and juxtacortical lesion counts and disease duration in MS per VRF group....212
Figure 7.3. Infratentorial lesions in MS with and without VRF....216
Figure 7.4. Lesion probability distribution analysis....220
Figure 8.1. Number of lacunae and age in MS with VRF and non-MS with VRF....230
Figure 8.2. Percentage of cases with lacunae (a.), central pons lesions(b.) and microbleeds (c.) per group....231
Figure 8.3. Subtraction maps MS VRF minus non-MS VRF....234
Figure 9.1. Summary of key findings....239

List of Tables

Table 1.1 Microcirculation: normal structure and changes with aging, cSVD and in MS....21
Table 1.2. Summary of core brain MRI and pathology features in MS and cSVD....35
Table 1.3. Brain MRI studies on the impact of VRF on MS brain lesions....54
Table 1.4. Clinical features of all cohorts used for the in vivo Brain imaging study....63
Table 1.5. Brain MRI sequences and protocol from each participating centre....64
Table 2.1. Demographic features of MS and non-MS cases studied in Chapter 2....72
Table 2.2. Other causes of death in MS and non-MS cases....73
Table 2.3. Atheroma scores according to pathologist....75
Table 2.4. Correlation matrix for individual SysVasc features included in the SysVasc Score 75
Table 2.5. SysVasc in MS and non-MS....78
Table 2.6. Models to study the effect of MS diagnosis on SysVasc and Atheroma Scores....81
Table 3.1. Details of Antibodies used in Chapter 3 and Chapter 5....92
Table 3.2. cSVD scored features....96
Table 3.3. Clinical details of the cohort used in Chapter 3, for all cases and cases binned above and the median age at death....103
Table 3.4. Frequencies of each cSVD individual pathological features per brain region in non-MS and MS outside plaque....106
Table 3.5. Numerical results of the multivariate linear regression stepwise model to predict Global cSVD Index considering age at death, SysVasc score and MS diagnosis....113
Table 3.6. Numerical results of the multivariate linear regression analysis to predict Global cSVD Index taking into SysVasc score above and below the median age at death....113
Table 3.7. Numerical results for binary logistic models to predict the influence of MS on individual cSVD pathologies adjusting for age at death and SysVasc burden....116
Table 4.1. Additionally scored cSVD features....127

Table 4.2. Periarteriolar and perivenular inflammation per brain region in non-MS and MS (outside plaque).....132
Table 5.1. Demyelination outcomes per brain region.....154
Table 5.2. Numerical results of the Poisson loglinear regression stepwise model to predict total number of plaques and number of active plaques.....161
Table 5.3. Numerical results of the Poisson loglinear regression stepwise model to predict total number of plaques and number of active plaques, segregated by age at death.....164
Table 5.4. Relationship between each cSVD individual pathology, periarteriolar and perivenular inflammation and total number of plaques and number of active, segregated by age at death.....167
Table 6.1. MS and cSVD imaging surrogate markers quantification in MS without VRF and non-MS with VRF.....189
Table 6.2. Clinical data and WML volumes of the cohort included for probabilistic mapping 193
Table 7.1. Clinical features and MS imaging markers quantification of the MS cohort used in Chapter 7 stratified by VRF.....207
Table 7.2. Poisson loglinear model to predict the number of Dawson fingers and juxtacortical lesions considering the presence of any VRF and disease duration.....211
Table 7.3. Summary of the Poisson log-linear models to predict the number of Dawson fingers and juxtacortical lesions considering.....214
Table 7.4. Clinical data and WML volumes of the cohort included for probabilistic mapping 218
Table 8.1. Clinical features of the cohorts included in Chapter 8 and summary of cSVD imaging markers visual scoring results.....229
Table 8.2. Clinical features and WML volumes of the MS with VRF and non-MS with VRF groups used for lesion probabilistic analysis.....232

Abbreviations

BBB – blood brain barrier
BMI – body mass index
CAA - cerebral amyloid angiopathy
CI – confidence intervals
CIS – clinically isolated syndrome
CNS - central nervous system
CSF – cerebrospinal fluid
cSVD - cerebral small vessel disease
DAWM – diffusely abnormal WM
DMT- disease modifying treatments
EAE - experimental autoimmune encephalomyelitis
EBV – Epstein-Barr virus
EDSS - expanded disability status scale
FLAIR- fluid-attenuated inversion recovery
FFPE - formalin–fixed paraffin-embedded
FWM – frontal white matter
H&E – haematoxylin and eosin
IS -ischaemic stroke
LVH – left ventricular hypertrophy
MRI – magnetic resonance imaging
MAG – myelin associated glycoprotein
MAGNIMS - Magnetic Resonance Imaging in MS
MI – myocardial infarction
MS - multiple sclerosis
NAWM – normal appearing WM
OCBs – oligoclonal bands
OWM – occipital white matter
PHL – peri-arteriolar hemosiderin leakage
PLP – proteolipid protein
PPMS – primary progressive multiple sclerosis
PSD – peri-arteriolar space dilatation
RRMS – relapsing remitting multiple sclerosis
SMA- smooth muscle actin
SPMS – secondary progressive multiple sclerosis
SWI – susceptibility-weighted imaging
SysVasc – systemic vascular disease
VRF- vascular risk factors
WM – white matter
WML – white matter lesions

1 Introduction

1.1. Multiple Sclerosis (MS) and vascular disease: key reasons to study an interaction

Multiple sclerosis (MS) is a chronic inflammatory demyelinating and neurodegenerative disease of the central nervous system (CNS) (Lassmann *et al.*, 2007) that affects 2.5 millions of people worldwide (Koch-Henriksen and Sørensen, 2010; Kingwell *et al.*, 2013; Aarli *et al.*, 2014). MS is a heterogeneous disease but commonly manifests in young adults initially with transient episodes of neurological dysfunction (relapses) relating to flares of acute CNS inflammation. After several decades, the vast majority of these patients experience progressive accumulation of disability without relapses. This progressive phase of the disease is driven by neuronal/axonal loss disproportionate to inflammatory activity (Vukusic and Confavreux, 2007; Lublin *et al.*, 2014) and is mostly refractory to currently disease modifying therapies (DMT).

Age is one of the stronger predictors of entry into the progressive phase and accumulation of severe disability (Confavreux and Vukusic, 2006; Tutuncu *et al.*, 2013; Scalfari *et al.*, 2014) and factors known to be associated with aging, such as hypoxia (Desai *et al.*, 2016), mitochondrial dysfunction (Currais, 2015) and iron accumulation (Ward *et al.*, 2014), among others, may be important contributors to neuronal damage, and by extent, disability in MS.

Changes in the body vasculature, including the brain, occur with aging and with the presence of vascular risk factors (VRF), such as hypertension, smoking, diabetes, dyslipidaemia and physical inactivity. Cerebral small vessel disease (cSVD) is the term used for pathological processes that affect cerebral small arterioles, capillaries, and venules (Pantoni, 2010; Esiri *et al.*, 2015) (Wardlaw *et al.*, 2013*a*), leading to ischaemia, white matter (WM) lesions (WML) and neuronal loss (Zlokovic, 2011). VRF and vascular disease could potentially contribute to age-related neurodegenerative pathology seen in MS (**Figure 1.1.**) (Geraldes *et al.*, 2017).

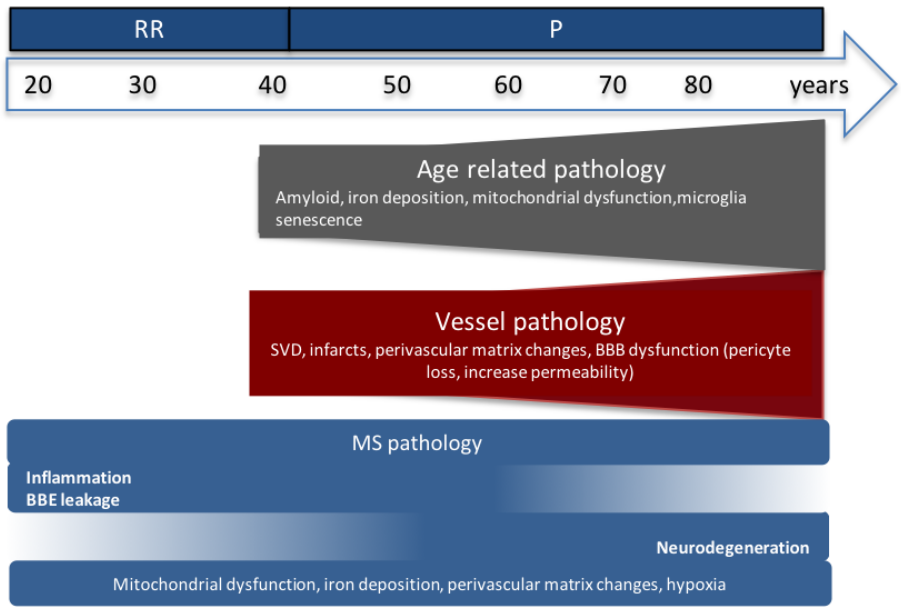

Figure 1.1. Aging with MS

Adapted from (Geraldes et al. 2017). BBB, blood–brain barrier; RR, relapsing–remitting MS; P, progressive MS.

In this thesis introduction, the key aspects of MS and vascular disease will be reviewed, focusing on cSVD. The typical pathological and radiographical characteristics of MS and cSVD, together with the impact of these two disorders on the cerebral microvasculature, their overlapping features and possible additive effects will be critically analysed and gaps in the literature highlighted. This aims to provide the background for the two complementary approaches I have chosen to gather a better insight into the interaction between MS and vascular disease, which will be summarised at the end of this chapter.

1.2. Brief overview on the cerebral microcirculation

The cerebral circulation can be classified according to vessel size into macro- and microcirculation (Jones, 1970; Kiliç and Akakin, 2008; Kulik *et al.*, 2008), as illustrated in **Figure 1.2.** Micro-vessels do not provide sufficient collateral flow to perfuse tissue when a penetrating arteriole or venule is blocked (Blinder *et al.*, 2013). This contributes to deep WM vulnerability to ischaemia because its major blood supply is via long medullary arterioles (Brown and Thore, 2011*b*, Wardlaw *et al.*, 2013*a*). Communication between the brain parenchyma and the microvasculature is mediated through the neurovascular unit that includes different structures including the pericytes that act as capillary sphincters and participate in blood flow regulation (Hall *et al.*, 2014). Key structural features and functions of the normal microvasculature are summarized in **Table 1.1.** (Kulik *et al.*, 2008; Iadecola and Anrather, 2011; Lau *et al.*, 2013; Bardehle *et al.*, 2015; Prakash and Carmichael, 2015; Segarra *et al.*, 2015; Zhao *et al.*, 2015; Spencer *et al.*, 2018)**.**

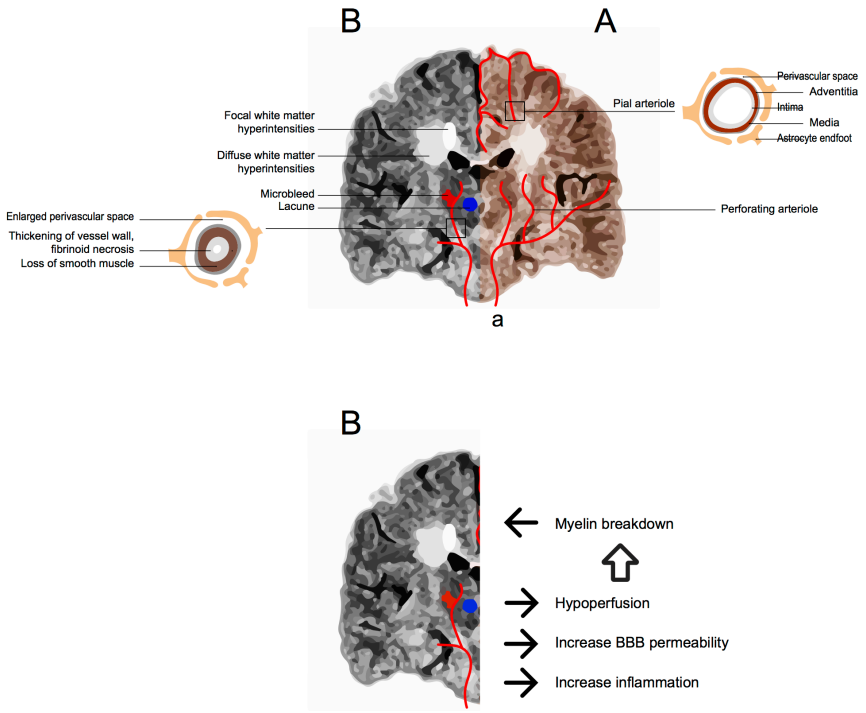

Figure 1.2. Cerebral microcirculation

A- Cerebral circulation is divided into macrocirculation (**a**) that includes the internal carotid and vertebral arterial systems and (**b**) microcirculation. The microcirculation is composed of pial and perforating arterioles, capillaries and venules. **Pial arterioles** give rise to **superficial perforating arterioles** that course centripetally entering the brain at right angles to its surface, branching and terminating as end arteries. **Perforating arterioles** also arise from the main artery branches and irrigate the basal ganglia, deep WM and brainstem. Perforating arterioles lie within the Perivascular Spaces (PVS), where vessel wall components are in close contact with the astrocyte end feet, and terminate as end arteries (i.e. without shunts) in capillary beds. The capillary plexus drains into venules (not shown). **B - Potential interaction between cSVD and MS.** Longstanding MS Brain MRI (FLAIR coronal section), showing focal and diffuse periventricular WM hyperintensities adjacent to the lateral ventricles. A perforating artery affected by cSVD is illustrated where enlargement of the perivascular space, thickening of the vessel wall with significant reduction of the vessel lumen is present. These vessel changes are associated with subsequent vessel occlusion leading to lacunae, vessel rupture causing microbleeds, hypoperfusion, blood brain barrier damage and subsequent myelin break down. This could cause additional WM damage and neuronal loss in MS. (Geraldes et al. 2017).

Table 1.1 Microcirculation: normal structure and changes with aging, cSVD and in MS

Microcirculation	Structure	Function	Aging	SVD	MS
Pial arteries **Perforating arteries**	Surrounded by CSF and pia-arachnoid and glia limitans. Three vessel wall layers: 1. *tunica adventitia* (mostly collagen and fibroblasts) 2. a *tunica media* (smooth muscle) 3. a *tunica intima* (single layer of endothelial cells and internal elastic lamina)	1. Nutrition 2. Cerebral blood flow regulation 3. Vasophylic neuroblast migration	1.Tortuousity 2.Thickened walls 3.Loss of elastin and smooth muscle 4. Reduced coverage by pericytes and perivascular nerve plexus	1.Severe thickening vessel wall 2.Arteriosclerosis/ fibrinoid necrosis 3. Enlarged PVS 4. Vascular ectasia 5.Amyloid wall infiltration 6.PVS hemosiderin deposition	1.Enlarged PVS Scarce information
Capillary	Single layer of endothelial cells	1. Nutrition 2.Cerebral blood flow regulation 3. Immune response	1.Increased diameter 2. Basal membrane thickening, reduplication and vacuolization 3. Increased vessel wall hyalinosis and fibrosis 4. Reduced coverage by pericytes	1.Perivascular rarefaction 2. Increased endothelial permeability	1. Increase endothelial permeability, with protein leakage, red blood cell extravasation 2. Perivascular inflammation
Venules	Thin-walled vessels: 1. *tunica adventitia* (mostly collagen and fibroblasts) 2. a *tunica media* (thin layer of smooth muscle) 3. a *tunica intima* (single layer of endothelial cells) No valves.	1. Metabolite clearance 2. Cerebral blood flow regulation	1.PVS collagenosis	1. Vessel wall and PVS collagenosis	1.Thickening of vessel wall, vessel tortuosity 2.Intramural fibrinoid deposition, wall reduplication 3. Iron deposition 4. Enlarged PVS 5. PVS collagenosis 6. Perivascular inflammation 7. Thrombosis
Neurovascular Unit	1. Endothelial cells 2. Pericytes 3. Vascular smooth muscle cells 4. Astrocytes 5. Basal membrane 6. Neurons 7. Perivascular macrophages 8. Mesenchymal stromal cells	1.Immune response regulation (adaptive and innate immune responses regulation of leukocyte transfer) 2. Transport of substances 3. Blood flow 4.Angiogenesis regulation 5. Coagulation and fibrinolysis	1.Endothelial cell increased permeability 2. Reduced pericytes	1. Endothelial cell increased permeability	1.Changes in endothelial cell tight and adherens junction expression (occludine, claudins, cadherins, zonula-ocludens), with increase permeability 2.BM/extracellular matrix abnormalities 3.Dynamic changes in mesenchymal stromal cells

(adapted from Geraldes et al. 2017) CSF – cerebrospinal fluid, PVS – perivascular space

1.3. MS overview

1.3.1. Clinical summary and natural history

The onset of MS clinical neurological symptoms, resulting from bouts of focal CNS inflammation, typically occurs around the second or third decade of life (Compston and Coles, 2002; Brownlee *et al.*, 2017). Though 10% of the cases present before the age of 18 years (Yeshokumar *et al.*, 2017), MS before the age of 10 is extremely rare (Waldman *et al.*, 2016) and only around 4.5% of patients are diagnosed after the age of 50 years (Lotti *et al.*, 2017).

In the majority of cases, the onset of MS is characterized by an initial attack, defined as clinically isolated syndrome (CIS) consisting of an unpredictable episode of either monocular visual loss (due to optic nerve inflammation or optic neuritis), sensory and motor symptoms (often due to spinal cord inflammation or myelitis), brainstem, cerebellum or cerebral hemisphere symptoms. The symptoms present sub-acutely and last more than 24 hours but usually less than 4 weeks (Filippi *et al.*, 2018). However, it is increasingly recognized that during the years preceding the emergence of these neurological symptoms, that often lead to MS diagnosis, health care use due to pain, depression, chronic fatigue and other non-specific symptoms is increased, indicating that there is a prodromal phase of the disease (Wijnands *et al.*, 2017; Disanto *et al.*, 2018), which is yet to be fully characterized. Further support that CNS maybe targeted before neurological symptoms, is the fact that lesions with typical features of MS can be incidentally found in CNS imaging performed for a reason other than suspicion of MS. Though a careful exclusion of alternative

diagnosis is recommended, this cohort of patients is at risk of a future symptomatic neurological event, that will lead to the diagnosis of MS, and has been defined as radiological isolated syndrome (De Stefano *et al.*, 2018).

In around 85% of MS patients, recurrence of these discrete events of neurological dysfunction, or relapses, characterise the initial relapsing-remitting phase (RRMS). RRMS is heterogeneous in terms of relapse frequency, severity and recovery, but it is generally accepted that the accumulation of disability in this phase relates to relapses and that in-between these events there is no accumulation of neurological dysfunction. The average relapse frequency is around 1.1 per year early in the disease but seems to decrease with advancing disease and age (Patzold and Pocklington, 1982).

The vast majority of patients with RRMS will then enter a phase characterised by progressive, irreversible disability that occurs independently of relapses, or the secondary progressive phase (SPMS). A minority of MS patients (10-15%) will have progressive disability independent of relapses, for at least 1 year from disease onset and this phenotype has been named primary progressive MS (PPMS). Age at onset of PPMS is usually around the 40 years (Koch *et al.*, 2007) and common symptoms of both progressive phenotypes include walking difficulties, due to lower limb weakness and increased muscular tone, bladder symptoms, such as urinary retention or incontinence, fatigue and cognitive dysfunction (Compston and Coles, 2008; DeLuca *et al.*, 2015).

The onset of disease progression is age dependent and occurs around the age of 40 years (Koch *et al.*, 2007; Tutuncu *et al.*, 2013; Confavreux and Vukusic, 2014; Scalfari *et al.*, 2014) and seems to be somehow unrelated to the presence or duration of a pre-progression symptomatic disease course (Zeydan and Kantarci, 2018). Relapses can occur in both SPMS and PPMS but they are much less common in these MS subtypes (Lublin, 2014).

1.3.2. Epidemiology and risk factors

MS is the commonest non-traumatic disabling neurological disease to affect young adults in Europe (Kobelt *et al.*, 2017). Disease prevalence tends to increase with the distance from the equator (Aarli *et al.*, 2014), northern European countries with a prevalence of around 100-120/100000 inhabitants and of 15-60/100000 in southern European countries. This latitude gradient together with migration studies, showing that the risk of MS for those who migrate from a low risk country to a high-risk country before adolescence is similar to that of those who are born and reside in the high-risk country, implicate environmental and life-style factors in the risk of MS (Olsson *et al.*, 2017). Among those, Epstein-Barr virus (EBV) infection, smoking, low vitamin D and lack of sun exposure and adolescent obesity are well-established MS risk factors and their link with MS will be detailed below (O'Gorman *et al.*, 2012; Belbasis *et al.*, 2015; Olsson *et al.*, 2017). However, others, such as night shift work (Gustavsen *et al.*, 2016), solvent exposure (Bell and DeLuca, 2018; Hedström *et al.*, 2018), bacterial infections (Wagley *et al.*, 2018), high dietary salt and changes in gut microbiota (Bell *et al.*, 2018) may also increase susceptibility to MS.

Individuals who have had symptomatic infectious mononucleosis in early adulthood have around 2-fold increased risk of developing MS (Giovannoni *et al.*, 2010). Although several genetic and molecular mechanisms suggest a link between EBV activation in the brain of MS patients leading to intrathecal B-cell transformation (Fierz, 2017), a causal relationship between EBV infection and MS has not been established.

Smoking associates with a 1.5-fold risk of developing MS and there seems to be a dose-response relationship (Handel *et al.*, 2011; Salzer and Sundstrom, 2013; Weinstock-Guttman *et al.*, 2013). Passive smoking has also been linked to an increased MS risk but the use of oral tobacco (Hedström *et al.*, 2013) associates with a decreased risk of MS (Hedström *et al.*, 2011), suggesting that respiratory airway or lung irritation is a key factor. This is in line with the recent association between solvent exposure (Hedström *et al.*, 2018) and MS risk. Smoking also has a negative impact on MS clinical and radiological outcomes. Not only does it increase the risk of early conversion from CIS into clinically definite MS (Di Pauli *et al.*, 2008), but it also accelerates the conversion from RRMS into SPMS (Healy *et al.*, 2009; Wingerchuk, 2012). A cross-sectional study has shown that each additional year of smoking after the diagnosis of MS accelerates the time to conversion to SPMS by 4.7%, patients who continued smoking reaching SPMS at 48 versus 56 years of age for those who quit (Ramanujam *et al.*, 2015). Smoking is pro-inflammatory and has been associated with several immune-mediated disorders (Perricone *et al.*, 2016). It is hypothesised that lung irritation leads to change of local lymphocytes genetic

expression which then acquire the capability of migrating into the CNS, where they promote demyelination, activate microglia and induce a plethora of cytotoxic responses (Perricone *et al.*, 2016; Olsson *et al.*, 2017).

Vitamin D and its metabolites have pleomorphic roles in both nervous system health and disease (DeLuca *et al.*, 2013). In addition to the above mentioned latitude and migrant studies, the link between vitamin D and MS is based on epidemiological studies showing a lower MS risk in individuals with a higher exposure to sunlight, either over their life course (Tremlett *et al.*, 2018) or *in utero* (Cruz *et al.*, 2016; Nielsen *et al.*, 2017), with high circulating levels of vitamin D (Munger *et al.*, 2006) or with vitamin D enriched diets (Cortese *et al.*, 2015). Low vitamin D levels also seem to enhance MS activity and clinical disability (Ascherio *et al.*, 2014). The mechanisms by which vitamin D deficiency influences MS susceptibility and clinical outcomes are not completely understood. However, it is well established that vitamin D affects several immune-cell types, including macrophages, dendritic cells, B and T-cells (Mora *et al.*, 2008) and its deficiency may lead to abnormal immune responses and in turn to MS (DeLuca *et al.*, 2013).

The association between high body mass index (BMI) in adolescence and a higher risk of MS (2-fold) was shown in large epidemiological studies and factors such as the pro-inflammatory state seen in obese individuals, increased leptin levels or gut microbiota dysregulation have been proposed has possible explanations of this association (Huitema and Schenk, 2018).

Genetic factors are also linked with MS susceptibility. Population-based studies estimated that the relative risk of MS in a sibling of an MS patient is increased 7-fold (Westerlind *et al.*, 2014). Though genetic factors fail to fully explain MS susceptibility, a strong association between genes within the HLA complex and MS has been consistently reported, particularly class I and II genes. Variants of HLA class II genes encode products that present antigens to CD4+ T lymphocytes, whereas class I encoded proteins are involved in antigen presentation to CD8+ lymphocytes. Presence of class II variant *HLA-DRB1*1501* increases the risk of MS by around 3-fold (Sawcer *et al.*, 2011). Genome-wide association studies have identified several other gene regions associated with increased MS susceptibility but with each of the individual genes having only a minor effect (Mitrovič *et al.*, 2018). Almost all of these gene regions seem to be involved in immune mechanisms.

Interactions between MS environmental and genetic risk factors and between each individual environmental risk factors have been reported (Olsson *et al.*, 2017). For example, HLA allele interactions with smoking, EBV infection and adolescent obesity increase the risk to develop MS by around 14 to 15-fold. Obesity has been associated with decreased vitamin D bioavailability and compromised immune response to viral infections and a combination of EBV infection and obesity increases the risk of MS 14-fold (Hedström *et al.*, 2014*a*).

Females are thought to be at higher risk of developing MS. Indeed, MS is more common in women but the sex ratio has changed in the past few decades, being almost 1:1 in the beginning of the 20th century it is now around 3:1 (Orton *et*

al., 2006). Such an increase in MS incidence in women is possibly explained by the increase of smoking and obesity as well as changes in reproductive behaviour (Ponsonby *et al.*, 2012). Despite having a higher MS incidence, females do not have a poorer prognosis compared with men suggesting a biological mechanism of resilience (Voskuhl and Gold, 2012). Female preponderance is less marked in PPMS (Koch *et al.*, 2007).

Altogether the epidemiology and risk factors of MS suggest that MS is triggered by an environmental factor in a genetically susceptible individual, where the immune response is disturbed (Marrie and Tremlett, 2011).

1.3.3. Immunology, inflammation and neurodegeneration

Although MS is an organ-specific disease featured by immune-mediated myelin destruction, as described below, a specific auto-antigen has not been identified in MS despite extensive research. Unlike neuromyelitis optica associated with anti-aquaporin-4 antibodies, MS does not meet the full definition of an autoimmune disease (Lemus *et al.*, 2018). Nevertheless, a complex interplay between environment and genetic factors strongly impacts the CNS immune response. The inflammatory reaction that occurs within the CNS is thought to be triggered by an putative environmental factor outside the CNS, and/or represents a response to a degenerative process that is intrinsic to the CNS (Mallucci *et al.*, 2015). In the CNS-extrinsic (periphery) model, autoreactive T-cells that are activated at peripheral sites (either by molecular mimicry, bystander activation or co-expression of T-cell receptors with different specificities) will access the CNS along with B-cells and monocytes. This

hypothesis has been tested using the animal model of MS, experimental autoimmune encephalomyelitis (EAE), where CNS antigens and immune stimulants are inoculated, generating pathogenic CD4+ T helper 1 (Th1) cells and Th17 cells, that will then cross the blood brain barrier (BBB) to exert their deleterious actions, including myelin and axonal damage. In the CNS-intrinsic model the infiltration of autoreactive lymphocytes is thought to be a secondary phenomenon, either targeting a currently unknown CNS infection or in response to a primary CNS neurodegeneration, again of unknown cause (Dendrou *et al.*, 2015).

Whatever model is considered, activated T-cells within the CNS will activate a cascade of inflammatory events that culminate with direct myelin and axonal damage but also stimulate a B-cell response which will then produce an intrathecal antibody response. This response can be documented in up to 95% of MS patients by the presence of cerebro-spinal fluid (CSF) oligoclonal bands (OCB). OCB are clonally restricted immunoglobulins, detected by isoelectric focusing, secreted by plasma cells into the CSF. Though a hallmark of ongoing inflammation within the CNS, they are non-specific and have been documented in many other conditions (i.e. viral encephalitis, paraneoplastic syndromes) (Pryce and Baker, 2018). The antigenic targets for OCB have yet not been clarified. Recent studies suggest that OCBs may target ubiquitous, intracellular targets, suggesting that they develop secondary to CNS damage (Brändle *et al.*, 2016).

Not only adaptive immune mechanisms are involved in MS immuno-pathogenesis but innate immune responses, mediated through monocyte-derived macrophages and microglia also play a key role in disease progression. Perivascular macrophages likely recruit peripheral leukocytes by producing chemokines and other inflammatory markers and presenting CNS antigens. In the parenchyma, activated microglia and monocytes produce cytotoxic mediators, phagocytose myelin and reactivate infiltrating auto-aggressive T-cells. Activated microglia are not only seen around areas of demyelination, as will be described below, but also in normal appearing WM (NAWM). Although monocytes, microglia and perivascular macrophages can promote inflammation, they can also supress it and, by clearing myelin debris, parenchymal phagocytes may actually promote the recruitment of oligodendrocytes and thus of remyelination (Bogie *et al.*, 2014).

Of note, most of what is known from MS immunology comes from EAE models which often do not replicate the progressive phase of the disease (Kipp *et al.*, 2017). While it is clear that CNS inflammation is a key feature of MS, the exact role of all the immune system players is still not fully understood, particularly in progressive MS. The inflammatory response tends to fade with increased age and disease duration whereas other mechanisms leading to neurodegeneration, such hypoxia, oxidative injury, mitochondrial dysfunction, energy failure and iron accumulation along with age-related neurodegeneration are amplified (Mahad *et al.*, 2015). While several DMTs target the inflammatory response in MS, there is a desperate need for drugs

that halt neurodegeneration, particularly in progressive MS (Salvetti *et al.*, 2015; Correale *et al.*, 2017).

1.3.4. Classical MS features detected by imaging and its pathological correlates

MS lesions occur in different areas of the CNS and can be detected *in vivo* using magnetic resonance imaging (MRI) and on *post mortem* examination. Typical conventional MRI (Geraldes *et al.*, 2018) and corresponding pathology features (Filippi *et al.*, 2019) are summarized in **Table 1.2.** and illustrated in **Figure 1.3.**

WM hyperintensities (bright) lesions (WMH) or T2/fluid-attenuated inversion recovery (FLAIR) imaging sequences are key features of MS, corresponding to different degrees and types of pathology (Moore *et al.*, 2008; Lassmann, 2011; Klawiter, 2013; Laule *et al.*, 2013; DeLuca *et al.*, 2015; Frischer *et al.*, 2015).

The pathological hallmark of MS is the presence of the MS plaque, a focal well-demarcated demyelinated lesion with inflammation and variable degrees of axonal loss (but usually relatively preserved) and reactive gliosis within the white and grey matter. MS plaques are seen in MRI as focal WML, usually hyperintense on T2/FLAIR and with different degrees of hyperintensity on T1-weighted imaging. Lesion formation is a dynamic process, with different degrees of infiltration by monocytes/macrophages, microglia, T and B-cells. The extent of macrophage/microglia lesion infiltration, the special distribution of these cells and their content of myelin degradation products makes are used to classify lesion activity. In active lesions a dense infiltrate of

macrophages/microglia is present all over the lesion and can be subdivided in active demyelinating and active post-demyelinating considering the content of myelin debris seen within these cells. In mixed active/inactive and post-demyelinating lesions macrophages/microglia are seen at the lesion border only and in inactive lesions few of these cells are seen (Kuhlmann T et al. Acta Neuropathol 2017). Active plaques tend to associate with significant BBB breakdown and this can be visualized *in vivo* by contrast agent (gadolinium) leakage from the blood vessels into the parenchyma, the so-called contrast-enhanced lesions. Radiological lesions can resolve (Reich *et al.*, 2015) as inflammation and oedema die out but may also persist, usually when irreversible tissue loss has occurred (Fisher *et al.*, 2007). Some of these lesions are seen as T1-hypointensities and owing to their dark appearance were named as 'black-holes'. The proportion of each type of WML changes over time: older patients with longer disease duration having more inactive than active lesions as seen in pathology (Frischer *et al.*, 2015) and imaging (Tortorella *et al.*, 2005).

While no area is typically spared, there are regions of predilection for these focal WML such as the periventricular and juxtacortical WM, the optic nerve and spinal cord (Miki *et al.*, 1998; Compston and Coles, 2002; Geraldes *et al.*, 2018) (**Figure 1.3.**). The underlying substrate for this topographic predilection is not fully understood, but some observations suggest that the relationship between MS lesions and the cerebral vessels is important. Persistent T2 lesions are more common in central areas of the brain relative to the peripheral regions, whereas acute, transient contrast enhancing lesions are more evenly distributed throughout the cerebral WM (Lee *et al.*, 1999). This suggests that

additional factors, such as WM susceptibility to hypoxia may contribute to persistent tissue damage in some areas such as the periventricular WM (Martinez Sosa and Smith, 2017). Focal WML occur at sites of high venous density and also in watershed areas of low arterial blood flow (Haider *et al.*, 2016) further supporting a dynamic interaction between MS pathology and the cerebral circulation.

Myelin constituents may also be diffusely affected. In diffusely abnormal WM (DAWM) myelin phospholipids and certain myelin proteins such as myelin associated glycoprotein (MAG) are reduced with relative preservation of other constituents such as proteolipid protein (PLP) (Laule *et al.*, 2013). DAWM is usually visualized in MRI as diffuse, with poorly defined boundaries, mild T2/FLAIR hyperintensities and has been shown to associate with reduced tissue integrity, as measured by quantitative MRI techniques (Laule *et al.*, 2011). However, in practice differentiating histological changes in NAWM from DAWM may be challenging.

While cortical and deep grey matter pathologies are important features of progressive MS that associate with clinical disability (Calabrese *et al.*, 2012*b*; DeLuca *et al.*, 2015), sensitivity to detect lesions in these areas on conventional MRI is relatively poor, particularly for the cerebral cortex. That being said, new non-conventional MRI techniques, including higher field strength and sequences that supress the signal from WM and CSF, allowing the images to show a superior delineation of the cortical grey matter (Geurts *et al.*, 2011), enabled better quantification of cortical pathology *in vivo*. Some of these

techniques are likely to be incorporated in routine clinical imaging. Meningeal inflammation, sometimes extensive and organized as follicle-like structures, characterises the late stages of MS and correlates with cortical microglia activation, demyelination and neuronal loss (Howell *et al.*, 2011). The relationship between cortical lesions and the cerebral vasculature has not been fully explored. However, leakage of cortical vessels with fibrinogen extravasation has been shown to be increased in MS compared with controls and to associate with neuronal loss (Yates *et al.*, 2017), further supporting that the NVU plays a crucial role in MS pathology (Spencer *et al.*, 2018) .

Iron deposition, which is diffuse in the brain parenchyma, particularly in the thalamus and basal ganglia, is recognised as a feature of MS pathology (Adams, 1988) but has only been recently assessed *in vivo* with susceptibility weighted (SWI) MRI (Hametner *et al.*, 2013) (**Table 1.1.**). SWI is also useful to document the association between focal WML and venules, by detecting the low signal of deoxyhaemoglobin in venous blood, which appears as a linear or rounded hypointensity in the middle of the focal WM hyperintensity and was named the "central vein sign" (Sati *et al.*, 2016).

Finally, neuronal loss and consequent whole brain volume and regional atrophy are important features of MS and have a stronger correlation with clinical disability than total WML volumes (Fisher *et al.*, 2000; Cifelli *et al.*, 2002; Bermel and Bakshi, 2006; Jacobsen *et al.*, 2014).

Table 1.2. Summary of core brain MRI and pathology features in MS and cSVD

	MS		cSVD	
	Conventional Brain MRI lesion features	Histopathology of respective MRI abnormalities	Conventional Brain MRI lesion features	Histopathology of respective MRI abnormalities
T2/ FLAIR WMH	Focal lesions Sharply defined ! U or S shaped juxtacortical ovoid appearance ! perpendicular to the lateral ventricles (Dawson fingers) ! corpus callosum ! optic nerve ! spinal cord ! pons periphery Diffuse WML periventricular/occipital	Myelin loss (all constituents) Different degrees of axonal loss At high venule density and arterial watershed areas Active - rich in macrophages and lymphocytes Inactive - minimal macrophage infiltration Myelin loss with selective reduction of phospholipids	Focal lesions Watershed regions ! central pons ! sparing of the spinal cord ! less frequent in the corpus callosum ! sparing U fibres Diffuse WML: Symmetrical 1.Mild periventricular WM 2.Irregular periventricular WM 3.Punctate deep WM 4. Deep partial confluent/confluent WM	Myelin loss Axonal loss Myelin loss with selective reduction of phospholipids, MAG 1.Loss of ventricular ependymal. Mild-to-moderate fibrosis of the subependymal layer. 2.Loosening of the fibre network around "tortuous venules". Minor arteriosclerotic vessel changes 3. Severe axonal and myelin loss and reactive gliosis Incomplete infarcts. Fibrohyalinotic and arteriosclerotic vessels. Mild tissue changes surrounding dilated PVS Myelin loss and atrophic neuropil around fibrohyalinotic arterioles 4.Axonal loss and astrogliosis. Myelin, axon and oligodendrocyte loss, focal transitions to complete infarcts.
T1 T1 GAD	Transient hypointensities Widespread WM Persistent hypointensities Periventricular >juxtacortical ↑perivascular spaces CEL - Widespread in WM Different patterns: nodular, punctate, ring or open-ring	Increase extracellular space due to oedema tissue loss Perivascular collagenosis and inflammatory cuffs within these enlarged spaces Macrophage/microglia, lymphocytic infiltrates BBB disruption	**Lacunae**- hypointense areas >2 mm and <15 mm in the perforating arteries territory more in putamen and pallidum, followed by the pons (central), thalamus, caudate nucleus, internal capsule and corona radiate (usually at the edge of WMH) Arteriosclerosis cSVD - Along the lenticulostriate arteries entering the basal ganglia through the anterior perforated substance; CAA SVD – pial and superficial perforating arteries Enhancement may be seen in the context of acute stroke	Irregular cavitations with scattered fat-laden macrophages, reactive gliosis and myelin loss ↑perivascular spaces Perivascular collagenosis Acute ischaemic changes – red hypoxic neurons, inflammatory infiltrate
SWI	Diffuse hyposignal Basal Ganglia Cortex	Perivascular iron deposition Iron in activated macrophages/microglia at the edges of WML Iron precipitation in microbleeds	**Microbleeds** -small rounded 2-10mm hypointensities not well visualized on T2. Arteriosclerosis cSVD - Deep WM, basal ganglia and brainstem in arteriosclerosis-related cSVD Cerebral Amyloid SVD – cortex, convexity/sulcus hypointensitiees	Microscopic bleeds, small lacunae , hemosiderin containing macrophages in PVS Microscopic and macroscopic bleeds; β- amyloid vessel wall deposition

! Differentiating features between MS and cSVD, WMH- WM Hyperintensities, WML – WM lesions, FLAIR – fluid attenuated inversion recovery, SWI – susceptibility weighted imaging, CEL – contrast enhancing lesions, MAG –myelin associated glycoprotein

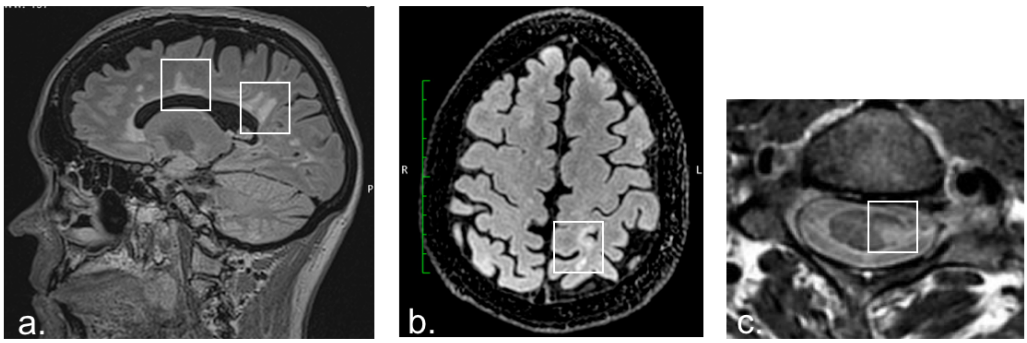

Figure 1.3. Typical imaging features of MS with conventional MRI

a. So-called Dawson fingers (boxes), visible as ovoid, hyperintense, periventricular lesions perpendicular to the body of the lateral ventricle and/or to the callosal junction, shown in a sagittal fluid-attenuated inversion recovery (FLAIR) image. **b.** An S-shaped juxtacortical lesion (box) in an axial FLAIR image, **c.** Eccentric short spinal cord lesion (box) that are typical of MS, shown in an axial T2-weighted image. (Geraldes *et al.*, 2018)

1.4. Age- VRF- related cSVD

1.4.1. The aging brain

Brain volume and myelin loss occur during "normal aging" (Taki *et al.*, 2013). At a cellular level there are several changes, such as microglia hyperactivity, cellular senescence, stem cell exhaustion, altered intercellular communication, genomic instability, mitochondrial dysfunction and free radical generation, loss of proteostatis and dysregulated nutrient sensing (Chen *et al.*, 2010; Pfefferbaum *et al.*, 2012; López-Otín *et al.*, 2013; Jiang and Cadenas, 2014). These changes also affect the cerebral vessels particularly arterioles and also veins (Kalaria, 1996; Farkas *et al.*, 2006, Brown and Thore, 2011*b*; Wu and Roks, 2014). Cerebral vasoreactivity is impaired in aged brains and changes in the nitric oxide pathways (Lourenço *et al.*, 2015), reduction of

endothelin-A and beta-adrenergic receptors have been reported (Schutzer *et al.*). This age-related degeneration of brain vessels may impair local perfusion (Iadecola, 2013). With aging, there is increased BBB permeability and BBB-pericyte injury (Farrall and Wardlaw, 2009; Oakley and Tharakan, 2014; Montagne *et al.*, 2015). Other neuronal signalling changes, serotonin, acetylcholine and other vasoactive neurotransmitters may also affect cerebral blood flow control (Drake and Iadecola, 2007). All these factors may predispose to ischaemic/hypoxic injury. Structural age-related microvascular changes have been summarized in **Table 1.1**.

1.4.2. Cardiovascular disease and VRF

Cardiovascular disease is the leading cause of global deaths and disability-adjusted life years. Over 95% of all vascular deaths are attributable to ischaemic heart disease, stroke, hypertensive heart disease, cardiomyopathy, rheumatic heart disease and atrial fibrillation (Joseph *et al.*, 2017). The risk of developing symptomatic cardiovascular disease can be predicted using various prediction models. Vascular disease risk is primarily driven by age (Groenewegen *et al.*, 2016) but modifiable risk factors such as dyslipidaemia (i.e. high blood levels of cholesterol and/or triglycerides), smoking, obesity, arterial hypertension, physical inactivity and diabetes mellitus are important contributors (Joseph *et al.*, 2017). Young males also have a higher risk of cardiovascular events than young females (Spence and Pilote, 2015), suggesting that inherent sex differences may influence the development of vascular disease.

Atherosclerosis, defined by the formation and growth of plaques within the arterial wall with concurrent loss of vascular elasticity, and subsequent blood flow reduction

through the affected vessel, is the main underlying mechanism that leads to symptomatic vascular disease. Despite being closely linked to the above mentioned modifiable VRF, atherosclerosis is a chronic, inflammatory, progressive disease that begins at young ages (Webber *et al.*, 2012) and that steeply increases with age. The atheroma plaques tend to occur at artery bifurcations, where shear stress promotes endothelial lesions, and to affect the aorta and coronary arteries earlier in life, and the cervical and intracranial arteries later on (Roberts *et al.*, 1959; Qiu and Fratiglioni, 2015).

It appears that atherosclerotic progression is the result of both the accumulation of signals and processes that exacerbate inflammation within the vessel wall, and a loss of repair mechanisms, as a consequence of aging and VRF (Head *et al.*, 2017). The initial stages of atheromatous disease involve an inflammatory insult to the endothelial cells lining the arterial lumen. Injured endothelial cells express adhesion molecules that enable migration of monocytes into the vessel intima, which then differentiate into macrophages and "begin to engulf lipid and lipid products forming foam cells" (Head *et al.*, 2017), which will form a fatty streak. Inefficient clearance of these fat laden macrophages leads to a growing lipid-rich necrotic core, followed by smooth muscle cell migration to the intima to form a fibrous cap. Rupture of this cap leads to thrombus formation and subsequent cardiovascular events (Head *et al.*, 2017). VRF can enhance atheroma formation by different mechanisms. For example, smoking induces vascular dysfunction that is initiated by reduced nitric oxide bioavailability and further by the expression of adhesion molecules and subsequent endothelial dysfunction. Moreover smoking induces the adherence of platelets and

macrophages and promotes the development of a procoagulant and inflammatory environment (Messner and Bernhard, 2014).

Although hyperlipidaemia is a key driver of atherosclerosis, growing evidence indicates that soluble and cellular and immune factors associated with chronic inflammation can promote atherogenesis independent of hyperlipidaemia (Angelovich *et al.*, 2015). This is supported by the increased risk of atherosclerosis in a number of inflammatory conditions, such as sepsis, systemic lupus erythematosus (SLE) (Wu *et al.*, 2016) and rheumatoid arthritis (RA) (Giles, 2015), which is independent of traditional cardiovascular risk factors including lipid levels (Angelovich *et al.*, 2015).

1.4.3. cSVD overview

1.4.3.1. Classification, risk factors and clinical features

The term cSVD encompasses all the pathological processes that affect the small vessels of the brain (<300 μm diameter), including small arteries and arterioles but also capillaries and veins. An aetiological classification of these diseases has been suggested (Pantoni, 2010) and includes the following 6 cSVD types: type 1 or arteriolosclerosis (age-related and VRF-related cSVD), type 2 or sporadic and hereditary cerebral amyloid angiopathy (CAA), type 3 or inherited or genetic cSVD distinct from CAA, type 4 or inflammatory and immunologically mediated cSVD, type 5 or venous collagenosis and type 6 including other cSVD.

Type 1, also generally named sporadic cSVD, is the most common form of cSVD (Wardlaw *et al.*, 2013*a*), followed by sporadic CAA which is also strongly linked with aging (Haglund and Englund, 2002; Love *et al.*, 2014; Esiri *et al.*, 2015), the other types, in particular the inherited SVD are rare. This thesis will focus primarily on type 1 cSVD.

VRF such as hypertension, diabetes, smoking, hyperlipidaemia and obesity, associate with an increased risk of type 1 cSVD even in younger populations (Von Sarnowski *et al.*, 2013). The relationship between cSVD and large artery atheroma is still unclear, some studies reporting an association between the two (Xu, 2014; Song *et al.*, 2016) but others suggesting they are two independent processes (Wardlaw *et al.*, 2014).

Clinical manifestations of this type of cSVD are varied. cSVD accounts for one fourth of all causes of stroke, is a major cause of cognitive decline and dementia and has been linked to urinary and walking dysfunction (Baezner *et al.*, 2008; Poggesi *et al.*, 2008;

Chen *et al.*, 2010; Smallwood *et al.*, 2012; Liu, 2014; Caplan, 2015; Qiu and Fratiglioni, 2015; Staals *et al.*, 2015).

1.4.3.2. Classical features of MRI cSVD and its pathological correlates

Morphological vascular changes in the age-related cSVD are summarized in **Table 1.1.** (Deramecourt *et al.*, 2012; Smallwood *et al.*, 2012; Iadecola, 2013) and illustrated in **Figure 1.2.** Of the microvasculature, arterioles are particularly affected with vessel wall thickening and tortuosity. Type 1 cSVD predominantly affects the perforating arterioles that feed the basal ganglia, deep WM and pons. Although sporadic CAA principally affects cortical arterioles, the underlying subcortical WM may be affected and show signs of damage because these arterioles supply blood to this area. Thickening of small cerebral veins, type 5 SVD, has been an increasingly recognised pathology also associated with aging (Moody *et al.*, 1995; Brown *et al.*, 2002; Keith *et al.*, 2017).

Small vessels with a diameter <500 μm, cannot be studied in vivo, and signs of parenchymal damage, such as WML, lacunae (Duering *et al.*, 2013, Wardlaw *et al.*, 2013*a*; Caplan, 2015), enlarged perivascular spaces (Farrall and Wardlaw, 2009, Wardlaw *et al.*, 2013*a*; Loos *et al.*, 2015; Charidimou *et al.*, 2017; Brown *et al.*, 2018) and microbleeds (Cordonnier *et al.*, 2007; Gouw *et al.*, 2011; Janaway *et al.*, 2014) are used as cSVD surrogate markers on MRI. A summary of these key cSVD imaging features and its pathology correlates is depicted in **Table 1.2.** Of note, most imaging studies have looked at the prevalence of cSVD in older adults (above the age of 50 years) and studies that included younger adults will be highlighted below. The frequency of each of type 1 cSVD pathologies (i.e. arteriolosclerosis) in healthy or VRF

only young adults (below the age of 50) is unclear since cSVD *post mortem* studies have focused on older cohorts.

cSVD-related WML, seen as WM hyperintensities on FLAIR/T2 brain MRI without prominent hypointensities on T1 images (Fazekas *et al.*, 1998; Fernando *et al.*, 2006; Gouw *et al.*, 2011) are also called leukoaraiosis. Leukoaraiosis occurs in 5-10% of people aged 20-40 years (Charil *et al.*, 2006; Thorn *et al.*, 2019) and in up to one third of people aged 65-84 years (Breteler *et al.*, 1994). While very commonly found in the periventricular area, WML distribution patterns seem to differ according to the different risk factors; periventricular lesions are seen more in males and smokers whereas the deep WM is more commonly affected in hypertensives (Rostrup *et al.*, 2012). At a microscopic level, loss of myelin components, in particular a selective loss of MAG and relative preservation of PLP, is a feature of cSVD WM abnormalities (Fazekas *et al.*, 1993; Fernando *et al.*, 2006; Gouw *et al.*, 2008; Barker *et al.*, 2013). Lacunae are defined as small (3-15 mm diameter) round or ovoid subcortical infarcts in the territory of one perforating arteriole with an MRI signal similar to the CSF (hypointense in T1 and hyperintense on T2). The prevalence of lacunae also increases with age, occurring in up to 8% of 55 to 59 year-old healthy adults, raising to 23% in the 65 to 72 year-old group (Bryan *et al.*, 1999). Lacunae are increased in young adults with type 1 diabetes (4 out of 191, 2.1 %), compared with age matched controls (0 out of 30, 0%) (Thorn *et al.*, 2019). Cerebral microbleeds detected with SWI reflect hemosiderin deposits in/around the vessel walls and are a marker of vasculopathy that is more commonly due to CAA (in which microbleeds have a primarily lobar distribution (Rosand *et al.*, 2005)) or simple arteriolosclerosis (in which they are primary in the deep grey matter and WM (Lee *et al.*, 2004)). In 8 595 stroke-free individuals (mean age 66.7± 5.6 years) from a Western population, 624 (7.3%) had

microbleeds (Yakushiji *et al.*, 2019). This cSVD marker was present in around 8% of healthy American adults younger than 55 years (Daugherty and Raz, 2017) but higher percentages can be seen in young adults with VRF such as hypertension (Ni *et al.*, 2018), diabetes (Thorn *et al.*, 2019) and smoking (Kim *et al.*, 2012).

Presence of VRF and cSVD imaging markers also associate with generalized and focal brain atrophy (den Heijer *et al.*, 2005; Nitkunan *et al.*, 2011; Beauchet *et al.*, 2013; Launer *et al.*, 2015; Moulton *et al.*, 2015; Tuladhar *et al.*, 2015) and reduced perfusion in the NAWM (Thomas *et al.*, 2015).

1.5. Differentiating MS from cSVD with MRI

Although direct comparison between MS and cSVD has rarely been performed (Schmidt *et al.*, 2006; Theocharakis *et al.*, 2009), the location and shape of WML as well as their signal behaviour on different sequences, seem to be useful in differentiating the two disorders (Aliaga *et al.*, 2014; Chen *et al.*, 2016; Filippi *et al.*, 2016; Okuda *et al.*, 2017). Lesions in the optic nerve, juxtacortical areas, periphery of the brainstem and posterolateral cervical spinal cord indicate MS rather than cSVD, as do lesions that are irregular in shape or appear as Dawson fingers (**Figure 1.3.a.**) WML in cSVD spare the U-fibres, affect the central pons and are associated with lacunae and microbleeds.

Microbleeds reported in patients with MS might have been due to concomitant vascular disease (Zivadinov *et al.*, 2016) as they were not observed when patients with vascular disease were excluded (Eisele *et al.*, 2016). Although

only 2 studies quantified microbleeds in MS, it is generally accepted that the presence of this imaging marker indicates cSVD.

Optimized SWI protocols can detect the central vein sign in around 80% of MS lesions at 3T, but this is present in a smaller proportion of cSVD WML: a cut-off of 45% is highly predictive in distinguishing between the two conditions (Mistry *et al.*, 2016; Samaraweera *et al.*, 2017). However, visualizing all lesions is not practical in the clinical setting, and this cut-off maybe less accurate in older patients with MS and vascular comorbidities (Sati *et al.*, 2016).

Cortical lesions may be a useful discriminator between MS and other conditions (Calabrese *et al.*, 2012*b*, *a*). However, it is still not clear if they can be easily distinguished from cortical microinfarcts, especially in older MS and/or patients with VRF (van Dalen *et al.*, 2015; Hilal *et al.*, 2016).

It is accepted that spinal cord lesions do not occur with aging (Thorpe *et al.*, 1993) or sporadic cSVD (Lycklama à Nijeholt *et al.*, 2000; Bot *et al.*, 2002) and thus, in the appropriate context, indicate MS.

Few, small sample studies have used non-conventional imaging techniques to compared MS with cSVD (Reidel *et al.*, 2003; Kapeller *et al.*, 2005; Öztoprak *et al.*, 2014), but their usefulness in clinical practice has not been established.

1.6. MS and vascular disease: evidence for a possible interaction

In the previous sections clinical, imaging and pathological features of both MS and cSVD that may be useful in distinguishing the two disorders were described. Features that are difficult to tear apart and/or exist in both disorders, such as DAWM, brain volume loss and perivascular space dilation, were also identified.

This thesis aims to explore a possible interaction between MS and vascular disease. It is possible that MS *per se* leads to worse vascular disease but also that VRF and vascular disease associate with worse MS outcomes. The theoretical rationale and the evidence that supports each of these possible relationships will be highlighted below.

1.6.1. MS associates with worse vascular disease

1.6.1.1. Rationale

The chronic inflammatory milieu seen in MS may directly lead to microvasculature and NVU damage leading to abnormalities in the fibrinolytic pathways (East *et al.*, 2005; Bardehle *et al.*, 2015), impairing angiogenesis (Lengfeld *et al.*, 2014) and vascular repair.

Also, as mentioned above, inflammation is a major driver of atherosclerosis and an increased risk of cardiovascular disease and accelerated atherosclerosis is observed in other inflammatory conditions (Angelovich *et al.*, 2015; Head *et al.*,

2017; Santovito and Weber, 2017). The relationship between inflammation and cSVD has not been sufficiently explored but the following data suggest that it deserves more attention: 1) systemic inflammation is associated with cSVD (Miwa *et al.*, 2016); 2) genes associated with inflammatory pathways are upregulated in cSVD brains (Ritz *et al.*, 2015); and 3) prominent inflammatory infiltrates are found in some CAA subtypes (Auriel *et al.*, 2016). In MS, perivascular inflammation may increase cerebral vessel vulnerability to VRF-related damage, thus contributing to increase of cSVD.

Another argument to suggest that MS may associate with a higher burden of vascular disease is that some environmental factors that predispose to atherosclerosis may be more prevalent in MS. Among these factors smoking (Messner and Bernhard, 2014; Belbasis *et al.*, 2015), obesity (Van Gaal *et al.*, 2006, Hedström *et al.*, 2014*b*; Marck *et al.*, 2016) and sodium intake (Staessen *et al.*, 2003; Farez *et al.*, 2015) are of particular relevance since they associate with both disorders. Vitamin D deficiency has also been linked to increased cardiovascular disease risk (Brewer *et al.*, 2011), though the causality of this association still warrants further investigation (Papandreou and Hamid, 2015). More importantly , MS patients are at higher risk of immobility and frailty (Lauretani *et al.*, 2017; Hanlon *et al.*, 2018) and thus, potentially, of vascular disease.

1.6.1.2. 'MS vascular theory' and evidence of microcirculation changes in MS

Early pathology studies traced MS lesions to draining CNS veins and capillaries, surrounded by perivascular inflammatory cell infiltrates (Rindfleisch, 1863; Dawson, 1916; Putman and Adler, 1937; Rae-grant *et al.*, 2014). Dynamic changes of microvessel wall components have been recently described in MS and seem to relate to disease duration and inflammation (Iacobaeus *et al.*, 2017). Structural microvasculature changes reported in MS are summarized in **Table 1.1.** and include thickening of vessel walls, and sometimes vessel thrombosis (Putman and Adler, 1937; Adams, 1988; Gay and Esiri, 1991; Wakefield *et al.*, 1994; Beggs, 2013; Iacobaeus *et al.*, 2017). The latter findings led to disappointing trials using anticoagulants (Putman and Chiavacci, 1947) and hyperbaric oxygen (Bennett and Heard, 2010) as a treatment for the disease, that were followed by reduced interest in the role of vessels in MS pathology. During the last decade, the hypothesis of venous insufficiency in MS patients was raised, given the claim that venous blood flow alterations were more prevalent in MS patients, however this observation was not replicated in larger, more controlled studies (Zamboni *et al.*, 2008; Kugler *et al.*, 2015). The "central vein sign" demonstrated *in vivo* on SWI (Sati *et al.*, 2016) further supports post-mortem observations that WML often occur around veins. However, it is somehow surprising that the arterioles remain intact in longstanding MS and the current published literature does not rule out that structural or functional arteriole changes play a role in MS pathology.

In MS, enlargement of the perivascular spaces, particularly at the brain convexity, associates with brain atrophy (Kilsdonk *et al.*, 2015) and with perivascular protein

changes (Gay and Esiri, 1991; van Horssen *et al.*, 2005; Mohan *et al.*, 2010), further pointing to a possible relationship between vascular pathology and MS severity. Structural abnormalities of perivascular spaces adjacent to venules have been mentioned above, but it is not clear if spaces around pial and penetrating arterioles are spared in MS. Meningeal inflammation spreads into convexity perivascular spaces (Howell *et al.*, 2011), but whether this only occurs around veins or also is observed around arterioles is not specified. The temporal profile of these vascular and perivascular changes in MS in the context of age-related vascular changes requires further study. Even if not directly related to MS, arteriole changes are predictable as part of aging and increased VRF. However, cSVD has not been systematically quantified so far in MS.

1.6.1.3. Hemodynamic changes in MS

Several studies have found that patients with MS have reduced cerebral perfusion (Rashid *et al.*, 2004; D'haeseleer *et al.*, 2011, 2015). Cerebral blood flow is reduced in non-enhancing WML (Sowa *et al.*, 2015) and in the cortical and subcortical grey matter associating with higher disability scores and T2 lesion load (Paling *et al.*, 2014; Lapointe *et al.*, 2018). Chronic MS plaques are more prevalent in WM regions with lower relative perfusion (Holland *et al.*, 2012) and hypoperfusion associated with T1 hypointensities (Narayana *et al.*, 2014). The observed hypoperfusion in MS appears to be a primary phenomenon and not merely a consequence of neuronal death (Saindane *et al.*, 2007), taking into account the fact that reduced cortical and deep grey matter cerebral blood flow is present in all disease course subtypes (Elsankari *et al.*, 2013) even in the absence of corresponding volume loss (Debernard *et al.*, 2014; Paling *et al.*, 2014). However, large, longitudinal studies

are still needed to confirm that hypoperfusion precedes neurodegeneration. Reduced cerebrovascular reactivity has also been reported in MS and impaired dilator capacity of cerebral arterioles to vasomotor stimulation has been proposed as a possible contributor to MS hemodynamic changes(Marshall *et al.*, 2014).

1.6.1.4. Hypoxia in MS

MS inflammation and associated NVU dysfunction (Alexander *et al.*, 2011) may lead to tissue hypoxia (Lassmann, 2003; D'haeseleer *et al.*, 2015). In the animal model, EAE, acute tissue hypoxia develops rapidly in response to inflammation, triggers enlargement of vessel lumen and increases vessel number, and is related to the neurological deficits (Davies *et al.*, 2013). Reducing tissue hypoxia may be an underestimated therapeutic target since it may reduce demyelination in animal models (Desai *et al.*, 2016).

There has been an increased interest in the relationship between angiogenesis and MS (Girolamo *et al.*, 2014; Lengfeld *et al.*, 2014; Salvetti *et al.*, 2015) but few studies have investigated the relationship between tissue hypoxia and structural microvasculature abnormalities in MS (Davies *et al.*, 2013). MS WML and classic ischaemic WM disease share some histopathological changes (Lassmann, 2003; De Keyser *et al.*, 2008). Using vascular distance maps, larger MS lesions tend to be further from vessels (Kozinska *et al.*, 2004) and it has been shown that MS lesions tend to accumulate not only in areas of high venule density but also in watershed areas (Haider *et al.*, 2016) where hypoxia due to low arterial perfusion may amplify hypoxia and mitochondrial dysfunction (Mahad *et al.*, 2009). It is not clear how these changes relate to the microvasculature, in particular the contribution of the

arterioles or of downstream players, such as capillary pericytes and surrounding astrocytes (De Keyser *et al.*, 2008; Hall *et al.*, 2014) in hypoxia development is not known.

1.6.1.5. Prevalence of VRF and cardiovascular disease in MS

Studies have shown that MS patients have a greater prevalence of VRF, such as smoking and increased BMI, compared to the general population while other VRF, such as hypertension, diabetes and hyperlipidaemia do not differ significantly between groups (Marrie *et al.*, 2015).

MS patients have reduced life expectancy that is estimated to be between 7-14 years compared to individuals without the disease (Scalfari *et al.*, 2014). Though increased mortality can be directly related to MS, cardiovascular diseases are also important contributors (Goodin *et al.*, 2014). MS is associated with an increased rate of myocardial infarction (Marrie *et al.*, 2019), and possibly of heart failure and ischaemic stroke, particularly in the first years after diagnosis (Christiansen *et al.*, 2010; Christiansen, 2012). The reported increased cardiovascular disease soon after MS diagnosis might be due to surveillance bias and later in the disease course may relate to venous disorders in progressive MS (Ahmed *et al.*, 2019), suggesting that immobilization may be a predisposing factor (Roshanisefat *et al.*, 2014). The heterogeneity among studies on the incidence and prevalence of cardiovascular disorders in MS makes it difficult to fully understand the epidemiology of vascular comorbidity in MS (Marrie *et al.*, 2014). There is scarce information on global atherosclerosis burden in MS patients assessed clinically or with vascular imaging, though an increase of subclinical markers of atherosclerosis has been reported in

a small group of MS patients particularly in those with reduced physical activity (Ranadive *et al.*, 2012).

1.6.1.6. cSVD imaging and pathology correlates in MS

After an extensive search for publications assessing cSVD imaging markers in MS, only two MRI studies looking at the prevalence of microbleeds were found and have shown conflicting results (Eisele *et al.*, 2016; Zivadinov *et al.*, 2016), as described in section 1.5. An imaging-pathological study aiming to track iron in 2 MS brains showed iron precipitation in aggregates typical of microbleeds. Indeed, both cases were older than 60 and one had significant VRF and evidence of severe atherosclerosis at autopsy (Bagnato *et al.*, 2011). An older pathology study also reported perivenular hemosiderin deposition related to MS plaques in 21 out of 70 MS cases, of which 4 had coexistent cardiovascular disease (Adams, 1988). Studies quantifying periarteriolar iron and/or assessing the relationship between iron deposition and the presence of cSVD in MS were not found in the searched literature. In longstanding MS, basal ganglia T1 hypointensities along with diffuse WM changes have been reported but no information regarding vascular comorbidities was provided (Renard *et al.*, 2010). Since no imaging-pathological correlation had been performed, the findings could be related to MS and/or cSVD pathology.

In summary, there is evidence of microvasculature and hemodynamic changes in MS to suggest that the arteriole may play an important role in MS pathology. However, it is unclear if there are arteriolar and periarteriolar structural changes in MS. Epidemiological studies suggest that MS associates with a higher burden of

vascular comorbidities but atherosclerosis burden has not been objectively assessed in MS. Finally, it is unknown if the burden of cSVD pathology or imaging surrogate markers are increased in MS compared with non-MS.

1.6.2. VRF and vascular comorbidities lead to worse MS outcomes

1.6.2.1. Rationale

The presence of VRF associates with increased disability (e.g. gait impairment) and mortality in people without MS (Shi and Wardlaw, 2016). Their effect on MS outcomes could be merely an additive effect of non-MS pathology or they may directly impact MS pathology. In favour of the latter hypothesis would be shared risk factors, such as smoking, that may have an inherent effect on MS lesion development. Also, the presence of systemic and cerebral vascular disease may promote an increase of MS lesion burden and inflammation. The exact relationship between cSVD and brain damage is incompletely understood (Pantoni, 2010, Wardlaw *et al.*, 2013*a*; Rosenberg *et al.*, 2016) but factors such as hypoperfusion/ischaemia due to reduced vessel lumen size, impairment of perivascular drainage, BBB dysfunction (Bridges *et al.*, 2014) and subclinical inflammation may lead to oligodendrocyte damage (Maki *et al.*, 2013) and loss of myelin causing WML and neuronal loss (Huang *et al.*, 2010; Pantoni, 2010; Hase *et al.*, 2018). NVU dysfunction leading to neuronal-vascular uncoupling, has been implicated in perpetuating tissue damage in ischaemia (Zlokovic, 2011; Hall *et al.*, 2014). The presence of cSVD in MS patients may represent the extra hit that hinders compensatory mechanisms. In this case, neurovascular-uncoupling and hypoperfusion with consequent chronic hypoxia and tissue damage could exacerbate MS related demyelination (**Figure 1.2 B**)

1.6.2.2. The effect of VRF and vascular comorbidities on MS clinical, MRI and pathological outcomes

The presence of any vascular comorbidity (diabetes, hypertension, hypercholesterolemia, heart disease, and peripheral vascular disease) associated with increased risk of more severe MS-related disability (Tettey *et al.*, 2014; Dagan *et al.*, 2016; Marrie, 2017; Zhang *et al.*, 2018). Tobacco smoking has also been associated with increased and faster progression of clinical disability in MS (Healy *et al.*, 2009; Shirani and Tremlett, 2010; Heydarpour *et al.*, 2018). The underlying substrate for the poor clinical outcomes seen in MS with vascular comorbidities has not been explored so far.

Few MS imaging studies have taken into account the effect of VRF on lesion distribution and size and brain atrophy (**Table 1.3.**) (Healy *et al.*, 2009; Zivadinov *et al.*, 2009; Weinstock-Guttman *et al.*, 2011; Kappus *et al.*, 2015; Pichler *et al.*, 2019). American MS patients with one or more VRF have shown an increased lesion burden and more brain atrophy compared to MS patients without VRF (Kappus *et al.*, 2015). Smoking alone has been associated with an increased burden of contrast enhancing lesions indicating a direct impact on MS pathology and not only a mere increase in cSVD related WML. However, for the other VRF and vascular comorbidities it is not clear whether the increase in WML load relates with an increase of "MS-like" lesions or "vascular-like" lesions.

Table 1.3. Brain MRI studies on the impact of VRF on MS brain lesions

Author. year	Study information	Number of clinical definite MS patients/controls	Vascular Risk factor	MRI outcomes	Main MRI findings
Healy BC et al. 2009	Single centre, cross sectional survey and longitudinal follow up (3.2 years)	1045 (first MRI)/0	Tobacco Smoking	Whole brain volume T2 LV BPF	Current smokers had a lower BPF compared with never-smokers. T2 LV was higher in current smokers than in never smokers. No differences between Ex-smokers and never smokers.
Zivadinov R. (2009)	Single centre cross-sectional	368/0	Tobacco Smoking	T1 LV T2 LV CEL number and volume BPF	Ever Smokers with higher number of CEL, T1 and T2 LV when compared with non-smokers Lower BPF in smokers
Weinstock-Guttman B (2011)	Single centre, retrospective, cohort	210/0	Fasting lipid profile (HDL, LDL, triglycerides, total cholesterol, cholesterol/HDL ratio) BMI	CEL T2 LV T1 LV BPF	Higher HDL associated with a low CEL LV Higher triglyceride levels associated to higher CEL LV No associations with T2-LV and T1-LV with any of the lipid profile variables
Farez M et al.	Single centre cohort (prospective)	First group – 70 Replication - 52	Sodium intake (low, medium, high)	T2 LV	Patients with higher sodium intake had a greater chance of developing a new T2 lesions and had increased T2 LV
Kappus et al. (2015)	Single centre cohort (prospective)	326 RRMS 163 SPMS /175 HC	HT, heart disease, smoking, overweigh/obesity, type 1 DM	T1 and T2 LV Normalised brain parenchyma volume, GM, WM and lateral ventricle volume	In MS patients HT and heart disease associated with decrease GM and cortical volumes Overweight/obesity associated with increased T1-LV and smoking with decrease whole brain volume.
Pichler A et al. 2019	Single centre cohort (prospective)	61 CIS 21 RRMS	HT, hyperlipidaemia, DM, smoking	T2 LV Normalised brain parenchyma volume, cortical GM, WM, thalamic and basal ganglia volumes Percentage of brain volume change	Patients with more than 1 VRF had a lower brain volume at baseline but had no increased brain volume loss at 3.5 years follow up. VRF had no effect on T2 LV

BPF - Brain parenchymal fraction; BMI – body mass index; LV – lesion volume; CEL – contrast enhancing lesions, GM – grey matter, White Matter – WM, HT – hypertension, DM- diabetes mellitus, HC -healthy controls

To date, no pathology study has looked at the effect of systemic or cerebral vascular disease on MS pathological outcomes.

In summary, although VRF and vascular comorbidities associate with worse clinical and imaging outcomes in MS, it is not clear if this relates to a higher burden of MS lesions.

Taking in to account the above summarized gaps in the literature my main research questions are:

1. Does MS associate with worse systemic and cerebrovascular disease?
2. Does the presence of VRF/vascular disease associate with a higher burden of MS lesions?

1.7. Thesis Overview

1.7.1. Research hypotheses

This thesis aims to improve the understanding of the relationship between vascular disease and MS. My overarching hypotheses are:

1. MS associates with a higher burden of systemic and cerebral vascular disease compared with non-MS.
2. VRF/vascular disease associates with a higher burden of MS lesions

To test these hypotheses, a *post mortem* and an *in vivo* study were designed. In the first, the effect of MS diagnosis on objective measures of systemic and cerebro-vascular disease was assessed and the relationship between these measures and MS pathology outcomes was analysed. In the second, the effect of VRF on MS imaging markers and of MS on cSVD imaging outcomes was determined.

This thesis is presented as a series of 7 results chapters that each include the following sections: Introduction and Aims, Materials and Methods, Results, Summary of the main findings and Discussion.

Chapter 2: In this chapter it is hypothesised that MS associates with a higher burden of systemic vascular disease (SysVasc). A global measure of systemic atheroma and vascular related end-organ damage was obtained from autopsy reports and the extent of SysVasc was compared between MS (n=85) and age and sex-matched non-MS cases (n=68) (**Figure 1.4**).

Chapter 3: In this chapter it is hypothesised that MS influences the extent of cSVD. The extent and distribution of cSVD, using recently published definitions and concentrating on arteriolar pathology, was assessed in 4 brain regions in MS (n=42) and compared with age and sex-matched non-MS cases (n=39) (**Figure 1.4**).

Chapter 4: In this chapter it is hypothesised that MS associates with a characteristic small vessel vasculopathy, including not only small vein but also arteriole/periarteriolar inflammation and damage. Frequency and distribution of venous collagenosis and inflammation, as well as arteriolar/periarteriolar damage and inflammation were explored in MS (n=42) and compared with non-MS cases (n=39), in 4 brain regions (**Figure 1.4**).

Chapter 5: In this chapter it is hypothesised that SysVasc and cSVD impacts MS demyelination and plaque activity. The relationship between SysVasc and cSVD and plaque area, number and activity were assessed in the MS cohort (n=42) (**Figure 1.4**).

Chapter 6: In this chapter it is hypothesised that some imaging markers are specific for MS and others for cSVD. To test this hypothesis, MS and cSVD imaging markers were compared between a group of MS cases without VRF (N=93) and non-MS cases with VRF (N=43) (**Figure 1.5**).

Chapter 7: In this chapter it is hypothesised that VRF associate with a higher burden of MS imaging markers and influence WML distribution. The extent of visually quantified MS imaging markers was obtained from brain MRI and compared between MS without VRF (n=93), and age and sex-matched MS cases with VRF (N=108). Lesion probabilistic maps were compared between MS without VRF (N=33) and MS with VRF (N=43) (**Figure 1.5**).

Chapter 8: In this chapter it is hypothesised that MS influences the burden of MRI surrogate markers of cSVD and associates with a higher burden of WML in vascular locations. The burden of cSVD markers was assessed in MS with VRF (n=108) and non-MS cases with VRF (n=43) brain MRIs and WML probabilistic maps were compared in a subgroup of MS with VRF (N=43) and of non-MS with VRF (N=26) (**Figure 1.5**).

1.7.2. Study design

1.7.2.1. Post mortem study design and sample size considerations

From a larger study population where SysVasc was scored (Chapter 2) a smaller cohort was selected for brain histology (Chapters 3, 4 and 5) (**Figure 1.4.**). Both the collection of autopsy report data and brain tissue analysis were done in adherence to the ethical regulations from Oxford Brain Bank's NHS Research Ethics Service (REC approval reference number 15/SC/0639). Permission for data collection, where no explicit objection for research use, is given by the patient or next of kin in accordance with UK Human Tissue Act regulations.

There are no studies in the literature assessing the burden of SysVasc in MS. cSVD, has never been assessed post mortem MS brain tissue and most cSVD studies have looked at non-MS cases older than 50 years. Sample calculation for the comparison of cSVD between MS and non-MS cases took into account the confidence intervals (CI) of each of the individual cSVD pathologies included in the most recent consensus paper on cSVD scoring (Skrobot *et al.*, 2016). In this study 65 normal subjects were compared with 48 cognitive impaired cases and the odds ratio for global arteriolosclerosis was 3.82 (95%CI 1.32-11.09), for global periarteriolar space dilatation (PSD) 4.0 (95%CI 1.3-12.29) and for microinfarcts 6.63, (95%CI 1.34-32.8). The calculated sample size (using G*Power calculator version 3.1) for each of these cSVD features was 43, 38 and 8, respectively. I aimed to include a minimum of 38 MS and 38 non-MS cases in the *post-mortem* study, which is a considerable large sample, considering brain tissue availability. However, this sample size estimation is limited by the lack of data regarding the prevalence of cSVD pathologies in younger adults.

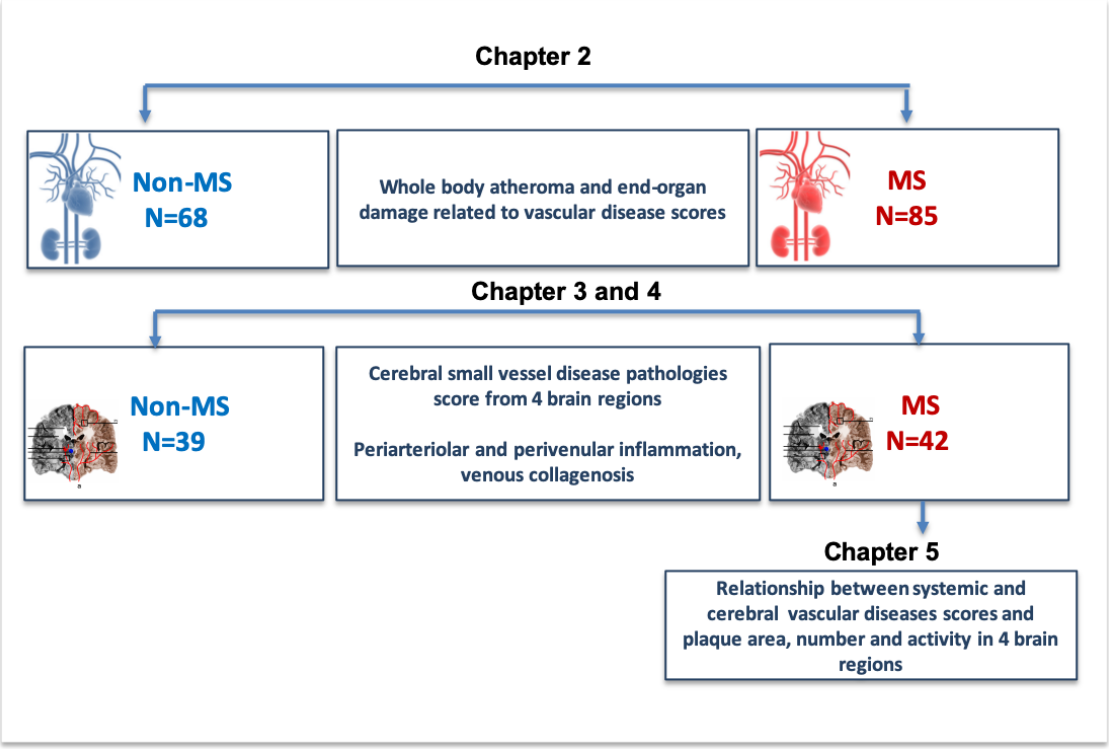

Figure 1.4. *Post mortem* study design

The *post mortem* study was designed to compare objective measures of SysVasc (Chapter 2) and cSVD (Chapter 3 and 4) between MS and age and sex-matched non-MS cases. The effect of both systemic and cerebral vascular disease on MS pathology outcomes was then assessed (Chapter 5).

Eighty-five MS cases were selected from a total of 111 MS cases and 68 out of 90 age and sex-matched non-MS cases, where autopsies were performed between 1971 and 2007 at the Neuropathology department, Oxford University Hospitals. The majority of autopsies were performed for medical interest, regarding patients followed at the Oxford University Hospitals, 3 (1 MS and 2 non-MS) for medico-legal purposes and 3 (1 MS and 2 non-MS) as part of the Oxford Project to Investigate Memory and Ageing (OPTIMA) study (Smallwood *et al.*, 2012). From these two initial groups brain tissue was analysed in 42 MS and 39 non-MS cases, after cases with no available tissue or with confounding central nervous system disorders were excluded.

1.7.2.2. In vivo brain imaging study design and sample size considerations

The imaging study was designed to test whether VRF make "MS-like" lesions worse or if MS associates with a higher burden of cSVD. To test the first hypothesis MS with no

VRF was compared with MS with VRF and to test the second MS with VRF was compared with non-MS with VRF, but first lesion specificity was assessed by comparing MS without VRF with non-MS with VRF (**Figure 1.5.**).

Sample size estimations were made taking into account a previous study on the effect of smoking on WML volumes (Zivadinov *et al.*, 2009). In this study WML volumes were compared between 240 never smokers (mean 13.5±2) and 128 ever smokers (mean 15.7±3). Using G*Power calculator version 3.1 a total of 60 (30 ever smokers + 30 never smokers) subjects were estimated to be needed for a power of 0.95. Recent papers testing a possible MS-specific marker (Samaraweera *et al.*, 2018), the central vein sign, have found significant differences between a group of 23 RRMS patients and 16 cSVD patients. For the purpose of visual scoring an estimated sample of 30 MS cases and 30 non-MS cases with VRF would be needed for a power of 0.95.

A multicentre retrospective observational case-control study was set up to obtain the study groups. Anonymised clinical and imaging data was obtained from 5 Magnetic Resonance Imaging in MS (MAGNIMS) consortium centres: Graz, London, Rome, Barcelona, Amsterdam (**Figure 1.6.**). Each centre was asked to contribute with triads of age- and sex-matched MS cases with and without VRF and with non-MS cases with VRF, to minimize bias related to scanner differences. All the MRI and clinical data sets were first collated, anonymised and stored at the contributing sites in accordance with the local research ethics regulations. The imaging and clinical data were collated centrally in Oxford, quality controlled and visually inspected by myself (RG).

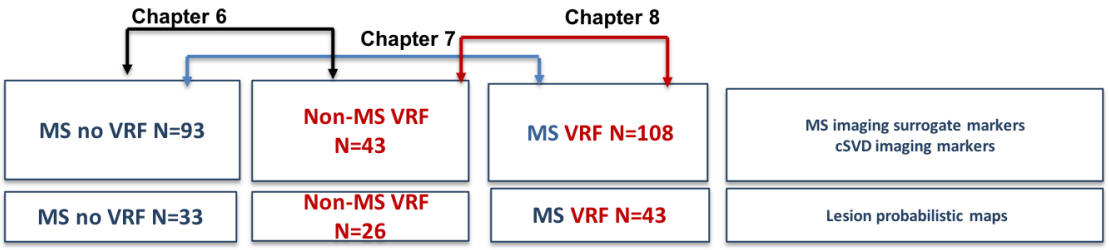

Figure 1.5. *In vivo* brain imaging study design

The *in vivo* brain imaging study was designed to test the influence of VRF on MS imaging surrogate markers, by comparing MS with and without VRF (Chapter 7) and the influence of MS on cSVD imaging surrogate markers by comparing MS with VRF and non-MS with VRF (Chapter 8). The specificity of both MS and cSVD imaging markers was initially assessed by comparing MS without VRF and non-MS with VRF (Chapter 6). WML distribution was available for comparison in a subset of cases.

Pairs of age and sex matched MS cases with and without VRF were obtained from 5 MAGNIMS centres (see Figure 1.6), all of which are tertiary centres (University Hospitals), with specialized Multiple Sclerosis clinics. The non-MS cases with VRF were part of two studies looking at brain lesions in diabetic patients and were obtained from two of the five participating MAGNIMS centres (see Figure 1.6).

a) Cohorts and Clinical data

All MS and non-MS cases were assessed by a neurologist and diagnosis confirmed. Male or females, age 35 or above MS without VRF, age- and sex matched MS with VRF and non-MS with VRF, with available MRI, were included. MS cases were diagnosed according to the 2010 McDonald criteria and exclusion criteria were presence of previous stroke or high risk for cardioembolic stroke (e.g. atrial fibrillation, valvular heart disease), history of any neurological disorder or known brain lesions unrelated to MS. The following demographic and clinical data were collected by each participating study centre, at the time of MRI: sex, age at the time of MRI scan, disease

duration and phenotype, Expanded Disability Status Scale (EDSS) and DMT. Presence of the following VRF (yes/no) was recorded: 1.arterial hypertension (ever) (Mancia *et al.*, 2007); 2. hypercholesterolemia (ever) (Catapano *et al.*, 2016); 3. diabetes mellitus according to WHO definitions (Sacks *et al.*, 2011) self-reported smoking status – positive of patients smoked more than 10 cigarettes a day for at least 6 months (Pichler *et al.*, 2019). Patients were considered to be in the VRF group when they had one or more of the above conditions.

Clinical Information and VRF profile for each of the cohorts per participating centre is summarized in (**Table 1.4**).

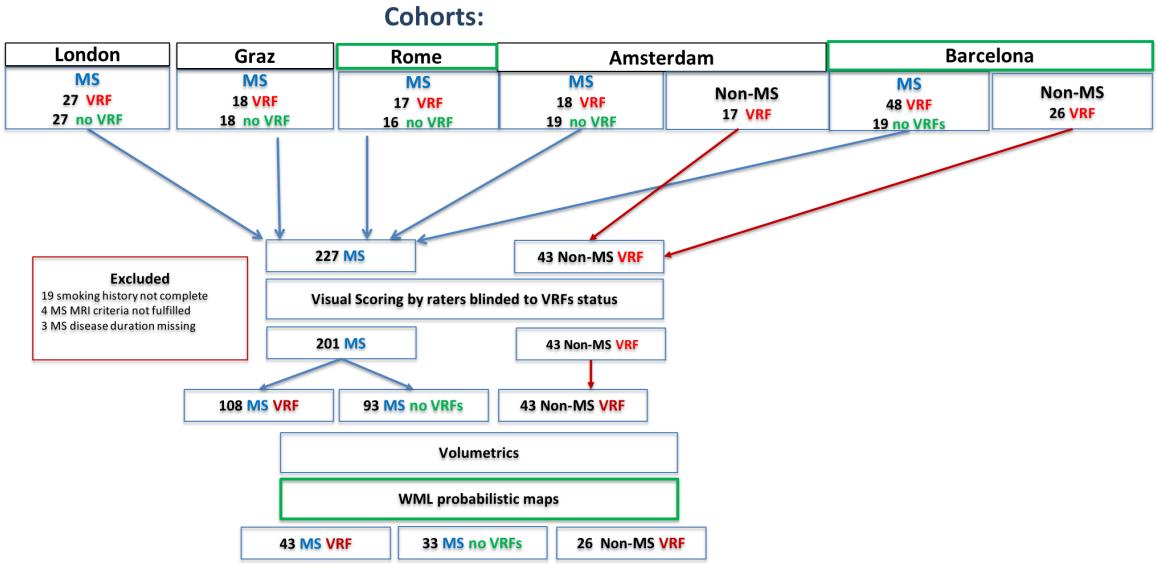

Figure 1.6. Cohorts included in the *in vivo* brain imaging study

227 MS and 60 non-MS cases were initially scored by a rater blinded to clinical information. Clinical data was later analysed separately and 4 cases were excluded since they did not fulfil dissemination in space MRI criteria and 22 cases with incomplete clinical information were also excluded. Lesion probabilistic analysis was performed only in a subset of cases from Barcelona and Rome (green boxes).

Table 1.4. Clinical features of all cohorts used for the *in vivo* Brain imaging study.

	MS					Non-MS	
	Graz (N=36)	London (N=54)	Amsterdam (N=35)	Rome (N=33)	Barcelona (N=43)	Amsterdam (N=17)	Barcelona (N=26)
Mean age (SD), years	42.3 (5.9)	51.0 (7.8)	56.7 (6.7)	43.5 (5.6)	45.2 (6.9)	43.2 (7.0)	68.5 (4.9)
% females (N)	50.0 (18)	70.4 (38)	51.4 (18)	75.8 (25)	62.8 (27)	58.8 (10)	65.4 (17)
Median disease duration (range), years	2.6 (0-26.1)	12.3 (0.5-47.8)	16.4 (8.8-34.8)	13.0 (3-26)	11.3 (0.4-31.3)	NA	NA
VRF % (N):							
Ex-smoker	NA	24.1 (13)	28.6 (10)	9.1 (3)	18.6 (8)	0	38.5 (10)
Smoker	13.9 (5)	22.2 (12)	20.0 (7)	30.3 (10)	39.5 (17)	17.6 (3)	19.2 (5)
HT	30.6 (11)	20.4 (11)	40 (14)	6.1 (2)	14.0 (6)	58.8 (10)	NA
DysL	16.7 (6)	9.3 (5)	2.9 (1)	18.2 (6)	16.3 (7)	64.7 (11)	NA
DM	0	1.9 (1)	14.3 (5)	6.1 (2)	4.7 (2)	100 (17)	100 (26)

SD – standard deviation, HT – arterial hypertension, DysL – dyslipidaemia, DM- diabetes, NA – not available/applicable

b) <u>Imaging sequences</u>

The following image sequences were requested from the different centres, obtained from 3 Tesla brain MRIs (**Table 1.5.**), with variable sequence protocol depending on the source of the data but established of high quality:

- Brain 3-dimensional (3D) high resolution isotropic T1- weighted image – this is the optimal protocol for measuring brain volume using SIENAX method, it is also used for lesion visual scoring in which case 2-dimentional (2D) scans were also considered if transversal sections available.
- Brain axial Fluid Attenuated Inversion Recovery (FLAIR) weighed images are standard protocols for WML visual scoring. For automatic WML volume and lesion probabilistic analysis 3D 1mmx1mmx1mm DICOMS were required as well as centre permission for image transfer for lesion segmentation with IcoBrain MS software and this was only given by Barcelona and Rome centres.

- T2*-weighed images (Gradient-Echo, GRE) are standard SWI protocols for microbleed scoring but not routinely done in MS. SWI was only available from 2 centres (Graz and Barcelona) and only a total of 34 pure MS cases, 46 MS with VRF and 26 non-MS with VRF were available.

Table 1.5. Brain MRI sequences and protocol from each participating centre

Site	**T1 and FLAIR**	
	MS	**Non-MS**
Graz Number cases Voxel size - FLAIR - T1 FLAIR TE, TR Lesion segment.	 **36** 0.86x0.86x3 mm 1x0.5x0.5 mm 69, 9000 No	NA
London Number cases Voxel size - FLAIR - T1 FLAIR TE, TR Lesion segment.	 **54** 1x1x3mm 1x1x3mm 25, 8000 No	NA
Amsterdam Number cases Voxel size - FLAIR - T1 FLAIR TE, TR Lesion segment.	 **34** 0.97x0.97x1 mm 0.94x0.94x1 mm 129.5, 8000 No	 **34** 1.3x1.3x1.3 1x1.1.mm 385, 6500 No
Rome Number cases Voxel size - FLAIR - T1 FLAIR TE, TR Lesion segment.	 **33** 0.48x0.48x3.3 1x1x1 mm MS 89, 9000 Yes	NA
Barcelona Number cases Voxel size - FLAIR - T1 FLAIR TE, TR Lesion segment.	 **43** 1x1x1 mm 1x1x1 mm 394, 5000 Yes	 **26** 1x1x3mm 1x1x1 mm 93, 9000 Yes

2 The influence of MS on systemic atherosclerosis and vascular end-organ damage

2.1.Introduction

Increased immobility and frailty (Lauretani *et al.*, 2017; Hanlon *et al.*, 2018), immune dysregulation or increased smoking exposure could potentially contribute to an increase of SysVasc in MS compared to matched non-MS.

SysVasc is an important cause of death in MS (Goodin *et al.*, 2014; Capkun *et al.*, 2015) and the prevalence of cardiovascular disease seems to exceed that of the general population (Marrie *et al.*, 2014; Marrie, 2017). However, it is difficult to ascertain, from the epidemiological studies, if MS patients have a higher burden of atherosclerosis. *Post mortem* studies, may provide unique objective measures of atheroma and vascular end-organ damage burden but no *post mortem* study has been set up, to date, to evaluate SysVasc burden in MS. The work described in Chapter 2 aims to fill in this literature gap and to answer the following research question:

- Is SysVasc burden increased in MS compared with age and sex-matched non-MS?

My working hypothesis is that MS cases will have a higher burden of SysVasc than non-MS cases. To test this hypothesis, my aims are to:

a. Devise a SysVasc score based on autopsy reports
b. Validate this SysVasc score and apply it to a cohort of pathologically confirmed MS and to non-MS cases
c. To compare SysVasc, as measured by the devised score, between MS and age and sex-matched non-MS cases

2.2. Material and Methods

2.2.1. Study population

A human autopsy cohort of pathologically confirmed MS and age- and sex-matched non-MS cases older than 35 years from the Oxford Brain Bank (1971-2007) were selected for study. Each case had post-mortem brain material and comprehensive brain and full body autopsy reports (including of the vascular system) available for analysis. The majority of autopsies were performed for medical interest, regarding patients followed at the Oxford University Hospitals, 3 (1 MS and 2 non-MS) for medico-legal purposes and 3 (1 MS and 2 non-MS) as part of the OPTIMA study (Smallwood *et al.*, 2012).

2.2.2. Assessment of Clinical data and SysVasc using autopsy reports

2.2.2.1. Demographic and clinical data

Age, sex, cause of death, year of death, main diagnosis (MS, non-MS), MS disease duration (from first symptom onset to death) and the identification of the pathologist who performed the autopsy were recorded. Cause of death was not known at the time of case selection and was assessed by two independent raters (myself, RG, and Prof Margaret Esiri, ME) and by a third rater (Prof Gabriele De Luca, GD), wherever there was disagreement. Death due to MS was considered when no other cause of death was documented and MS brain lesions were considered to be fatal (i.e. extensive brainstem lesions). Information regarding the presence of VRF (hypertension, dyslipidaemia, smoking, diabetes) and of immobility was collected, where available.

2.2.2.2. Construction of a SysVasc score from autopsy reports

The data collected in autopsy reports was reviewed and a standardised questionnaire that encompassed routinely collected SysVasc-related pathology elements was developed, as outlined in **Figure 2.1**. This questionnaire was then used, by two independent raters (ME, RG), to score the extent of atherosclerosis and end organ damage from autopsy reports, with disagreements in any of the data being adjudicated by a third, independent rater (GD). The extent of atheroma (in the aorta, coronary, cervical – carotids and vertebral - arteries), indicators of end-organ damage (including left ventricular hypertrophy (LVH), myocardial infarction (MI), macroscopic large vessel ischaemic stroke (IS), and renal hypertensive disease (RH)), and heart weight (in grams (g)) were assessed and recorded (as outlined below). The spectrum the atheroma severity was assessed based on commonly used descriptors outlined in **Figure 2.1.** legend and a semi-quantitative score was subsequently devised as follows: 0 – not present, 0.33 – "mild", 0.66 – "moderate", 1 – severe.

A semi-quantitative score (from 0 to 3) was used to assess the severity of intracranial (Circle of Willis) atherosclerosis/atheroma based on descriptions in the autopsy reports, as follows: 0=normal; 1=atheroma was present but no artery was more than 50% occluded; 2=if one vessel was 50% or more occluded; 3= if more than one vessel was 50% or more occluded (Esiri *et al.*, 1997).

LVH was scored by a composite of heart weight and documented evidence of left ventricular hyperplasia (Grajek *et al.*, 1993), as follows: 0 – < 400g and no hyperplasia present; 0.5 - < 400g and mild to moderate left ventricular hyperplasia present or LVH

not described but heart weight >400g; and 1– > 400g and mild to moderate LVH present or with severe LVH documented independent of heart weight.

Individual variables that were recorded in more than 80% of the reports and had a substantial or above inter-rater agreement (as outlined in section 2.2.4) were used. As a high correlation was expected between some of the individual variables (Aono *et al.*, 2015) and to minimize Type I errors (Song *et al.*, 2017), pre-determined SysVasc-related composite variables were defined as follows (**Figure 2.1**):

- **Atheroma Score** – average of individual atheroma variables from the different scored arteries
- **End organ Damage Score** – average of individual end organ damage variables (i.e. IS, MI)
- **SysVasc Score** – Average of Atheroma and End Organ Damage Scores

2.2.2.3. Testing the validity of the SysVasc score

To test if the obtained SysVasc score performed as expected, its relationship with age at death and vascular causes of death was investigated in the whole cohort. It was expected that the score increased with age at death and that cases that died of other causes of death had lower scores than cases that died with vascular deaths, not only MI and IS (which by the nature of the score would have higher values), but also cases of that died of other vascular causes of death such as pulmonary embolism, where immobility might not only contribute to this fatal outcome but also to an increase of atheroma and vascular end-organ damage.

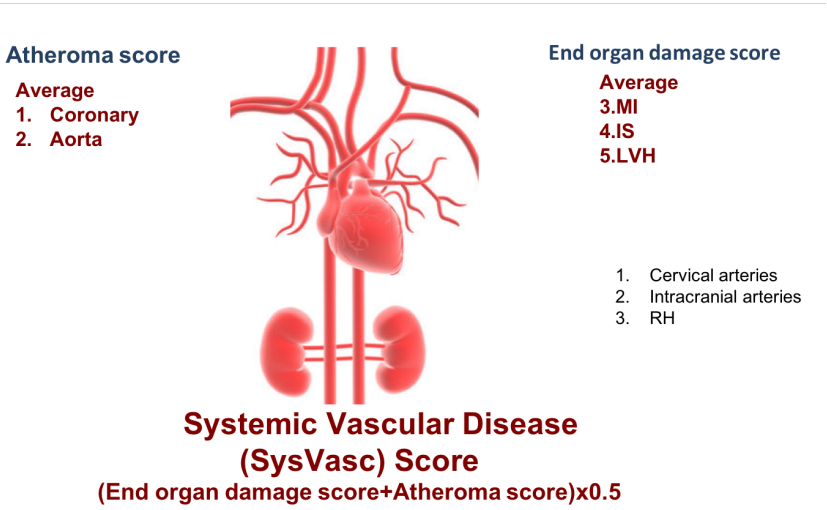

Figure 2.1. SysVasc score construction.

Routinely standardized autopsy reports were assessed and the spectrum of atheroma burden in the aorta, coronary, cervical and intracranial arteries was determined to later devise a semi-quantitative score, using the following commonly used descriptors: not present - ”normal ”, ”free of atheroma”; “mild” - “slight”, “expected atheroma for age, “fatty infiltration only”; “moderate – “luminal narrowing of 10-49%”, “non-significant stenosis”; severe – “ occlusion”, “significant narrowing”, “ulcerated plaque/thrombus”. Presence of MI, IS, RH, and severity of LVH (not present/mild to moderate/severe) were assessed as measures of vascular related end-organ damage. Since information on aorta and coronary atheroma, MI, IS and LVH, was consistently available and retrieved without significant variability these variables were included in the final scores. **Atheroma score** was obtained by averaging the aorta and coronary atheroma scores, and the **End Organ score** by averaging MI, IS and LVH. A final global **SysVasc score** was obtained by the average of the Atheroma and End Organ Scores.

2.2.3. Statistical analysis

Distribution of data was assessed analytically and graphically and transformed, as required. Three-way contingency tables, Chi-square or Fisher Exact tests, parametric and nonparametric tests were applied, as appropriate. Continuous data are presented as mean ± standard deviation (SD) where normally distributed and as median and interquartile range (IQR) or range where non-normally distributed. Categorical data are presented as counts or percentages, as relevant. Correlations between continuous

normally distributed pathological variables were assessed using Pearson's correlation coefficients (r), for non-normally distributed variables or categorical variables Spearman rank coefficients (r_s) and Kendall rank coefficients (r_τ) were used, respectively. Inter-rater agreement was measured by free marginal multi-rater kappa coefficient (Randolph, 2005) and interpreted as defined below (Landis and Koch, 1977): 0 – less than chance agreement, 0.01-0.2 – slight agreement, 0.21-0.4 – fair agreement, 0.41-0.6 – moderate agreement, 0.61-0.8 – substantial agreement, 0.81-0.99 – almost perfect agreement. Cronbach's Alpha was used to check the internal consistency of the pre-defined composite variables and if below 0.6 composite variables were not used for subsequent analysis.

Binary logistic regression was used to investigate if the SysVasc score associated with vascular deaths, adjusting for age at death. Regression plots and simple linear models (Model 1) and with interaction terms (Model 2) were used to determine the influence of MS on SysVasc and Atheroma scores while accounting for the relationship between age at death and these scores in MS and non-MS cases. Results are presented as regression coefficients (B) or their exponentials (EXP (B)) and respective 95% CI. To account for a possible bias of our comparator group towards SysVasc, a sensitivity analysis excluding death due to MI and/or IS was carried out and SysVasc Scores between MS and non-MS segregated by cause of death were compared. All tests of hypothesis were carried out using two-sided tests and p-values of less than 0.05 were considered significant. SPSS version 23 and Graph Prism 7 were used for statistical analyses and plots.

2.3. Results

2.3.1. Cohort characteristics

A total of 201 reports were assessed of which 156 were included from MS (n=85; mean age 61.1±11.9 years, 54.1% females) and non-MS (n=68; mean age 58.5±12.3 years, 50.0 % females) cases for further study, as outlined in **Figure 2.2.**

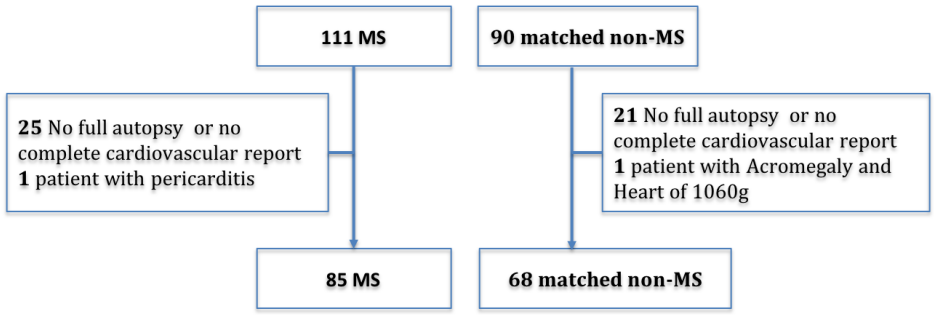

Figure 2.2. Cohort Selection for autopsy reports scoring.

A total of 111 MS and 90 age- and sex-matched non-MS cases with available autopsy reports were selected from the Oxford Brain Bank database. After analysing the autopsy reports, 25 MS and 21 non-MS cases were excluded due to missing data or confounding factors that interfered with classification of LVH.

Clinical features of MS and non-MS cases are summarised in **Table 2.1**. Age and sex did not differ between the two groups. Year of death was 1984±9.6 in MS cases and 1988.9±9.7 in non-MS cases (p=0.007). VRF were more commonly reported in non-MS cases (42.6%) but information regarding this variable was missing in most of the MS cases reports (78.8%). Immobility was more commonly mentioned to be present in MS (69.4%) than in non-MS autopsy reports (30.9%), p<0.001.

As for causes of death, infection was more frequent in MS (23.5%) compared to non-MS (5.3%) (p=0.004), while cancer, MI, and/or IS death was more common in non-MS (**Table 2.1.).** Other causes of death did not differ between MS and non-MS groups (**Table 2.2.**).

Table 2.1. Demographic features of MS and non-MS cases studied in Chapter 2

	MS (N=85)	**Non-MS (N=68)**	**p**	**MS no MI and/or IS death (N=79)**	**Non-MS no MI and/or IS death (N=56)**	**P**
Female n (%)	46 (54.1)	34(50.0)	0.630	41(51.9)	29 (51.8)	0.99
Age at death (years) mean (SD)	61.1 (± 11.9)	58.5 (± 12.3)	0.190	60.9 (12.0)	57.7(12.5)	0.18
Disease duration (years) median(IQR)	19 (16.3)	NA	NA	16 (17.0)	NA	NA
Year at death median(IQR)	1984(9.6)	1988 (9.7)	0.007**	1984 (9.4)	1989 (9.9)	0.006
Immobility			<0.001**			<0.001**
Present	59 (69.4)	21 (30.9)		54 (68.4)	17 (30.4)	
Not present	1 (1.2)	36 (52.9)		1 (1.3)	28 (50)	
Unknown/not mentioned	25 (29.4)	11 (16.2)		24 (30.4)	11 (19.6)	
Vascular Risk Factors			0.03*			0.07*
Not mentioned	67 (78.8)	39 (57.4)		65 (82.3)	35 (62.5)	
1	14 (16.5)	20 (29.4)		11 (13.9)	15 (26.8)	
2	3 (3.5)	5 (7.4)		2 (2.5)	3 (5.4)	
>2	1 (1.2)	4 (5.9)		1 (1.3)	3 (5.4)	
Causes of death n (%),						
Pulmonary embolism/DVT	10(11.8)	6(8.8)	0.61	10 (12.7)	6 (10.7)	0.73
Infection	42 (49.4)	12 (17.6)	0.001**	42 (53.2)	12 (22.2)	<0.001**
Cancer	5 (5.9)	16 (23.5)	0.004**	5 (6.3)	16 (28.6)	0.001**
MI and/or IS	6 (7.1)	12 (17.6)	0.048	NA	NA	
MS	3 (3.5)	NA		3 (3.8)	NA	
Other	19 (22.3)	22 (32.4)	0.27	19 (24.1)	22 (39.3)	0.06

Left columns summarize data for all cases and on the right of those where Myocardial Infarction (MI) and/or Ischaemic stroke (IS) recorded as causes of death were excluded NA – not applicable, not available. *p<0.05, **p<0.01

Table 2.2. Other causes of death in MS and non-MS cases

	MS	Non-MS
Infection N (%)		
Total	42	12
- Pneumonia	34 (81.0)	8 (66.7)
- pyelonephritis	3 (7.0)	1 (8.3)
- septicaemia	0	1 (8.3)
-meningitis/encephalitis	2 (4.8)	2 (16.7)
- skin infection	2 (4.8)	0
- peritonitis	1 (2.4)	0
Cancer N (%)		
Total	5	16
- Bladder	1 (20.0)	2 (12.5)
- Lung	0	5 (31.3)
- Gynaecological	1 (20.0)	2 (12.5)
- GI	1 (20.0)	2 (12.5)
- Haematological	0	3 (18.8)
- CNS	1 (20.0)	2 (12.5)
- Breast	1 (20.0)	0
Other causes of death	19	22
Total		
- Metabolic	1 (5.3)	5 (22.7)
- GI bleed/perforation	4 (21.1)	3 (13.6)
- Suicide (intoxication/overdose/hanging)	4 (21.1)	6 (27.3)
- Asthma/Asthma/another lung disease	5 (26.6)	1 (1.5)
- Non-atheromatous vascular disease	1 (13.6)	3 (13.6)
- Trauma	2 (9.1)	1 (1.5)
- Anaemia	1 (4.5)	1 (1.5)
- CNS disorder	1 (4.5)	1 (1.5)

2.3.2. Construction of a SysVasc score from autopsy reports

One pathologist (ME) performed 88 out of the 156 (56.4%) (MS, n=46; non-MS, n=42) of the selected autopsies. Causes of death, and scores for aorta and coronary atheroma categories did not differ between pathologists, in particular no differences were observed between ME and all other pathologists combined (**Table 2.3.**).

Variables were systematically recorded in all cases and substantial to almost perfect agreement between raters was found for coronary and aorta atheroma, MI, IS and LVH. It was only possible to obtain a reproducible scoring of cervical artery atheroma in 34 MS cases (moderate to severe in 8 cases) and 27 non-MS cases (moderate to severe in 6 cases), and of large artery intracranial atheroma in only 34 MS cases (moderate to severe in 6 cases) and in 30 non-MS cases (moderate to severe in 8 cases). Inter-rater agreement on RH was low (0.3) since presence of other renal pathologies (i.e. infection, hydronephrosis) confounded the diagnosis. In cases with an agreement above 0.65, RH was present in 5 out of 36 non-MS cases and 6 out of 41 MS cases. Cervical/ intracranial atheroma and RH were not further included in any of the composite variables or analysis in this Chapter.

Correlation matrix between each individual SysVasc feature is depicted in **Table 2.4.**

Table 2.3. Atheroma scores according to pathologist

Coronary atheroma n (%)	**ME** **Non-MS (N=46)**	**All other pathologists** **non-MS (N=25)**	**ME** **MS (N=42)**	**All other pathologists** **MS (N=43)**
Not present Mild Moderate Severe	15 (32.6) 11 (23.9) 9 (19.6) 11 (23.9)	7 (28.0) 10 (40.0) 5 (20.0) 3(12.0)	18 (42.9) 7 (16.7) 12 (28.6) 5 (11.9)	12 (27.9) 19 (44.2) 5 (11.6) 7 (16.3)
Aorta Atheroma n (%)	**ME** **Non-MS (N=42)**	**All other pathologists** **Non-MS (N=25)**	**ME** **MS (N=40)**	**All other pathologists** **MS (N=35)**
not present Mild Moderate Severe	9 (21.4) 13 (31.0) 12 (28.6) 8 (19.0)	5 (20.0) 8 (32.0) 8 (32.0) 4 (16.0)	12 (30.0) 14 (35.0) 6 (15.0) 8 (20.0)	8 (22.9) 16 (45.7) 7 (20.0) 4 (11.4)

Table 2.4. Correlation matrix for individual SysVasc features included in the SysVasc Score

	Aorta atheroma	**Coronary atheroma**	**MI**	**LVH**	**IS**
Aorta atheroma	1	0.571**	0.312**	0.193*	0.124
Coronary atheroma	0.571**	1	0.496**	0.258**	0.154
MI	0.312**	0.496**	1	0.272**	0.157*
LVH	0.193*	0.258**	0.272**	1	0.265**
IS	0.124	0.154	0.157**	0.265**	1

MI – myocardial infarction, LVH left ventricular hypertrophy, IS – ischaemic stroke,

r_τ coefficients significance is highlighted: **p<0.01, *p<0.05

Cronbach's alpha was 0.76 for the 2 items of Atheroma Score (aorta and coronary atheroma) and 0.65 for the 5 items of SysVasc Score (aorta, coronary atheroma, MI, IS, LVH), therefore, these composite variables were used as a global measure of Atheroma and SysVasc burden, respectively. On the other hand, Cronbach's alpha was 0.4 for End Organ damage Score (MI, IS, LVH). For this reason, MI, IS and LVH were presented

separately and the predefined End Organ Damage Score was not used as a measure of overall end organ damage.

2.3.3. SysVasc score validity

As expected, the SysVasc score was positively correlated with age at death (r=0.37, p<0.001). Consistent with SysVasc Score being a valid measure of overall cardiovascular burden, higher mean scores were found in cases (MS and non-MS) who died of MI and/or IS (N=18, 0.59±0.19) and PE/DVT (N=16, 0.42± 0.29) compared to cases that died of other causes (N=41, 0.26± 0.03) (p<0.05) (**Figure 2.3**). In a binary logistic model to predict PE/DVT deaths in all cases except those who died of MI/IS and adjusting for age at death, the SysVasc score associated this outcome (EXP(B)=18.1, 95%CI 1.7, 191.1, p=0.016).

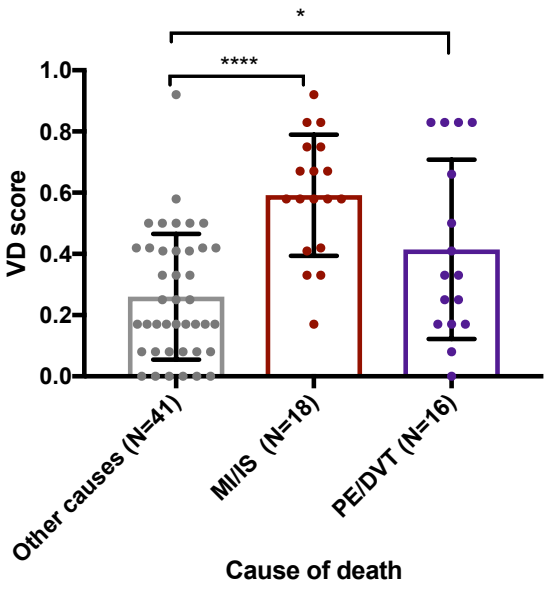

Figure 2.3. SysVasc Scores in vascular and non-vascular causes of death in the whole cohort.

****p<0.0001, *p=0.03, t-test

2.3.4. SysVasc in MS and non-MS

2.3.4.1. Individual SysVasc pathologies and SysVasc score in MS and non-MS

Frequencies of Aorta and Coronary Atheroma, MI, IS and LVH as well as Atheroma, and SysVasc Scores are outlined in **Table 2.5.** Moderate-severe atheroma and LVH was found in approximately a third of the MS cases (atheroma: 29.4% aorta, 34.1% coronary; LVH 28.2%) while MI (15.3%) and IS (8.2%) were not as commonly present. In the univariate analysis and after adjusting for age and sex MI and IS did not differ between MS and non-MS cases (**Table 2.5**)

LVH was significantly higher in non-MS even after excluding MI and/or IS deaths. In this latter group, MS cases had lower heart weights than non-MS cases (B=-39.2, 95%CI -71.4, -6.93, p=0.02), after adjusting for age and sex (**Figure 2.4.** and **Table 2.5.**). LVH was less frequent in MS women (6 out of 41, 14.6%) when compared to non-MS women (14 out of 30, 46.7%), even after excluding MI and/or IS deaths (p=0.003). In a binary regression model to determine the influence of MS on the presence of LVH, adjusting for age at death and sex, non-MS cases showed to have 3.5-fold more LVH than MS cases (EXP (B)=3.5, 95%CI 1.7,7.1, p<0.001).

Atheroma scores did not differ between groups in univariate analysis (**Table 2.5**.) but comparisons taking in account age at death will be detailed below (section *2.3.4.2*).

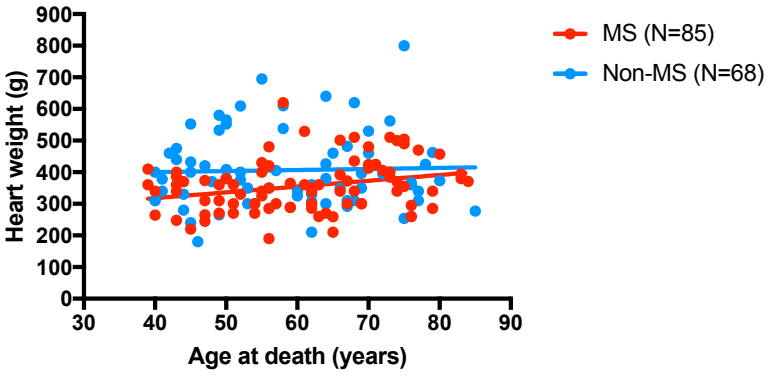

Figure 2.4. Heart weight variation with age at death in MS and non-MS cases

Table 2.5. SysVasc in MS and non-MS

	MS (N=85)	Non-MS (N=68)	p	MS no MI and/or IS death (N=79)	Non-MS no MI and/or IS death (N=56)	p
Atheroma						
Aorta Atheroma n **(%)**			0.2			0.23
not present	20 (23.5)	13 (19.1)		20 (25.3)	12 (22.4)	
Mild	30 (35.3)	21 (30.9)		30 (38.0)	19 (33.9)	
Moderate	13 (15.3)	19 (27.9)		9 (11.4)	14 (25.0)	
Severe	12 (14.1)	11 (16.2)		12 (15.2)	8 (14.3)	
NA	10 (11.8)	4 (5.9)			3 (5.4)	
Aorta atheroma score mean(SD)	0.41 (± 0.34)	0.48 (± 0.34)	0.19	0.39 (±0.34)	0.44 (± 0.33)	0.33
Coronary atheroma n **(%)**			0.81			0.81
Not present	30 (35.3)	21 (30.9)		30 (38.0)	19 (33.9)	
Mild	26 (30.6)	21 (30.9)		25 (31.6)	19 (33.9)	
Moderate	17 (20.0)	12 (17.6)		17 (21.5)	10 (17.9)	
Severe	12 (14.1)	14 (20.6)		7 (8.9)	8 (14.3)	
Coronary atheroma score mean(SD)	0.37 (± 0.35)	0.42 (± 0.37)	0.43	0.3 (±0.32)	0.37 (± 0.34)	0.58
Atheroma Score mean (SD)	0.39 (± 0.31)	0.45 (± 0.31)	0.25	0.36 (±0.29)	0.41 (±0.31)	0.41
End organ damage						
Myocardial infarction n(%)	13 (15.3)	10 (14.7)	0.83	8 (10.1)	5 (8.9)	0.82
Ischaemic stroke n (%)	7 (8.2)	9 (13.2)	0.36	6(7.6)	4 (7.1)	0.92
LVH n (%)			<0.01**			<0.01*
not present	61 (71.1)	31(45.6)		59 (74.7)	27 (48.2)	
mild to moderate	7(8.2)	10 (11.8)		6 (7.6)	10 (17.9)	
severe	17 (20.0)	26(38.2)		14 (17.7)	18(32.1)	
NA		1 (1.5)			1 (3.6)	
Heart weight mean (SD)	356 (± 82.3)	406 (± 120)	<0.01**	352 (±80.9)	388.6 (± 112.3)	0.03*
SysVasc Score mean (SD)	0.27 (± 0.24)	0.35 (±0.24)	0.06	0.25 (±0.22)	0.29 (±0.23)	0.17

SD – standard deviation, LVH – left ventricular hypertrophy, *p<0.05

2.3.4.2. The relationship between SysVasc and Atheroma Scores and age at death in MS and non-MS

SysVasc Scores increased with age at death in MS (N=85, r=0.59, p<0.001) but this association was not significant in non-MS (N=68, r=0.19, p=0.18) (**Figure 2.5 a.**).

In a simple linear regression model, to test the effect of MS on SysVasc, taking age at death into account, MS cases have a lower burden of SysVasc than non-MS (B=-0.09,95%CI -0.16,-0.02, p=0.01) and similar results were found after excluding MI and/or IS deaths. To effectively compare the coefficients of the MS and non-MS of SysVasc on age at death regression lines, a convenient simple linear model with an interaction term was assumed (statistical analysis outputs are presented in **Table 2.6.**). For the SysVasc score, the coefficient for the interaction term was significantly different from zero, confirming that the effect of age at death on SysVasc is different between MS and non-MS cases. The analysis of the data, after excluding the MI and/or IS causes of death yielded similar results. The appearance of the graphical display, confirmed by the numerical output, showed that the conclusions were not different from those obtained including all causes of death.

As for SysVasc score, the Atheroma score increased with age at death in MS and non-MS groups, as depicted in **Figure 2.5 b**. The effect of age on atheroma was found to be stronger in MS (N=85, r=0.62, p<0.001) compared to non-MS (N=68, r=0.28, p=0.06) cases. In a simple linear regression model, MS did not seem to significantly influence Atheroma score. However, when adding an interaction term, the same pattern of results to those seen for SysVasc was found when doing the regression of the Atheroma Score on age at death, with and without MI and/or IS deaths (**Table 2.6**.).

Overall, MS cases have lower SysVasc and Atheroma scores at younger ages at death than the non-MS cases but this is reversed at older ages at death.

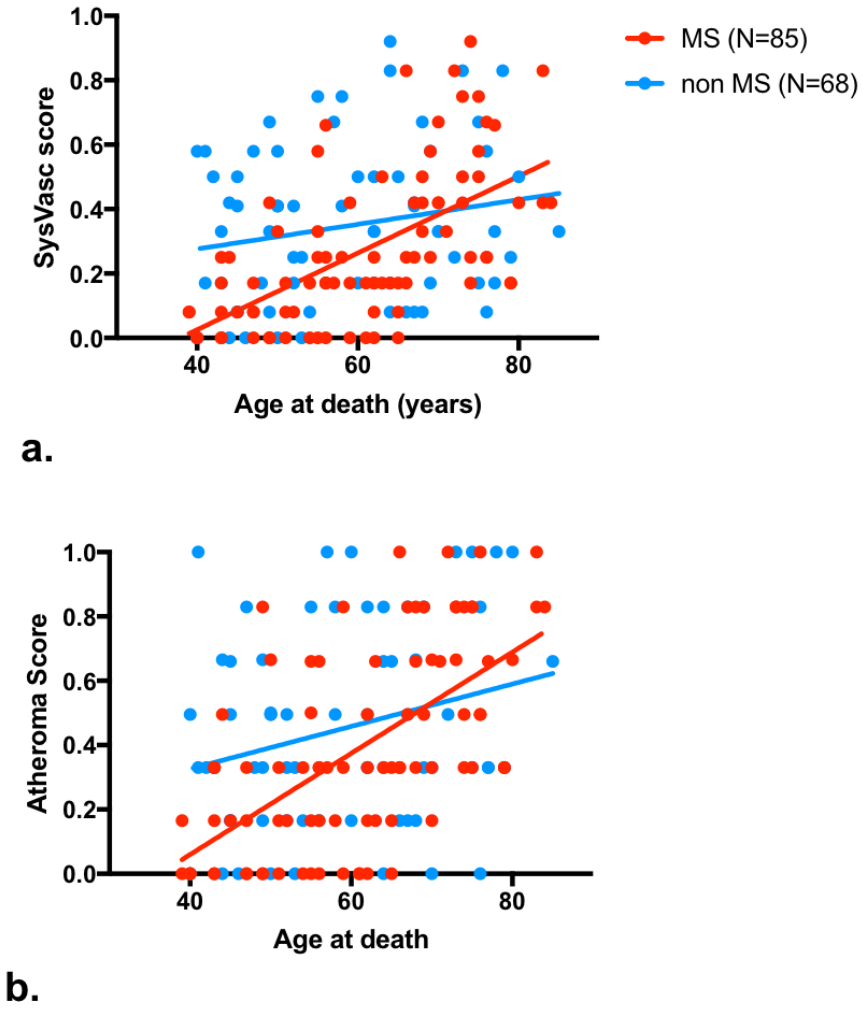

Figure 2.5. Regression plots of SysVasc and atheroma on age, for MS and non-MS cases

Table 2.6. Models to study the effect of MS diagnosis on SysVasc and Atheroma Scores

		SysVasc Score			Atheroma score		
Case	**Parameter**	**B**	**95%CI for B**	**p**	**B**	**95%CI for B**	**p**
All cases							
Model 1	Intercept(b_0)	-0.130	-0.310,0.500	0.150	-0.230	-0.45,-0.020	0.05
	Age(b1)	0.080	0.005,0.010	<0.001**	0.010	0.008,0.020	<0.001**
	MS(b_2)	-0.090	-0.160,-0.020	0.010*	-0.090	-0.18,0.003	0.059
F-statistic: 17.13 on 2 and 152 DF, p<0.001					F-statistic: 19.8 on 2 and 152 DF, p<0.001		
Model 2	Intercept (b_0)	0.123	-0.132,0.378	0.341	0.063	-0.260,0.390	0.701
	Age(b1)	0.004	0.000-0.008	0.079	0.007	0.001,0.010	0.017 *
	MS(b_2)	-0.572	-0.923, -0.220	0.002**	-0.632	-1.080,-0.190	0.006 **
	Age*MS(b_3)	0.008	0.002,0.014	0.007**	0.009	0.002,0.016	0.002 **
F-statistic: 14.43 on 3 and 152 DF, p<0.001					F-statistic: 15.75 on 3 and 152 DF, p<0.001		
No MI/IS							
Model 1	Intercept(b_0)	-0.070	-0.32,0.020	0.080	-0.285	-0.510,-0.060	0.013*
	Age(b1)	0.008	0.005,0.010	<0.001**	0.012	0.008,0.016	<0.001**
	MS(b_2)	-0.075	-0.146,-0.005	0.036*	-0.080	-0.170,0.011	0.085
F-statistic:16.1 on 2 and 134 DF, p<0.001					F-statistic:21.3 on 134 and 2 DF,p <0.001		
Model 2	Intercept (b_0)	0.055	-0.195, 0.205	0.664	- 0.037	-0.363,0.290	0.825
	Age(b1)	0.004	0.000, 0.008	0.050	0.008	0.002,0.013	0.07 *
	MS(b_2)	-0.449	-0.787,-0.111	0.010*	-0.529	-0.972,-0.086	0.02 *
	Age*MS(b_3)	0.006	0.001, 0.120	0.027*	0.008	0.000,0.015	0.043 *
F- statistic: 12.74 on 3 and 134 DF, p<0.001					F-statistic: 15.9 on 3 and 134 DF, p<0.001		

Numerical results of a simple linear model (Model 1) and with an interaction term (Model 2) to study the effect of MS diagnosis on SysVasc and Atheroma Scores, taking in account age at death, for all cases and excluding MI and/or IS deaths. The linear model with an interaction term was used to compare the two regression lines for the MS and non-MS groups. The estimated equation of the model is $y= b_0 + b_1 x_1 + b_2 x_2 + b_3 x_1 x_2$ where y is the response variable (SysVasc or Atheroma score), x_1 represents the variable age and x_2 is a binary variable with $x_2 = 1$ if the subject belongs to the MS group and $x_2 = 0$ if the subject belongs to the non-MS group. If $x_2=0$ we have $y=b_0+b_1x_1$, and b_0 and b1 are the intercept and the slope of the regression line associated with the non-MS group. If $x_2=1$ we have $y= (b_0+b_2) + (b_1+b_3) x_1$, b_0+b_1 and b_1+b_3 are, respectively, the intercept and the slope of the regression line of the MS group. The coefficient b_2, indicates how much higher (lower) the intercept of the line for the MS group is than the intercept of the line for the non-MS group, while the coefficient of the interaction, b_3, measures the differential between the slopes of the two regression lines.

*p<0.05, **p<0.01

2.4. Summary of main findings

1. Causes of death in the studied *post mortem* cohort were similar to those reported in epidemiological studies in MS and the general population
2. SysVasc Score is a reliable and robust scoring for the severity of cardiovascular burden since high levels of inter-rater agreement were found, consistency between its constituent variables documented and it behaved as expected, increasing with age at death, being higher in vascular deaths compared with non-vascular deaths.
3. LVH is less common in MS compared with non-MS but no differences were found in Atheroma, MI and IS
4. SysVasc score is lower in MS compared with non-MS
5. SysVasc and Atheroma burden are lower in MS cases who died young but increased more steeply with age of death in MS than in non-MS cases

2.5. Discussion

The first aim of this chapter's work was to devise a simple, standardized method for autopsy report data collection. This method produced reliable variables and a consistent SysVasc score that closely associated with age and vascular deaths, supporting its validity. Previous studies have quantified coronary and aorta atheroma burden from autopsy reports in the general population (Thej *et al.*, 2012; Webber *et al.*, 2012). However, to my best knowledge, a global cardiovascular score considering both atheroma and end-organ vascular related burden has not been proposed before. SysVasc score proved to be useful in comparing cardiovascular disease burden between MS and non-MS, as discussed below, and may be a simple and useful tool to

test the relationship between SysVasc and brain pathology, not only in MS but in other disorders.

The SysVasc score was applied to a representative cohort of MS and non-MS cases, since causes of death in both groups of cases were similar to those previously reported in other populations (Goodin *et al.*, 2014; Jick *et al.*, 2014; Capkun *et al.*, 2015). Moderate-severe aorta and coronary atherosclerosis was observed in around one third of non-MS cases in line with what has been reported in previous autopsy studies in non-MS (Thej *et al.*, 2012).

Another important aim of this study was to compare SysVasc between MS and non-MS. Contrary to the initial hypothesis, SysVasc, was not increased in MS when compared to age matched non-MS cases. LVH was actually less commonly found in MS than in non-MS cases. These findings somehow challenge the reported association between MS and SysVasc in epidemiological studies (Christiansen, 2012; Marrie *et al.*, 2014, 2019; Murtonen *et al.*, 2018).

The incidence of objective measures of atherosclerosis in MS has not been previously studied. Only one *in vivo* study reported increased subclinical surrogate markers of atherosclerosis, as measured by forearm blood flow, arterial compliance and pulse wave velocity, in 33 MS cases compared with 33 healthy controls but with no differences in intima-media thickness, an early marker of atherosclerosis, were found (Ranadive *et al.*, 2012), thus not contradicting our autopsy findings.

In our study, LVH was significantly lower in MS compared with non-MS, even adjusting for age at death. Cardiac deconditioning and atrophy has been linked to sedentarism (Vis *et al.*, 2012) and increased immobility/inactivity may have led to lower heart weights in MS compared with non-MS. LVH is closely related with hypertension (Gosse, 2005) and it is possible that MS patients have a lower prevalence of hypertension as suggested in some epidemiological studies (Marrie *et al.*, 2014; Simpson *et al.*, 2014). Putative explanations for a lower rates of hypertension in MS include: 1. the immune system may play an essential role in the pathogenesis of not only MS (Dendrou *et al.*, 2015) but also in hypertension (Rodríguez-Iturbe *et al.*, 2014) and cardiovascular remodelling, such as LVH (Diamantopoulos *et al.*, 2003) ; 2. there are gender differences in the susceptibility for both disorders, with MS being more common in younger women (Golden and Voskuhl, 2017), who have a lower risk of arterial hypertension compared to age-matched men (Sandberg *et al.*, 2015); 3. there may be some genetic overlap between MS and systolic blood pressure control (Wang *et al.*, 2016).

MI or large artery IS was not seen in excess in MS compared to non-MS group. A systematic review of observational studies looking at the prevalence of vascular comorbidities in MS suggested increased prevalence of ischaemic heart disease, congestive heart failure and IS in MS when compared to healthy controls (Marrie *et al.*, 2014). However, in this review problems with study quality, heterogenicity and potential bias are acknowledged. In particular, MS patients may have more health care contact than non-MS cases and thus more investigations and recorded diagnosis. This surveillance bias could explain the reported increased risk of cardiovascular disease in the first years after MS diagnosis compared to age-matched controls (Christiansen

et al., 2010; Christiansen, 2012; Roshanisefat *et al.*, 2014). Moreover, existing large case-control studies rely on broad diagnostic categories frequently including different vascular disorders, i.e. PE/DVT and MI, in the same category (Marrie *et al.*, 2014; Tettey *et al.*, 2014) and reported differences between MS and age-matched controls may be due to an excess of embolic vascular disorders but not specifically a higher burden of atherosclerosis. That being said, a recent Canadian population-based study reported a 1.6 fold increased hazard for MI in MS compared with age and sex-matched non-MS, even after adjusting for traditional VRF (Marrie *et al.*, 2019). More than 40 percent of the MS cases included in this study were older than 55 years of age and, as will be discussed below, SysVasc and Atheroma burden steeply increases with age at death in MS and atherosclerosis could account for an increased risk of MI in older patients. Nevertheless, it is possible that a non-accounted for structural cardiac dysfunction in MS may predispose to MI. Cardiac microvascular changes are more common as a cause of MI in women than in men (Mehta *et al.*, 2016). Whether such changes are enhanced in MS warrants further investigation.

IS was not increased in our MS cohort compared with non-MS. Adding to the small sample size limitations, I acknowledge that only large artery related IS was assessed and that MS may predispose to cSVD related ischaemic lesions instead. This hypothesis will be tested in Chapter 3.

To fully understand the interaction between MS and SysVasc, the effect of age at death in both disorders needs to be considered. Age is one of the most important predictors of SysVasc in the general population. Age may also be a marker of disease severity in

MS, MS cases that die young potentially having worse disease and this hypothesis will be explored in subsequent Chapters.

MS cases that died at young ages have less SysVasc than age- and sex-matched non-MS cases but the reverse is seen in cases that die after the age of 65 years. These observations argue against a common underlying mechanism predisposing for both MS and cardiovascular disease and even suggest that inherent factors present in MS may protect against SysVasc at young ages. However, SysVasc burden steeply increases with age at death in MS but this association is weaker in non-MS. MS cases that died after the age of 65 years, possibly having a longer exposure to VRF and to chronic inflammation, tended to have more SysVasc than non-MS. Increased immobility at older ages in MS might also be an important factor for SysVasc accumulation. In this study, information about mobility was not always available and was limited (i.e. no information on severity, time course) and its impact on SysVasc could not be further analysed. Other confounding factors, such as a lower prevalence of cancer in MS (Koch-Henriksen *et al.*, 1998; Goodin *et al.*, 2014; Capkun *et al.*, 2015), could explain a possible excess of SysVasc in MS patients that live up to older ages, since an inverse association has been reported between atherosclerosis and cancer (Li *et al.*, 2015).

I recognise that these findings need to be taken with caution given the inherent biases in *post mortem* studies. Young MS cases with less severe disease and older MS cases with higher disease burden may not have been included and different results may have been found if they were. Medication history might be different between the two groups but this information was not available. Another possible limitation is that pathologists

were not blinded for cases and control diagnosis and may have underestimated SysVasc in MS cases. However, a standardized autopsy report was used and no differences were found across pathologists. Finally, *post mortem* studies only have access to a single time point and the direction of the herein found relationships are difficult to establish. Factors not directly related to MS might explain the development of systemic atherosclerosis in MS patients. Larger *in vivo* studies, ideally longitudinal with information on other possible confounders such as mobility and steroid use, are needed to document a possible arterial dysfunction in MS and to assess the relationship between MS duration and atheroma progression.

However, the present work has important strengths: 1. sample size is considerably large for a *post mortem* study; 2. brain and whole-body full autopsy data was available for study; 3. data was obtained from an MS cohort with no DMT exposure avoiding the possible bias of a DMT effect on SysVasc.

In conclusion, in this study a robust and reliable SysVasc score was devised and evidence that objectively measured SysVasc is lower in MS is provided. A different relationship between age at death and SysVasc in MS compared with non-MS was documented and this interaction needs to be considered when studying cerebrovascular disease in MS. The present work sets the stage to further explore the effect of SysVasc on brain pathology in MS.

3 The influence of MS on type 1 cSVD

3.1. Introduction

In the previous chapter, a score to quantify SysVasc was developed and was shown to steeply accumulate with age at death in MS.

MS patients with vascular comorbidities, such as diabetes, hypertension, heart disease, hypercholesterolemia and peripheral vascular disease, will need a walking aid sooner than those without vascular comorbidities (Marrie *et al.*, 2010). It is possible that these VRF and comorbidities associate with a concomitant higher burden of cerebrovascular disease. However, the prevalence and extent of cSVD has never been explored in MS.

SysVasc score is an objective marker of vascular comorbidities and it may be positively associated with cSVD burden, both in MS and non-MS. Owing to chronic inflammation, immobility and frailty (Gisterå and Hansson, 2017; Hanlon *et al.*, 2018) cSVD burden may be higher in MS. The main Chapter 3 research question is:

1. Is cSVD burden higher in MS compared with non-MS, taking age and SysVasc into account?

It is possible that cSVD burden is higher in MS than in non-MS. To test this hypothesis, my aims are to:

a. devise a valid cSVD score using consensual cSVD pathologic measures
b. apply this score to a pathologically defined *MS post mortem* cohort and an age- and sex-matched non-MS cohort, where SysVasc has previously been assessed.

c. compare the burden of cSVD, as measured by the devised score, between MS and non-MS considering age and SysVasc.
d. explore the influence of MS on individual cSVD pathologies, considering age and SysVasc.
e. explore inside MS plaque cSVD and compare it with outside plaque cSVD, in the MS cohort

3.2. Materials and Methods

3.2.1. Study population

A post-mortem cohort of MS (n=42) and non-MS (n=39) cases on whom the extent of SysVasc scores were previously obtained from the cohort described in Chapter 2, section 2.3.1 with available brain tissue and information on cervical and intracranial atheroma were used for study. Cases with severe brain damage (i.e. brain trauma, any brain tumour) or cases with disorders known to associate with vascular injury (i.e. subarachnoid haemorrhage, cerebral venous thrombosis; extensive bilateral macroscopic stroke) or inflammation (i.e. brain infection) were excluded. Age, sex and causes of death were obtained from autopsy reports as previously described (section 2.2.2.1). Brain weight (g) was available for all cases.

3.2.2. Tissue sampling

For each case, 10% formalin–fixed paraffin-embedded (FFPE) tissue from the following 4 areas was obtained (**Figure 3.1**):

- Frontal WM (FWM) at the level of the frontal horn of the lateral ventricle
- Occipital WM (OWM) at the level of the occipital horn

- Basal Ganglia (BG) lenticular nucleus, and when not available, caudate nucleus at the level of the frontal horn of the lateral ventricle
- Pons at the level of the facial nucleus

As FWM, OWM and BG are typically affected by age-related cSVD, these areas are typically included in most cSVD pathological scoring systems (Deramecourt *et al.*, 2012; Smallwood *et al.*, 2012; Craggs *et al.*, 2014; Skrobot *et al.*, 2016) and were used for this purpose in the current study. While the pons is not usually included in cSVD scoring systems, it is of interest given that it is irrigated by perforating arterioles that may be affected by cSVD (Caplan, 2015) and is commonly affected in MS (Brainin *et al.*, 1987).

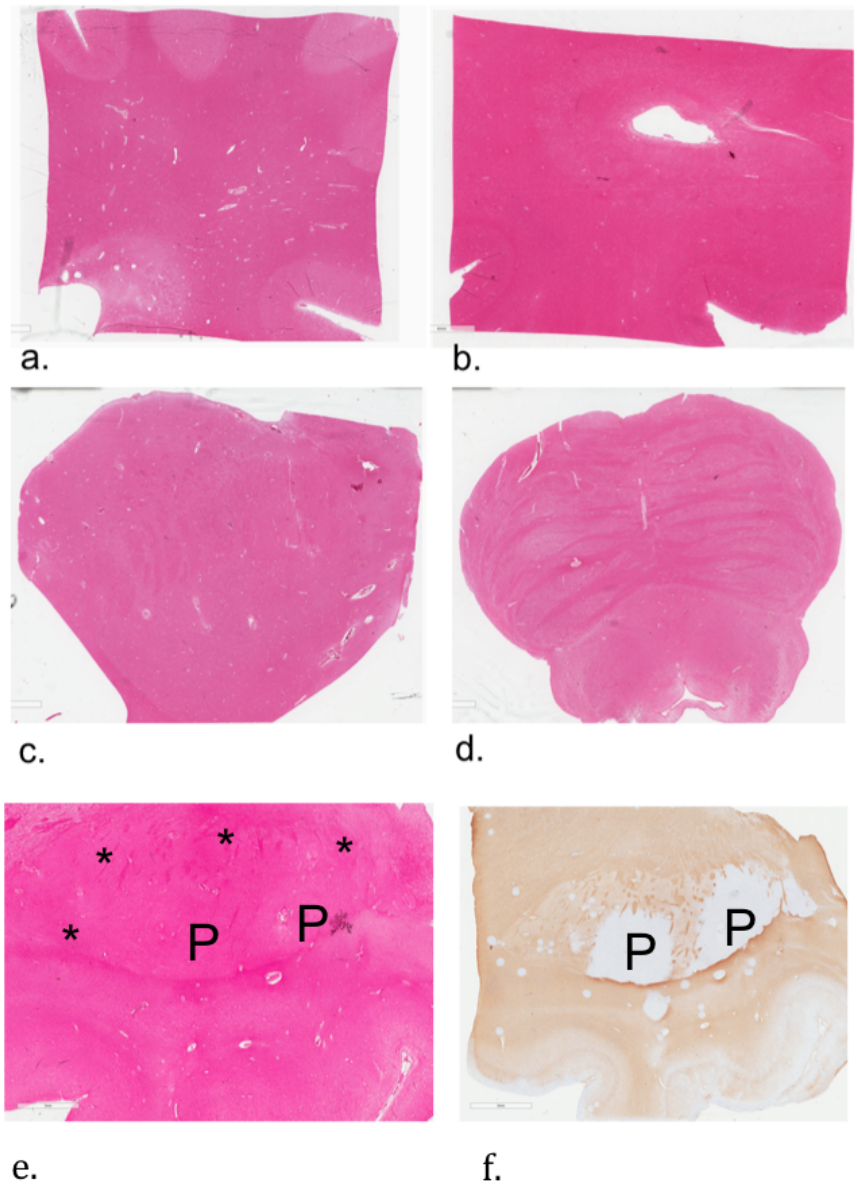

Figure 3.1. Sampled brain areas for cSVD scoring

Four brain areas were sampled both in MS and non-MS cases to be further stained with H&E and SMA-immunostained for cSVD scoring. The figure depicts H&E FFPE stained sections from non-MS cases of **a.** FWM at the level of the frontal horn of the lateral ventricle; **b.** OWM at the level of the occipital horn; **c.** BG; **d.** pons at the level of the facial nucleus and from an MS case of **e.** BG and **f.** an adjacent BG PLP FFPE stained section. In MS adjacent sections were stained with PLP and plaque areas were identified as areas of complete PLP loss (details on MS plaque analysis in Chapter 5 sections 5.3.3. and 5.3.4). In MS, cSVD was scored outside (1mm from plaque border) plaque (*) and inside plaque (**P**).

3.2.3. Neuropathological Evaluation

3.2.3.1. Scoring cSVD pathologies using consensual definitions and Global cSVD Index construction

FFPE 10 μm sections of the FWM, OWM, BG and pons were stained with H&E and immunostained with primary antibodies for myelin PLP and smooth muscle actin (SMA) (counterstained with haematoxylin) (**Table 3.1**). SMA was chosen since it proved to be useful in differentiating arterioles from small veins (**Figure 3.2**). The wall of small veins is known to thicken with ageing and in the presence of VRF, especially in the periventricular area (Keith *et al.*, 2017). Further, venous wall fibrosis has been described in MS (Mohan *et al.*, 2010) and could be difficult to differentiate from arteriolosclerosis in this group of patients (Brown and Thore, 2011*a*) on H&E stain alone further justifying the use SMA to help distinguish small veins from arterioles (see **Figure 3.2**).

Table 3.1. Details of Antibodies used in Chapter 3 and Chapter 5

Antibody	Clone	Classification	Pre-treatment	Dilution	Supplier	Catalogue Number
PLP	plpc1	Monoclonal mouse	Microwave citrate pH6.0	1:1000	AbD Serotec	MCA8399
SMA	1A4	Monoclonal mouse	Microwave TRIS-EDTA pH9.0	1:50	Dako	M0851
CD68	PGM-1	Monoclonal mouse	Microwave citrate	1:100	Dako	M0876

Stain	Vein	Artery
Haematoxylin &Eosin	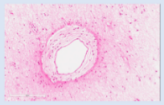	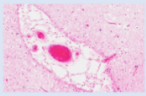
Van Gieson Elastin	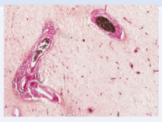	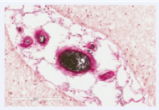
Smooth muscle Actin	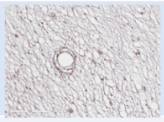	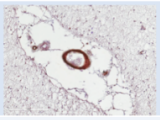
Hamartin	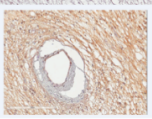	

Figure 3.2. Differentiation between damaged small veins and arterioles in MS.

Cerebral arteries are thin-walled for their calibre but with a smooth muscle and internal elastic layers and virtually no elastic fibres in the other vascular wall layers. In contrast, veins have a thin wall almost devoid of smooth muscle cells. Pathological thickening of small veins walls could potentially make their distinction from damaged arterioles challenging. On H&E, morphological differences, such as a more intensely stained media, were helpful to distinguish small veins with a thickened wall due to collagen accumulation from arterioles. Arterioles had evidence of a smooth muscle layer labelled with anti-SMA and anti-Hamartin (expressed in arteriole smooth muscle (Johnson *et al.*, 2001) primary antibodies and an elastic lamina labelled by Van Geison Elastin staining. These characteristic arteriole features were still preserved in presence of perivascular inflammation or space widening. For the purpose of this study, the use of H&E and SMA staining in tandem was found to be the most effective way to differentiate arterioles and veins in this study formalin fixed tissue (Smyth *et al.*, 2018).

H&E stained histology sections of the four brain areas of interest were scanned 20X magnification using Scannoscope and images were analysed with Aperio ImageScope software. cSVD was assessed in the whole section for the pons and basal ganglia as in the FWM and OWM 2mm from the ventricular surface. The periventricular area has been avoided in most cSVD scoring studies (Skrobot *et al.*, 2016) and will be explored in Chapter 4.

In MS outside and inside plaque cSVD was scored. MS plaques, were defined as well demarcated areas of complete demyelination, seen as complete absence of PLP immunostaining (see Chapter 5, section 5.2.4. for full description of plaque analysis). cSVD scoring was obtained inside the largest plaque seen in the PLP stained sections adjacent to the H&E section (**Figure 3.1 e**). In the FWM and OWM if the largest plaque was periventricular the second largest, non-periventricular plaque was also scored. Plaques below 200μm^2 were excluded.

All vessels with a clearly delineated cross-sectional lumen measuring 20-150 μm in diameter were selected and analysed. The extent of cSVD was assessed using established definitions (Skrobot *et al.*, 2016), detailed in **Table 3.2**.

Agonal state has not been factored in previous cSVD scoring studies (Smallwood *et al.*, 2012; Skrobot *et al.*, 2016) and was not considered in the present study. Contrary to transcriptomic and proteomic studies (Tashjian *et al.*, 2019), I would not expect a significant effect of agonal state on the studied structural cSVD pathologies such as arteriolosclerosis, PHL, microinfarcts. PSD due to acute cerebral oedema associates with loose appearance of myelinated areas, rarefaction of subpial spaces and a vacuolar appearance of the grey matter neuropil (Yates *et al.*, 1975). However, cases where generalized brain oedema could be present (i.e. due to traumatic brain injury) were excluded from the analysis. Moreover, the shape PSD and pattern of perivascular tissue changes was considered when scoring the presence PSD (i.e. loosening of the neuropil around the vessel or the presence of fibrotic tissue in a well demarcated perivascular space), to differentiate longstanding perivascular changes from end-of-

life acute changes. For the same reasons, perivascular red blood cell leakage was not considered to be due to a microbleed unless structural findings such as arteriolar wall disruption, or agglomerates of hemosiderin laden macrophages were present.

Table 3.2. cSVD scored features

SVD scoring using established definitions (Skrobot et al. Brain 2016)		Example
1.Arteriosclerosis and arteriolosclerosis*:	0= normal or mild thickening of the vessel media, mild fibrosis 1= partial loss of smooth muscle cells in the media, moderate hyaline fibrosis or complete loss of smooth muscle cells in the media, severe hyaline fibrosis, lumen stenosis	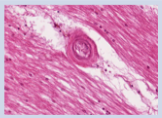
2.Fibrinoid necrosis and microaneurysms:	0= absent 1= present	
3.Perivascular space dilation :	0= from absent to perivascular space ≥ the artery diameter in a minority of sections 1= perivascular space is ≥ the artery diameter in the majority of sections	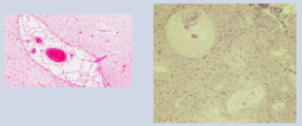
4.Perivascular haemosiderin leakage:	0= absent or <3 haemosiderin granule deposits in the perivascular space 1= ≥3 haemosiderin deposits in the perivascular space	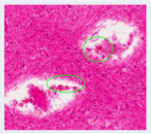
5.Microinfarcts, Lacunar infarcts, 6.Large infarcts	0= absent 1= present	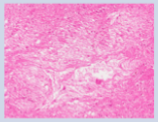
7. Microhaemorrhage	0= absent 1= present	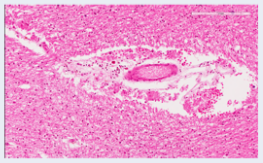

*Arteriolosclerosis - hyaline thickening of walls of vessels <150 μm in diameter; micro-infarcts - ischaemic lesion found on microscopic examination but nor visible to the naked eye; lacunar infarct - cystic lesion visible to the naked eye but <1cm in diameter; large infarcts - maximum diameter >1cm; microhaemorrhage - haemorrhagic lesion, with parenchymal involvement, found on microscopic examination which is not visible to the naked eye. Examples of perivascular space dilatation in MS (left) and non-MS (right) are shown.

Sections would be scored positive if arteriolosclerosis, PSD or hemosiderin leakage was found in 3 or more vessels. Though specific stains for hemosiderin were not used (i.e. Pearls Prussian blue), H&E has been shown to be sensitive to capture perivascular hemosiderin (Alwahaibi, and Al-Himali, 2012) and has been widely used in cSVD scores that include this pathological feature (Deramecourt *et al.*, 2012; Skrobot *et al.*, 2016). In the H&E sections, hemosiderin, an iron storage complex, was typically found in cells (usually macrophages) as intracellular gold-brown granules (**Table 3.2, example 4**). Observation of one of the other features (i.e. microbleeds, microinfarcts), defined as outlined in **Table 3.2.** legend, in the section was sufficient to attribute a positive score. Microinfarcts and larger infarcts (>1cm) were defined as lesions with neuronal/axonal loss and gliosis (Erten-Lyons Neurology 2013).

Total scores for each of the pathological features were obtained (i.e. **Total arteriolosclerosis**: pons+BG+FWM+OWM arteriolosclerosis). The sum of each of the total scores contributed to a **Global cSVD Index**. In MS, the Global cSVD Index was obtained from non-plaque areas.

Inside MS Plaque cSVD was obtained for each studied brain region: sum of all plaques cSVD/number of plaques. A **Global Inside Plaque cSVD Index** was obtained by summing FWM, OWM, BG and Pons Inside Plaque cSVD.

To better assess the differences between in plaque and outside plaque cSVD, comparisons were made between the largest plaque and non-plaque regions of the same section for each individual cSVD pathology.

cSVD ratings were obtained by one rater (RG) with inter-rater reliability assessed in a subset of cases by an experienced neuropathologist (ME). The two raters were blinded for SysVasc scores. Cases with different severities of cSVD from the OPTIMA cohort (Smallwood *et al.*, 2012) previously scored by ME were used as a training cohort for cSVD analyses. As features of MS pathology may be evident in sections assessed for cSVD thereby unblinding the assessor, a subset of the sampled 1x1x1mm squares were coded and scored by two independent raters blinded to the diagnosis and block location (RG and Dr Damian Jenkins, DM). These results were compared with the whole section scoring results.

3.2.3.2. Testing the validity of Global cSVD Index

If Global cSVD is a valid measure Index of cSVD it is expected to increase with age at death, associate with vascular deaths and to be positively correlated with vascular WML (Barker *et al.*, 2013). These lesions usually appear as diffuse areas of myelin loss or rarefaction, defined as weakly stained/pale and loose appearance of WM myelinated fibres (Skrobot *et al.*, 2016). It is expected that the Global cSVD Index positively correlates with myelin rarefaction.

Myelin rarefaction was scored 2mm away from the periventricular lining in all sampled brain sections and outside plaque in MS cases, as outlined **in Figure 3.3**. A positive score (1) was attributed if loosening or pallor of WM myelinated fibres was seen as seen in PLP immunostained sections (**Figure 3.3**).

A **total myelin rarefaction score** was obtained by adding the score of each of the 4 studied brain areas.

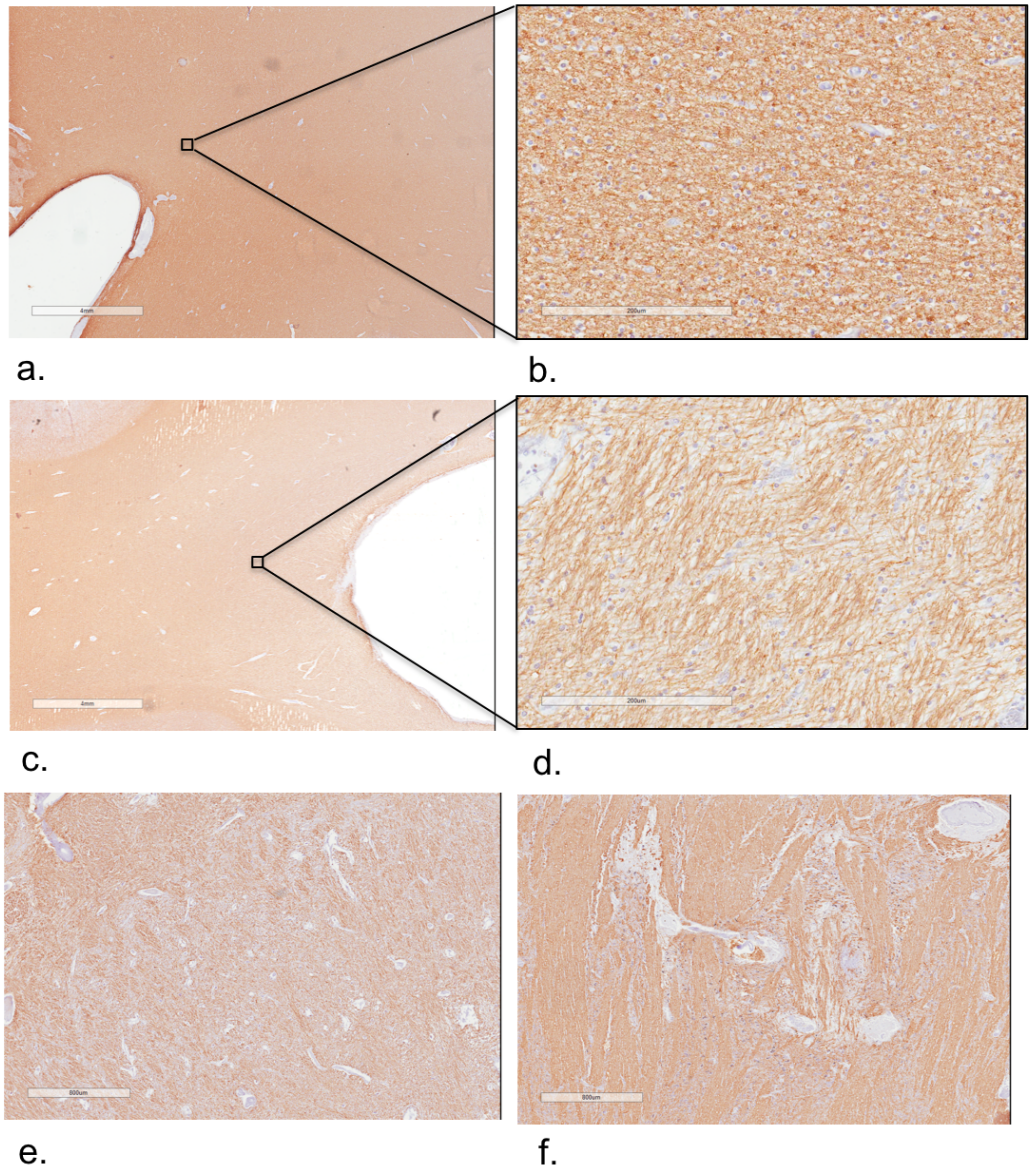

Figure 3.3. WM rarefaction scoring in PLP immunostained sections.

Normal FWM PLP is observed at lower (**a.**) and higher (**b.**) magnification (score =0). Frontal WM rarefaction is depicted at lower (**c.**) and higher(**d.**) magnification (score=1). Loosening of myelin fibres can also be detected in the basal ganglia (**e.**) and central pons (**f.**) (score 1).

3.2.3.3. SysVasc burden and cervical/intracranial artery atherosclerosis assessment

SysVasc Score was obtained as a measure of cardiovascular burden, as previously

described in Chapter 2, section 2.2.2.2. The variables included were aorta, coronary and cervical artery atheroma, MI, IS and LVH. Cervical/intracranial atherosclerosis scoring was available for a subset of cases as described in Chapter 2.

3.2.4. Statistical Analysis

Descriptive statistics, univariate analysis and inter-rater agreement was performed as described in Chapter 2, section 2.2.3. Internal consistency of the individual cSVD pathologies grouping to the Global cSVD Index was assessed by the Cronbach's alpha. Both inter-rater agreement and internal consistency were used as reliability measures of Global cSVD Index, while the validity of this index was assessed by determining its association with age at death, vascular causes of death and WM myelin rarefaction. Binary and ordinal logistic regression models were used to investigate if the Global cSVD Index associated with vascular deaths and to WM myelin rarefaction, respectively, adjusting for age at death.

Stepwise regression models were fitted to evaluate the influence of MS on Global cSVD Index whilst controlling for age at death, sex, *post mortem* delay and the SysVasc score. Only predictors that significantly correlated ($p<0.05$) with the outcome variable were included in the final models. The best model was chosen considering variable distribution, the interaction between variables and the overall performance of the model. The Variance Inflation factor (VIF) was used to test for multicollinearity and if VIT values lower than 5 levels variables were included in subsequent regression analysis. Considering that an interaction between age at death and SysVasc in MS versus non-MS has been documented in the previous chapter, similar analysis was repeated on groups stratified above and below the median age at death. Binary

regression models were used to explore the effect of MS on each individual cSVD pathology (presence/absence of the feature in any of the studied regions), whistle adjusting for age at death and SysVasc score. Results of these models are presented as regression coefficients (B) or their exponentials (EXP (B)) and respective 95% CI. All tests of hypothesis were carried out using two-sided tests and p-values of less than 0.05 were considered significant, except when more than 5 hypotheses were tested, where a p-value of less than 0.01 was considered significant.

SPSS version 25 and Graph Prism 7 were used for the statistical analysis and plots.

3.3. Results

3.3.1. Cohort characteristics

A total of 42 MS (mean age 60.6 ±12.9 years, 57.1% females) and 39 non-MS (mean age 58.8 ±12.9 years, 56.5 % females) cases, where SysVasc burden was previously characterised (Chapter 2), were included for cSVD assessment. The cohort selection flowchart is depicted in **Figure 3.4**.

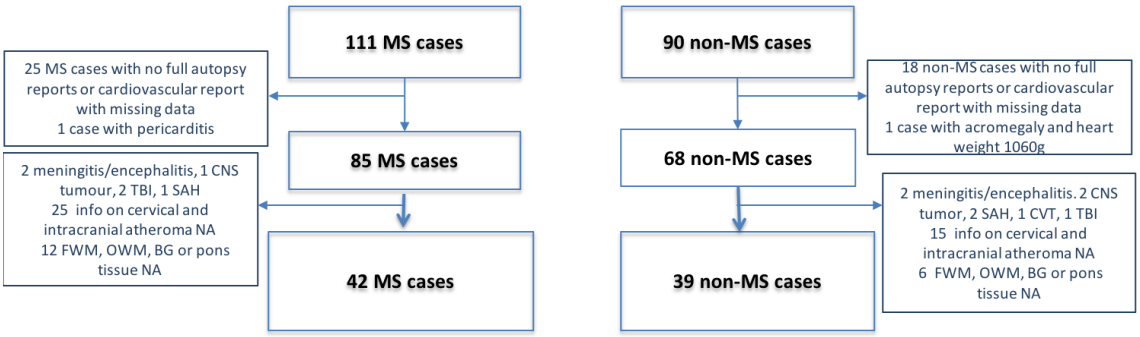

Figure 3.4. Cohort selection for histology analysis.

MS cases and non-MS cases with severe brain damage were excluded: brain trauma, herpes encephalitis, meningitis, brain tumour, complete territorial ischaemic stroke. NA – not available

Demographic and clinical features of the cohort used in this chapter are shown in **Table 3.3.** No differences in age, sex, year of death, or post-mortem delay were found between the selected MS and non-MS cases. Causes of death were different between the two groups: infection was more commonly seen in the MS group (40.5% in MS versus 12.8% in non-MS, p=0.006) and cancer in the non-MS group (0% in MS versus 28.2% in non-MS, p=0.0001). Similar differences were observed between MS and non-MS cases when split above and below the median age at death. Vascular deaths were more common in both groups who died after the age of 60 years. The two MS cases in whom the cause of death was attributed to MS died before the age of 60 years. Brain weight tended to be lower in MS cases than non-MS cases (1275.1 ±185.1g in MS versus 1351.9 ±180.4 g in non-MS, p=0.09) (see **Table 3.3.** for full details).

Table 3.3. Clinical details of the cohort used in Chapter 3, for all cases and cases binned above and the median age at death.

	MS (N=42)	**Non-MS** (N=39)	**p**	**MS**		**Non-MS**	
				=<60(N=20)	**>60 (N=22)**	**=<60 (N=21)**	**>60(N=18)**
Mean age, years (SD)	60.6 (±12.9)	58.8 (±12.9)	0.53	48.8 (6.3)	71.3(6.2)	48.5 (6.2)	70.8 (6.5)
%Females (N)	57.1 (24)	56.4 (22)	0.95	55.0 (11)	59.1 (13)	52.4 (11)	61.1 (11)
Median Year at death (IQR)	1981 (20)	1984(16)	0.493	1982 (17)	1981 (23)	1988 (19)	1985 (16)
Cause of death			0.001				
PE/DVT	11.9 (5)	10.3 (4)	ns	15.0 (3)	9.1 (2)	4.8 (1)	16.7 (3)
Infection	40.5 (17)	12.8 (5)	**	35.0 (7)	45.5 (10)	19.1 (4)	5.5 (1)
Cancer	0	28.2 (11)	**	0	0	33.3 (7)	22.2 (4)
MI/IS	7.1 (3)	17.9 (7)	ns	0	13.6 (3)	9.5 (2)	27.8 (5)
MS	4.8 (2)	NA		10.0 (2)	0	0	0
Other	35.7 (15)	30.8 (12)	ns	40.0 (8)	31.8 (7)	33.3 (7)	27.8(5)
Mean post-mortem delay in hours (SD)	54.8 (±31.2)	45.8 (±23.9)	0.152	55.3 (34.9)	54.5 (27.9)	45.6 (26.3)	46.1 (21.5)
Mean brain weight in grams (SD)	1275.1 (±185.1)	1351.9 (±180.4)	0.086	1288.7 (140.6)	1262 (220.6)	1342.8 (169.8)	1361.1 (195.9)

Comparisons made between total MS and non-MS **p<0.01

3.3.2. Scoring cSVD pathologies and Global cSVD Index construction

3.3.2.1. Inter-rater agreement in cSVD scoring and Global cSVD score internal consistency

cSVD pathological features seen in non-MS and MS (outside and inside plaque) per brain area analysed are depicted in **Table 3.4**. None of these features was associated with *post mortem* delay or year of death. PSD, arteriolosclerosis, hemosiderin leakage and microbleeds were the most commonly seen pathological features both in non-MS and MS cases. Micro-infarcts were rarely seen in both groups and macro infarcts and fibrinoid necrosis/microaneurysms were only observed in non-MS (**Table 3.4** and **Figure 3.8.**).

Substantial to almost perfect inter-rater agreement, as measured by Cohen's Kappa, was found for arteriolosclerosis (0.7) and perivascular hemosiderin leakage (0.88) with agreement being only moderate for perivascular space dilatation (0.46) scores and fair for microbleeds and infarcts (0.35). No differences were found between whole section cSVD scoring and individual squares cSVD scoring. In the latter, case raters made a correct diagnosis (i.e. MS versus non-MS) in only 20% of the cases. Cronbach's alpha indicated good internal consistency (0.61) for the variables included in the Global cSVD Index (total arteriolosclerosis, total PSD, total periarteriolar hemosiderin leakage (PHL), total fibrinoid necrosis, total infarcts, total microbleeds).

The **Global cSVD Index**, obtained by summing the individual cSVD scores from all brain areas, ranged from 1 to 11 in MS and from 0 to 12 in non-MS (maximum total score possible = 28). We recall that in MS this score was obtained from non-lesional areas. Global Inside plaque cSVD will be analysed separately at the end of this chapter.

Table 3.4. Frequencies of each cSVD individual pathological features per brain region in non-MS and MS outside plaque.

		Arteriolosclerosis	Periarteriolar space dilatation	Periarteriolar hemosiderin leakage	Microbleeds	Micro-infarcts	Large infarcts	Fibrinoid Necrosis
% (N) in one or more areas	**Non-MS (N=39)**	**61.5 (24)**	**64.1 (25)**	**46.2 (18)****	**35.9 (14)**	**15.4 (6)**	**2.6 (1)**	**5.1(2)**
% (N) in one or more areas	**MS out plaque (N=42)**	**61.9 (26)**	**85.7 (36)**	**78.6 (33)****	**33.3 (14)**	**2.4 (1)**	**0 0**	**0 0**
Pons % (N)	**Non-MS (N=39)**	12.8 (5)	23.1(9)**	7.7 (3)	10.3 (4)	2.6 (1)	0	0
	MS out-plaque (N=42)	11.9 (5)	52.4 (22)**	19.0 (8)	19.0 (8)	2.4 (1)	0	0
BG % (N)	**Non-MS(N=39)**	51.3 (20)	51.3 (20)	17.9 (7)	17.9 (7)	5.1 (2)	2.6 (1)	5.1 (2)
	MS out-plaque (N=42)	45.2 (19)	35.7 (15)	30.9 (13)	14.3 (6)	2.4 (1)	0	0
FWM % (N)	**Non-MS(N=39)**	33.3 (13)	35.9(14)	41.0 (16)	2.6 (1)	2.6 (1)	0	0
	MS out-plaque (N=42)	31.0 (13)	54.8 (23)	45.2 (19)	0	0	0	0
OWM % (N)	**Non-MS(N=39)**	20.5 (8)	35.9 (14)	35.9 (14)**	15.4 (6)*	5.1 (2)	0	0
	MS out-plaque (N=42)	35.7 (15)	54.8 (23)	64.3 (27)**	2.4 (1)*	0	0	0

Comparisons were made between non-MS and MS outside plaque (Chi-square test or Fisher exact test**p<0.01, *p<0.05).)

3.3.2.2. Testing the validity of Global cSVD Index

Consistent with being a valid score the Global cSVD Index increased with age at death in the whole cohort (N= 81, r=0.39, p<0.001) (**Figure 3.5 a.**). Global cSVD was higher in MS and non-MS cases that died secondary to vascular causes (N=19, median 8, IQR 3-10) compared to those that died of other causes of death (N= 62, median 4, IQR 2-6), p=0.009 (**Figure 3.5 b**.). In a binary logistic regression to predict vascular deaths (MI and or IS, PE/DVT) adjusting for age at death, the Global cSVD Index associated with this outcome (EXP (B) =1.23, 95%CI 1.03,1.48, p=0.02).

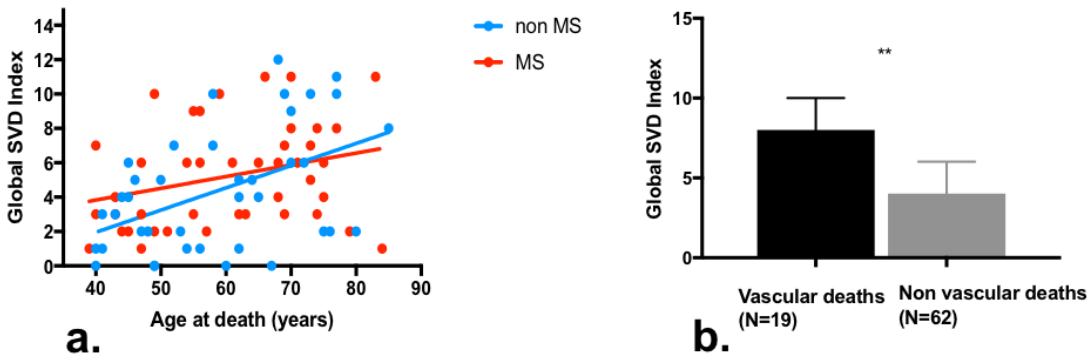

Figure 3.5. Global cSVD and Age at death in non-MS and MS

(**a**) and Global cSVD Index and all vascular causes of death (PE/DVT, MI, IS, other vascular) versus all non-vascular causes of death (all cases) (**b**) Consistent with being a valid score the Global cSVD Index increases with age at death and associates with vascular causes of death. **Mann-Whitney test p=0.009

Also, in favour of Global cSVD Index validity, in an ordinal logistic regression to predict total myelin rarefaction score, adjusting for age at death, this Index (B=0.23, 95%CI -0.02,0.05, p=0.004) associated with this outcome.

3.3.3. Global cSVD Index, SysVasc Score and cervical/intracranial atheroma in MS and non-MS

3.3.3.1. Global cSVD Index

Overall Global cSVD Index did not differ between MS (median 5.5, IQR 1-7.25) and non-MS (median 4 IQR 1-7) cases (p=0.146) (**Figure 3.6 a.**). When stratified by cause of death, no differences were found between MS and non-MS cases except in those that died from infection, where Global cSVD Index (n= 17, median 4, IQR 3-7) was higher than non-MS (n= 5, median 2, IQR 0.5-4) cases (p=0.01). cSVD scores for each brain region studied in MS and non-MS are highlighted in **Figure 3.6 b.** cSVD scores did not differ between MS and non-MS cases in any of the brain regions studied although there was a trend towards increased cSVD in the pons and OWM in MS compared to non-MS cases (p<0.09 for each).

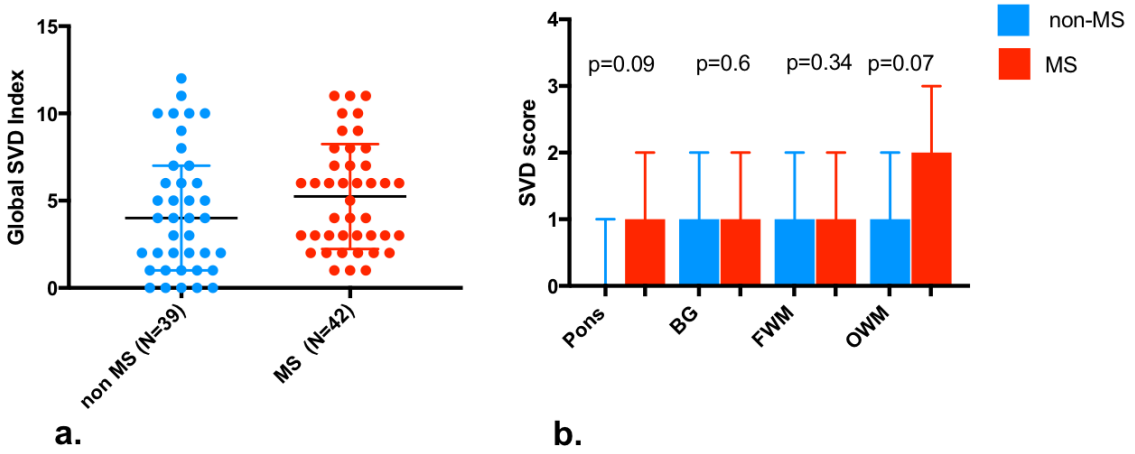

Figure 3.6. Global cSVD Index and cSVD per brain region in non-MS and MS (outside plaque)

3.3.3.2. SysVasc Score and cervical/intracranial arteries atheroma

SysVasc score did not differ between MS (0.31±0.29) and non-MS cases (0.32±0.23), p=0.63. It was possible to obtain a reproducible scoring of cervical artery in 34 out of 42 MS cases and 27 out of 39 non-MS cases and no differences were found between the groups (p=0.42). Large artery intracranial atheroma information was available in 34 out of 42 MS cases and in 30 out of 39 non-MS cases and this score did not differ between the two groups (p=0.31).

3.3.4. The influence of MS on Global cSVD Index considering age at death and SysVasc Score

As described above, overall Global cSVD Index did not differ between MS and non-MS cases. However, we have shown that age at death has an impact on the extent of SysVasc (Chapter 2) and cSVD (this chapter) in MS and non-MS cases.

The relationship between Global cSVD and SysVasc seems to be different in MS, where a positive correlation is found (r=0.46, p=0.002) compared with non-MS, where no significant association is seen (r=0.22, p=0.17) (**Figure 3.7 a.**). However, in a stepwise multivariate linear regression model built to predict Global cSVD Index considering age at death, SysVasc Score and MS status (**Table 3.5**), MS diagnosis does not associate with Global cSVD Index (B=0.74, 95%CI -0.59, 2.07, p=0.27). This the model explained 19.8% of the variance of Global cSVD Index.

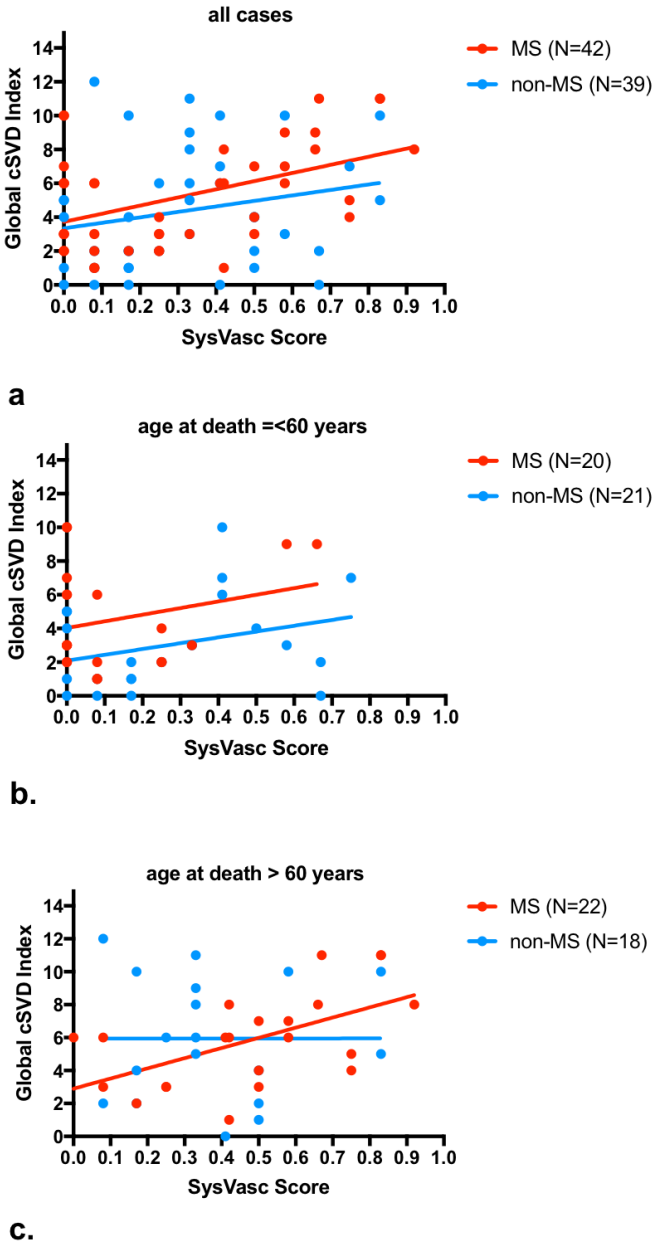

Figure 3.7. Relationship between SysVasc score and Global cSVD Index in all non-MS and MS and segregated by age at death

a. In all MS cases Global cSVD index severity increased with SysVasc burden but this association was not seen in all non-MS. For the same amount of SysVasc cSVD burden is higher in MS compared with non-MS in the younger at death group (**b.**) but this difference is not significant in the older at death group (**c.**) (see **Table 3.6** for details). In both age groups the burden of cSVD steeply increases with SysVasc severity in MS. However, in non-MS this association is only seen in the young at death group.

Since we had previously shown that the relationship between age at death and SysVasc score differed in MS versus non-MS, especially below the age of 65 years, the relationship between SysVasc score and Global cSVD was explored below (**Figure 3.7 b.**) and above (**Figure 3.7 c**.) the median age at death and a multivariate linear model to predict Global cSVD Index, considering SysVasc and MS diagnosis was run in each of these age at death groups (**Table 3.6**). Of note, no significant differences were found in demographic features and causes of death between age categories (**Table 3.4**)

In cases with age at death =<60 years, MS disease status impacted the extent of cSVD (B =2.03, 95%CI0.14, 3.92, p=0.036), as suggested by the graphical appearance of the data, where the intersect of the MS regression line was higher than of the non-MS line (**Figure 3.7 b.**). In contrast, in cases with age at death > 60 years, MS disease status did not impact cSVD (B =-0.50, 95%CI -2.5, 1.6, p=0.63) (**Figure 3.7 c.**).

Table 3.5. Numerical results of the multivariate linear regression stepwise model to predict Global cSVD Index considering age at death, SysVasc score and MS diagnosis.

Model	Parameter	B	95%CI	p	VIF
1	Intercept	-1.11	-4.32,2.1	0.49	
	Age at death	0.09	0.05,0.15	<0.01**	1.0
F –statistic: 14.1 on 1 and 79 DF, p<0.001					
2	Intercept	-0.48	0.02-0.13	0.77	
	Age at death	0.75	0.02, 0.13	0.01*	1.278
	SysVasc score	2.53	-0.3,5.3	0.08	1.278
F –statistic: 8.84 on 2 and 78 DF, p<0.001					
3	Intercept	-0.725	-4.0, 2.5	0.66	
	Age at death	0.073	0.01, 0.13	0.02*	1.278
	SysVasc score	2.62	-0.22,5.46	0.07	1.272
	MS	0.741	-0.59,2.07	0.27	1.008
F –statistic: 6.3 on 3 and 77 DF, p=0.001					

R^2 Model 1=0.152, R^2 Model 2=0.185, R^2 Model 3=0.198, VIF – variance inflation factor (measure of collinearity); DF – degrees of freedom, **p<0.01,* p<0.05

Table 3.6. Numerical results of the multivariate linear regression analysis to predict Global cSVD Index taking into SysVasc score above and below the median age at death

Model	Parameter	B	95%CI B	p
Age <=60	Intercept	2.03	0.34,3.72	0.020*
	MS_nonMS	2.03	0.14, 3.93	0.036*
	Systemic VD score	3.69	-0.39,7.77	0.075
Age >61	Intercept	4.46	2.24,6.68	<0.001**
	MS_nonMS	-0.50	-2.61,1.61	0.634
	Systemic VD score	3.96	-0.34, 8.26	0.070

R^2 Model (age <=60) = 0.140, R^2 Model (age >61) = 0.09; **p<0.01,* p<0.05

3.3.5. The influence of MS on individual cSVD pathologies

The Global cSVD Index is a composite variable. Some of its variables may be influenced differently by MS. The proportions of all individual cSVD pathologies in MS and non-MS per brain region are depicted in **Table 3.4.** Micro- and large infarcts as well as fibrinoid necrosis were rarely seen. **Figure 3.8.** illustrates the frequencies of the most commonly seen cSVD pathologies: arteriolosclerosis, PSD. PHL and microbleeds, in MS (outside plaque) and non-MS, per brain region. Overall, arteriolosclerosis did not differ between MS and non-MS cases. PSD and PHD were more commonly found in MS compared to non-MS, especially in the pons and OWM, while microbleeds and microinfarcts tended to be more common in non-MS, especially in the OWM.

In binary logistic regression models to predict individual cSVD pathologies, considering age at death and SysVasc burden, MS cases are more likely to have PSD (EXP (B)= 3.9, 95%CI 1.17,13.2, p=0.03) and PHL (EXP (B)=4.14, 95%CI 1.55,11.0, p=0.005) but tend to have less microinfarcts (EXP (B) =0.11, 95%CI 0.01, 1.03, p=0.05). MS did not influence arteriolosclerosis or microbleeds (see **Table 3.7.** for full results).

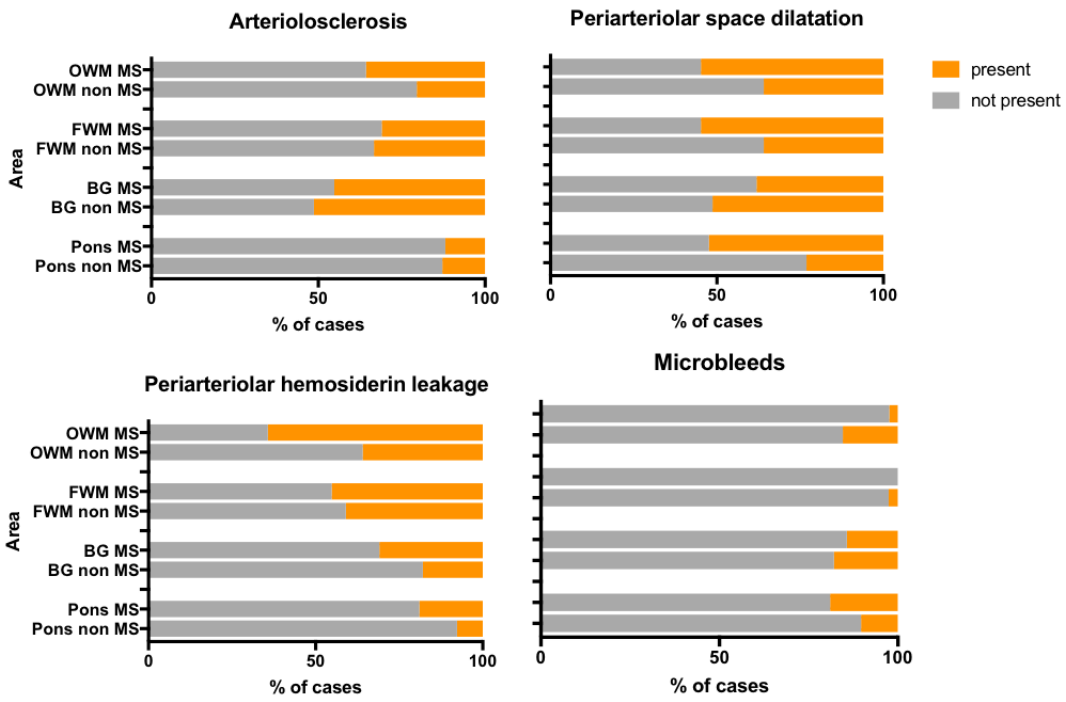

Figure 3.8. Individual cSVD pathologies per brain region in non-MS and MS (outside plaque).

All MS (N=42) and non-MS (N=39) cases were compared (exact proportions in Table 3.4.).

Table 3.7. Numerical results for binary logistic models to predict the influence of MS on individual cSVD pathologies adjusting for age at death and SysVasc burden.

	Arteriolosclerosis			Periarteriolar space dilatation			Periarteriolar hemosiderin leakage			Microbleeds			Micro-Infarcts		
Parameter	**Exp B**	**95%CI for Exp B**	**p**	**Exp B**	**95%CI for Exp B**	**p**	**Exp B**	**95%CI for Exp B**	**p**	**Exp B**	**95%CI for Exp B**	**p**	**Exp B**	**95%CI for Exp B**	**p**
Age at death	0.98	0.95,1.03	0.60	0.93	0.89,0.98	0.02*	0.97	0.93,1.01	0.17	0.97	0.93,1.01	0.13	0.97	0.91,1.04	0.38
SysVasc	0.25	0.03,1.90	0.18	0.32	0.02,4.31	0.39	2.44	0.30,19.68	0.52	0.69	0.09,5.01	0.72	0.97	0.91,1.04	0.38
MS	1.02	0.41,2.56	0.96	3.92	1.17,13.12	0.03*	4.14	1.55,11.04	<0.01**	0.83	0.32,2.14	0.71	0.11	0.01,1.04	0.05

*p<0.05, **p<0.01

3.3.6. The influence of MS on cSVD considering age at death cervical/intracranial large artery atheroma.

In the subset of cases where cervical and intracranial atheroma was available, the relationship between each of these variables and Global cSVD Index was explored, considering the MS diagnosis status and adjusting for age at death. Intracranial large artery atheroma associated with Global cSVD Index (EXP(B)=25.0, 95%CI 3.9,161.1, p=0.001) and the same was seen for cervical artery atheroma (EXP (B)=24.8, 95%CI 3.8, 161.4, p=0.001). MS did not influence cSVD in the whole cohort. However, as seen for SysVasc, in the young at death (=<60 years) group MS associated significantly with higher Global cSVD Index, even after adjusting for cervical atheroma (EXP(B)= 9.76, 95%CI 1.5,61.6, p=0.015).

3.3.7. Inside plaque cSVD and its relationship with outside plaque cSVD and SysVasc

3.3.7.1. The Global Inside Plaque cSVD Index and individual inside plaque cSVD pathologies

Inside plaque cSVD was scored in 38 out of the 42 MS cases. Thirty-seven plaques in the FWM, 31 in the OWM, 30 in the pons, and 22 in the BG were analysed. In the FWM, a second non-periventricular largest plaque was scored in 10 cases and in the OWM in 8 cases. A total of 18 periventricular, 13 subcortical and 8 juxtacortical plaques were scored in the FWM. In the OWM 18 periventricular, 11 subcortical and 3 juxtacortical plaques were examined. **Global Inside Plaque cSVD Index** was 3.1±2.3 (range 0-8.5) and was significantly lower than the corresponding Global cSVD Index (5.23±2.3) in the MS cases with at least one plaque (N=38) (p=0.0006).

To better assess the differences between in plaque and outside plaque cSVD, comparisons were made between the largest plaque and non-plaque regions of the same section and the results of the most commonly found cSVD pathologies are summarized in **Figure 3.9**. Only 1 microinfarct was seen inside a FWM plaque, no large infarcts or fibrinoid necrosis/microaneurysms were observed.

The FWM was assessed in 29 MS cases, the OWM in 23, the BG in 22 and the pons in 30. Arteriolosclerosis was more frequently seen outside (50.0%, 11 out of 22) plaque than inside plaque (27.7%, 5 out of 22) in the BG, p=0.001. Similar differences were found in the FWM where arteriolosclerosis was present in 31.1% (9 out of 29) outside versus and only in 10.3% (3 out of 29) inside plaque, p<0.001. No differences were found between outside and inside plaque arteriolosclerosis in the pons (5 out of 30, 16.6% vs 6 out of 30, 20.0%, p=0.990) or OWM (30.4% vs 26.1%, p=0.630). PSD was significantly more common inside (25 out of 30, 83.3%) than outside (15 out of 30, 50.0%) plaque in the pons (p=0.001) and BG (17 out of 22, 77.3% inside versus 10 of 22, 45.4% outside plaque, p=0.06). PHL was observed more frequently outside than inside plaque in all areas but differences were significant at the FWM (75% versus 25%, p=0.036) and OWM (69.6% versus 13.0%, p<0.001). No other asymmetries in the frequencies of other individual cSVD features were observed between plaque and non-plaque areas.

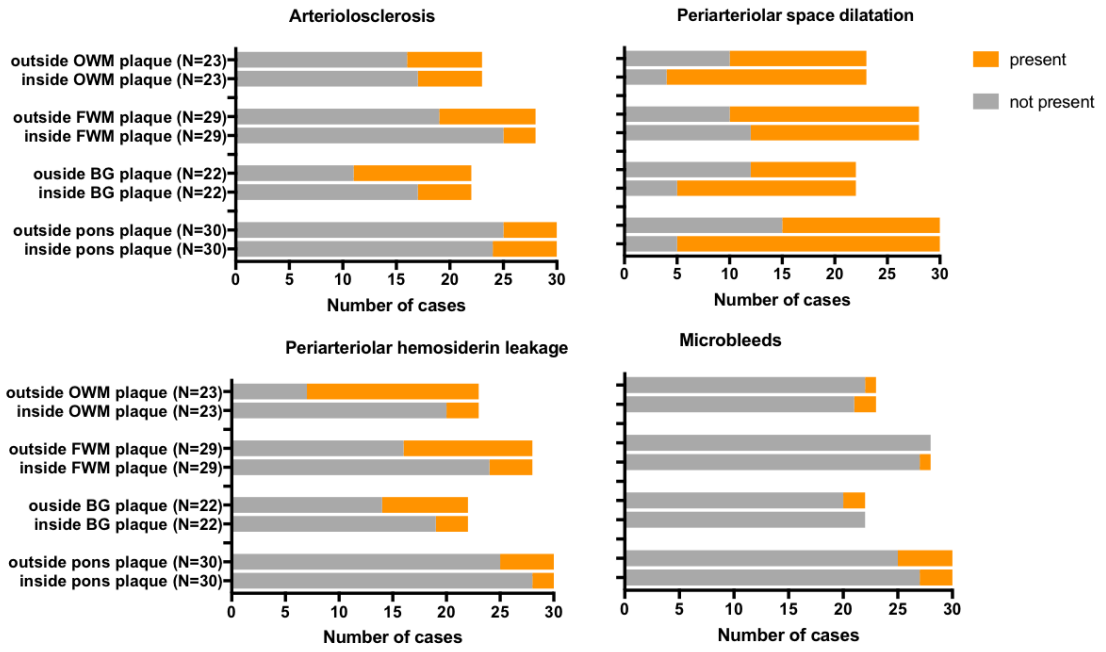

Figure 3.9. Inside and outside plaque cSVD per brain area

3.3.7.2. The relationship between Global Inside Plaque cSVD Index, Global cSVD Index and SysVasc

The Global Inside Plaque cSVD Index did no associate with Global cSVD Index (outside plaque) (N=39, r=0.12, p=0.45) nor with the SysVasc (r=-0.23, p=0.15) and this was still true after considering age at death (data not shown).

3.4. Summary of main findings

1. A robust and valid measure of cSVD type 1 burden, the Global cSVD Index, was devised and significantly associated with age at death, vascular deaths and myelin rarefaction
2. Global cSVD Index steeply increased with SysVasc in MS, but this association was not seen in non-MS
3. In cases that died at the age of 60 years or below, for the same SysVasc burden MS cases had a higher Global cSVD Index than non-MS cases. Global cSVD Index did not differ between MS and non-MS, considering SysVasc, in the older at death age group.
4. MS associates with a higher burden of PSD and PHL and with fewer microinfarcts but has no influence on arteriolosclerosis or microbleeds.
5. Overall arteriolosclerosis and periarteriolar hemosiderin deposition were more commonly seen outside plaque and PSD inside plaque. Global Inside Plaque cSVD Index was lower than Global cSVD Index and the two indexes were not correlated.

3.5. Discussion

A reliable and robust Global cSVD Index was devised, including several cSVD pathological features (Skrobot *et al.*, 2016), as a global measure of type 1 cSVD and thus of arteriolar and periarteriolar damage.

The frequencies of each cSVD pathology found in this study are similar to those reported in previous studies, except for PSD, PHL and microbleeds. *Skrobot et al*. reported arteriolosclerosis in one or more of the studied areas in 69% of the controls,

PSD were seen in 8%, infarcts being rare (5%) and haemorrhages, fibrinoid necrosis or microaneurysms were not observed. Although we have used long term formalin fixed tissue no correlation between year of death and PSD scores was found. A possible explanation of the discrepancy between these results and previous studies is that, in the present study, scores were obtained from magnified scanned images and this may have increased sensitivity to detect PSD, PHL, and microbleeds compared to the traditional microscopic scoring.

Global cSVD Index steeply increases with SysVasc in MS, but this association is not seen in non-MS. The relationship between large artery arteriolosclerosis and cSVD in the general population is unclear and has not been explored in MS. In non-MS cases large artery atheroma has been reported to have only a small effect on brain WM changes, an indirect marker of cSVD (Wardlaw *et al.*, 2014), but other studies suggest a stronger association between cervical (Ding *et al.*, 2017), intracranial (Del Brutto and Mera, 2017) and aortic arterial atheroma (Song *et al.*, 2016) and other cSVD imaging markers. This association may be influenced by increased systemic and atheroma plaque inflammation (Ding *et al.*, 2017) suggesting that inflammation may strengthen the relationship between SysVasc and cSVD, as seen in MS cases included the present study.

One of this work's main findings is that in cases that died at the age of 60 or below, for the same SysVasc burden MS cases had a higher Global cSVD Index than non-MS cases. It is possible that MS cases that die at young ages have severe active MS, with a higher burden of inflammation that might contribute to peri-arteriolar damage outside plaque. This hypothesis will be tested in Chapter 5 but for the moment, in this age at

death group, features of an arteriolopathy outside MS plaques were observed and this has been ignored in the past. The arteriole plays an insignificant role in the classical MS pathological descriptions and the peri-arteriolar changes may be an end process of ongoing inflammation. Indeed, a higher burden of imaging markers of cSVD, particularly perivascular space enlargement, has been demonstrated in other inflammatory disorders, such as SLE (Wiseman *et al.*, 2016) and perivascular hemosiderin deposition has been induced in an animal model of inflammation (Sumbria *et al.*, 2016).

Global cSVD Index did not differ between MS and non-MS, considering SysVasc, in the cases that died above the age of 60 years. MS cases that survived to later ages had the opportunity to be exposed to VRF for a longer period of time and may have had a less aggressive MS. In this older age at death group MS alone does not influence cSVD. However, in presence of SysVasc, MS cases have an excess of cSVD compared with non-MS. This data supports that MS patients with vascular comorbidities have an increased risk of cerebral cSVD and this might be a contributor factor for worse clinical outcomes.

The association between SysVasc burden and cSVD has not been found in non-MS cases that died above the age of 60, whereas a positive association was seen in those that died at younger ages. A similar discrepancy can be found in the literature, studies reporting no relationship between cSVD and large artery atheroma including older cases (Wardlaw *et al.*, 2014) than those included in studies where a positive relationship was found (Song *et al.*, 2016). Increased internal carotid artery stiffness has been related to cSVD burden *in vivo* in cases below the age of 70 years but not

above this age (Lau *et al.*, 2018). These reports and this study results suggest that the nature of the relationship between large artery atheroma and cSVD is influenced by age. Nevertheless, I am aware that in the spread of Global cSVD Indexes documented in this study is relatively narrow in both MS and non-MS groups and different relationships could potentially be observed if cases with the full spectrum of cSVD burden are included (i.e. older cohort).

A higher burden of PSD, both outside and inside plaque and of PHL outside plaque was seen in MS compared with non-MS. PSD has been described in MS and associated with brain volume loss (Kilsdonk *et al.*, 2015) but whether these corresponded to peri-arteriolar space dilatation or only to peri-venular space dilatation had not been investigated to date. Hemosiderin deposition around plaque and peri-plaque veins and venules has been described in up to 21 out of 70 MS cases (30%) (Adams, 1988) but had not been quantified around arterioles. In line with this chapter's results, iron content has shown to be highest in NAWM, followed by the peri plaque WM, and lowest inside plaques (Popescu B et al. Acta Neuropathol 2017). The accumulation of plaques in specific anatomic locations, such as the periventricular areas, where the density of arterioles is lower than in the adjacent subcortical areas, may have led to an underestimation of cSVD pathologies inside plaque. Nevertheless, the arteriole seems to be predominantly affected outside plaque.

The fact that only PSD and PHL but not arteriolosclerosis was seen in excess in MS, especially in young at death cases, with a low SysVasc burden, suggests that the observed arteriolar and peri-arteriolar changes relate to MS and not to an increased burden of type 1 cSVD.

4 The influence of MS on cerebral periarteriolar/perivenular inflammation and venous collagenosis

4.1. Introduction

In the previous chapter it was shown that MS influences PSD and PHL, especially in cases that died young, but not other type 1 cSVD pathologies. Inflammatory and immunological mediated cSVD have been considered to be a separate type of cSVD, the type 4. MS has not been included as a cause of cSVD but it is possible that the acute and chronic inflammatory CNS milieu characteristic of MS might lead to small vessel injury. While looking at the most common age- and VRF- related cSVD type pathologies, I have concentrated, in that chapter, on the arteriole and did not consider other pathologies that might be relevant for MS pathology such as periarteriolar/perivenular inflammation and venous collagenosis.

Changes in the small venules, with thickening of the vessel wall and collagenosis feature in MS, particularly within the MS plaque (Adams *et al.*, 1987; Dal-Bianco *et al.*, 2015). In non-MS, more attention has been recently paid to venous collagenosis (type 5 cSVD) (Moody *et al.*, 1995; Brown *et al.*, 2002; Ibrahim *et al.*, 2017; Keith *et al.*, 2017; Hartmann *et al.*, 2018) as an important driver of WML burden, periventricular infarcts and cognitive dysfunction. These venous changes occur preferentially around the ventricles but the periventricular cSVD has never been quantified specifically in this area in MS. Chapter 4 main research questions are:

1. Is periarteriolar and perivenular inflammation, outside and inside the MS plaque, increased in MS compared with non-MS considering age at death and

SysVasc? How does periarteriolar and perivenular inflammation relate with the Global cSVD Index?

It is possible that MS associates with increased periarteriolar and perivenular inflammation compared with non-MS.

To test this hypothesis, I aim to:

a. compare peri-arteriolar and peri-venular inflammation between MS (inside and outside plaque) and non-MS cases;
b. to investigate the relationship between these two pathologies and the Global cSVD Index.

I would also like to explore the following questions:

2. What is the influence of MS on periventricular cSVD burden?
3. What is the influence of MS on venous collagenosis?

It is possible that MS associates with a higher burden of cSVD in the periventricular area and with a higher burden of venous collagenosis both outside plaque and in the periventricular area. To test these hypotheses, my aims are to:

c. compare frontal WM periventricular cSVD between MS and non-MS cases
d. quantify and compare venous collagenosis, in and outside the periventricular area, between MS and non-MS cases.

Finally, I will also explore and describe cSVD changes that may be specific to MS.

4.2. Materials and Methods

4.2.1. Study population and tissue sampling

Brain tissue was obtained from pathologically confirmed MS (N=42) and non-MS (N=39) cases where SysVasc burden had been characterized and tissue sampling was performed as described in Chapters 2 and 3, sections 2.2.2 and 3.2.

4.2.2. Neuropathological assessment

FFPE 10 μm sections of the FWM, OWM, BG and pons were stained with H&E and immunostained with primary antibodies for myelin PLP and for SMA (counterstained with haematoxylin) as described in Chapter 3 (section 3.2.3). Stained histology sections of the 4 brain areas of interest were scanned 20X magnification using Scannoscope and images were analysed with Aperio ImageScope software.

4.2.2.1. Periarteriolar and perivenular inflammation and venous collagenosis scoring

Adding to the well-established cSVD features described in Chapter 3, section 3.2.3.1, morphological changes in the small cerebral arterioles and veins and their surrounding perivascular space were explored and described in this chapter's **Table 4.1.** Periarteriolar and perivenular inflammation was scored in the FWM, OWM, BG and pons. **Total periarteriolar** and **total perivenular** scores were then obtained by summing the scores from all areas.

Venous collagenosis scoring was performed in the pons and FWM only and in this section the periventricular area was scored separately as describe below for non-MS and MS (**Figure 4.1 a.**).

Table 4.1. Additionally scored cSVD features

Additional scored features		Example
Medium caliber (50-150 μm) and smaller veins collagenosis	0= absent 1= present ≥10% of partial occluded or occluded small veins in the examined area	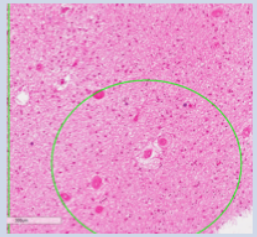
Larger veins collagenosis	0=absent 1=five or more concentric wall layers were seen in a cross sectional section of the vessel and this was observed in three or more veins of the examined area	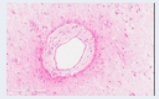
Perivenular inflammation	0= absent 1= present (> 5 WBC in the perivascular space)	
Periarteriolar inflammation	0= absent 1= present (> 5 WBC in the perivascular space)	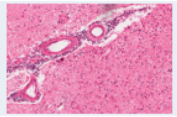

4.2.2.2. Scoring cSVD in the FWM periventricular area

In the periventricular FWM (within 5 mm from the ventricle lining) cSVD scoring (including all features described in Chapter 3, section 3.2.3.1, **Table 3.2**. and those described in this chapter **Table 4.1**) was performed in 15 1x1x1 mm squares as depicted in **Figure 4.1 a.** In the FWM WM sections of MS cases, cSVD scoring was split into 3 regions:

- Periventricular FWM outside plaque (within 5 mm from the ventricle lining). In this region cSVD scoring was performed in 15 1x1x1 mm squares as depicted in **Figure 4.1 a.**
- Periventricular FWM inside plaque (**Figure 4.b**.)
- FWM outside plaque (**Figure 4.b**.)
- FWM inside plaque (**Figure 4.b**.)

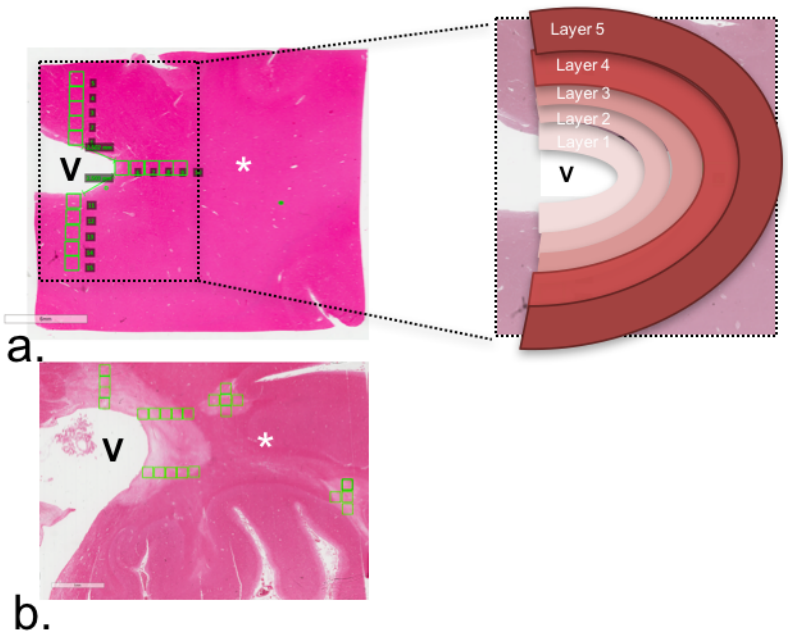

Figure 4.1. Scoring of cSVD in FWM

Scoring of FWM sections in non-MS (**a**.) and MS (**b**.) In the periventricular area 15 squares were scored from the ventricle (V) surface outwards. Median cSVD scores from the three squares adjacent to the ventricle was calculated to compute Layer 1 cSVD score and the same was repeated for the next group of three squares lying outwards from layer 1 as illustrated within the dashed rectangles (**a**.). The whole FWM 5mm from the ventricular surface was scored (white stars). In MS cSVD inside plaques (periventricular, subcortical or juxtacortical) was scored separately (**b**. green squares cross).

4.2.3. Statistical Analysis

Descriptive statistics, univariate analysis was performed as described in Chapter 2, section 2.2.3. Ordinal and binary regression models were fitted to evaluate the influence of MS diagnosis on outside plaque all areas peri-arteriolar, peri-venular inflammation and venous collagenosis whilst controlling for age at death, sex, post mortem delay and SysVasc score. All tests of hypothesis were carried out using two-sided tests and p-values of less than 0.05 were considered significant. SPSS version 25 and Graph Prism 7 were used for the statistical analysis and plots.

4.3. Results

4.3.1. Cohort characteristics

Forty-two out of the 85 MS cases (mean age 60.6 ±12.9 years, 57.1% females) and 39 out of the 68 non-MS cases (mean age 58.8 ±12.9 years, 56.5 % females), where cardiovascular burden as measured by the SysVasc Score (Chapter 2) and cSVD (Chapter 3), as measured by the Global cSVD Index, were previously characterized, were included for neuropathological assessment. Demographic and clinical features of the cohort used in Chapter 4 were described in Chapter 3 (section 3.3.1).

4.3.2. Periarteriolar and perivenular inflammation

4.3.2.1. Periarteriolar and perivenular inflammation in MS outside plaque and non-MS

The frequencies of periarteriolar and perivenular inflammation, per brain region, in non-MS and MS cases (outside plaque) are summarized in **Table 4.2** and **Figure 4.2** and described below.

Peri-arteriolar inflammation in one or more regions was higher in MS outside plaque (76.2%) than in non-MS cases (59.0%), p=0.01 and this difference was driven by the pons (38.1% in MS compared to 10.3% in non-MS, p=0.009) and FWM (54.8% in MS compared to 30.8% in non-MS, p=0.04) (**Figure 4.2 a.**). In a ordinal logistic regression model to predict all areas outside plaque periarteriolar inflammation, adjusting for age at death, sex, and SysVasc, MS cases were 3.4 times more likely to present this outcome (EXP(B)= 3.44, 95%CI 1.51, 7.83, p=0.003).

In MS, outside plaque periarteriolar inflammation did not correlate with the Global cSVD Index ($r\tau$=0.04, p=0.74). Though it correlated with PSD ($r\tau$=0.27, p=0.01), no association was found with any other individual cSVD pathologies in this group. In non-MS cases peri-arteriolar inflammation did not correlate with Global cSVD Index ($r\tau$=0.06, p=0.68) nor with any of the individual cSVD pathologies studied (data no shown).

Perivenular inflammation in one or more regions was significantly more common in MS outside plaque (61.9%) than in non-MS cases (15.4%), p<0.001. This difference was observed in all studied brain areas (**Figure 4.2 b.**). In an ordinal logistic regression model, MS cases had 10 times more perivenular inflammation (EXP(B)=10.3, 95%CI 3.5, 30.47 p<0.001) than non-MS cases.

Perivenular inflammation did not associate with the Global cSVD Index in MS (outside plaque) ($r\tau$=-0.16, p=0.23) nor in non-MS cases ($r\tau$=0.24, p=0.08).

In MS, peri-venular inflammation correlated with peri-arteriolar inflammation ($r\tau$=0.32, p=0.015). No other significant relationships were found between perivenular inflammation with any of individual cSVD features in MS and non-MS cases.

Table 4.2. Periarteriolar and perivenular inflammation per brain region in non-MS and MS (outside plaque)

		Periarteriolar Inflammation	Perivenular Inflammation
% (N) in one or more areas	**Non-MS (N=39)** **MS out-plaque (N=42)**	**59.0 (23)** **76.2 (32)**	**15.4 (6)** **61.9 (26)**
Pons % (N)	**Non-MS (N=39)**	10.3 (4)**	5.1 (2)**
	MS out-plaque (N=42)	38.1 (16)**	31.0 (13)**
BG % (N)	**Non-MS (N=39)**	15.4 (6)	7.7 (3)*
	MS out-plaque (N=42)	31.0 (13)	28.6 (12)*
FWM % (N)	**Non-MS (N=39)**	30.8 (12)*	7.7 (3)**
	MS out-plaque (N=42)	54.8 (23)*	31.0 (13)**
OWM % (N)	**Non-MS (N=39)**	38.5 (15)	7.7 (3)**
	MS out-plaque (N=42)	52.4 (22)	33.3 (14)**

Comparisons were made for non-MS versus MS outside plaque only Chi-square/Fisher exact test *p<0.05, ** p<0.01

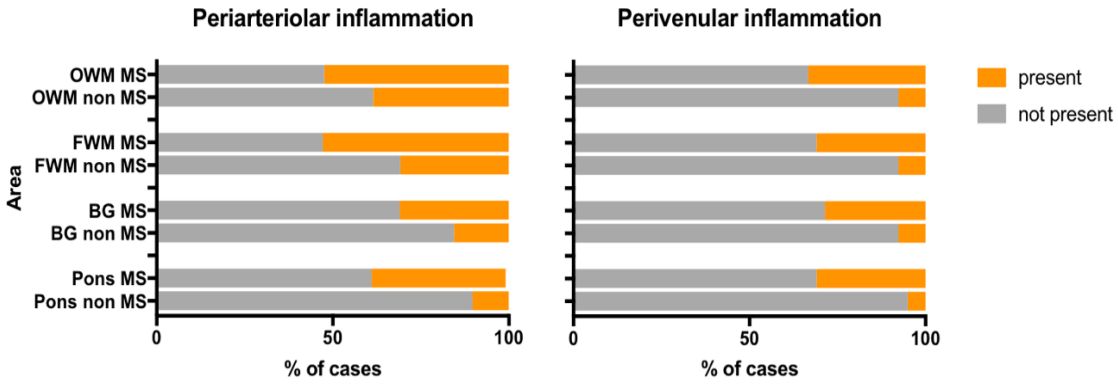

Figure 4.2. Periarteriolar (a) and perivenular (b) inflammation per brain region in non-MS and MS (outside plaque)

4.3.3.2 Periarteriolar and perivenular inflammation in MS outside plaque versus inside plaque

Periarteriolar inflammation inside plaque in one or more areas was present in 20 out of 38 (52.6%) of the MS cases with plaques but a higher proportion of these cases showed outside plaque periarteriolar inflammation (30 out of 38, 78.8%), p=0.02. This was evident in all brain areas but particularly when comparing the outside plaque FWM (23 out of 29, 79.3%) with inside plaque within cases (8 out of 29, 27.6%, p<0.001), similarly to what was previously done in Chapter 3, section 3.3.71. and illustrated in **Figure 4.3**.

Plaque perivenous inflammation in one or more areas was present in 25 out of 38 (65.8%) of the MS cases with plaques and overall a similar a proportion of perivenular inflammation was seen outside plaque (65.8%). However, when perivenular inflammation was compared per brain region, this feature was more commonly seen inside plaque (18 out of 30, 60.0%) than outside plaque (10 out of 30, 33.3%), p=0.04 in the pons but differences were not significant in the other brain areas (**Figure 4.3**).

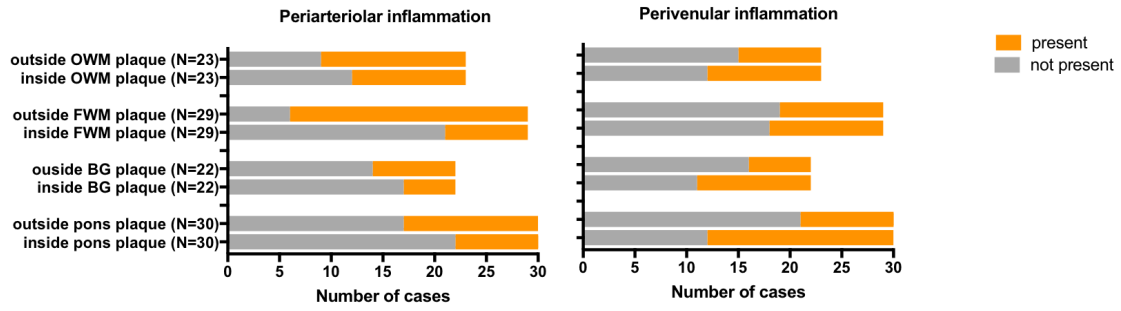

Figure 4.3. Periarteriolar and perivenular inflammation inside and outside plaque per brain area

4.3.3. FWM periventricular cSVD in non-MS and MS

cSVD was scored in the FWM periventricular area, as described in **Figure 4.1 a.**, in non-MS cases and MS cases outside periventricular plaques. A total of 178 arterioles (0.32±0.17 arteriole per mm^3) with a diameter of 20-150 μm was observed in non-MS and 115 (0.24±0.14 arteriole per mm^3) in MS. **Figure 4.4.** illustrates cSVD scoring per layer in MS and non-MS. cSVD scores in the periventricular area of non-MS cases and of MS cases with no periventricular plaques were lower than cSVD scores outside the periventricular area with similar scores (median=0, range 0-1) in both groups (p=0.53).

The proportion of cases with one or more of each cSVD pathology was also explored. The most common pathological feature was PSD seen in 51.4% (18 out of 35) non-MS and 69.4% (16 out of 23) MS cases in the total periventricular area. Arteriolosclerosis was observed 22.8 % (8 out of 35) of non-MS and in 21.7 % (5 out of 23) MS cases. PHL was only present in the periventricular area in 5.7% (2 out of 35) non-MS cases and was absent in this region in MS cases. These proportions were not significantly

different. None of the other individual cSVD features were identified in FWM periventricular area.

The proportion of cases with a median cSVD score of 1 in all areas was similar in non-MS (2.9%, 1 out of 35) and MS cases (8.6%, 2 out of 23), p=0.56 and no differences between the groups were found for individual periventricular layers. In non-MS, outside periventricular area FWM cSVD correlated with layer 4 (r=0.43, p=0.01) and layer 5 (r=0.35, p=0.042) cSVD but not with layers 1 to 3 cSVD. In MS cases no correlation was found between any of the periventricular layers cSVD and FWM cSVD outside the periventricular area.

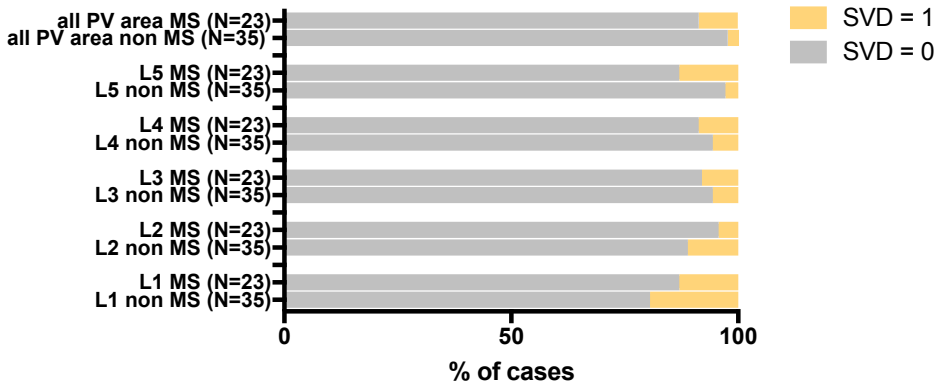

Figure 4.4. cSVD per FWM periventricular layer in non-MS and MS cases without periventricular plaques.

L1 adjacent to the ventricle and L5 4 cm from the ventricle; all PV area = median cSVD of all layers

4.3.4. Venous collagenosis

In the FWM, **outside the periventricular area**, venous collagenosis was present in 5 out of 42 (11.9%) MS cases (outside plaque) while it was rarely seen in non-MS (1 out

of 39, 2.6%) p=0.118 (**Figure 4.5.**). Outside periventricular FWM area venous collagenosis did not correlate with age at death (non-MS r= -0.06, p=0.96, MS r= -0.48, p=0.71), nor with FWM outside periventricular area cSVD scores (non-MS $r\tau$= 0.12, p=0.32, MS $r\tau$ = -0.05, p=0.72) and was not related to SysVasc (non-MS $r\tau$= 0.21, p=0.30, MS $r\tau$ = -0.19, p=0.09) in any of the groups.

Periventricular FWM vein collagenosis was found in Layer 1 only in non-MS cases (N=35, 13.5%). Similar frequencies of large (8.0%) and small vein (10.0%) collagenosis were seen in non-MS. In MS, it was present in both Layer 1 (21.7% of 23 MS cases with no periventricular plaque) and 2 (21.7% of 23 MS cases with no periventricular plaque) but not in the outer periventricular layers (**Figure 4.5.**). Small vein collagenosis was seen in 6.0% of MS cases whilst large vein collagenosis was observed in 18.0%. Small vein collagenosis was only seen in Layer 1 in both MS and non-MS. FWM periventricular venous collagenosis tended to increase with FWM venous collagenosis outside the periventricular area in MS ($r\tau$=0.35, p=0.06) but no association was seen in non-MS ($r\tau$=0.19, p=0.30). No association was found between FWM periventricular venous collagenosis and age at death, cSVD inside or outside the periventricular area, or with SysVasc, in any of the groups.

In the pons **outside plaque venous collagenosis** was significantly more common in MS (21.4%, 9 out of 42) than in non-MS (5.1%, 2 out of 39) (p=0.002).

Large vein collagenosis was seen inside 20 out of 31 (64.5%) FWM plaques, 23 out of 31 (74.2%) OWM plaques, 10 out of 22 (45.5%) BG plaques and 10 out of 30 (33.3%) pons plaques.

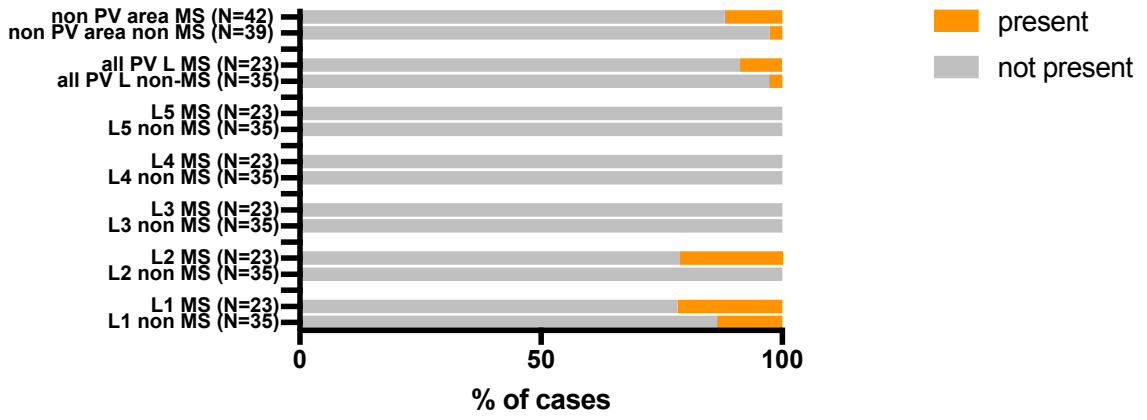

Figure 4.5. Venous collagenosis per FWM periventricular layer and outside PV area in non-MS and MS cases without periventricular plaques.

L- layer, PV – periventricular, L1 adjacent to the ventricle and L5 4 cm from the ventricle.

4.3.5. Description of peri-arteriolar changes in MS

Although PSD is a feature of cSVD it can be found in MS. Possible differentiating features will be described below. While in age/VRF related cSVD the whole perivascular tissue can show some loosening, in MS very well demarcated perivascular spaces were observed in some cases with strands of fibrous material inside these spaces that resembled veils (**Figure 4.6.**).

In MS, these periarteriolar veils were detected in 16.6 % (7 out 42 cases) outside plaque FWM, 37.7% (14 out of 37 plaques) inside FWM plaques, but were rarely seen in non-MS FWM (5.1%, 2 out of 39 cases). They were detected in in 23.8% (12 out of 42) outside plaque OWM and in 41.9%(13 out of 31 plaques) OWM plaques and were uncommon in non-MS OWM (2 out of 39, 5.1%) (**Figure 4.7.**). In a binary regression model to predict presence of veils (FWM or OWM) including MS disease status, age at

death and SysVasc as explanatory variables, MS associated with more of this pathological outcome (Exp (B)=6.59, 95%CI 1.85,23.48, p=0.004).

In MS, the presence of arteriolar veils did not associate with the Global cSVD Index ($r\tau$=0.14, p=0.30) but was negatively associated with SysVasc burden ($r\tau$=-0.29, p=0.03). This characteristic type of PSD did not correlate with periarteriolar ($r\tau$=0.089, p=0.52) nor with perivenular ($r\tau$=0.209, p=0.14) inflammation.

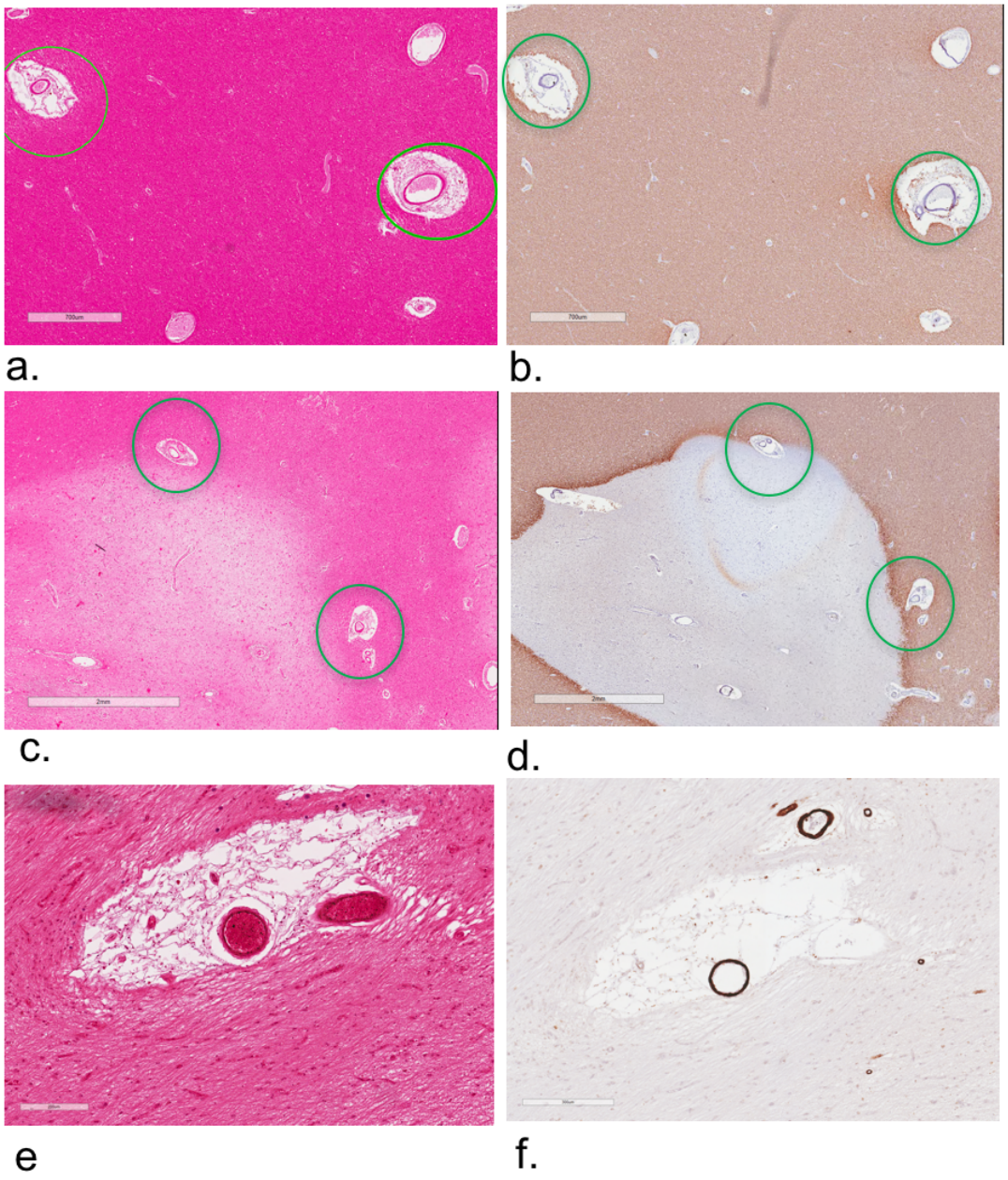

Figure 4.6. Periarteriolar veils

Perivascular space dilatation was found in MS cases around arterioles as seen in H&E stain of FWM (**a.** (green circles), **c.** and **e.**) and in SMA staining (**f.**). These PSDs were found in areas of normal PLP staining (**b.** (green circles)) and at plaque edges (**d.** (green circles)). The latter were classified as inside plaque veils.

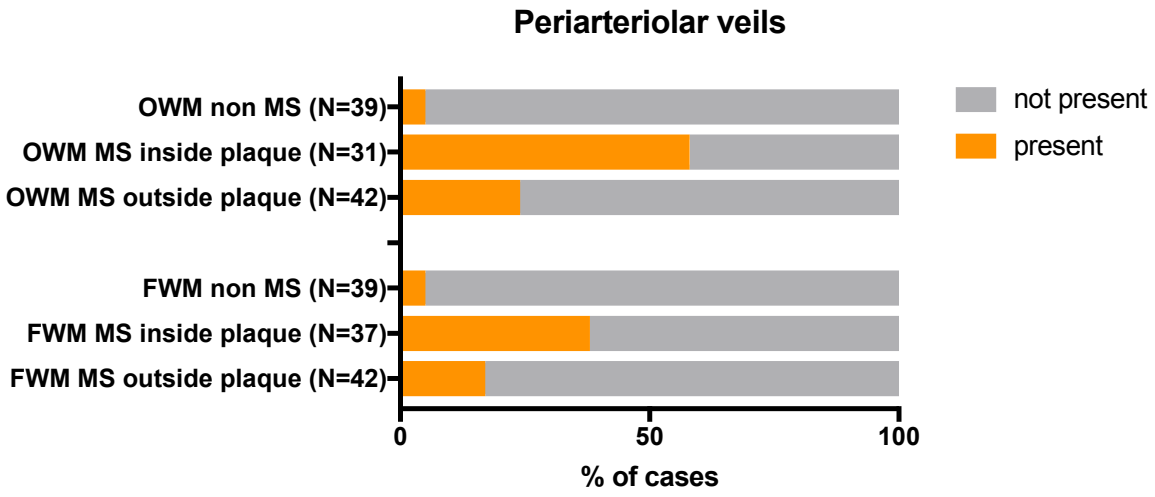

Figure 4.7. Peri-arteriolar veils in MS (inside and outside plaque) and non-MS

4.4. Summary of the main findings

1. Periarteriolar inflammation was 3.4 times more common in MS outside plaque than in non-MS. This feature associated with PSD and was more commonly seen outside than inside the MS plaque.
2. Perivenular inflammation was 10 times more likely to occur in MS outside plaque than in non-MS. This feature correlated with periarteriolar inflammation but not with any other cSVD pathology.
3. In the FWM periventricular area, cSVD pathologies, especially periarteriolar hemosiderin deposition, were seen in similar low proportion both MS and non-MS cases
4. Venous collagenosis was seen in non-MS mostly in an area adjacent to the ventricular wall and rarely outside the periventricular areas, while in MS, venous collagenosis was seen in a higher proportion outside this area, even outside the MS plaque.

5. Up to one fifth of the MS cases present well demarcated, enlarged periarteriolar spaces, often filled with fibrous tissues, resembling veils. This pathologic feature is rarely seen in non-MS.

4.5. Discussion

This study has shown that, periarteriolar inflammation was increased in MS, particularly outside plaque. *In vivo*, cerebral blood flow was found to be reduced in NAWM in MS compared with controls (Law *et al.*, 2004) and this could relate with reduced axonal activity, astrocyte metabolism, increased concentrations in endothelin (D'haeseleer *et al.*, 2011) or fibrin deposition and occlusion of small veins and capillaries (Putman and Adler, 1937; Wakefield *et al.*, 1994). Nevertheless, peri-arteriolar inflammation might contribute to the hemodynamic changes found in NAWM. Moreover, it is also possible that, despite still being present at end-stage MS, periarteriolar inflammation plays an important role in early MS pathology. Indeed, the expression of an important extracellular matrix component (laminin) receptor, predominantly restricted to the arterioles, has shown to be upregulated in the acute and later stages of an EAE model of chronic progressive MS. The upregulation of this receptor is thought to be a response to the threat of leukocyte infiltration and to aim at strengthening the linkage between basal lamina laminin and the cytoskeletal proteins of endothelial cells, resulting in enhanced BBB integrity (Welser *et al.*, 2017). The efficiency of arteriole response to inflammation may then be a key factor for the development of further MS pathology.

This study sheds some light on the distribution of cSVD in MS and non-MS, by exploring the FWM periventricular area. This area is commonly affected in age/VRF related cSVD

and MS. The fact that this brain region is poorly vascularized (Martinez Sosa and Smith, 2017) may be partially responsible for its vulnerability to damage. In MS, particularly in the SPMS phase, tissue structural abnormalities in the NAWM seem to be greatest near the ventricles, as measured by magnetization transfer ratios (Liu *et al.*, 2015). I have scored cSVD pathologies in concentric layers from the frontal horn periventricular wall, in both MS and non-MS, and found no differences between the two groups. Indeed, cSVD scores were much lower in the inside the periventricular area than the outside. For these reasons, major arteriolar structural changes in this brain region are unlikely to explain the above-mentioned gradient of tissue loss in MS periventricular NAWM.

Periarteriolar hemosiderin deposition was absent in MS in periventricular FWM, outside plaque, in line with other studies looking at iron content in periventricular lesions (Li *et al.*, 2016; Bagnato *et al.*, 2018). Considering that this area is prone to axonal loosening, with consequent decrease in oligodendrocytes - an important source of iron - a lower iron content may be expected even in non-lesional periventricular areas.

In line with the literature, this study confirmed that small veins are frequently affected in MS, venous collagenosis being particularly common in the MS plaque. However, outside plaque venous collagenosis, including in the periventricular area, was much less frequently seen and was only slightly more common in MS than in non-MS. This was particularly true for small vein collagenosis that occurs adjacent to the ventricular surface, which did not differ between groups. Nonetheless, a gradient of venular changes could be seen in both groups, venous collagenosis being observed most

exclusively at the inner periventricular layers but in MS extending slightly more outwards than in non-MS.

As previously shown, PSD features in MS pathology. Herein I have identified characteristic enlargement and morphology of the peri-arteriolar spaces, which, having the appearance of a well compartmentalized space where crossing strands of fibrous tissue could be observed, which were named “veils”. Cuffs of inflammatory cells in the Virchow-Robin spaces have been described to be prominent features of acute MS plaques (Esiri and Gay, 1990). They were commonly seen around venules, where the perivascular space was described to contain strands of fibrin, and were also found in areas of preserved myelin (Adams *et al.*, 1985). Inflammatory perivascular cuffs are also seen in the animal model experimental encephalomyelitis around post-capillary venules (Agrawal *et al.*, 2013). Likewise, it is possible that the periarteriolar space is affected in MS but this has not been clearly documented in the literature. Most studies do not use markers to differentiate small veins from arterioles and this may sometimes be challenging. I have used SMA immunostaining, along with the morphological features seen in H&E, to identify small arterioles. By doing so I am confident that “veils” were seen around arterioles.

Periarteriolar “veils” were clearly more commonly seen in MS than in non-MS but the relevance of these structures in MS pathology remains to be explored. Veils might represent the remnants of resolved periarteriolar inflammation. In MS at any one time, an eventual stimulating effect may be confined to the cells in the perivascular space. This confinement of the inflammatory reaction to this space might avoid active

damage of the surrounding myelin (Esiri and Gay, 1990) and this could explain why these structures were also seen in NAWM.

Although this study has contributed to the better understanding of cSVD in MS, many aspects of this association have not been addressed. I have concentrated on the most common cSVD features. CAA, the second most common type of cSVD in the general population, was not studied and the exact burden of periarteriolar/perivenular inflammation has not been quantified nor further characterized. This study was restricted to brain regions that are commonly affected in in age/VRF cSVD and thus the full spectrum of vascular changes in MS may not fully be appreciated. Nevertheless, by using objective pathology measures in a unique cohort where information on SysVasc was available, this study has evidenced that, as in other inflammatory disorders, MS leads to small vessel vasculopathy.

5 The influence of systemic and cerebral vascular disease on MS pathological outcomes: a *post mortem study*

5.1. Introduction

In the previous chapters have improved the knowledge on the relationship between SysVasc and cSVD in MS and implicated MS in the injury of cerebral small vessels. Yet the influence of the devised measures of vascular disease on MS pathology outcomes has not been studied.

In this thesis I aim to further advance the understanding on how vascular comorbidities influence MS pathological and radiological outcomes. As previously mentioned, the presence of vascular comorbidities in MS has been associated with faster MS disability progression (Marrie *et al.*, 2010) and increased WML load as assessed by brain imaging (Kappus *et al.*, 2015). One possible explanation for this association is that SysVasc and cerebrovascular disease adversely affects MS pathological outcomes; by contributing to hypoxia and hypoperfusion they may influence MS lesion distribution and expansion (Frischer *et al.*, 2015; Desai *et al.*, 2016; Haider *et al.*, 2016; Geraldes *et al.*, 2017; Martinez Sosa and Smith, 2017). Furthermore, SysVasc and cSVD may promote BBB breakdown (Bridges *et al.*, 2014; Brown *et al.*, 2018) and, consequently exaggerate CNS inflammatory response, in MS. However, the relationship between post mortem measures of cardiovascular and cerebrovascular burden and MS pathological outcomes has not been investigated so far. My main research questions and hypotheses for this chapter are:

1. Does SysVasc associate with a higher burden of demyelination and MS lesion inflammatory activity?

- It is possible that demyelination load and lesion activity increases with SysVasc severity

2. What is the relationship between demyelination and MS lesion inflammatory activity and outside plaque cerebral cSVD?
    - I hypothesize that the Global cSVD Index severity will associate with a higher demyelination burden and MS lesion activity

To test these hypotheses, my aims are:

1. To investigate the effect of cardiovascular disease burden, as measured by the SysVasc Score, on the total number and area of MS plaques and on the number of active plaques in an MS *post mortem* cohort
2. To investigate the relationship between outside plaque cSVD, as measured by the Global cSVD Index, and the total number and area of MS plaques and on the number of active plaques in an MS *post mortem* cohort.

I would also like to explore the following research question and hypothesis:

3. What is the relationship between each individual cSVD pathology and MS demyelination and lesion inflammation outcomes?
    - It is possible that some of the cSVD pathologies will have a stronger association with MS demyelination and lesion inflammation outcomes.

To explore this hypothesis, I aim to determine the relationship of each cSVD pathology with the total number and area of MS plaques and the number of active plaques in the same MS *post mortem* cohort.

5.2. Materials and Methods

5.2.1. Study population

Brain tissue was obtained previously described in Chapter 3 section 3.2.1, of pathologically confirmed MS where SysVasc and cSVD had been characterized and where information on the extent of cervical and intracranial atheroma was available (Chapter 3, section 3.3.1, **Figure 3.4**)

5.2.2. Macroscopic global WML burden assessment

Macroscopic global WM burden was classified by an experienced pathologist (ME) with a semi-quantitative score (mild, moderate, severe) in whole formalin-fixed MS brains cut in 1 cm slices. The slice with the highest number of lesions was chosen as shown in **Figure 5.1 a.** and the total area of WML quantified using a point grid ratio (number of points on lesions/total number of points of WM) (**Figure 5.1 b.**).

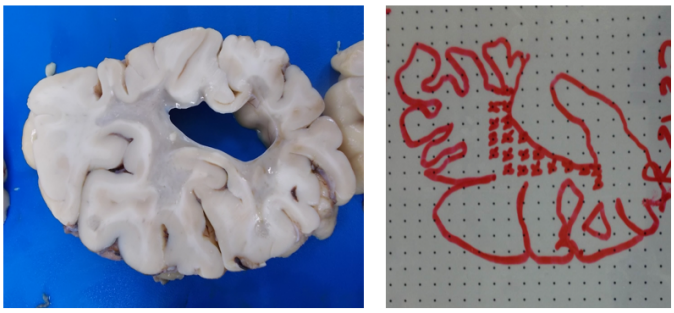

Figure 5.1. Macroscopic global WML assessment

Whole brain formalin-fixed 1 cm slices were examined and the slice with the highest lesion load was chosen (**a.**). A point grid was applied on top of the slice and the WM lesional area marked (red crosses) and the total WM area delineated (**b.**) The total macroscopic WML burden was obtained by dividing the number of points on lesions by the total number of WM points.

5.2.3. Tissue sampling and neuropathological evaluation

FWM, OWM, Pons and BG sections were obtained as explained in Chapter 3, section 3.3.2. Adjacent FFPE sections of these 4 brain areas were stained with H&E, immunostained with primary antibodies for myelin PLP, activated microglia (CD68) and SMA (for details see Chapter 3, section 3.2.3, **Table 3.1**). When possible, frontal and occipital cortex was included in the FWM and OWM sections.

5.2.4. Assessment of demyelination

MS plaque areas were defined as well demarcated (with sharp borders) areas of complete loss of PLP (**Figure 5.2**). Plaques were counted in each brain region and the total number of plaques was obtained by summing all regions plaque counts . Plaque area and the total WM area, for FWM and OWM and the area of the tissue in the slide, for the pons and basal ganglia, was obtained using ImageScope analysis tool (micro square metres μm^2). The percentage of plaque area was calculated for each brain region as follows (**Figure 5.2**):

a) Frontal and occipital WM – WM plaque area divided by total sampled WM area
b) Pons and Basal ganglia – WM/GM plaque area divided by total sampled area
c) Frontal and Occipital Cortex – GM plaque area divided by total cortical area. Analyses were restricted to cases where all cortical layers were present, to avoid over or under estimating of cortical lesion burden. This meant that a significant amount of cortical area was not included.

The overall percentage of plaque area was determined for each by combining proportional plaque area measures derived from a) and b). Cortical demyelination

area was analysed separately. A percentage of total cortical demyelination was obtained by the sum of Frontal and Occipital demyelination.

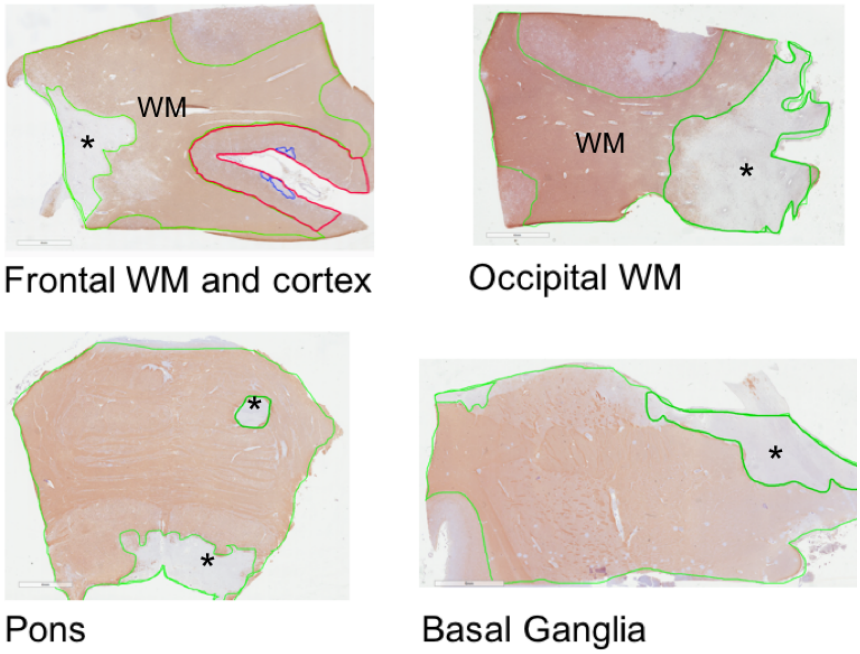

Figure 5.2. Assessment of MS demyelination.

Plaque (*), frontal and occipital WM, and pons and basal ganglia total tissue areas were delineated using ImageScope tools. The adjacent corresponding H&E section was scored for cSVD inside (largest plaque) and outside plaque as described in Chapters 3 and 4. Total cortical area (where all cortical layers were present) (red) and cortical plaque demyelination (blue) were also obtained.

The stage of demyelination was determined for each plaque using CD68 immunohistochemistry as per the most recent classification (Kuhlmann *et al.*, 2017) and grouped for analysis as follows:

a) Active – macrophage infiltration throughout the lesion centre and/or border (includes active demyelinating lesions and mixed active/inactive post demyelinating lesions) (**Figure 5.3**)
b) Inactive – minimal macrophage infiltration with sharp border of demyelination

The number of active and inactive plaques was obtained per each area. The total percentage of active plaques was obtained by dividing the number of active plaques in FWM, OWM, Pons and BS by the total number of plaques in these areas. The percentage of inactive plaques was obtained in the same way.

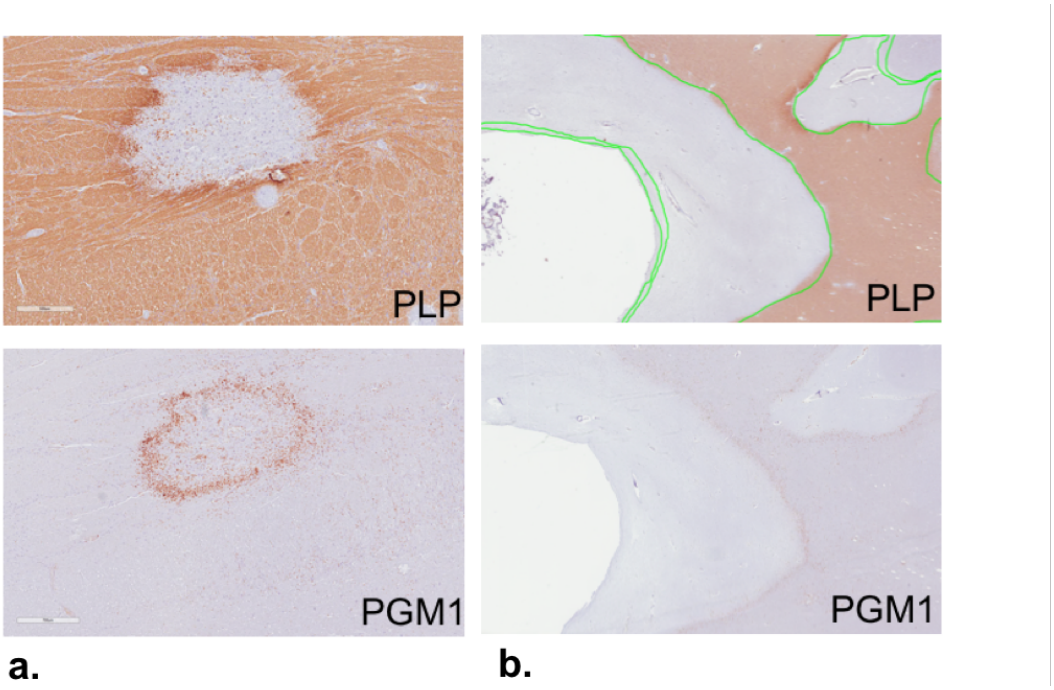

Figure 5.3. Plaque activity classification.

Plaques were defined well demarcated areas of complete PLP, a marker of myelin, loss. In active demyelinating plaques (**a.**) a diffuse infiltration of activated macrophages, PGM1 positive, was seen within the whole lesion and in mixed active/inactive post demyelinating lesions (**b.**) these cells would be seen at the lesion border.

5.2.5. SysVasc and cerebrovascular disease assessment

SysVasc score was obtained from the following variables: aorta, coronary and cervical artery atheroma, MI, IS and LVH, as described in Chapter 2, section 2.2.2.2. A semi-quantitative score was used to score the severity of intracranial atherosclerosis (Esiri *et al.*, 1997) as described in Chapter 2, section 2.2.2.2. The extent of cSVD was assessed as described in Chapter 3, section 3.2.3.1, by using an outside plaque Global cSVD Index obtained by the sum score of arteriolosclerosis, PSD, PHL, microbleeds, micro and macro infarcts and fibrinoid necrosis of all studied brain areas.

5.2.6. Statistical analysis

Descriptive statistics and univariate analysis were performed as described in Chapter 2, section 2.2.3. Regression models were fit to evaluate the influence of SysVasc and Global cSVD Index, on demyelination and plaque activity outcomes, whilst controlling for age at death, and other factors with significant association with the outcome variables, as per univariate analysis. For count variables with a Poisson distribution (i.e. total number of plaques, of active plaques), Poisson loglinear models were used. Continuous variables that were still not suited for linear regression after the appropriate transformations (i.e. percentage of plaque area) were binned above and below the median and binary regression models were used. Regression coefficients (B) or their exponential EXP (B) along with the respective 95% CI will be presented. All tests of hypothesis were carried out using two-sided tests and p-values of less than 0.05.

Age at death may affect plaque load and activity (Frischer *et al.*, 2015) and correlates with SysVasc score (Chapter 2) and Global cSVD Index (Chapter 3). To better understand the effect of this confounding factor an additional analysis was pre-planned where cases were binned above and below the median age at death. The relationship between total number of plaques, percentage of WM, cortical plaque area, active and inactive plaques with SysVasc and Global cSVD Index were explored within each age at death category.

SPSS version 25 and Graph Pad Prism 7 were used for the statistical analysis and plots.

5.3. Results

5.3.1. Cohort characteristics

A total of 42 MS cases was included (mean age 60.60 ±12.9 years, 57.1% females, mean disease duration 19.9±12.76 years). MS cohort selection flowchart is depicted in Chapter 3, section 3.3.1, **Figure 3.4**, and MS cases clinical features are also summarized in Chapter 3, section 3.3.1**, Table 3.3.** Unfortunately, clinical phenotype information could only be retrieved in 31 cases, 30 of all included cases (N=42) being SPMS (71.6%). More patients died of vascular disease above the age of 60 years, less of other causes and none of MS. As expected disease duration was higher in the older at death group (mean 26.5±14.2 years) compared with the young at death group (14.8±6.5 years), p=0.002 but no differences were found for sex (p=0.99), median year at death (p=0.71) or post mortem delay (p=0.74).

5.3.2. Demyelination and plaque activity outcomes

A good correlation was found between the WML burden assessed by the pathologist, using the semi-quantitative score, and the percentage of total plaque area ($r\tau$=0.67, p<0.001). A strong correlation was also found between the macroscopic global WML assessment (median 5.1 IQR 9.1) and the percentage of overall plaque area (r_s=0.79, p<0.001) and total number of plaques (r_s=0.49, p=0.003) and only these latter outcomes were used for subsequent analysis as measures of global WM demyelination. The vast majority of MS cases (90.5%, 38 out of 42) had one or more plaques in each of the 4 sampled brain areas, with a median of 5 (Range 0-25) plaques. A strong correlation was found between total plaque number and plaque area (r_s=0.822, p<0.001), 2 cases only with significant discrepancies between the two

variables (one with high plaque area and low number of plaques and another with low plaque area and high number of plaques). A summary of the demyelination outcomes per brain region is depicted in **Table 5.1**. are described below.

The burden of WML between FWM, OWM, BG and pons was positively correlated (data not shown). The majority of the cases presented plaques in all studied areas but they were more common in the pons and FWM. Most cases presented active and inactive plaques.

Table 5.1. Demyelination outcomes per brain region

Total N cases= 42	**Pons**	**Basal Ganglia**	**FWM**	**OWM**	**Total**
Number of cases with plaques (%)	31 (73.8)	28 (66.6)	29 (69.0)	24 (57.1)	38 (90.5)
Median total number of plaques (IQR)	1 (4)	1 (2.25)	1 (2.25)	1 (1)	5 (9.0)
Median percentage of plaque area (IQR)	1.75 (11.5)	2.11 (10.8)	0.72 (10.2)	1.56 (16.8)	2.75 (13.1)
Median total number of active plaques (IQR)	0 (3.25)	0 (1)	0.5 (2)	0 (1)	2.0(8.5)
- **Active**	0 (0)	0 (0)	0 (0)	0 (0)	0 (2)
- **Mixed active/inactive**	0 (3)	0 (1)	0 (1)	0 (1)	1 (6)
% cases with 1 or more active plaques (N)	45.2 (19)	30.9 (13)	52.4 (22)	38.1 (16)	71.4 (30)
Median number of inactive plaques (IQR)	0 (1)	0.5 (1)	0 (1)	0 (0)	2.0 (1.0)
% cases with 1 or more inactive plaques	40.5 (17)	50.0 (21)	28.6 (12)	19.0 (8)	76.2 (32)

It was possible to assess cortical demyelination in 37 out of 42 cases (88.8%) (any region), the frontal cortex (adjacent to sampled FWM) was available for assessment in 28 out of the 42 cases and occipital cortex (adjacent to sampled OWM) in 25 out of 42 cases. Median percentage area of frontal cortex demyelination was 4.9% (IQR 27.5), median percentage area of occipital cortex demyelination was 12.5% (IQR 19.5) and median percentage area of total cortical demyelination was 13.8% (IQR 23.7). The

percentage of total cortical demyelination increased with the percentage of overall plaque area (r_s=0.577, p<0.001).

Post mortem delay was not associated with the percentage of plaque area (r_s=0.024, p=0.882, the total number of plaques (r_s=0.008, p=0.96), the number of active (r_s=-0.081, p=0.62) nor with the number inactive plaques (r_s=0.79, p=0.63). Year at death did not associate with any of the MS pathology outcomes except with the total number of active plaques (r_s=0.343, p=0.026) and percentage of active plaques (r_s=0.504, p=0.001).

5.3.3. The relationship between MS pathology outcomes and age at death and disease duration

Increased age at death associated with lower burden of demyelination as measured by the total number of plaques (N=42, r_s=-0.564, p<0.001) and with percentage of total plaque area in all sampled areas (N=42, r_s=-0.507, p=0.001). The same relationship was observed in all studied areas (data not shown). The number of active plaques was also inversely correlated with age at death (N=42, r_s=-0.564, p<0.001) as was the number of inactive plaques (N=42, r_s=-0.465, p=0.002), but the proportion of active plaques tended to decrease with age at death (N=42, r_s=-0.26, p=0.09) (**Figure 5.6.**).

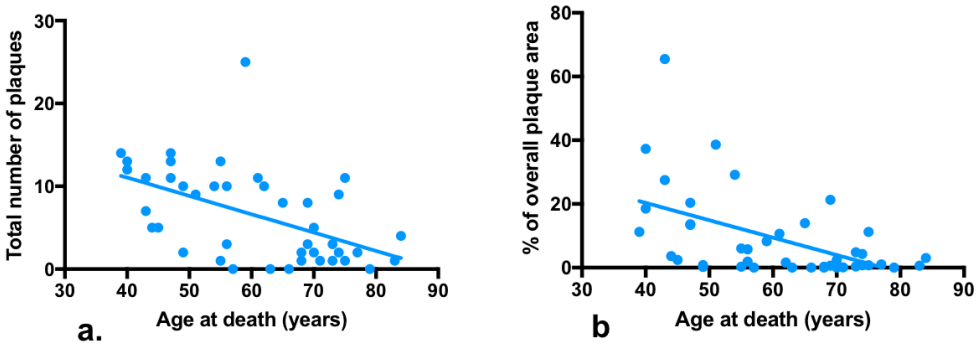

Figure 5.4. Relationship between total number of plaques (a), percentage of overall plaque area (b).

The total area of cortical demyelination was inversely correlated with age at death (N=37, r_s= -0.380, p=0.02) (**Figure 5.5**) and this was mainly driven by occipital cortex demyelination (N= 25, r_s= -0.575, p=0.003) , since a similar relationship was not seen with frontal cortex demyelination (N=28, r_s=-0.257, p=0.187).

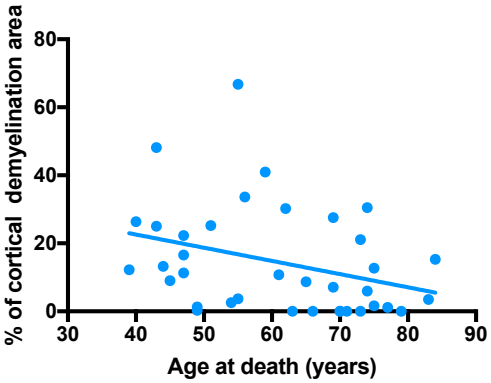

Figure 5.5. Percentage of cortical demyelination area and age at death.

No significant association was found between MS disease duration and total number of plaques (N=42, r_s=-0.206, p=0.197), of active (N=42, r_s=-0.129, p=0.420) or inactive plaques (N=42, r_s=-0.111, p=0.49), total plaque area (N=42, r_s=-0.176, p=0.272) or total area of cortical demyelination (N=37, r_s=-0.059, p=0.73). As seen for the whole

cohort, disease duration did not associate with any of the MS pathological outcomes after binning cases above and below the median age at death (**Figure 5.6**).

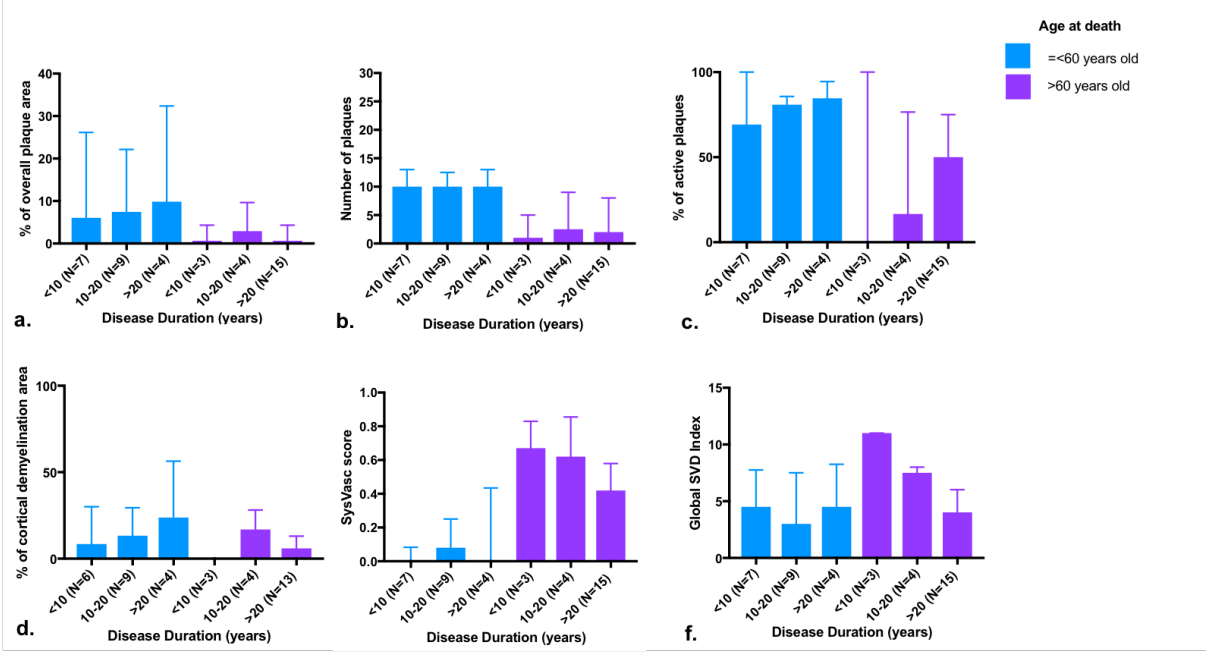

Figure 5.6. The relationship between disease duration and MS pathology outcomes, SysVasc and cSVD segregated by age at death

5.3.4. The relationship between MS pathology outcomes and SysVasc

MS disease duration did not correlate with SysVasc (N=42, r_s=0.15, p=0.36) (**Figure 5.6 e.**).

As SysVasc burden increased the total number of plaques (EXP(B)=0.19, 95%CI 0.10,0.38, p<0.001) and number of active plaques (EXP(B) = 0.09, 95%CI 0.04, 0.22, p<0.001) decreased, after adjusting for age at death (**Table 5.2**, Model 2). Similar results were found adjusting for year at death (data not shown). Though in univariate

analysis the percentage of total plaque area was also inversely correlated with SysVasc (N=42, r_s=-0.492, p=0.001), after adjusting for age in a binary logistic model to predict above or below the median plaque area this association was no longer significant (EXP (B)= 0.04, 95%CI 0.001,1.21, p=0.06). No other significant associations were seen between SysVasc and the other MS pathology outcomes.

To better appreciate the relationship between SysVasc and the MS pathology outcomes, accounting for age at death, I have taken a similar approach to that of Chapter 3, and have binned the data above and below the median age at death. In MS cases that died at younger ages (=<60 years old) no significant correlations were found between SysVasc and overall plaque area (N=20, r_s=-0.41, p=0.08) (**Figure 5.7 a.**), total number of plaques (N=20, r_s=-0.252, p=0.284) (**Figure 5.7 b.**) or the percentage of active plaques (N=20, r_s=-0.130, p=0.58) (**Figure 5.7 c.**). In the older age at death group the percentage of active plaques significantly decreased (N=22, r_s=-0.5, p=0.02) (**Figure 5.7 c.**) with an increase of SysVasc burden but SysVasc did not impact any other MS pathology outcomes.

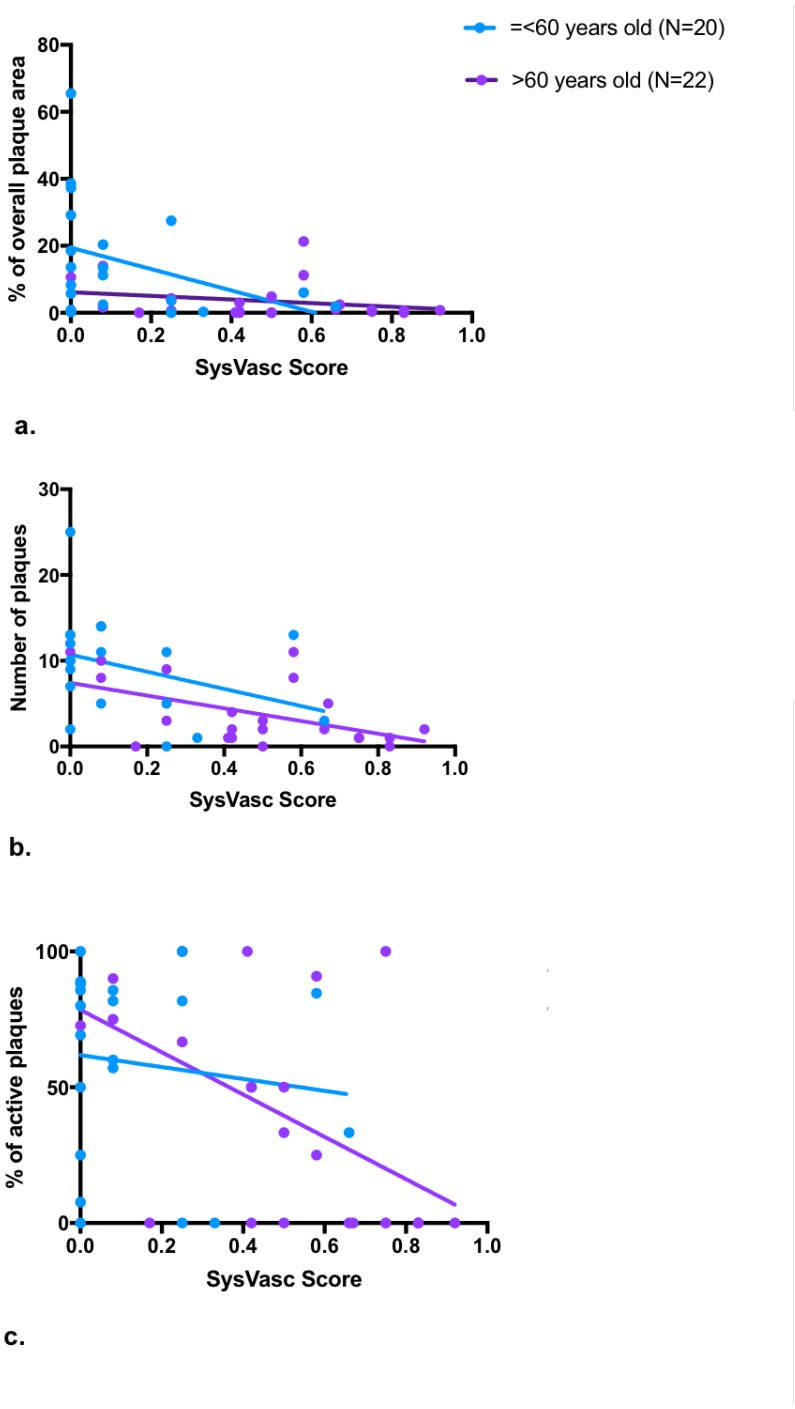

Figure 5.7. Relationship between MS pathology outcomes and SysVasc segregated by age at death

In the whole MS group, no significant association was found between total cortical demyelination and SysVasc (N=37, r_s=-0.239, p=0.155), though frontal cortex demyelination area (N=28, r_s=-0.377, p=0.048) tended to decrease with increasing

SysVasc burden but there was no significant effect on above/below median frontal cortical demyelination after adjusting for age at death (EXP(B) =0.11, 95%CI 0.003,4.9, p=0.25). SysVasc did not influence occipital cortex demyelination (N=25, r_s=-0.104, p=0.602). The relationship between cortical demyelination and SysVasc was different in cases that died at or below the age of 60 years, where a positive association was found (N=17, r_s=0.51, p=0.037), compared with those that died at older ages (N=20, r_s=-0.22, p=0.36), where no effect of SysVasc on cortical demyelination was seen (**Figure 5.8**).

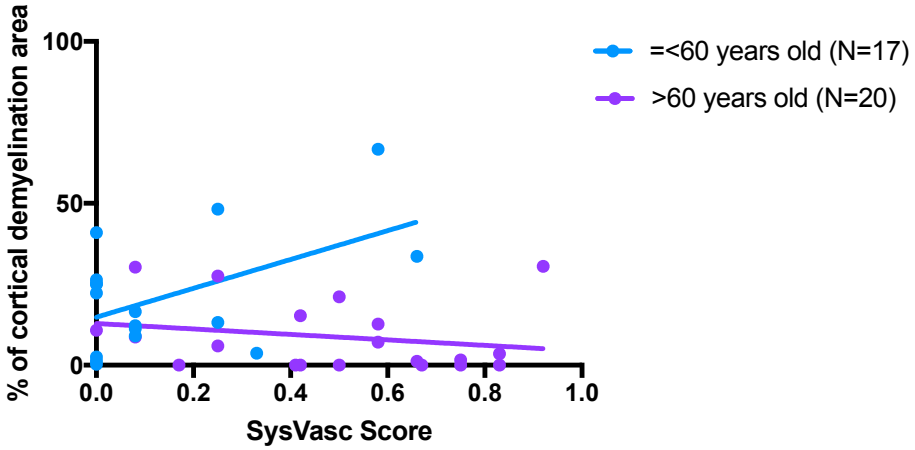

Figure 5.8. Percentage of cortical demyelination area and SysVasc segregated by age at death

5.3.5. The relationship between MS pathology outcomes and cSVD

5.3.5.1. Demyelination/plaque activity outcomes and Global cSVD Index

Overall Global cSVD Index did not associate with MS disease duration (r_s=-0.18, p=0.25) (**Figure 5.6 f.**).

In univariate analysis, the Global cSVD Index did not correlate with the total number of plaques (N=42, r_s=0.004, p=0.982) or the percentage of overall plaque area (N=42, r_s= -0.05, p= 0.751), number (N=42, r_s=-0.049, p=0.757) and proportion of active plaques (N=42, r_s=-0.114, p=0.47) or the number (N=42, r_s=0.151, p=0.336) or proportion inactive plaques (N=42, r_s=0.254, p=0.109). However, after adjusting for age at death and SysVasc, which has been previously shown to influence cSVD, Global cSVD Index significantly associated with the total number of plaques (EXP(B) = 1.1, 95%CI 1.05,1.15 p<0.001) and with the number of active plaques (EXP(B) = 1.12, 95%CI 1.01,1.17 p<0.001) (**Table 5.2**. Model 3, for the complete numerical results of the regression model). When added to the model, no significant impact of year at death was found and similar associations between SysVasc and Global cSVD Index with the number of active plaques were found (data not shown).

Table 5.2. Numerical results of the Poisson loglinear regression stepwise model to predict total number of plaques and number of active plaques

		Total number of plaques			Number of active plaques		
Model	**Parameter**	**EXP B**	**95%CI**	**p**	**EXP B**	**95%CI**	**p**
1	Age at death	0.96	0.95,0.97	<0.001**	0.96	0.95,0.97	<0.001**
2	Age at death	0.99	0.97,1.0	0.046	0.99	0.98,1.01	0.55
	SysVasc score	0.19	-0.101,0.38	<0.001**	0.09	0.04,0.22	<0.001**
3	Age at death	0.98	0.97,0.99	0.012*	0.99	0.97,1.01	0.247
	SysVasc Score	0.16	0.08,0.31	<0.001**	0.08	0.04,0.19	<0.001**
	Global cSVD Index	1.10	1.06,1.15	<0.001**	1.12	1.06,1.17	<0.001**

Global cSVD Index did not associate with the percentage of overall plaque area (EXP(B) =1.00, 95%CI 0.73,1.38 p=0.99) nor with the total number of inactive plaques (EXP(B) =0.58, 95%CI 0.19, 1.76, p=0.34).

Similarly, to what done for SysVasc, I have explored the relationship between Global cSVD and MS pathology outcomes in two different age at death categories, as illustrated in **Figure 5.9**. Overall percentage plaque area did not correlate with Global cSVD neither in the young (N=20, r_s=0.06, p=0.81) nor in the old age at death (N=22, r_s=0.05, p=0.75) categories. For the same Global cSVD Index values, cases that died at younger ages had higher plaque burden than those that died at older ages (**Figure 5.9 a**.). The Global cSVD Index did not correlate with the total number of plaques in the young age at death group (N=20, r_s=0.32, p=0.17) nor in cases that died at older ages (N=22, r_s=-0.02, 0.92) (**Figure 5.9 b**.). The relationship between Global cSVD Index and the percentage of active plaque was different in MS cases that died at younger ages when compared with those that died after the age of 60 (**Figure 5.9 c.**). In cases that died at younger ages the burden of Global cSVD tended to increase with the number of active plaques (N=20, r_s=0.31, p=0.08) but the association with the percentage of active plaques (N=20, r_s=0.2, p=0.42), was not significant. A reverse relationship was seen in MS cases that died at older ages, where higher levels of Global cSVD Index tended to associate with a lower number (N=22, r_s=-0.37, p=0.09) and percentage (r_s=-0.36, p=0.09) of active plaques (**Figure 5.9 c.**)

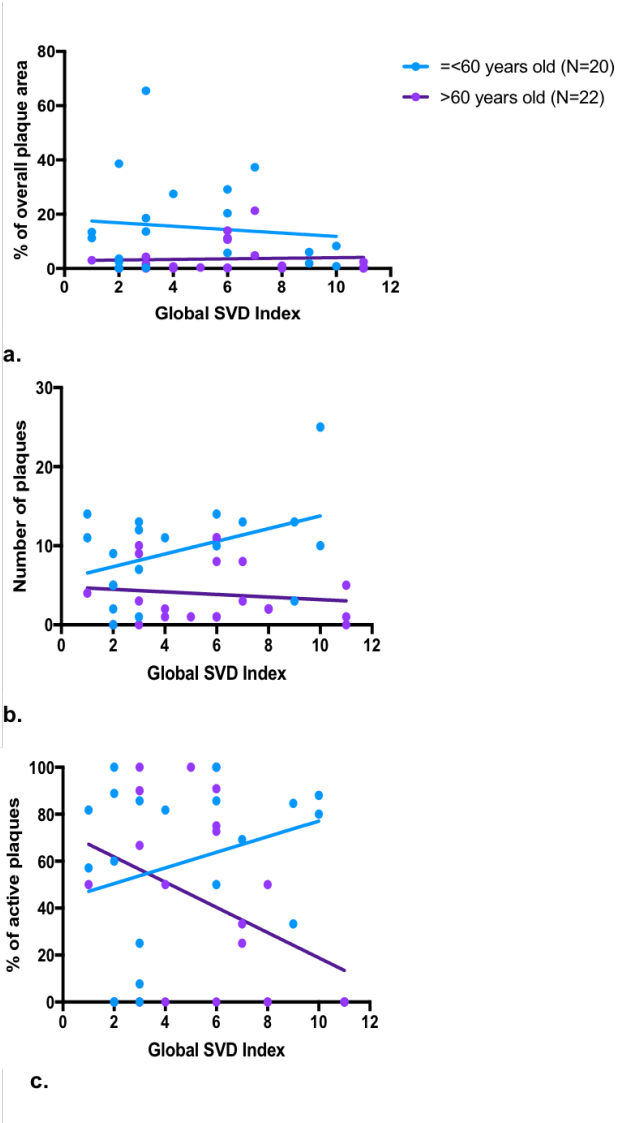

Figure 5.9. Relationship between MS pathology outcomes and Global cSVD Index segregated by age at death

Global cSVD Index relationship with the percentage of overall plaque area (**a.**); total number of plaques (**b.**) and percentage of active plaques (**c.**), above and below the median at death (60 years).

The results suggested by the graphical appearance of the data (**Figures 5.7 b.**, **5.7 c.** and **Figures 5.9 b.**, **5.9 c.**) were confirmed by repeating a stepwise multivariate model to predict the total plaque number and the number of active plaques, considering age at death and SysVasc in the two age at death categories (**Table 5.3.**). As expected a

negative association between total plaque number and SysVasc was observed in both age categories and a positive correlation between total plaque number and Global cSVD Index was seen only in the young at death (=<60 years) group. Similar relationships were seen for the number of active plaques, SysVasc being negatively correlated with the number of active plaques in both age categories and Global cSVD showing a positive association with this plaque activity outcome only in MS cases that died at younger ages (=<60 years).

Table 5.3. Numerical results of the Poisson loglinear regression stepwise model to predict total number of plaques and number of active plaques, segregated by age at death

		Total number of plaques			Number of active plaques		
Model		**EXP B**	**95%CI**	**p**	**EXP B**	**95%CI**	**p**
Age=<60	SysVasc Score	0.24	0.10,0.55	<0.001**	0.29	0.12,0.73	0.009*
	Global cSVD Index	1.10	1.05,1.15	<0.001**	1.15	1.09,1.21	<0.001**
Age >60	SysVasc Score	0.11	0.04,0.28	<0.001**	0.04	0.01,0.14	<0.001**
	Global cSVD Index	1.07	0.97,1.18	0.153	0.97	0.86,1.10	0.64

Cortical demyelination was not related with Global cSVD Index (N=37, r_s=-0.09, p=0.58) (**Figure 5.10 a.**), even after taking age at death and SysVasc into account (EXP(B) =0.89, 95%CI 0.68,1.15, p=0.37). Although the associations are not significant, the graphical appearance of Global cSVD Index on cortical demyelination for MS cases that died at the age of 60 or below shows positive relationship (N=17, r_s=0.28, p=0.27) whereas a negative association is seen for those who died after the age of 60 years (N=20, r_s=-0.19, p=0.42) (**Figure 5.10 b.**).

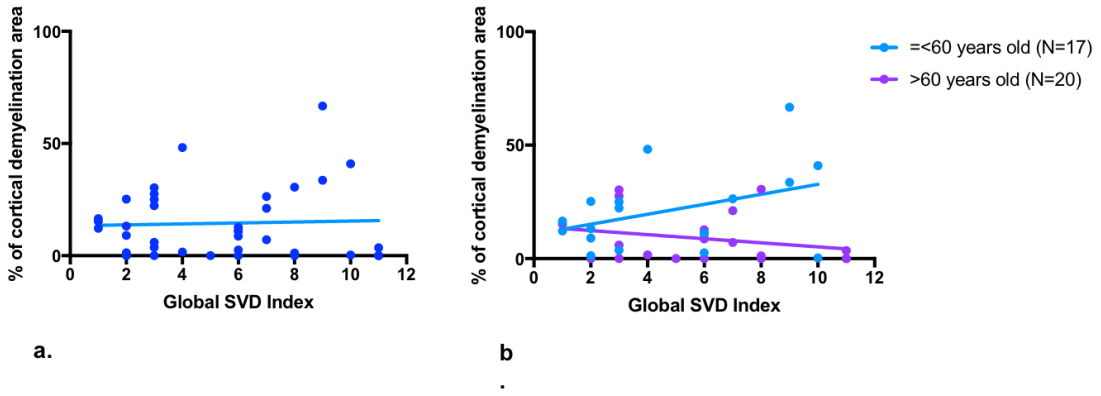

Figure 5.10. Percentage of cortical demyelination area and Global cSVD Index for all cases (a) and segregated by age at death (b).

5.3.6. MS pathology outcomes and individual cSVD pathologies

The association of each individual cSVD pathology outside the MS plaque and MS pathology outcomes was only explored for the most common cSVD pathologies (seen in >10 cases): arteriolosclerosis, PSD, PHL, periarteriolar and perivenular inflammation. I have also explored the relationship between MS pathology outcomes and well demarcated PSD, with fibrous material, described in the previous chapter, the "veils".

In the whole MS group arteriolosclerosis (EXP(B)=1.27,95%CI 0.98,1.64, p=0.06) tended to associate with a higher total number of plaques, accounting for age at death and SysVasc and this association was significant in cases who died at or below the age of 60 years, but not at older ages (**Table 5.4**). Similarly, arteriolosclerosis associated with a higher number of active plaques (EXP (B)=1.45, 95%CI 1.07,1.97, p=0.016), this association being driven by cases that died before the age of 60 years (**Table 5.4**). No

association was seen between this cSVD pathology and the number of inactive plaques, the percentage of plaque area or of cortical demyelination.

All areas PSD associated with the total number of plaques (EXP(B)=1.56, 95%CI 1.22, 2.01, p=0.001), number of active plaques (EXP(B)= 1.39 95%CI 1.03,1.88, p=0.03) and inactive plaques (EXP(B)=1.9, 95%CI 1.20,3.06, p=0.006) allowing for age and SysVasc and this was also driven by cases that died at younger ages (**Table 5.4**). PSD did not associate with the percentage of plaque area or with cortical demyelination.

PHL associated with the number total number of plaques (EXP (B)= 1.47, 95%CI 1.15,1.88, p=0.002), of active plaques (EXP (B)= 1.71, 95%CI 1.26,2.34, p=0.001), and again this was driven by cases that died at younger ages (**Table 5.4**). PHL did not associate with the number of inactive plaques, plaque area or with cortical demyelination.

Periarteriolar inflammation associated with the total number of plaques (EXP(B)=1.56, 95%CI 1.19,2.02, p=0.001) and tended to be more common with more active plaques (EXP (B)= 1.36, 95%CI 0.99,1.86, p=0.05) and this related with a strong association between periarteriolar inflammation and these two MS pathology outcomes at younger ages of death (**Table 5.4**).

Perivenous inflammation did not associate with any of the MS pathology outcomes in the whole group or in the above and below the mean age at death groups, except for a negative association with the number of active plaques in the young at death group (**Table 5.4**).

Finally, presence of "veils" associated with a higher total number of plaques (EXP (B)=1.33, 95%CI 1.02,1.72, p=0.03), and with the number of inactive plaques (EXP (B)=2.55, 95%CI 1.57,4.14, p<0.001), but did not associate with the number of active plaques, plaque area or cortical demyelination.

Table 5.4. Relationship between each cSVD individual pathology, periarteriolar and perivenular inflammation and total number of plaques and number of active, segregated by age at death

		Total number of plaques			Number of active plaques		
		EXP B	**95%CI**	**p**	**EXP B**	**95%CI**	**p**
Age <=60	**Arteriolosclerosis**	1.64	1.14,2.35	0.007*	2.02	1.32,3.11	0.01*
	PSD	1.63	1.21,2.19	0.001**	1.47	1.03,2.09	0.03*
	PHL	1.48	1.08,2.01	0.013*	2.28	1.54,3.39	<0.001**
	Periarteriolar inflammation	1.61	1.17,2.23	0.004**	1.51	1.04,2.21	0.03*
	Perivenular Inflammation	0.82	0.61,1.09	0.18	0.66	0.46, 0.94	0.02*
Age >60	**Arteriolosclerosis**	0.75	0.46,1.22	0.25	0.55	0.28,1.08	0.08
	PSD	1.77	0.94,3.32	0.08	1.36	0.57,3.23	0.48
	PHL	1.63	1.01,2.64	0.04*	1.19	0.65,2.18	0.56
	Periarteriolar inflammation	1.67	1.05,2.65	0.03*	1.42	0.80,2.51	0.23
	Perivenular Inflammation	1.24	0.74,2.08	0.41	1.20	0.65,2.21	0.55

The exponential of the regression coefficients adjusted for age at death and SysVasc, obtained for each individual cSVD pathology in separate Poisson models are summarized in the table. **p<0.01, *p<0.05

5.3.7. The relationship between MS pathology outcomes and intracranial artery atheroma burden

Information on intracranial artery atheroma was available in 34 out of the 42 MS cases. Intracranial artery atheroma burden did not impact the total number of plaques (B =1.4, 95%CI -4.1,6.9, p=0.61), the percentage of overall plaque area (B =2.37, 95%CI -12.16, 16.92, p=0.741), the number of active plaques (B =-0.70, 95%CI -5.88,4.47, p=0.783), nor the number of inactive plaques (B =2.06, 95%CI -0.402, 4.52, p=0.098), taking age at death and SysVasc into account.

5.4. Summary of the main findings

1. MS pathology outcomes were influenced by age at death.
2. The total number of plaques and the number of active plaques was inversely related with SysVasc, this relationship being stronger in cases who died after the age of 60 years. SysVasc did not influence plaque area or the number of inactive plaques.
3. Overall SysVasc did not have an effect on cortical demyelination burden but this relationship was different in cases that died at young ages, where a positive correlation was seen, compared with those that die after the age of 60 years.
4. The burden of cSVD was higher in MS cases with a higher plaque load and more active plaques. This association was driven by cases who died before the age of 60 years.
5. PHL and periarteriolar inflammation associated with a higher total number of plaques and of active plaques in the whole MS group and a similar association

was seen for arteriolosclerosis and PSD in MS cases who died before the age of 60 years.

6. Presence of "Veils" associated with a higher number of inactive plaques

5.5. Discussion

Contrary to what was predicted, increased SysVasc associated with lower total plaque burden and inflammation. In line with the initial hypothesis, cSVD burden associated with higher plaque number and activity.

The assumption that age at death was inversely correlated with MS lesion burden was confirmed in this study, in line with previous work from our group where cortical demyelination was found to be more extensive in MS cases that died at younger ages (Yates *et al.*, 2015). In present cohort, plaque activity was also influenced by age at death, the percentage of active plaques decreasing with an increase of age at death, as has also been shown by Frischer at al. (Frischer *et al.*, 2015). In this study, looking at 120 MS cases and 2476 plaques, the probability curves for active and inactive plaques on age at death were inversed, the former decreasing with age at death, intersecting at the age of 49 years of age.

Considering the important age at death effect on MS pathology outcomes and the fact that a different relationship between age at death and vascular disease outcomes had been documented in the previous chapters, I have used different approaches to account for this effect, all of which led to uniform findings.

Firstly, SysVasc was inversely correlated with plaque number and the percentage of active plaques. The link between MS plaque load and activity and a global cardiovascular burden measure, the SysVasc, accounting for aorta and coronary atheroma, LVH, MI and IS was herein explored for the first time. Kappus et al. (Kappus *et al.*, 2015) looked into the effect of VRF and comorbidities on brain MRI outcomes of 489 MS patients, mean age 47.3 (SD 10.9) and has shown that a combination of hypertension, heart disease and overweight/obesity was associated with increased T2 WML volume in the overall MS cohort. However, it is difficult to discern how each individual VRF impacts MS clinical, imaging and pathology outcomes or whether their effect is related to vascular disease (i.e. higher atheroma burden and consequent end-organ damage,) or to other disease mechanisms. Moreover, the Kappus et al. study included younger American MS cases, many on DMTs, whereas the present *post mortem* study, included older British cases with no DMT exposure. These differences may also explain the discrepancies between the two studies findings. Most importantly, vascular comorbidities may affect other aspects of MS pathology at younger ages, such as neuronal loss or cortical demyelination.

In fact, in the present study, cortical demyelination was positively associated with SysVasc Scores only in cases that died young. VRF have shown to associate with brain volume loss, particularly with lower cortical grey matter (Pichler *et al.*, 2019) in early MS. If a higher burden of cortical demyelination is responsible for this association has not yet been investigated.

In older at death cases, the fact that both the total number of plaques and of active plaques decreases as SysVasc increases, independently of age at death, may have several possible explanations.

One possibility is that MS cases with known SysVasc may have been on medication with an effect on MS pathology outcomes. Unfortunately, I did not have access to medication history but median age at death of the MS cohort is 1981 and I can assume that most of MS cases have not been exposed to the currently accepted standard ischaemic heart disease treatment (Endo, 2010; Valgimigli, 2019). Most importantly, patients with concomitant cardiovascular disease might have had a higher likelihood of being advised to stop smoking than those without cardiovascular disease and this may have had an impact on MS pathology outcomes.

Another potential explanation for a negative correlation between SysVasc and plaque number is that remote ischaemic conditioning (RIC) related to symptomatic arterial stenosis may have an impact on WML formation. RIC is a phenomenon in which a brief period of ischaemia of one organ or tissue provides protection to another organ or tissue against a sustained ischaemic-reperfusion injury (Meng *et al.*, 2012) and it may lower the recurrence of stroke, attenuate inflammation and coagulation, improve cerebral circulation in cases with intracranial arterial stenosis (Meng *et al.*, 2015) and reduce T2 WML in cSVD (Wang *et al.*, 2017). One possible mechanism for this neuroprotective effect against ischaemia is the upregulation of hypoxia-inducible factor-1 in microglia (Huang *et al.*, 2014). MS lesions tend to occur in watershed areas (Haider *et al.*, 2016) and hypoxia plays an important role in MS demyelinating lesion development (Desai *et al.*, 2016). In the older at death cases SysVasc scores were

higher than in the younger at death MS cases, possibly predisposing to higher likelihood of ischaemia/hypoxia elsewhere in the body. This might have remotely mitigated MS demyelinating brain lesions, as it has been reported for cSVD WML (Wang *et al.*, 2017).

Another key finding of the current study is that cSVD burden, as measured by the Global cSVD Index and individual cSVD pathologies, such as arteriolosclerosis, PSD and PHL, positively associated with plaque number and the percentage of active plaques. These relationships were driven by MS cases that died at the age of 60 years or below and were independent of SysVasc.

In the young age at death group cSVD burden may be increased through two concomitant mechanisms. On one hand, highly inflammatory MS, as seen in cases that die young, seems to be associated with an arteriolopathy, translated by enlargement of the periarteriolar spaces. Brain imaging studies support these findings since enlarged PSD have been associated with contrast enhancing lesions (Wuerfel *et al.*, 2008). However, the distinction between perivenular and PSD is challenging in brain MRI studies. My study provides evidence that outside plaque periarteriolar spaces dilatation associate with increased lesion load and inflammation. On the other hand, I have also shown for the first time that in young at death MS cases arteriolosclerosis associates a higher burden of active plaques, indicating that the inflammatory milieu in MS may contribute to this cSVD pathology. In Chapter 3, is was shown that Global cSVD Index burden was higher in MS compared with non-MS, particularly in young at death cases, but overall arteriolosclerosis was not significantly increased. Yet lesion burden and activity had not been considered. A cross talk between the immune

response seen in MS and the pathways that lead to arteriole damage is plausible. Activated macrophages, which typically feature the MS active plaque, are also present in cSVD deep WML (Forsberg *et al.*, 2018) but how they may impact arteriolosclerosis development is unclear. An imbalance towards a T-helper 1 CD4+ T cells (Th1) activation compared to T-helper 2 CD4+ T cells (Th2) features active MS (Dendrou *et al.*, 2015) and this imbalance has shown to be pro-atherogenic in non-MS cases (Ketelhuth and Hansson, 2016) and could possibly contribute to arteriolosclerosis in highly active MS.

As for MS patients who died after the age of 60 years, cSVD burden seemed to be independent from all studied MS pathological outcome measures. In the previous chapter, it was shown that in this age group cSVD depended on SysVasc burden. The majority of the cases included in this MS cohort had entered the SPMS phase. Age-related cSVD may be contributing to neuronal loss, in the older age at death group, with low plaque burden (Frischer *et al.*, 2009), and consequently to disability progression independent of relapses, and this needs to be further investigated.

Outside plaque PHL and periarteriolar inflammation were tightly associated with the number of active plaques in the whole cohort, suggesting that classical MS pathology, represented by the MS plaque runs together with a widespread non-plaque associated pathology, where the arteriole may play a key role.

Finally, the presence of periarteriolar "veils" did not associate with the number of active plaques but were linked with increased number of inactive plaques. This

supports that this type of PSD may represent the remains of resolved periarteriolar inflammation.

All the *post mortem* study biases mentioned in the previous chapters apply to the present study. Most importantly, the directionality of the observed associations cannot be determined with this cross-sectional study. Not only MS inflammation may impact cSVD development, but also BBB breakdown described in cSVD (Farrall and Wardlaw, 2009; Wardlaw, 2010) may promote inflammation (either focal or generalized) and/or neuronal damage in MS. The interaction between these two disorders needs to be further explored in animal models where the onset and development of cSVD and inflammatory demyelination can be better controlled (Kipp *et al.*, 2017; Horsburgh *et al.*, 2018).

In this cohort a positive correlation between year at death and the number of active plaques was found and this possibly translates the effect of long-term formalin storage of brain tissue on antigenicity. This relationship was factored when analysing the relationship between systemic and cerebral vascular disease and the number of active plaques. In spite of my attempts to account for the age at death confounding effect, young MS cases with mild disease and old MS cases with more severe disease may have been missed. Finally, in the present study, only plaque related demyelination was assessed and diffuse WM changes were not considered. MAG/PLP ratio declines with cSVD severity in non-MS cases (Barker *et al.*, 2013). In an exploratory qualitative assessment of MAG and PLP immunostained slides from MS and non-MS cases, I found that the variability due to tissue antigenicity made it difficult to obtain an accurate ratio with immunohistochemistry (data not shown). Exact quantification of these

proteins as suggested by Barker et al. (Barker *et al.*, 2013) in non-plaque areas may provide further insight into the relationship between cSVD and demyelination in multiple sclerosis.

Despite all the limitations, this data supports that active MS, as measured by the percentage of active plaques, associates with cSVD, particularly at younger ages. Patients included in the present study did not have access to the current DMT and we may expect that some drugs that target inflammation early in the disease may minimize vascular damage in MS, though this has not been tested so far. Nevertheless, dampening inflammation only may not be enough and it is possible that exposure to inflammation even if for a brief period early in life, may trigger cascades that lead to arteriolar damage later on (Kowara *et al.*, 2019), especially if patients are exposed to VRF. This may be particularly relevant in MS cases that live to older ages, where vascular disease seems to be common but independent from the classical MS pathological outcomes.

6 Specificity of imaging surrogate markers in differentiating MS from cSVD

6.1 Introduction

WML are common both in MS and cerebrovascular disease. Some lesion characteristics, such as shape and location, may help to differentiate these two disorders. Several WML characteristics are thought to associate more clearly with MS, namely: juxtacortical U or S shape, ovoid appearance perpendicular to the lateral ventricle (Dawson's fingers), involvement of the corpus callosum, and the involvement of the WM around the temporal horns of the lateral ventricles or the cerebellar peduncles (Aliaga *et al.*, 2014; Geraldes *et al.*, 2018). Markers of neurodegeneration or severe tissue loss, such as T1 WM hypointensities black-holes, and thalamic atrophy (Cifelli *et al.*, 2002; Riva *et al.*, 2009) are commonly seen in MS. "Vascular" WML tend to be symmetrical, affect the watershed zones and spare the U-fibres, being frequently noted around the anterior horns of the lateral ventricles, spreading posteriorly along their lateral borders, in the deep WM region extending towards the precentral gyrus and around the posterior horns of the ventricles and centrum semiovale (Barkhof and Scheltens, 2002; Rostrup *et al.*, 2012). Additionally, vascular WML frequently associate with other cSVD imaging surrogate markers such as basal ganglia lacunae and perivascular space dilatation or microbleeds (Wardlaw *et al.*, 2013*a*). However, the performance of these imaging markers in discriminating MS from cSVD has rarely been tested (Geraldes *et al.*, 2018).

This thesis aims to understand the relationship between MS and vascular disease and, in the following chapters, will be tested whether the presence of VRF makes "MS-

lesions" worse (Chapter 7) or whether MS associates with worse cSVD (Chapter 8). In the present chapter I aim to identify imaging markers that are either strongly associated with MS or with cSVD, to later test these hypotheses.

In Chapter 6, my main research questions and hypotheses are:

a. What is the specificity of "MS-like" WML and neurodegenerative imaging markers associated with MS?
    - "MS-like" WML (i.e. Dawson fingers, juxtacortical lesions), black-hole burden and thalamic atrophy are specific for MS.
b. What is the specificity of cSVD imaging surrogate markers?
    - cSVD imaging surrogate markers (i.e. basal ganglia and lacunae, microbleeds) are specific for non-MS with VRF.

To test these hypotheses, these MS and cSVD imaging markers will be compared between MS without VRF and non-MS with VRF.

I also aim to explore the following question:

c. Is the WML distribution different in MS compared with cSVD?
    - Although several areas will overlap, the lesion distribution will differ between MS and cSVD.

To test this hypothesis, I will explore and compare WML probabilistic maps between MS with no VRF and non-MS with VRF.

6.2. Materials and Methods

6.2.1. Study design and cohorts

A multicentre retrospective observational case-control study was set up to compare MS cases without VRF ('Pure MS' or 'MS only') and non-MS cases with VRF ('Pure VRF' or 'VRF only'). Anonymised clinical and imaging data was obtained from 5 MAGNIMS consortium centres as described in Chapter 1, section 1.7.2.2. These are tertiary University Centres with expertise in MS research. The 'VRF only' group was derived from two studies on brain lesions in diabetic patients ran in two of the 5 participating MAGNIMS centres (Amsterdam and Barcelona).

A total of 93 FLAIR and T1-weighted brain MRI scans from MS patients without VRF and 43 from non-MS cases with VRF were scored for the presence of MS and cSVD imaging surrogate markers. Quality checks were performed as described in Chapter 1, section 1.7.2.2. Whole brain and thalamic volumes were obtained from the same cohort. A subgroup of MS cases without VRF (N=33) and non-MS cases with VRF (N=25), with SWI available, were scored for the presence of microbleeds. Another subgroup of MS without VRF (N=33) and non-MS cases with VRF (N=26) was included for lesion probabilistic map analysis (Chapter 1, section 1.7.2.2, **Figures 1.5.** and **1.6.**, **Tables 1.4.** and **1.5.**).

6.2.2. Imaging Analysis

6.2.2.1. Visual Scoring

A single investigator (RG), blinded to the VRF status performed visual scoring of the brain MRIs. A subset of MRI scans was scored twice on two separate occasions by RG and additionally scored by two other independent evaluators (Dr Maciej Juryńczyk,

MJ, and Dr Giordani dos Passos, GP) who were also blinded to clinical and demographic data) to ensure robust inter- and intra-rater agreement. All raters were neurologists with a special interest in MS. RG and MJ had previous experience MS lesion visual MRI scoring (Juryńczyk *et al.*, 2017*a*, *b*).

The following features were included in MS imaging surrogate markers scoring:

- Number of Dawson-fingers – these included well demarcated periventricular lesions that had an elongated, ovoid or flame-like shape, were perpendicular to the wall of the lateral ventricles and touched the ventricular lining, as seen in axial FLAIR (Chapter 1, section 1.3.4, **Figure 1.3 a.**).
- Number of juxtacortical lesions – these included all well demarcated lesions that touched the cortex as seen in both the axial FLAIR and T1.
- S- U-shaped juxtacortical lesions – a subset of the juxtacortical lesions which had an S or U shape (Chapter 1, section 1.3.4, **Figure 1.3 b.**).
- Number of infratentorial lesions - any lesion in the brain stem or cerebellum. If pons lesions were present they were classified as central, if present within a radius of 1.0 cm of the midpoint of the pons, or peripheral if beyond that circle.
- Presence of inferior temporal lobe lesions (yes/no)
- Black hole burden – black holes, defined as WML with a hypointense appearance relative to NAWM on T1- weighted image that are also hypointense in the corresponding FLAIR-weighted image (close to CSF signal), were classified as: not present, mild – 0 to 2 , moderate -3 to 4, severe - >4

MS cases with confluent periventricular lesions were excluded from the periventricular lesion and Dawson finger analysis and if confluent lesions extended up to the cortical-subcortical junction cases were also excluded from the juxtacortical lesion analysis.

The following features were included in cSVD imaging surrogate markers scoring:

- Basal ganglia lacunae number – a lacuna of presumed vascular origin, was counted when a round or ovoid, fluid filled cavity (signal similar to the CSF) of between 3 mm and 15 mm in diameter was seen in T1 and FLAIR sequences (**Figure 6.1**) (Wardlaw *et al.*, 2013*b*) in the caudate and lenticular nucleus and the thalamus.
- Basal ganglia perivascular space dilatation – basal ganglia perivascular spaces are defined as linear (parallel to the course of penetrating vessel), round or ovoid (perpendicular to the course of the vessel) spaces that are smaller than 3mm, with the same intensity signal as the CSF (hypointense on T1-weighted images and FLAIR), and occurring in the caudate and lenticular nucleus or adjacent deep WM (Wardlaw *et al.*, 2013*b*). Basal ganglia perivascular space dilatation was scored to be present when the diameter of more than 1 of these spaces measured 4 mm or more (Hansen *et al.*, 2015).
- Number of cerebral microbleeds – rounded area void of signal, 2-10 mm in diameters, with associated blooming seen on T2*-weighed MRI or other sequences that are sensitive to susceptibility effects (Wardlaw *et al.*, 2013*b*). Cerebral microbleeds were scored using the Microbleed Anatomical Rating Scale (MARS) (Gregoire *et al.*, 2009). In this scale the number of microbleeds is counted in different brain areas (infratentorial, deep grey and WM and the

different brain lobes), on the right and left and a final score is obtained by adding all the regional scores.

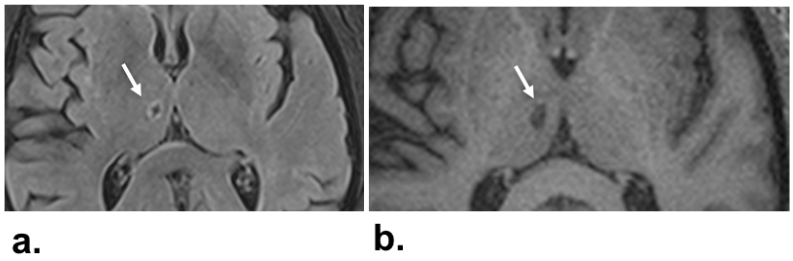

Figure 6.1. Basal ganglia lacuna example.

A right thalamic lacuna: a small ovoid cavity, hypointense in the centre of the lesion and slightly hyperintense at its border is seen on axial FLAIR) (**a.**) and T1 weighted images (**b.**) in a non-MS case with VRF (white arrows).

6.2.2.2. Whole Brain and thalamic volumes

Brain tissue volume, normalized for subject skull size, was estimated with SIENAX which forms part of the FMRIB Software Library (FSL) (Smith *et al.*, 2002, 2004). Brain extraction (removal of non-brain signal) was applied (Smith *et al.*, 2002) then the brain image was affine-registered to MNI152 space (Jenkinson *et al.*, 2002) using the skull image to determine the registration scaling, which was used to normalize for head size. Then, tissue-type segmentation with partial volume estimation was carried out (Zhang *et al.*, 2001) in order to calculate the total volume of brain tissue. Visual inspection of the results was performed and brain extraction parameters adjusted when needed.

Thalamic volumes were calculated using the automated segmentation tool FIRST (Patenaude *et al.*, 2011), also part of FSL, for each subject. They were then normalized for skull size (**Figure 6.2**). An average of the normalized left and right thalamic volumes per subject was obtained. The ratio between mean normalized thalamic volume and normalized whole brain volume was obtained.

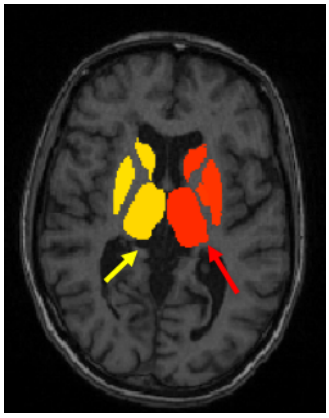

Figure 6.2 Example of basal ganglia and thalamus segmentation using FSL FIRST

Example of segmentation of the basal ganglia and the right (yellow arrow) and left (red arrow) thalamus with the automated too FSL FIRST, a model-based segmentation tool. The shape models used in FIRST are constructed from manually segmented images from the Centre for Morphometric Analysis, MGH, Boston. FIRST searches through linear combinations of shape modes of variation for the most probable shape given the observed intensities to the T1 image inputted.

6.2.2.3. WML volumes

An automatic lesion segmentation tool, MSmetrix (Icobrain software), was used for segmentation of WML. This tool uses a probabilistic model to detect WML as an outlier to normal brain, while segmenting the brain tissue into grey matter, WM and cerebrospinal fluid from 3D T1-weighted and FLAIR MR images (Jain *et al.*, 2015). This method seems to be reproducible even using images from different scanners (Jain *et*

al., 2016). Quality checks were performed by comparing the results of the automatic lesion segmentation with the visual scoring results and cases with significant discrepancies were excluded from the analysis. The following variables outcome measures were obtained: total, periventricular, subcortical and juxtacortical WML volume.

6.2.2.4. Lesion probabilistic maps

To determine if there was a significant difference in WML distribution between MS cases without VRF and non-MS with VRF lesion maps were compared. Probabilistic segmentation of T2 hyperintense lesions was performed on FLAIR and T1 images, in the native space, using Icobrain MS software (Jain *et al.*, 2015). These were subsequently thresholded and binarized to get labelled lesions in native space. These labelled lesions are warped into MNI space using both an AFFINE and non-rigid registration using niftyreg software (Ourselin *et al.*, 2002; Modat *et al.*, 2010). The obtained lesion masks were then summed and averaged for each subject group to create lesion probability maps. A group level comparison of lesion distribution was conducted using the non-parametric permutation testing tool Randomise with Threshold-Free Cluster Enhancement (TFCE) (Winkler *et al.*, 2014), with 500 iterations. This methodology combines cluster volume and amplitude information into a single parameter, the TCFE-score, by integrating over a range of thresholds for the statistical map. This analysis was repeated adding age and total lesion volumes (only if significantly different between the groups in univariate analysis) as nuisance variables. The TFCE-maps were thresholded at $p<0.01$.

6.2.3. Statistical analysis

Distribution of data was assessed analytically and graphically and transformed as required. Continuous normally distributed data are presented as mean ± standard deviation (SD) and continuous non-normally distributed variables are presented as median and interquartile range (IQR)/range. Count and percentage is depicted for categorical data. Inter-rater agreement was measured by free marginal multi-ratter kappa coefficient (Randolph, 2005) and interpreted as defined in Chapter 2, section 2.2.3. Three-way contingency tables, Chi-square or Fisher Exact test, parametric and nonparametric tests were applied as appropriate. For continuous and normally distributed variables one-way analysis of co-variance (ANCOVA) was used to detect between group differences with age and sex as nuisance covariables and a Bonferroni multiple comparisons correction applied. For count variables with a Poisson distribution, a Poisson loglinear model was used to compare the MS without VRF and non-MS with VRF groups, adjusting for age and sex. To compare binary variables, adjusting for age and sex, a binary regression model was used. A conservative $p<0.01$ was used to assess significance. A statistical trend was assumed if $p\leq0.05$.

Specificity, or true negative rate, was calculated for each imaging marker as: number of true negative cases/number of false positive cases +number of true negative cases and 95% CI calculated using MEDCALC statistical software. All other analyses were performed with SPSS version 25 and GraphPad prism version 7.

6.3. Results

6.3.1. Clinical features of the cohorts used for lesion visual scoring and volumetric analysis

Clinical features of the cohorts used in the imaging study are summarized in Chapter 1, section 1.7.2.2, **Table 1.4**. A cohort of MS with no VRF (N=93, mean age 47.2±8.2, 63.4% females) and non-MS cases with VRF (N=43, mean age 58.5 ±13.8, 61.7% females) was assessed for all the MS and cSVD imaging surrogate markers, except for microbleeds. Two cases had confluent lesions (one MS without VRF, one in non-MS with VRF) and it was not possible to obtain the Dawson finger and juxtacortical lesion number so they were excluded from this analysis. In one MS case a significant supratentorial artefact did not allow basal ganglia lacunae and perivascular space dilatation or black-hole scoring.

The non-MS with VRF group was older (N=43, mean age 58.5 ±13.8) than the MS without VRF group (N=93, mean age 47.2±8.2) ($p<0.001$). The VRF profile of the non-MS cases included was: 100% with diabetes, 23.3 % with arterial hypertension, 25.6% with dyslipidaemia, 18.6% current smokers and 23.3 % ex-smokers.

Due to several technical problems that could not be corrected at the pre-processing phase (corrupted T1, movement artefacts that significantly interfered with registrations) SIENAX could not be performed in 2 of 93 MS without VRF and FIRST could not be performed in 5. The non-MS with VRF cases were derived from 2 centres, Barcelona and Amsterdam. The Barcelona non-MS cohort with VRF was significantly older (N=26, 68.5±4.9 years) than the MS cases without VRF cohort (N=93, 47.2±8.2

years) (Chapter 1, section 1.7.2.2, **Table 1.4**.). Considering that brain volume is strongly associated with age, for volumetric analysis I have only included the 17 non-MS cases with VRF from Amsterdam which were age-matched (mean age 43.2±7.0 years) to the MS without VRF cases.

As previously mentioned, only a limited number of MS with no VRF and non-MS with VRF cases had SWI for microbleed scoring and from the available cases some had significant quality issues that did not enable accurate scoring. A total of 33 MS cases with no VRF (mean age 42.7±5.9 years, 54.5 % females) and of 25 non-MS with VRF cases (mean age 68.4±5.0 years, 64.0% females) were included in the microbleed analysis.

6.3.2. Inter-rater agreement for the visual scoring

Substantial inter-rater agreement was found for the number of Dawson fingers (0.66), the number of juxtacortical lesions (0.65) and the black-hole burden (0.70). Moderate agreement was found for U-S shape juxtacortical lesions (0.58). Substantial agreement was found for lacunae (0.67) and perivascular space dilatation (0.62) scoring and moderate agreement (0.55) for microbleeds scoring.

6.3.3. MS and cSVD imaging surrogate markers specificity

MS and cSVD imaging surrogate markers scoring results are summarised in **Table 6.1.** and depicted in **Figure 6.3** and **Figure 6.4**.

6.3.3.1. MS imaging surrogate markers visual scoring results

Significantly more Dawson fingers were seen in MS without VRF (median 2, IQR 4) than in non-MS with VRF (median 0, IQR 4), p<0.001. One or more Dawson fingers were seen in 78 % (72 out of 92) MS without VRF cases and in 9.3% (4 out of 43) non-MS with VRF cases, this difference being quite significant, p<0.001 (**Table 6.1.** and **Figure 6.3 a.**). The specificity of the presence of Dawson fingers to differentiate pure MS from the non-MS with VRF group was 90.7 % (95%CI 77.9,97.4).

One or more juxtacortical lesion was seen in 80.4 % (74 out of 92) of MS cases without VRF and in 6 out of the 43 non-MS with VRF (13.9%) cases (**Table 6.1** and **Figure 6.3 b.**), these proportions being significantly different, p<0.001. U-S shape juxtacortical lesions were only seen in MS cases and were present in 43.5% (40 out of 92) of the cases, p<0.001 (**Table 6.1**, **Figure 6.3 c**.). The specificity of juxtacortical lesions was 86.1% (95%CI 72.1,94.7). However, a 100% specificity (95%CI 96.4,100) was found for U-S shape juxtacortical lesions.

Of note, scoring of both Dawson fingers and juxtacortical lesions varied between the two centres that provided images from non-MS with VRF cases, none being detected in the Amsterdam cohort. This could reflect the age differences between the two cohorts, Barcelona cases being older (see Chapter 1, section 1.7.2.2, **Table 1.4**) but also due to sequence differences (see Chapter 1, section 1.7.2.2, **Table 1.5**).

Infratentorial lesions were more commonly seen in MS cases without VRF (52.7 %, 49 out of 93) than in non-MS with VRF (20.9 %, 9 out of 43), p<0.001 (**Table 6.1** and

Figure 6.3 d.). Lesion counts in this location were also higher in the MS group (median 1, IQR 2) compared with non-MS (media 0, IQR 0). The specificity of infratentorial lesions to differentiate MS from cSVD was 79.1 % (95%CI 63.9, 89.9). Peripheral pons lesions were observed in 31.2 % (29 out of 93) MS without VRF and in none of non-MS cases with VRF (**Figure 6.3 e.**). Presence of peripheral pons lesions showing a specificity for MS of 100% (95%CI 91.78, 100).

Inferior temporal lobe lesions were more frequently observed in MS (69.9 %, 65 out of 93) compared with non-MS (20.9 %, 9 out of 43), p<0.001 (**Table 6.1**). However, the specificity of this imaging feature for MS diagnosis was not as good (79.1%, 95%CI 63.9,89.9).

Moderate to severe black hole burden was seen in 43.4 % of MS cases with no VRF and in none of the non-MS cases with VRF (p<0.001). Presence of any black-hole had a specificity for MS of 93.0% (95%CI 80.9,98.5).

Table 6.1. MS and cSVD imaging surrogate markers quantification in MS without VRF and non-MS with VRF.

	MS Without VRF (N=93)	Non-MS with VRF (N=43)	p	Specificity	95% CI
MS imaging surrogate markers					
	N=92				
Median DF (IQR)	2 (4)	0 (4)	<0.001**		
% cases 1 or more DF (N)	78.2 (72)	9.3 (4)	<0.001**	90.7 %	77.9, 97.4
	N=92				
Median JCL (IQR)	2 (5)	0 (0)	<0.001**		
% cases 1 or more JCL (N)	80.4 (74)	13.9 (6)	<0.001**	86.1%	72.1,94.7
	N=92				
Median U-S JCL (IQR)	0 (1)	0	<0.001**		
% cases 1 or more U S JCL (N)	43.5 (40)	0	<0.001**	100%	96.4, 100
Median infratentorial lesions (IQR)	1 (2)	0 (0)	<0.001**		
% cases 1 or more lesion (N)	52.7 (49)	20.9 (9)	<0.001**	79.1%	63.9, 89.9
% cases with peripheral pons lesions (N)	31.2 (29)	0	<0.001**	100%	91.8,100
%inferior temporal lobe lesions (N)	69.9 (65)	20.9 (9)	<0.001**	79.1%	63.9,89.9
Black-hole burden	N=92		<0.001**	93.0%	80.9,98.5
Not present	40.2 (37)	93.0 (40)			
Mild	16.3 (15)	7.0 (3)			
Moderate	39.1 (36)	0			
Severe	4.4 (4)	0			
cSVD imaging surrogate markers					
	N=92				
Median BG Lacunae (IQR, range)	0 (0)	0 (0)	0.002**	97.9%	92.5, 99.7
% cases 1 or more lacunae (N)	2.2 (2)	16.3 (7)	0.005**		
	N=92	37.2 (16)	0.850	66.7%	56.1,76.1
% cases with one or more BG PSD (N)	33.7 (31)				
% cases with central pons lesions (N)	5.4 (5)	16.3 (7)	0.020*	94.6 %	87.9, 98.2
	N=33	N=25			
Median MARS (IQR,)	0 (0, 0)	0 (0)	0.180		
% cases with one or more microbleeds(N)	0	8.0 (2)		100%	89.4, 100

DF – Dawson fingers, JCL – juxtacortical lesions, IQR – interquartile range, PSD- perivascular space dilatation, BG- basal ganglia; **p<0.01, *p<0.05 Mann-Whitney test for non-parametric count variables, Chi-square or Fisher exact test for categorical variables

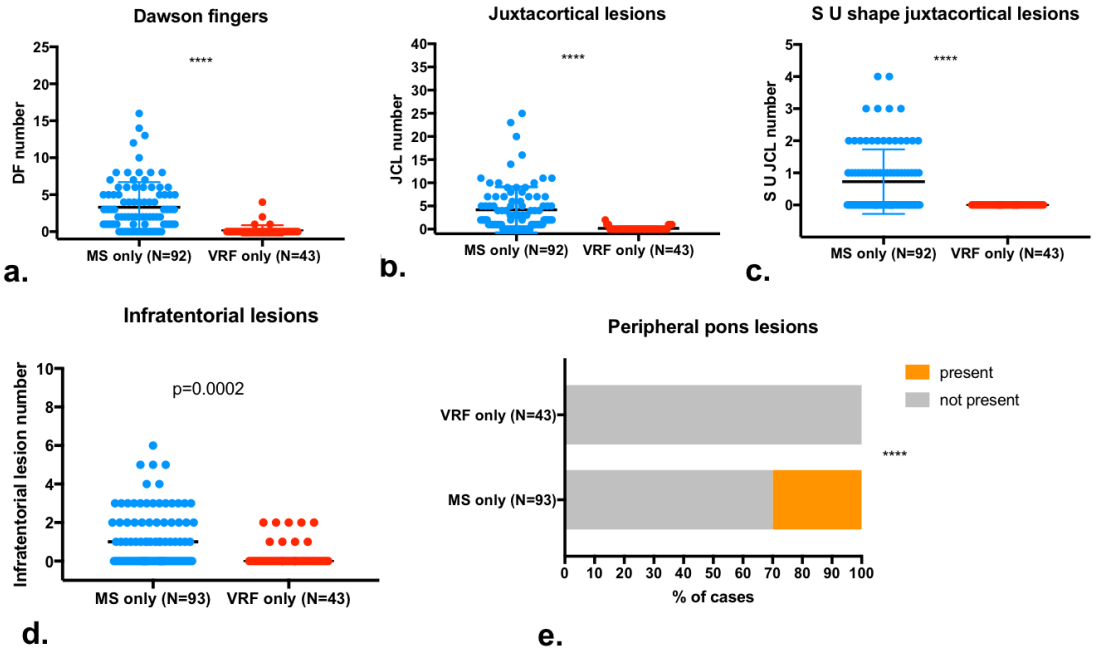

Figure 6.3. MS imaging surrogate marker visual scoring results in MS without VRF and non-MS with VRF.

Dawson fingers (DF) (**a.**), all juxtacortical lesions (JCL) (**b.**) and U or S shaped JCL (**c.**) number, as well as all infratentorial lesion number (**d.**) and the percentage of cases with peripheral pons lesions (**e.**) were compared between MS cases without VRF (blue dots) and non-MS cases with VRF (red dots). ****p<0.001 Mann-Whitney test for (**a.**), (**b.**), (**c.**); Fisher-exact test for (**e.**)

6.3.3.2. Thalamic/whole brain volume ratios

Whole brain volume and thalamic segmentations/volumetric analysis was obtained for 89 MS without VRF cases and 17 non-MS with VRF cases. The thalamic/whole brain volume ratio was not different in MS without VRF (0.51±0.06) compared with non-MS with VRF (0.52±0.07), after adjusting for age and sex, p=0.82.

6.3.3.3. cSVD imaging surrogate marker visual scoring results

Although lacunae counts were low in both groups, they were higher in non-MS with VRF (median 0, range 0-4) compared with MS without VRF (median 0, range 0-1), p=0.002. Lacunae were also more commonly seen in non-MS cases with VRF (7 out of 43, 16.3%) compared with MS cases with no VRF (2 out of 92, 2.2%), p=0.005 (**Table 6.1.** and **Figure 6.4 a.**). The specificity of the lacunae for non-MS with VRF diagnosis was 97.9 % (95%CI 92.5, 99.7).

Basal ganglia perivascular dilatation was seen in a similar proportion in non-MS with VRF (16 out of 43, 37.2%), p=0.85 (**Table 6.1.** and **Figure 6.4 c**.) and MS without VRF (31 out of 92, 33.7%). A poor specificity was found for this marker, 66.7% (95%CI 56.1,76.1).

Central pons lesions were seen in 5.4 %(5 out of 93) of MS without VRF and in 16.3% (7 out of 43) of non-MS with VRF cases (p=0.02) (**Figure 6.4 d.**). Specificity of this marker for non-MS with VRF diagnosis was 94.6% (95%CI 87.9, 98.2).

Microbleeds were not observed in MS and only present in 2 out of 25 (8.0%) of non-MS cases with VRF (**Figure 6.4 b.**) where it was possible to score this feature, so a specificity of 100% (95%CI 89.4, 100) of this marker for non-MS with VRF was observed.

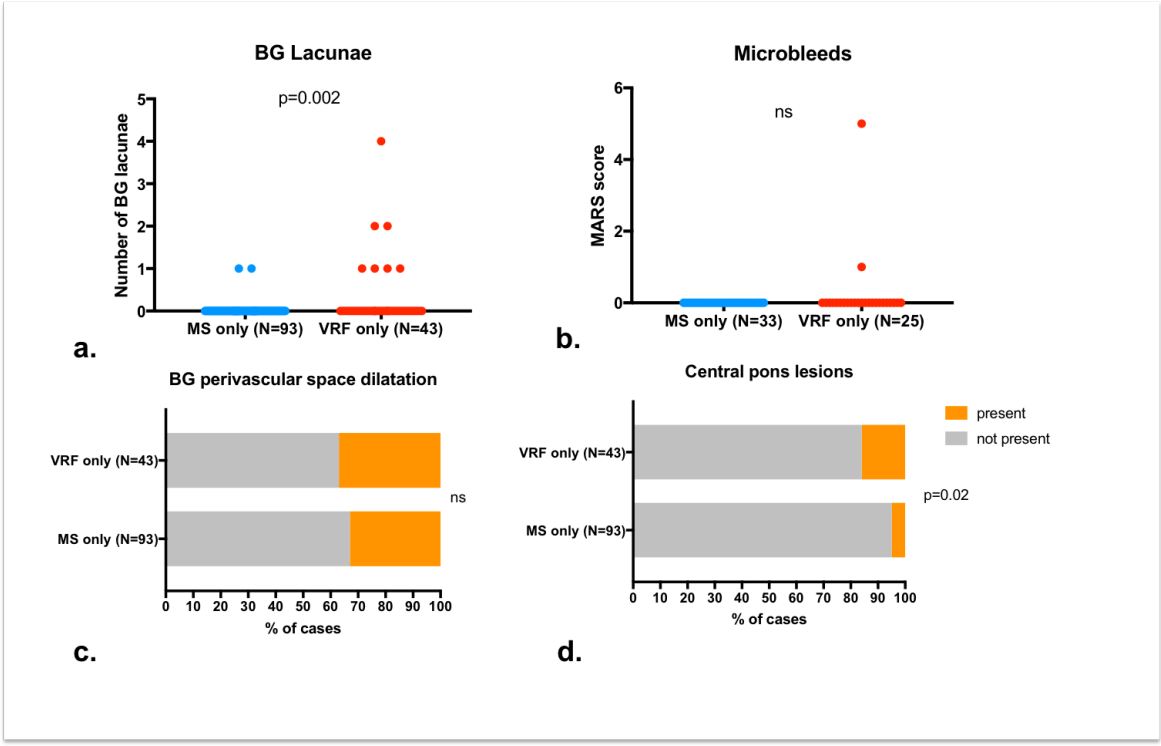

Figure 6.4. cSVD imaging surrogate markers visual scoring results in MS without VRF and non-MS with VRF.

6.3.4. Clinical features and WML volumes of the cohorts included on probabilistic mapping analysis

A total of 33 MS cases without VRF (mean age 44.0 ±6.5 years) and 26 non-MS with VRF cases (mean age 68.5 ±4.5 years) were included for WML volume segmentation and subsequent probabilistic mapping analysis. Clinical data and WML volumes of the cohort included in this analysis is summarized in **Table 6.2**. MS cases were significantly younger than non-MS cases (p<0.001). In the 26 non-MS cases with VRF, 19.2% (N=5) were current smokers, 38.5% (N=10) ex-smokers, 100% (N=26) were diabetic and no information regarding hypertension and dyslipidaemia was available. Quality of segmentation was thought to be good or moderate in the majority of the cases for supratentorial lesions, only in one case (MS without VRF) a major

discrepancy was found between juxtacortical lesion segmentation and juxtacortical lesion count and this case was excluded from the analysis.

The square root transformed WML volumes were compared between MS cases with no VRF and non-MS cases with VRF adjusting for age and sex. No significant differences were found between the two groups regarding total (p=0.81) or periventricular (p=0.59) WML volumes but juxtacortical lesion volumes tended to be higher in MS with no VRF (median=0.22, IQR 0.26) compared with non-MS with VRF (median 0, IQR 0.06, p=0.06) and deep WML volumes tended to be higher in non-MS with VRF (median=1.17 IQR 1.32) compared with MS without VRF (median=0.48, IQR=0.97, p=0.06) (**Table 6.2**.).

Table 6.2. Clinical data and WML volumes of the cohort included for probabilistic mapping

	MS no VRF (N=33)	Non-MS VRF (N=26)	p
Mean age (SD) (years)	44 (6.5)	68.5 (4.9)	<0.001**
% females (N)	75.8 (25)	65.4 (17)	
%MS Type (N) **CIS** **RRMS** **SPMS**	 27.3 (9) 69.7 (23) 3.0 (1)	NA	
Median Disease Duration (years) (IQR)	12.25(10.60)	NA	
Median FLAIR total WML volume (IQR)	7.15 (9.77)	7.23 (6.53)	0.81
Median FLAIR periventricular WML volume (IQR)	5.97 (9.28)	5.50(5.64)	0.59
Median FLAIR deep WML volume (IQR)	0.48 (0.97)	1.17(1.32)	0.06
Median FLAIR juxtacortical WML volume (IQR)	0.22 (0.26)	0 (0.06)	0.06

**p<0.01

6.3.5. Lesion distribution

The lesion probability distributions for the MS cases with no VRF and non-MS cases with VRF are shown in **Figure 6.5 A** and **B**, respectively. The distribution of the lesions throughout the brain tissue is widely variable which is reflected by the low probability

of lesions occurring in the same specific location in more than two patients. The area of highest probability of a lesion occurring in the MS with no VRF group was in the frontal WM adjacent to the right frontal horn (MNI coordinate -16.8 mm, 30.4 mm, 2 mm at a probability of 78.1%). In the non-MS with VRF group, the most likely place for a lesion to occur was also in the frontal WM adjacent to the right frontal horn (MNI coordinate -17.9 mm, 28.3 mm, 2 mm at a probability of 92.3%) and adjacent to the body of the right lateral ventricle (MNI coordinate -17.9 mm, -10.6 mm, 26 mm at a probability of 88.5%). The higher probabilities seen amongst the non-MS VRF group indicate a greater coherence of lesion location in this group. A direct comparison of the distributions is depicted in **Figure 6.5 C**, where the average of the MS with no VRF lesion map has been subtracted from the average non-MS with VRF lesion map. In both groups widespread lesions were observed in the supra and infratentorial WM and grey matter, with several areas being similarly affected. However, in the infratentorial compartment more MS lesions were found in middle cerebellar peduncles whereas more vascular lesions were seen in the central pons. In the non-MS with VRF group, no lesions were seen in the medulla oblongata but this area was affected in MS. More MS lesions than vascular lesions were present in the inferior temporal lobe, adjacent to the temporal horn. Although periventricular lesions were commonly seen in both groups, the MS with no VRF showed more lesions around the posterior aspect of the lateral ventricles, including the occipital horn, than the non-MS with VRF group and despite MS lesions being common in the anterior part of the lateral ventricles, vascular lesions were even more commonly seen in this area. Finally, vascular lesions affected the deep WM, spreading throughout the corona radiata more widely than MS lesions. Lesions in the corpus callosum as well as in the deep grey matter were seen in both groups.

Figure 6.5 D shows the voxel-wise permutation testing comparison of the lesion distributions in each group. Vascular lesions were significantly more likely than MS lesions adjacent to the frontal horn and body of the lateral ventricle (corrected p <0.01). After adding age as a nuisance variable this does not reach statistical significance, though the areas of higher likelihood are the same (p=0.11). Since total lesion load did not differ between groups this variable was not added to the design matrix and contrasts of the Randomize analysis. The lesional regions with the greatest likelihood to be in the MS group and not in the non-MS with VRF group were the periventricular area adjacent to the posterior lateral ventricle at the margin of the splenium of the corpus callosum (corrected p=0.16) and the inferior temporal lobe adjacent to the temporal horn (corrected p=0.20) but this did not reach statistical significance, possibly due to the high variability of MS lesions between subjects, each individual region having a low probability of having a lesion.

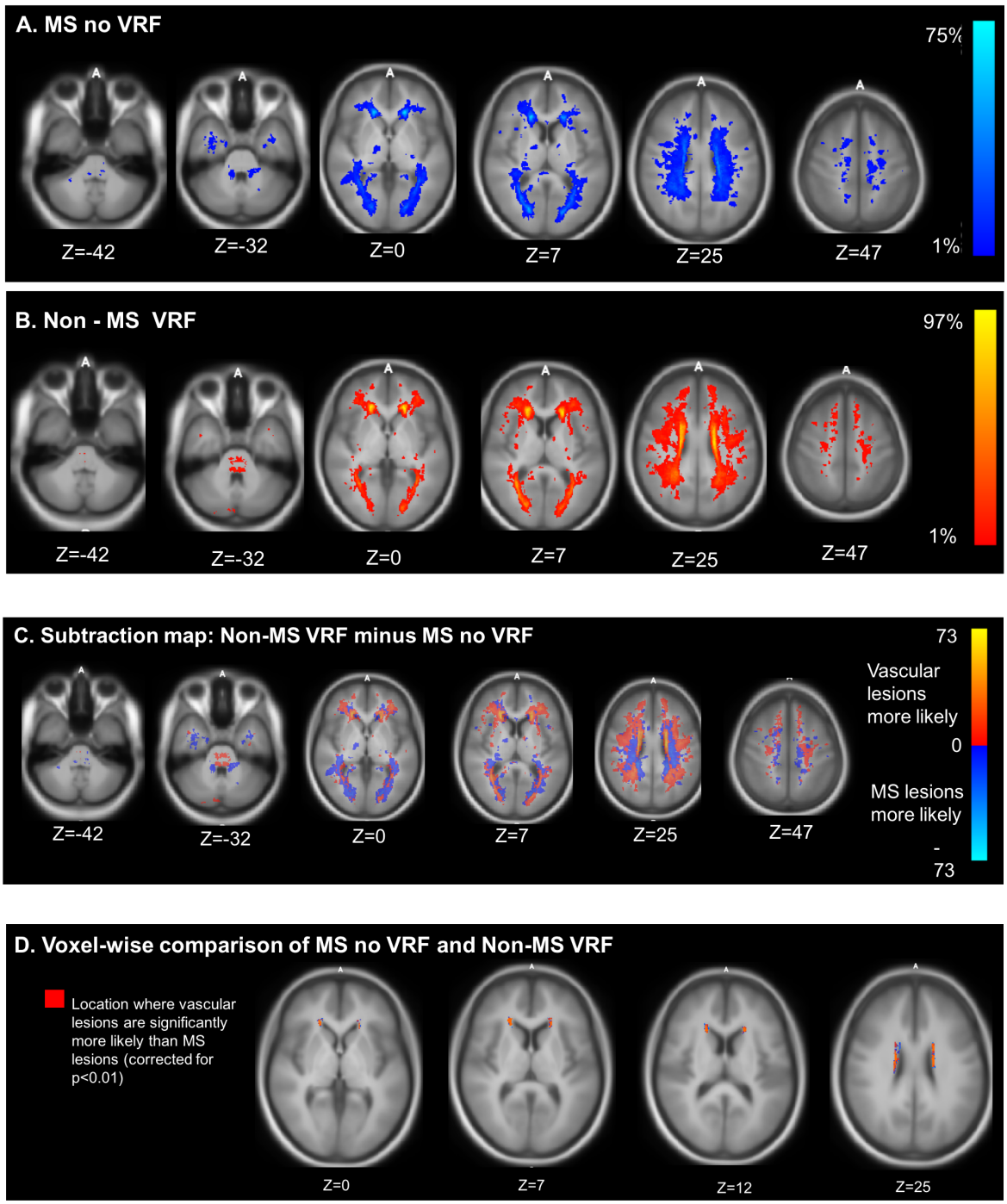

Figure 6.5. Lesion probability distribution analysis

A. Lesion probability distribution for 32 MS cases with no VRF. The colour scale (from 1 to 75%) represents the minimum to maximum probability of a lesion occurring in a particular space location. MNI standard space template Z coordinate is shown in mm. **B.** Lesion probability distribution for 26 non-MS cases with VRF. The colour scale (from 1 to 97%) represents the minimum to maximum probability of a lesion occurring in a particular special location. MNI standard space template Z coordinate is shown in mm. **C.** Subtraction map where

the average of the MS with no VRF lesion map has been subtracted from the average of non-MS with VRF group lesion map to allow a direct statistical comparison of the lesion distributions. Red to yellow represents where vascular lesions are more likely than MS lesions, a light blue to dark blue where MS lesions are more likely than vascular lesions. **D.** Voxel wise comparison of lesion probability maps showed that vascular lesions are significantly more likely than MS lesions adjacent to the body and to the frontal horn of the lateral ventricle, shown here in red (corrected $p<0.01$).

6.4. Summary of the main findings

1. U-S shaped juxtacortical lesions and peripheral pons lesions have the highest (100%) specificity for MS. Dawson fingers, all types of juxtacortical lesions and the presence of black-holes, are much more common in MS than in non-MS with VRF, with a good specificity but can also be seen in a small proportion of non-MS cases with VRF. Although more commonly seen in MS without VRF than in non-MS without VRF, inferior temporal lobe lesions specificity was lower than for the other imaging markers. Thalamic/whole brain volume ratio is not a useful discriminator between MS without VRF and non-MS with VRF.

2. The presence of basal ganglia lacunae and central pons lesions are strongly associated with non-MS with VRF with a good specificity for this diagnosis. However, basal ganglia perivascular space dilatation had a poor specificity for non-MS with VRF, since it was commonly seen in MS without VRF too. Microbleeds seem to be a specific marker for non-MS with VRF, though the small sample size and clinical differences between MS without VRF and non-MS with VRF need to be considered.

3. Despite the similarity in lesion distribution in the two groups, probabilistic WML map analysis showed that lesions in the frontal WM adjacent to the frontal horn and the anterior aspect of the body of the lateral ventricle were more likely to occur in the non-MS with VRF group than MS without VRF. Although they did not reach significance, the following lesions occurred more in pure MS than in pure VRF at the following locations: at the WM adjacent to the posterior lateral ventricle, at the periphery of the pons and in the medulla oblongata, while lesions in the central pons were more likely in VRF only. Overall juxtacortical lesion volumes tended to be higher in MS compared with non-MS and the reverse was seen for deep WML volumes.

6.5. Discussion

This study investigated, for the first time, the specificity of several brain imaging markers, seen on conventional MRI, by directly comparing MS cases without VRF and non-MS cases with VRF. Although direct comparison of imaging features between two disorders has proven to be quite useful in identification of disease discriminators (Juryńczyk *et al.*, 2017*b*; Cacciaguerra *et al.*, 2019) this approach has rarely been used to compare MS with cSVD (Schmidt *et al.*, 2006; Mistry *et al.*, 2016; Geraldes *et al.*, 2018). Moreover, until recently a VRF profile was not obtained in MS and most studies may have included cases with a mixture of MS and VRF associated WML.

I have identified imaging markers that strongly associate with MS and others that are strongly associated with the presence of VRF, some of which have a 100% specificity. The U-fibres commonly affected in MS (Brownell and Hughes, 1962) and were classically considered to be relatively preserved in cerebrovascular disease (Barkhof

and Scheltens, 2002). Although this latter assumption has rarely been tested *in vivo* before, it is not surprising that U and S shaped juxtacortical lesions were specific for MS. Some non-MS cases with VRF had a few juxtacortical lesions but none with a S or U shape. Though the U fibres receive blood supply from both the subcortical and medullary arteries stemming from the pial arteries it is possible that the cortical-WM junction (Akashi *et al.*, 2017) is not completely free from hypoxia/ischaemic injury, particularly in older patients with VRF (Salvadó *et al.*, 2019). In fact, I have found these lesions to be present only in the older non-MS with VRF cohort from Barcelona and not in the younger Amsterdam cohort. I would still consider juxtacortical WML to be quite specific for MS, even more in younger ages.

Periventricular lesions are common both in MS and cSVD. However well-demarcated, ovoid or flame-like shaped WML perpendicular to the wall of the lateral ventricles are thought to be typical of MS both in brain imaging (Horowitz *et al.*, 1989) and pathology studies (Dawson, 1916). These lesions, classically named as Dawson fingers, which have shown to be useful in differentiating MS from other inflammatory CNS disorders (Matthews *et al.*, 2013, Juryńczyk *et al.*, 2017*b*), have also shown to be useful to discriminated pure MS from VRF associated WML in the present study. Despite being high, the specificity of this imaging marker was not 100%. Less elongated periventricular lesions are usually seen in cSVD compared with MS (Okuda *et al.*, 2017). However, age-related venous collagenosis (type 5 cSVD), which may also be affected by VRF, has recently been associated with elongated periventricular lesions (Keith *et al.*, 2017) which may be difficult to distinguish from Dawson fingers.

Lesions located at the periphery of the pons have been described in MS (Nakashima *et al.*, 2001) and in theory, due to a rich vascularization, this area is not prone to cSVD. On the contrary, the central pons is supplied by perforating end-arterioles and is prone to ischaemic hypoxia and demyelination which underlies the FLAIR and T2 hyperintensities seen in this area in patients with cSVD (Pullicino *et al.*, 1995). However, these assumptions are based in very few observations and the role of these markers in discriminating MS from cSVD had not been tested so far and I was happy to confirm that peripheral pons lesions are quite specific for MS, whereas central pons lesions associate with cSVD.

Although black-holes can be seen in cSVD (Norrving, 2008) they seem to be more common and severe in MS, possibly translating a more marked neuronal damage in this group. Thalamic atrophy was not found to be useful in differentiating MS from non-MS with VRF. Few studies have investigated the effect of VRF on thalamic volumes. Although, the basal ganglia were found to be less susceptible to volume loss compared with the medial temporal lobe in presence of VRF, in a large cohort of elderly participants without MS (de Jong *et al.*, 2014), the literature is insufficient to conclude that VRF do not influence thalamic volumes. If indeed there is an effect, thalamic volumes differences between MS and cSVD may be smoothen.

The presence of infarcts in a brain MRI with WML is thought to suggest cerebrovascular disease instead of MS (Geraldes *et al.*, 2018) and this chapter's findings support that basal ganglia lacunae indicate cSVD more than MS. However, basal ganglia perivascular dilatation is seen in both MS and non-MS and this is in line with this thesis chapters 3 and 4 findings. Microbleeds seem to be specific of cSVD but

owing to the small number of cases analysed and the discrepancy between cohorts in terms of age these results need to be interpreted with caution. Nevertheless, similarly to what was found in this chapter, microbleeds were not detected in a larger cohort of MS cases without vascular comorbidities (Eisele *et al.*, 2016). It is also reassuring that the proportions of lacunae and microbleeds documented in the present study non-MS cases are similar to those reported in the few studies that have previously assessed these cSVD imaging markers in non-MS cohorts with a similar age distribution (Bryan *et al.*, 1999; Daugherty and Raz, 2017; Thorn *et al.*, 2019; Yakushiji *et al.*, 2019).

I explored the differences in lesion distribution between pure MS and non-MS with VRF attempting to find a non-pre-specified differentiating factor between the two conditions. By comparing probabilistic maps from pure MS and pure VRF I have identified some potential discriminating locations, in line with the visual scoring results. Although the WM adjacent to the frontal horn of the lateral ventricle was commonly affected in both groups in the present very conservative voxel-based analysis this area and the area adjacent to the anterior aspect of the body of the lateral ventricle was significantly more affected in VRF only compared with MS only. Rostrup et al. (Rostrup *et al.*, 2012) has shown that these are the most commonly affected areas in age-VRF related WM changes. In the same study deep WML were found to associate with VRF. In line with these observations, I have also found that the deep WM was more commonly affected in the non-MS with VRF group compared with the MS without VRF group. Infratentorial lesion distribution also differed between MS only and VRF only. MS more likely affected the middle cerebellar peduncles, in line with previous reports (Brainin *et al.*, 1987; Kincses *et al.*, 2011) and the medulla oblongata. On the other hand, this study confirms that central pons lesions are a feature of cSVD,

as previously suggested (Pullicino *et al.*, 1995; Caplan, 2015) but are much less common in MS. Also, the inferior temporal lobe had a higher probability of being affected in MS than in VRF only. However, these latter differences in lesion distribution did not survive voxel-based analysis, possibly owing to the small sample size.

This exploratory study of lesion distribution has several other limitations. Firstly, lesion segmentation was obtained with an automated tool, and, despite a moderate to good match with the visual inspection and a good reported accuracy and reproducibility of MSmetrix (Jain *et al.*, 2015, 2016), currently automated segmentation tools, MSmetrix included, are still less sensitive than the human eye to detect lesions (de Sitter *et al.*, 2017). Secondly, FLAIR and T1 MRI sequences were slightly different in MS only and VRF only, and only one centre contributed with scans for this latter group. Finally, age was not matched between the two groups and it is possible that younger non-MS cases would have less widespread WML, and thus differences between the two groups more evident. Also, periventricular lesions may occur with aging and it is possible the differences found in this area only relate to aging and not to VRF.

Despite these limitations, these results are in line with what has been described in the literature and suggests that significantly different features may be found in a larger study.

In conclusion, this study identified novel specific imaging markers of MS and cSVD, that may be useful in clinical practice, though this needs to be tested prospectively and in a broader population (i.e. older cohort, with different VRF, originating from non-

tertiary centres). Moreover, this work has now set the stage to test the influence of VRF on “MS-specific” markers and of MS on “cSVD- specific” markers.

7 The influence of VRF on MS imaging surrogate markers

7.1 Introduction

VRF, such as smoking and arterial hypertension associate with worse clinical outcomes in MS. Few imaging studies in MS have considered the effect of VRF on WML (Chapter 1, section 1.6.2.2, Table 1.3.). A higher burden of T2 WML volumes was reported in MS active smokers (Healy *et al.*, 2009; Zivadinov *et al.*, 2009) and in MS patients with concomitant hypertension and smoking (Kappus *et al.*, 2015). Since WML are common both in MS and cerebrovascular disease, it is not clear whether this increase of lesion load is due to a higher burden of "MS-like" or "vascular" WML. The main aim of the present chapter is to test the first hypothesis. In the previous chapter it was shown that juxtacortical lesions, particularly U and S shaped, Dawson-fingers, peripheral pons lesions and presence of black-holes have a good specificity for MS and the main Chapter 7 research question is:

1. Do VRF associate with a higher burden of these MS imaging surrogate markers?

To test if VRF associate with a higher burden of MS imaging markers, these markers will be compared between a group of MS cases without VRF and a group of age- and sex-matched MS cases with VRF.

I would also like to explore the following research question:

2. Do VRF influence lesion distribution in MS?

To test whether VRF associate with more lesions in a typical MS location lesion probabilistic brain lesion maps will be compared between MS without VRF and MS with VRF.

7.2. Materials and Methods

7.2.1. Study design and cohorts

A multicentre retrospective observational case-control study was set up to compare MS cases without VRF and age- and sex-matched MS cases with VRF. Anonymised clinical and imaging data was obtained from 5 MAGNIMS consortium centres as described in Chapter 1, section 1.7.2.2. From an initial total of 227 MS cases, with available FLAIR and T1-weighted brain MRI scans, 93 MS patients without VRF and 108 MS with VRF cases were included for analysis. A subgroup of MS with (N=43) and without (N=32 out of the initial 33, see Chapter, section 6.3.4) VRF were included in the lesion distribution probabilistic analysis.

7.2.2. Imaging Analysis

Visual scoring of MS imaging surrogate markers was performed as described in Chapter 6, section 6.2.2.1, in both MS without and with VRF. Imaging markers who have shown a specificity above 85% (Chapter 6, section 6.3.3.1) were included: total number of Dawson fingers, juxtacortical lesions, including S-U shaped, the presence of peripheral pons lesions and presence of black holes were included in the analysis. The specificity of the presence of any infratentorial lesion to differentiate MS without VRF from non-MS with VRF was below 85% but the lesion counts were significantly different between the two groups. Thus, I decided to also explore the effect of VRF on the total number of infratentorial lesions in MS.

Lesion segmentation, volumes and probabilistic maps were obtained as described in Chapter 6 sections, 6.2.2.3 and 6.2.2.4.

7.2.3. Statistical analysis

Descriptive statistics was performed as described in Chapters 2, section 2.2.3. and Chapter 6, section 6.2.3. Poisson log-liner regression models were used to determine the effect of presence of VRF on count variables with a Poisson distribution: number of Dawson fingers, number of juxtacortical lesions, adjusting for nuisance variables (i.e. age, disease duration). Binary logistic regression was used to test the effect of VRF on categorial variables: presence of peripheral pons lesions and of black-holes, adjusted for age and sex. Similar analysis was explored including each individual VRF: smoking, hypertension, dyslipidaemia, diabetes. Results will be presented as Exp (B) and 95% CI. Since multiple testing was involved in the analysis of MRI and clinical data, a conservative p=0.01 was used to assess significance. A statistical trend was assumed if p≤0.05. All analysis were performed with SPSS version 25 and GraphPad Prism version 7.

7.3. Results

7.3.1. Clinical features of the cohorts used for MS imaging markers visual scoring

Clinical features as well as the VRF profile of the MS cohorts used in Chapter 7 are summarized in **Table 7.1**. Clinical features of the different cohorts varied across centres was previously described in Chapter 1, section 1.7.2.2, **Table 1.4**. No significant differences were found between the MS without VRF and the MS with any VRF regarding age, sex, disease duration, MS subtype, EDSS or DMT. However, if segregated by VRF, hypertensive (N= 44, 50.6±9.3 years, p=0.03) and diabetic (N=10, 55.5±7.8 years, p=0.002) MS patients were significantly older compared with those with no VRF (N=47.2 ±8.2 years) (**Table 7.1**).

Three cases had confluent lesions (one MS without VRF, two MS with VRF) and it was not possible to obtain the Dawson finger and Juxtacortical lesion number, so they were excluded from the analysis.

Table 7.1. Clinical features and MS imaging markers quantification of the MS cohort used in Chapter 7 stratified by VRF.

	no VRF (N=93)	Any VRF (N=108)	Ever-smokers (N=85)	HT (N=44)	DysL (N=25)	DM (N=10)
Mean age (years) (SD)	47.2 (8.2)	48.3 (8.5)	48. 5(8.4)	50.6 (9.3)	49.4 (8.2)	55.5 (7.8)
% females (N)	63.4 (59)	62.0 (67)	62.4 (53)	61.4 (27)	64.0 (16)	50.0 (5)
%MS Type (N)						
CIS	20.4 (19)	13.9 (15)	9.4 (8)	13.6 (6)	20.0 (5)	10.0 (1)
RRMS	53.8 (50)	62.0 (67)	64.7 (55)	54.5 (24)	52.0 (13)	60.0 (6)
SPMS	18.3 (17)	15.7 (17)	18.8 (16)	18.2 (8)	16.0 (4)	30.0 (3)
PPMS	7.5 (7)	8.3 (9)	7.1 (6)	13.6 (6)	12.0 (3)	
Median Disease Duration (years) (IQR)	12.3 (12.8)	11.8 (11.7)	12.6 (10.7)	12.1 (16.0)	11.0 (16.3)	13.1 (15.4)
Median EDSS (IQR)	2.5 (4)	3.0 (4)	3.0 (4)	3.5 (4)	2.5 (4)	3.0 (4)
DMT						
None	47.3 (44)	42.6 (46)	38.8(33)	50.0 (22)	52.0 (13)	30.0 (3)
First line	47.3 (44)	44.4 (48)	45.9 (39)	43.2 (19)	36.0 (9)	50.0 (5)
Second line	5.4 (5)	9.3 (10)	10.6 (9)	6.8 (3)	12.0 (3)	10.0 (1)
NA		2.8 (3)	4.7 (4)			
	N=92	N=106	N=84	N=43		
Median DF (IQR)	2 (4)	2 (4)	3 (5)	2 (4)	2 (4)	1.5 (4)
% cases 1 or more DF (N)	78 (72)	78.3 (83)	82.1 (69)	72.1 (31)	80.0 (20)	70.0 (7)
	N=92	N=106	N=84	N=43		
Median JCL (IQR)	2 (5)	2 (5)	2.5 (7)	2 (5)	2 (8)	1.5 (3)
% cases 1 or more JCL (N)	80.4 (74)	84.0 (89)	86.9 (73)	81.4 (35)	80.0 (20)	70.0 (7)
	N=92	N=106	N=84	N=43		
Median U S JCL (IQR)	0 (1)	0 (1)	0 (1)	0 (1)	0 (1)	0 (1)
% % cases 1 or more U S JCL (N)	43.5 (40)	36.8 (39)	38.1 (32)	36.4 (16)	32.0 (8)	20 (2)
Median iTL (IQR)	1 (2)	1 (2)	1 (2)	0 (2)	1 (2)	0 (1)
% cases 1 or more iTL(N)	52.7 (49)	50.9 (55)	54.1 (46)	50 (22)	52.0 (13)	30.0 (3)
% peripheral pons lesion (N)	31.2 (29)	30.6 (33)	35. 3(30)	25.0 (11)	28.0 (7)	10.0 (1)
	N=92					
% black-holes (N)	59.1(55)	51.9 (56)	56.8 (46)	44.1 (19)	48.0 (12)	60.0 (6)

CIS – clinical isolated syndrome, RRMS – relapsing remitting MS, SPMS – secondary progressive MS, PPMS – primary progressive MS, DMT – disease modifying treatments, DF – Dawson fingers, JCL – juxtacortical lesions, iTL- infratentorial lesion, IQR – interquartile range

7.3.2. The relationship between MS imaging markers and age and disease duration

To appropriately determine the effect of VRF on each type of lesion we need to understand the relationship between lesion number with age and disease duration. No significant associations were found between age and any of the studied MS imaging markers. The number of Dawson fingers (r_s=0.31, p<0.001) and of juxtacortical lesions (r_s=0.26, p<0.001) including S-U shaped lesions (r_s=0.15, p=0.04), and the presence of black-holes (r_s=0.12, p=0.001) increased with disease duration. Disease duration did not influence infratentorial lesion number (r_s=0.02, p=0. 82) nor the presence of peripheral pons lesions ($r\tau$=0.3, p=0.66).

7.3.3. MS imaging markers visual scoring results: comparisons between MS with and without VRF

The results of visual scoring quantification of Dawson fingers, juxtacortical lesions, including those with a U or S shape and infratentorial lesions, segregated per VRF status are summarized in **Table 7.1**. Of note, less than half of the MS cases with or without VRF had U or S shaped juxtacortical lesions and the spread of these lesions counts was narrow in both groups. In the univariate analysis no significant differences were found between MS without VRF and MS with VRF regarding the total number of Dawson fingers (p=0.92) (**Figure 7.1 a.**), all juxtacortical lesions (p=0.59) (**Figure 7.1 b**.), S-U shaped juxtacortical lesions (p=0.25) (**Figure 7.1 c**.), infratentorial lesions (p=0.48) (**Figure 7.3 a.**), presence of black-holes (p=0.45), or of peripheral pons lesions (p=0.99).

The number of juxtacortical lesions was 26.0% higher in MS with VRF (Exp (B)=1.26, 95%CI 1.11, 1.44, p<0.001) compared with MS without VRF in a Poisson model adjusting for disease duration (**Table 7.2.**). In a similar model, no significant differences between the two groups were found regarding the number of S-U shaped juxtacortical lesions or of Dawson fingers (**Table 7.2.**). Presence of black-holes (Exp(B) = 1.2, 95%CI 0.7,2.2, p=0.48) and presence of peripheral pons lesions (Exp (B)=1.03, 95%CI 0.56, 1.87, p=0.94) did not differ between the two groups, in a binary logistic model, including disease duration as a nuisance variable .

As pre-planned, MS imaging markers scoring results were also segregated per VRF type (**Table 7.1**). Although univariate analysis did not show any significant difference between each MS cases with each individual VRF and MS cases without VRF (results not shown), the graphical display of Dawson fingers (**Figure 7.1 c.**) and juxtacortical (**Figure 7.1 d.**) lesion number per VRF type suggested that not all VRF had the same effect on these imaging markers.

Considering that smoking is the only non-treatable VRF and possibly with a longer time of exposure, I have segregated MS smokers from MS with no VRF and with VRF other than smoking and plotted the distribution of Dawson fingers and Juxtacortical lesions against disease duration (**Figure 7.2**). An excess of both these "MS-like" lesions was seen in the MS ever smoker group with no other VRF compared with MS cases without VRF or MS cases with VRF other than smoking.

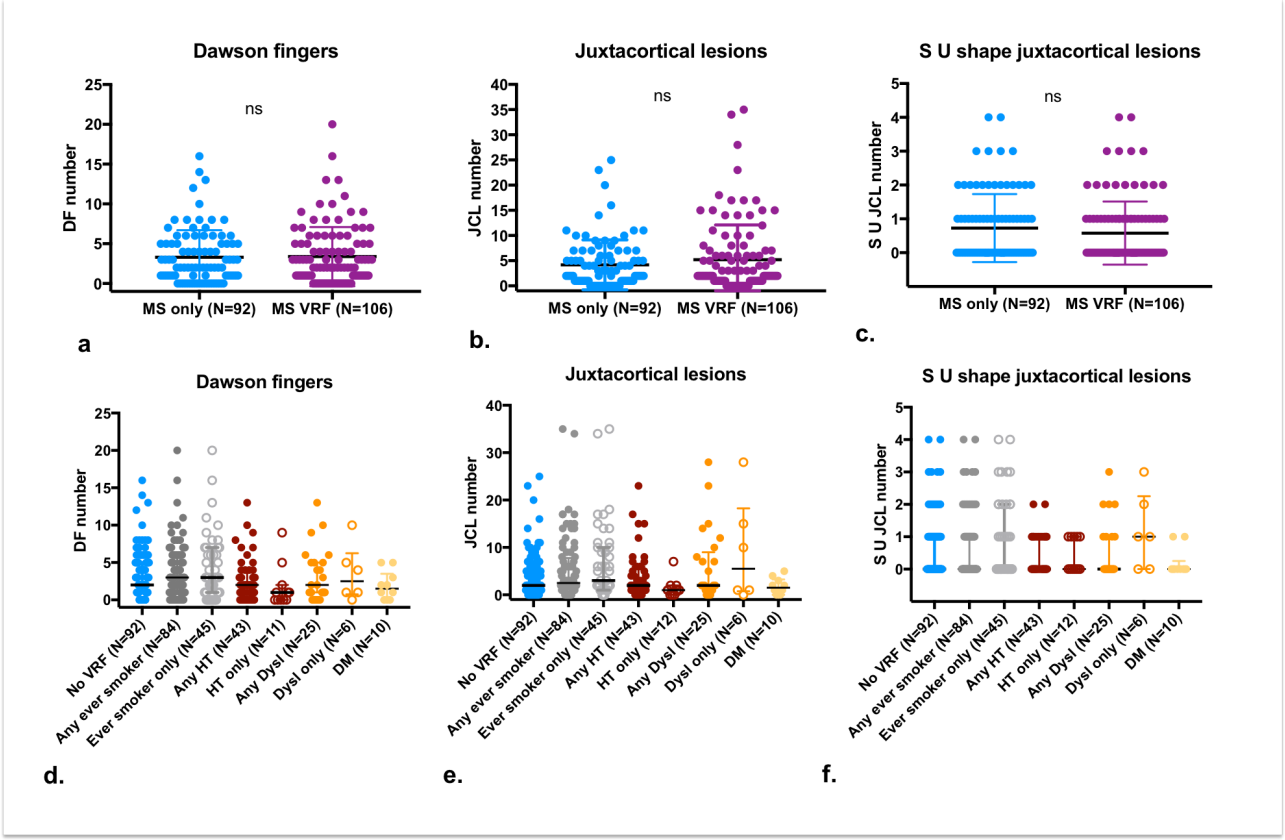

Figure 7.1. Comparisons of MS imaging markers between MS with and without VRF.

a. Dawson fingers, **b.** juxtacortical lesion number and **c.** U- S-shaped juxtacortical lesions were compared between MS with any VRF and without VRF. **d.** Dawson fingers, **d.** all and **e.** U- S-shaped juxtacortical lesions were further compared between MS cases segregated per type of VRF. MS ever smokers, hypertensives (HT) and with dyslipidaemia (DysL) were further subdivided in those with that VRF only or in combination with other VRF. ns - no significant differences were found between groups (Mann-Whitney test)

Table 7.2. Poisson loglinear model to predict the number of Dawson fingers and juxtacortical lesions considering the presence of any VRF and disease duration.

	Dawson fingers			Juxtacortical lesions (JCL)			U-S JCL		
Parameter	**Exp (B)**	**95%CI Exp (B)**	**p**	**Exp (B)**	**95%CI Exp (B)**	**p**	**Exp (B)**	**95%CI Exp (B)**	**p**
VRF=1	1.05	0.89,1.22	0.550	1.26	1.11,1.44	0.001**	0.81	0.57,1.15	0.26
Dis. Duration (years)	1.03	1.02,1.03	0.001**	1.02	1.01, 1.02	0.001**	1.02	1.00, 1.04	0.01*

**p<0.01

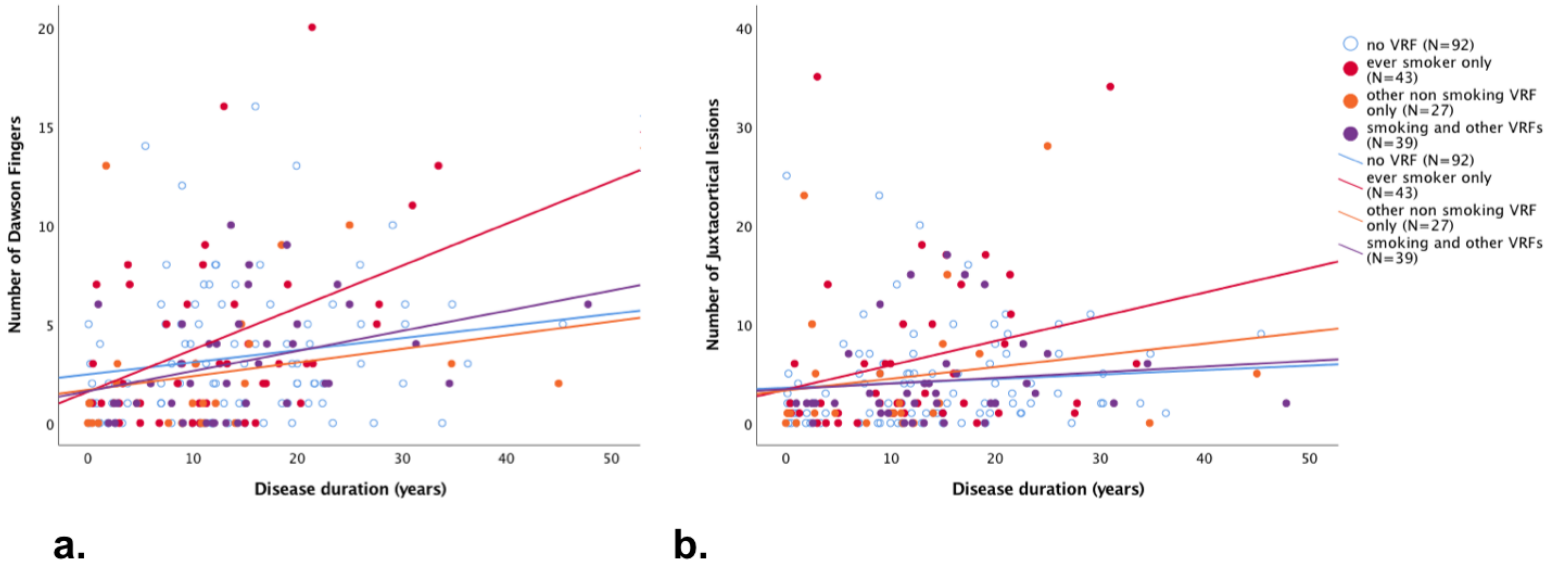

Figure 7.2. Dawson fingers and juxtacortical lesion counts and disease duration in MS per VRF group.

No VRF (blue line), smoking (red line), smoking and with other VRF (purple line) and only VRF other than smoking (orange line).

In a prespecified model to predict the number of Dawson fingers considering each individual VRF, including disease duration as covariate, smoking was associated with a higher burden of Dawson fingers (**Table 7.3.**). When the same model was applied to explain juxtacortical lesions divergent effects were seen for the different VRF. While ever smoking and presence of dyslipidaemia associated with a higher burden of juxtacortical lesions, the reverse was seen for diabetes, and hypertension showed no effect (**Table 7.3.**). No effect of any VRF was seen on U-S-shaped juxtacortical lesions (**Table 7.3.**).

Table 7.3. Summary of the Poisson log-linear models to predict the number of Dawson fingers and juxtacortical lesions considering each individual VRF separately, adjusting for disease duration and age.

	Dawson fingers			Juxtacortical lesions (JCL)			U-S JCL		
Parameter	**Exp (B)**	**95%CI Exp (B)**	**p**	**Exp (B)**	**95%CI Exp (B)**	**p**	**Exp (B)**	**95%CI Exp (B)**	**p**
Ever-smoker	1.23	1.05,1.43	0.009**	1.32	1.16,1.50	<0.001**	0.99	0.69,1.40	0.96
Hypertension	0.91	0.75,1.11	0.370	0.93	0.79,1.11	0.460	0.60	0.36, 1.00	0.05
Dyslipidaemia	0.98	0.78,1.24	0.890	1.32	1.10,1.57	0.002**	0.78	0.44,1.39	0.45
Diabetes	0.63	0.39,1.00	0.051	0.39	0.24,0.63	<0.001**	0.30	0.07,1.23	0.09

**p<0.01, Exp (B) for age and disease duration not shown

Infratentorial lesions were seen in 52.7 % (49 out of 93) of MS cases with no VRF, 50.9 % (55 out of 108) of MS cases with VRF. No statistically significant differences were seen in infratentorial lesion number between MS only and MS with VRF (**Figure 7.3 a**.), even after taking age and disease duration into account (EXP(B)=0.99, 95%CI 0.77,1.29, p=0.97). No significant differences were found between the different VRF groups (**Figure 7.3 b**), even after taking age and disease duration into account (data not shown).

The frequency of peripheral pons lesions was the same in MS without and MS with VRF (**Figure 7.3 c**.). In univariate analysis the proportion of cases with peripheral pons lesions did not significantly vary between MS ever-smokers, hypertensives, dyslipidemics, and diabetics and MS without VRF (**Table 7.1**). In an exploratory binary logistic model to determine the effect of each individual model on the presence of peripheral pons lesions, taking in to account nuisance variables, no significant effect of these VRF on peripheral pons lesions was observed (data not shown).

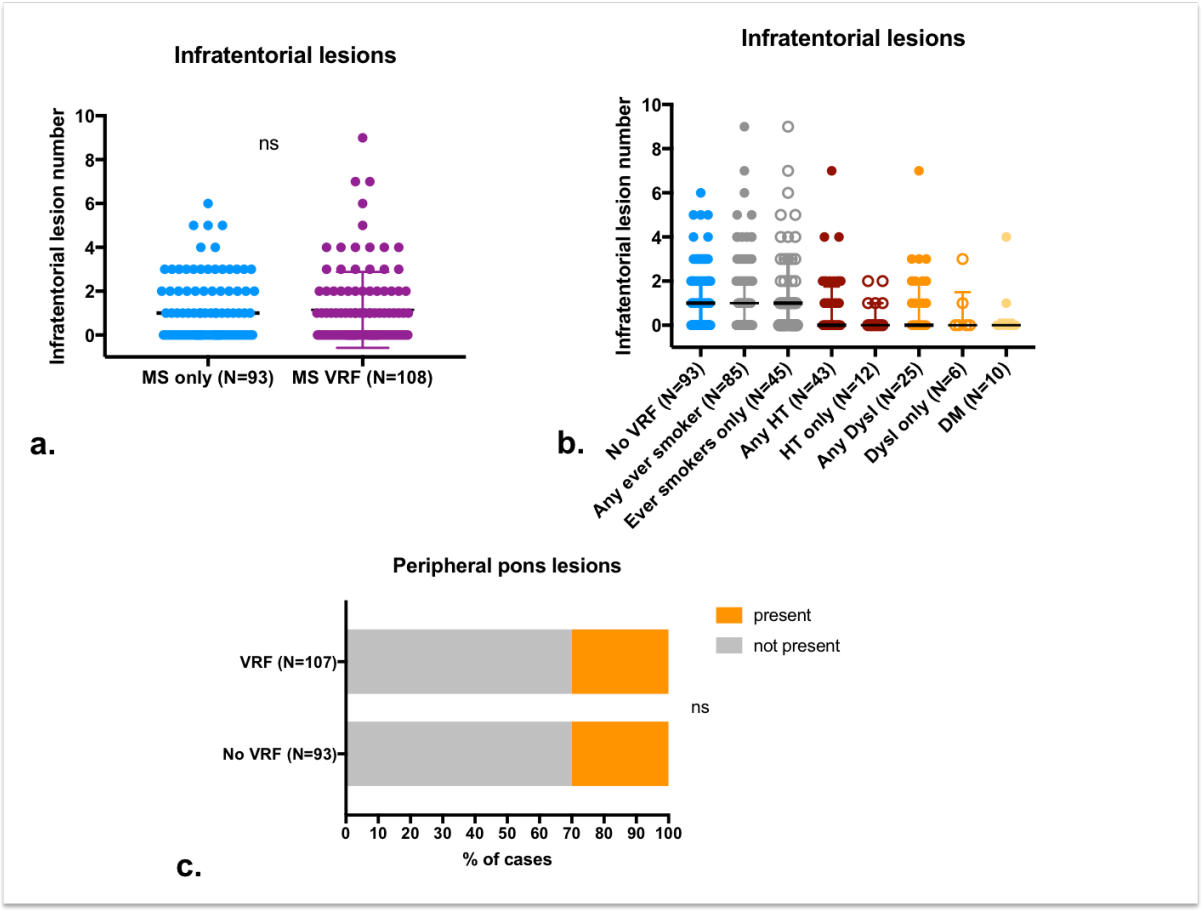

Figure 7.3. Infratentorial lesions in MS with and without VRF.

a. The number of infratentorial lesions was compared between MS cases without VRF and with VRF and **b.** were segregated per VRF type. MS ever smokers, hypertensives (HT) and dyslipidaemics (DysL) were further subdivided in those with that VRF only or in combination with other VRF. **c.** The percentage of MS cases with peripheral pons lesions was compared between MS with and without VRF. No significant differences (ns) were found between groups (Mann-Whitney test for **a.** and **b.**, Chi-square test for **c.**)

7.3.4. Clinical features and WML volumes of the cohorts use for probabilistic mapping analysis

A total of 33 MS cases without VRF (mean age 44.0 ± 6.5 years) and 43 with VRF (mean age 44.8 ±6.4 years) were included for WML segmentation and subsequent WML probabilistic mapping analysis. Clinical data and WML volumes of the cohort included in this analysis are summarized in **Table 7.4**. MS with and without VRF groups did not differ in terms of sex (p=0.68), disease type (p=0.79), disease duration (p=0.07). From the 43 MS cases with VRF, 65.1% (N=28) were current smokers, 18.6% (N=8) ex-smokers, 32.6% (N=14) had dyslipidaemia, 16.3% (N=7) hypertension and 9.3% (N=4) were diabetic.

The square root transformed WML volumes were compared between MS cases with no VRF and MS cases with VRF adjusting for age, sex and disease duration and no differences were found for any of the WML volumes (**Table 7.4**).

Table 7.4. Clinical data and WML volumes of the cohort included for probabilistic mapping

	MS no VRF (N=33)	MS VRF (N=43)	p
Mean age (SD)	44 (6.5)	44.8 (6.4)	0.37
% females (N)	75.8 (25)	69.8 (30)	0.68
%MS Type (N) **CIS** **RRMS** **SPMS**	 27.3 (9) 69.7 (23) 3.0 (1)	 20.9 (9) 76.7 (33) 2.3 (1)	0.79
Median Disease Duration (years) (IQR)	12.25(10.60)	9.5(11.20)	0.07
Median FLAIR total WML volume (IQR)	7.15 (9.77)	5.24 (8.06)	0.23
Median FLAIR periventricular WML volume (IQR)	5.97 (9.28)	4.01 (5.84)	0.21
Median FLAIR deep WML volume (IQR)	0.48 (0.97)	0.50 (0.64)	0.70
Median FLAIR juxtacortical WML volume (IQR)	0.22 (0.26)	0.18 (0.44)[!]	0.38

7.3.5. Lesion distribution

Due to poor segmentation one MS without VRF was excluded from probabilistic map analysis. The lesion probability distributions for the MS cases with no VRF and MS cases with VRF are shown in **Figure 7.4 A** and **B**, respectively. Similarly to what was shown for the MS without VRF group (Chapter 6, section 6.3.5), the most likely location for a lesion to occur in the MS group with VRF was also in the frontal WM, this time adjacent to the left frontal horn (MNI coordinate 17.9 mm, 28.3 mm, - 2 mm at a probability of 70.0%). A direct comparison between the two groups can be seen in **Figure 7.4 C** where the average of the MS with no VRF lesion map has been subtracted from the average MS with VRF lesion map. Inferior temporal lobe lesions were seen in both groups but were more likely in MS with VRF. Central pons lesions and lesions in both the splenium and the rostrum of the corpus callosum were more likely in MS with VRF compared with MS without VRF (**Figure 7.4 C**). However, no significant differences were found in the voxel-wise permutation testing comparison of the lesion

distributions in each group. The lesional regions with the greatest likelihood to be in MS with VRF compared with MS with no VRF was the periventricular region adjacent to the occipital horn of the left lateral ventricle (corrected p=0.59). Conversely, lesional regions with the greatest likelihood to be in the MS group without VRF compared with MS with VRF was the left parietal WM adjacent to the posterior aspect of the body of the lateral ventricle (corrected p=0.21).

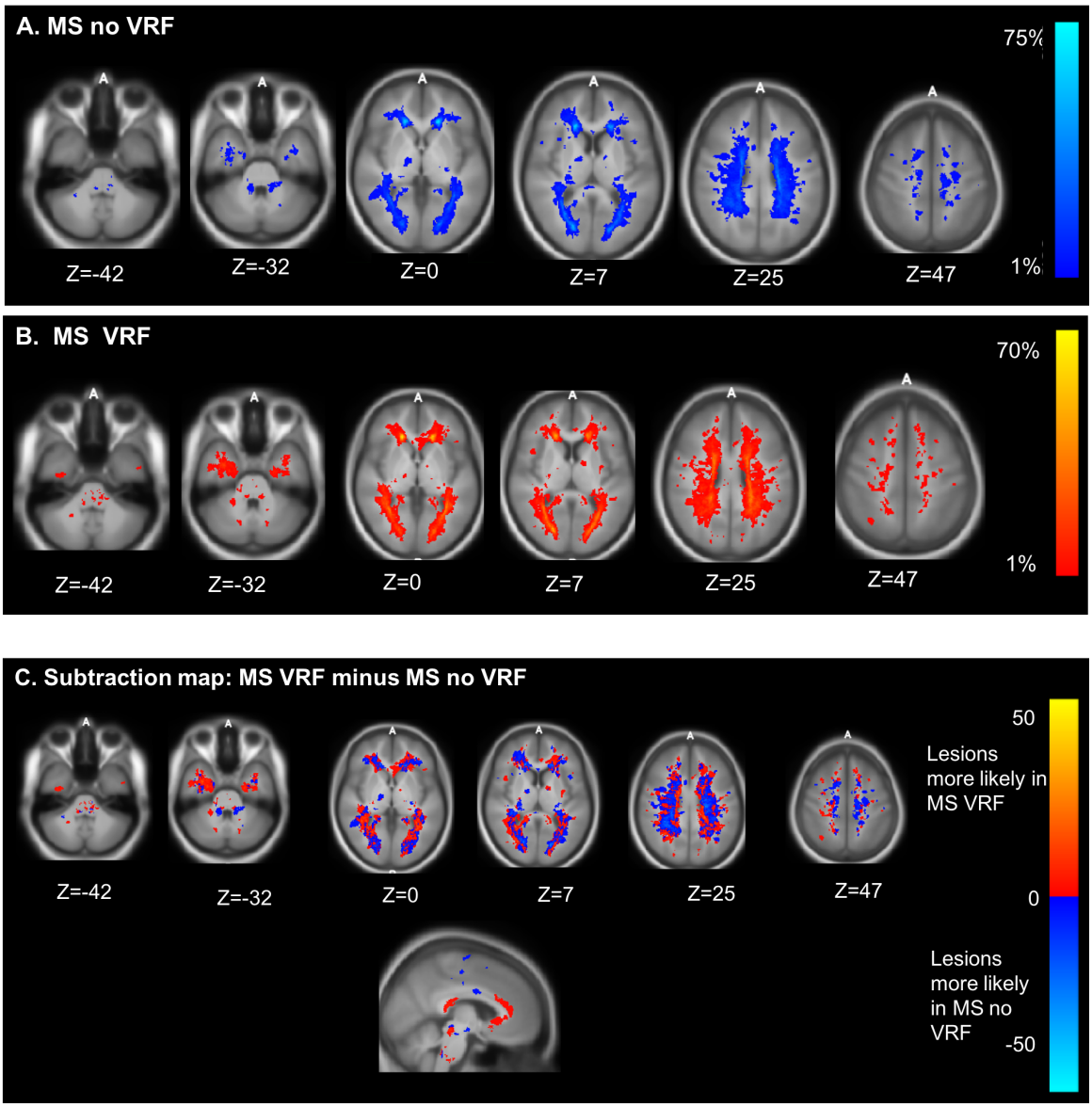

Figure 7.4. Lesion probability distribution analysis

A. Lesion probability distribution for 32 MS cases with no VRF. The colour scale (from 1 to 75%) represents the minimum to maximum probability of a lesion occurring in a particular space location. MNI standard space template Z coordinate is shown in mm. **B.** Lesion probability distribution for the 43 MS cases with VRF. The colour scale (from 0 to 70%) represents the minimum to maximum probability of a lesion occurring in a particular special location. MNI standard space template Z coordinate is shown in mm. **C.** Subtraction map where the average of the MS with VRF lesion map has been subtracted from the average of MS without VRF group lesion map to allow a direct statistical comparison of the lesion distributions, in transversal section in the upper section of the panel and in a sagittal view at the level of the corpus callosum in the lower section. Red to yellow represents where lesions

are more likely to be from the MS group with VRF, a light blue to dark blue where lesions are more likely to be in the MS group without VRF.

7.4. Summary of the main findings

1. Juxtacortical lesions burden was increased in MS with VRF compared with MS without VRF when considering disease duration. This was driven by the effect of smoking and dyslipidaemia, since diabetes had an opposite effect and hypertension had no effect. However, no impact of VRF on the more specific MS imaging marker, U-S-shaped juxtacortical lesions was found.
2. Overall VRF had no effect on Dawson fingers burden but smoking was independently associated with a higher number of this feature.
3. VRF did not influence the presence of peripheral pons lesions.
4. No single lesion location was significantly associated with the presence of VRF in MS. The lesional region with the greatest likelihood to be in MS with VRF compared with MS with no VRF was the periventricular region adjacent to the occipital horn of the left lateral ventricle. VRF presence in MS also associated with more central pons lesions and corpus callosum lesions.

7.5. Discussion

VRF and vascular comorbidities have been associated with worse clinical outcomes (Marrie *et al.*, 2010) and increased WML volumes (Kappus *et al.*, 2015), in MS. The present study contributed to advance the understanding of the nature of this association, since none of the previous studies looked at the effect of VRF on different types of brain lesions.

Overall VRF associated with a higher burden of juxtacortical lesions but not with, U and S shaped juxtacortical lesions, the Dawson fingers or peripheral pons lesions. To confirm the initial hypothesis, that VRF associate with a higher "MS-like" lesion burden an increase in at least two of these imaging markers would be expected, ideally of one of the more specific markers. Unfortunately, these specific markers, such as the U-S shaped juxtacortical lesions and the peripheral pons lesions occur less frequently and an impact on these rarer events may need a larger sample size. Moreover, the relationship between VRF and MS maybe more complex than anticipated.

A key finding of the present study is that the effect of VRF cannot be assessed altogether since each of the individual VRF has shown to have a distinct impact on MS imaging markers. Although the recognition that vascular comorbidities associate with a shorter interval into MS disability milestones (Marrie *et al.*, 2010) was an important finding, what is meant by vascular comorbidities still needs to be clarified.

Smoking has also been shown to significantly impact MS outcomes (Heydarpour *et al.*, 2018), including time to SPMS phase onset (Hernán *et al.*, 2005; Healy *et al.*, 2009). In the present study, smoking associated with a higher burden of Dawson fingers and juxtacortical lesions. This association may be independent of vascular disease. Smoking is an MS risk factor (Belbasis *et al.*, 2015) and has been linked with early conversion from CIS into clinically definite MS (Di Pauli *et al.*, 2008), though a causal relationship is still to be determined (Wingerchuk, 2012). The fact that smoking associated with a higher number of contrast enhancing lesions (Zivadinov *et al.*, 2009) supports that it may primarily affect MS pathology.

Dyslipidaemia associated with a higher burden of juxtacortical lesions. MS patients with hyperlipidaemia have been reported to have an increased relapse rate (Kowalec *et al.*, 2017) and higher triglyceride levels have been linked with a higher number and volume of contrast enhancing lesions, though no association with high T2 lesion volumes was found (Weinstock-Guttman *et al.*, 2011).

On the other hand, arterial hypertension does not seem to influence "MS-like" lesions. Three recent studies have also failed to find an association between arterial hypertension and T2 lesion volume or number despite showing a negative impact on clinical outcomes (i.e. walking speed, performance scores) and brain volume (Conway *et al.*, 2017; Dossi *et al.*, 2018; Pichler *et al.*, 2019). A large study reported that hypertensive MS patients experienced longer intervals to reach disability milestones compared with non-hypertensive MS cases (Dagan *et al.*, 2016). In light of these findings, the effect of hypertension on disease progression is not clear and needs to be better elucidated.

Diabetes has also been related to worse MS clinical outcomes (Conway *et al.*, 2017) but whether it affects lesion load is unclear. In the current study, diabetes associated with a lower burden of 'MS-like' lesions. However, these results need to be interpreted with caution since, a low number of patients was included in each individual VRF group, especially in the diabetes group, and no information regarding treatment was available. In opposition to smoking, all the other VRF can be treated and this may reduce their impact on WML. Moreover, some hypertensive and dyslipidaemia treatments have a putative neuroprotective role (Arun *et al.*, 2013; Chataway *et al.*,

2014) and antidiabetics may decrease the number of new or enlarging WML in MS (Negrotto *et al.*, 2016). Not only exposure to treatments may partially explain the different effects between smoking and hypertension/diabetes on "MS-lesions" but also exposure time needs to be considered. Smoking onset is usually around adolescence whereas hypertension and diabetes tend to occur later in life.

Contrary to what Kappus et al.(Kappus *et al.*, 2015) have found, VRF did not influence total lesion volume load, in the present study. An effect may not have been detected due to a smaller sample size. Moreover, the combinations of VRF (heart disease, hypertension and BMI>25 or hypertension and BMI>25), that have been associated with a higher WML burden in the Kappus et al. study were not investigated in the present work.

In terms of lesion distribution, the posterior WM, adjacent to the occipital horn, the corpus callosum and the central pons were more likely to be affected in MS with VRF than in MS only. However, this was not significant in the voxel-based analysis and these locations are not unequivocally related to MS. Although occipital WM and corpus callosum lesions are commonly seen in MS they are also seen with aging and hypertension (Rostrup *et al.*, 2012) and the integrity of the corpus callosum WM, as measured by diffusion MRI, has shown to be compromised in the elderly with VRF (Maillard *et al.*, 2015; Lao *et al.*, 2017). The central pons is classically affected by cSVD (Pullicino *et al.*, 1995; Caplan, 2015) and was more commonly affected in the VRF only cohort (Chapter 6). The same limitations discussed earlier in Chapter 6 apply to this exploratory probabilistic map analysis.

In summary, these findings suggest that not only there may be a direct influence of VRF on *"MS-like"* lesions but, although the present study was not designed to test this hypothesis, they possibly contribute to a higher burden of cSVD in MS.

8 The influence of MS on cSVD imaging markers

8.1. Introduction

MS is a chronic inflammatory disorder of the CNS and chronic inflammation may predispose to cerebral small vessel changes and consequent vessel occlusion or rupture. In Chapter 3, it was shown that MS *per se* associates with markers of cSVD, as seen in pathology, such as peri-arteriolar hemosiderin deposition and space dilatation. Moreover, the impact of SysVasc showed to be stronger on cSVD in MS compared with non-MS.

Few *in vivo* studies have looked at imaging cSVD surrogate markers in MS. Two studies investigated the prevalence of microbleeds in MS, one suggesting a slight increase of this marker in older MS patients when compared with healthy controls (Zivadinov *et al.*, 2016), and the other not detecting any case with microbleeds in the studied cohort (Eisele *et al.*, 2016). Whether MS associates with a higher burden of basal ganglia lacunae is unknown. In Chapter 6 it was shown that lacunae, central pons lesions and microbleeds are specific markers of cSVD. The main research question and hypothesis in Chapter 8 is:

1. Are these cSVD imaging surrogate markers increased in MS?
   - MS *per se* can exacerbate cSVD and associate with a higher burden of cSVD markers.

To test this hypothesis, I compare the presence of lacunae, central pons lesions and microbleeds in MS with VRF and non-MS with VRF.

I also explore whether MS associates with more lesions in a typical vascular location using probabilistic brain lesion maps which are compared in MS with VRF and non-MS with VRF.

8.2. Materials and Methods

8.2.1. Study design and study cohorts

A multicentre retrospective observational case-control study was set up to compare basal ganglia lacunae counts and presence of central pons lesions in MS cases with VRF (N=108) and non-MS cases with VRF (N=43), as described in Chapter 1, section 1.7.2.2. High-quality 3D T1 and FLAIR -weighted brain MRIs were obtained and clinical data collected as previously outlined in Chapter 1, section 1.7.2.2. A subset of cases, where SWI was available was additionally scored for microbleeds (MS VRF=37, non-MS VRF=26) and another subset was used to explore WML distribution (MS VRF=43, non-MS VRF = 26), as per Chapter 1, section 1.7.2.2.

8.2.2. Imaging Analysis

Visual scoring of cSVD imaging surrogate markers was performed as described in Chapter 6, section 6.2.2.1 in both MS with VRF and non-MS with VRF. Imaging markers that have shown a specificity above 85% were included in the analysis: lacunae and central pons lesions and, in a subset of cases, microbleeds.

Lesion segmentation, volumes and probabilistic map analysis were performed as described in Chapter 6, sections 6.2.2.3 and 6.2.2.4.

8.2.3. Statistical analysis

Descriptive statistics, data transformation and univariate analysis were done as described in Chapters 2, section 2.2.3. and Chapter 6, section 6.2.3. and Chapter 7, section 7.2.3.

Considering the distribution of lacunae and microbleed counts, these count variables were transformed into binary variables (0- not present, 1- present). A binary logistic regression model was used to determine the effect of MS on presence of lacunae, central pons lesions and microbleeds, where age was a covariate. Results are presented as EXP (B) and the respective 95% CI. Statistical significance was assumed if $p \leq 0.05$. All analyses were performed with SPSS version 25 and GraphPad prism version 7.

8.3. Results

8.3.1. Clinical features of the cohorts used in Chapter 8

107 from 108 MS with VRF and 43 non-MS with VRF cases were scored for lacunae and 108 for central pons lesions and the clinical features of the cohorts used for this analysis are summarised in **Table 8.1**. As mentioned above only a limited number of MS and non-MS cases had SWI for microbleed scoring and from the available cases some had significant quality issues that prevented accurate scoring.

MS with VRF cases were younger than non-MS with VRF. This latter group was formed from a younger cohort from Amsterdam (mean age 43.2 years, range 36-56) and an older cohort from Barcelona (mean age 68.8 years, range 60-77). Considering that age has shown to associate with cSVD imaging markers the MS with VRF group will be compared with all the available non-MS cases with VRF, but also with the younger

Amsterdam non-MS with VRF group. VRF profile differed between MS and non-MS cases, all non-MS cases being diabetic, whistle diabetes was the least common VRF in the MS group. Smoking which was the most common VRF in MS and was present in less than 50% of the non-MS cases. Data for hypertension and dyslipidaemia was not available from the Barcelona non-MS cohort (Chapter 1, section 1.7.2.2, **Table 1.4**), thus supporting the need to compare the MS cases with the Amsterdam cohort separately.

Table 8.1. Clinical features of the cohorts included in Chapter 8 and summary of cSVD imaging markers visual scoring results.

	MS VRF (N=108)	Non-MS VRF (N=43)	p[a]	Non-MS VRF Amsterdam (N=17)	p[b]
Mean age (SD) (years)	48.3 (8.5)	58.3 (13.7)	<0.01**	43.2 (7.0)	<0.01**
% females (N)	62.0 (67)	62.8 (27)	0.93	58.8 (10)	0.75
% cases with progressive disease (N)	22.2 (24)	NA		NA	
Median disease duration (years) (IQR)	11.8 (11.7)	NA	NA	NA	NA
%Ever smokers (N) **%Hypertensives (N)** **%Dyslipidemics (N)** **%Diabetics**	75.0 (81) 40.7 (44) 23.1 (25) 9.3 (10)	41.9 (18) 23.3 (10) 25.6 (11) 100 (43)	<0.01** 0.04* 0.83 <0.01**	17.6 (3) 58.8 (10) 64.7 (11) 100 (17)	<0.01** 0.19 <0.01** <0.01**
Median Lacunae N (range) **% cases 1 or more lacunae (N)**	N=107 0 (0-2) 6.5 (7)	0 (0-4) 16.3 (7)	0.06 0.06	0 0	0.28 0.59
% cases with central pons lesions	8.3 (9)	16.3 (7)	0.15	5.9 (1)	0.99
Median MARS (range) **% cases 1 or more microbleed (N)**	N=37 0 (0) 0	N=25 0 (0-5) 8.0 (2)	0.16	NA	NA

SD – standard deviation, IQR -interquartile range, MARS – Microbleeds Anatomical Rating scale, Not applicable/available –NA. [a] MS VRF versus all Non-MS VRF, [b] MS VRF vs Non-MS VRF Amsterdam, **p<0.01, *p<0.05 Mann-Whitney test for continuous variables, Chi-square or Fisher exact test for categorical variables

8.3.2. Relationship of cSVD markers with age

In the whole cohort the number of lacunae (N=150, r_s=0.29, p<0.001) increased with age (**Figure 8.1**), but age did not correlate with the presence of central pons lesions (N=151, rτ=0.11, p=0.12) or number of microbleeds (N=62, r_s=0.18, p=0.09).

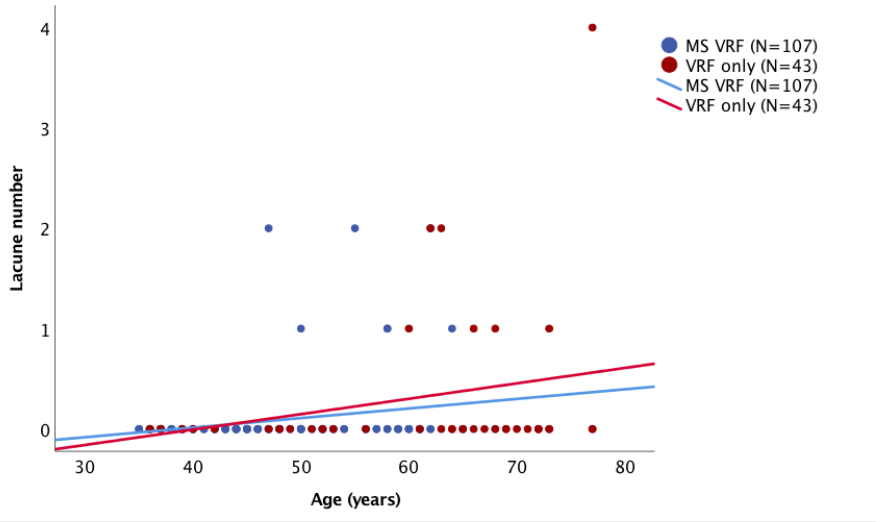

Figure 8.1. Number of lacunae and age in MS with VRF and non-MS with VRF

8.3.3. cSVD imaging surrogate markers in MS with VRF compared with non-MS with VRF

Lacunae number was low in both non-MS with VRF (median 0, range 0-4) and MS with VRF (median 0, range 0-2) groups, and no differences were found between the two groups p=0.06. The proportion of cases with any lacunae tended to be higher in the whole non-MS with VRF group (16.3%, 7 out of 43) compared with the MS with VRF group (6.5%, 7 out of 107), p=0.07 (**Figure 8.2 a.**). No significant differences between the two groups were found for central pons lesions (**Figure 8.2 b.**). Microbleeds were only observed in the non-MS with VRF group (**Figure 8.2 c**.).

No lacunae were observed in the non-MS VRF Amsterdam cohort and central pons lesion were only found in one case (5.9%), these proportions were not different from those observed in MS (**Table 8.1**).

MS did not associate with presence of lacunae (EXP (B)=0.86, 95%CI 0.19,3.79, p=0.86) nor with of central pons lesions (EXP (B)=1.5, 95%CI 0.43,5.1, p=0.53), in a binary regression model, adjusting for age. The same model was not applied to microbleeds owing to the low sample size and number of events.

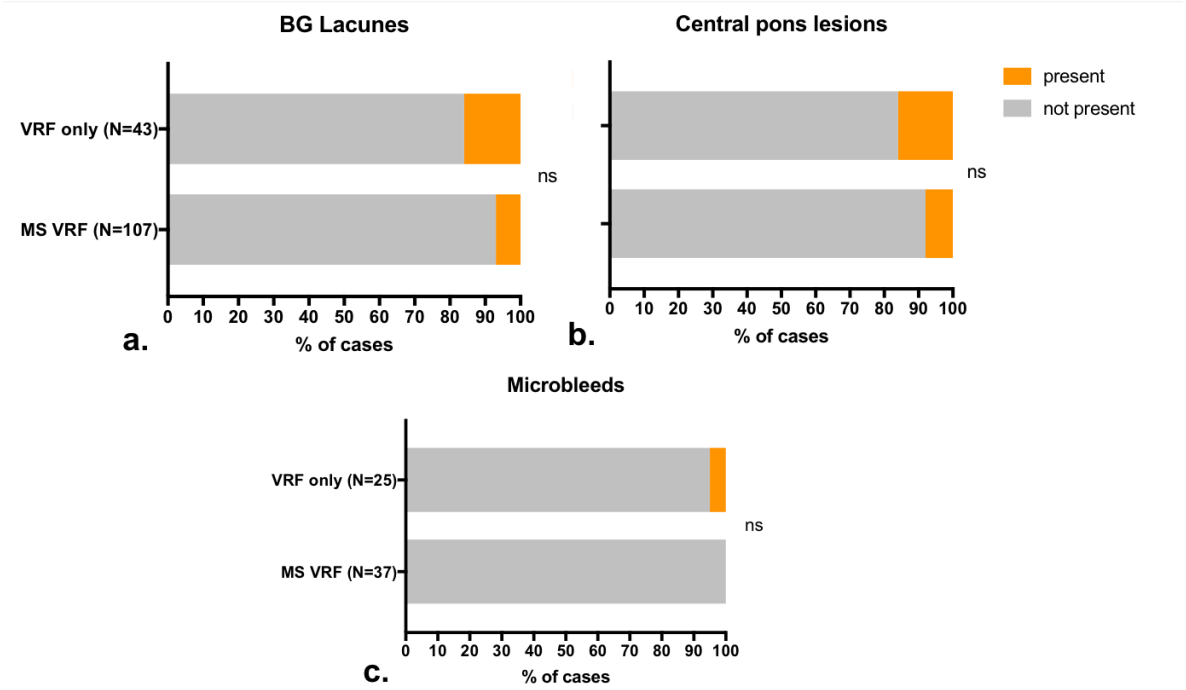

Figure 8.2. Percentage of cases with lacunae (a.), central pons lesions(b.) and microbleeds (c.) per group.

8.3.4. Lesion distribution

8.3.4.1. Clinical data and WML volumes of the cohorts used for lesion probabilistic analysis

Clinical data and lesions volumes of the cohorts used for lesion distribution analysis are depicted in **Table 8.2**. Non-MS with VRF (mean age 68.5±4.9 years) cases were older than the MS cases with VRF (44.8±6.4 years), p<0.001. Total WML volume was higher in non-MS with VRF than in the MS with VRF group, even after adjusting for age (p=0.05). Deep WML volumes were higher in the non-MS with VRF group than in the MS with VRF group, even after adjusting for age (p=0.014). Juxtacortical WML volume was higher in the MS group compared with non-MS but this was not significant when age was considered (p=0.32). Periventricular WML volumes did not differ between the two groups.

Table 8.2. Clinical features and WML volumes of the MS with VRF and non-MS with VRF groups used for lesion probabilistic analysis.

	MS VRF (N=43)	Non-MS VRF (N=26)	p
Mean age (SD)	44.8 (6.4)	68.5 (4.9)	<0.001**
% females (N)	69.8 (30)	65.4 (17)	0.79
Median FLAIR total WML volume (IQR)	5.24 (8.06)	7.23 (6.53)	0.03*
Median FLAIR periventricular WML volume (IQR)	4.01 (5.84)	5.5(5.64)	0.08
Median FLAIR deep WML volume (IQR)	0.50 (0.64)	1.17(1.32)	<0.001**
Median FLAIR juxtacortical WML volume (IQR)	0.18 (0.44)	0 (0.06)	<0.001**

**p<0.01, *p<0.05, t-test or Mann-Whitney test for continuous variables, Chi-square test for categorical variables

8.3.4.2. Lesion probabilistic map differences

The lesion probability distributions for the MS cases with VRF has been described in Chapter 7, section 7.3.5, **Figure 7.4 B** and for the non-MS group with VRF in Chapter 6, section 6.3.5, **Figure 6.5 B**. A direct comparison between the two groups is depicted in **Figure 8.3** where the average of the MS with VRF lesion map has been subtracted from the average of the non-MS with VRF group lesion map. Inferior temporal lobe lesions and corpus callosum lesions were more likely in MS with VRF. Central pons lesions were more likely in the non-MS with VRF, but were also seen in the MS with VRF group. Overall, the distribution of WML was similar between the MS with VRF and the non-MS with VRF groups. No significant differences were found in voxel-wise permutation testing comparison of the lesion distributions in each group, adjusting for age. In particular, an excess of WML in "vascular" locations was not seen in excess in the MS group with VRF. The lesional regions with the greatest likelihood to be in MS with VRF compared with MS with no VRF was the periventricular region adjacent to the occipital horn of the left lateral ventricle (MNI coordinate 19.6 mm, -41.9 2 mm, -2.0 mm, at a probability of 1.2%). Lesional regions with the greatest likelihood to be in the non-MS with VRF were the periventricular WM adjacent to the body (MNI coordinate -17.1 mm, -13.0mm, 27 mm, at a probability of 99.1%) and to the frontal horn of the right lateral ventricle (MNI coordinate -18.3 mm, -22.3mm, 14 mm, at a probability of 99.9%).

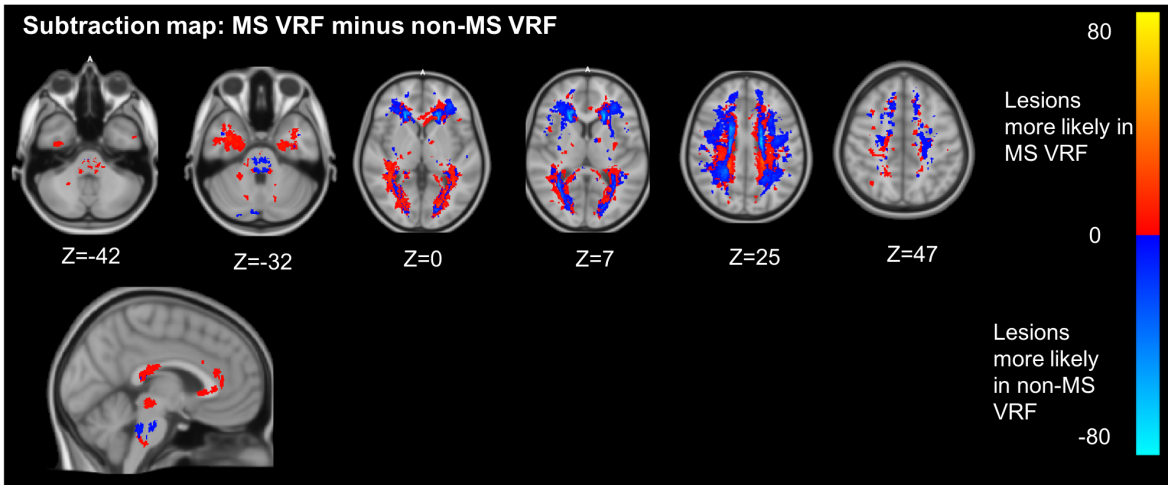

Figure 8.3. Subtraction maps MS VRF minus non-MS VRF.

Subtraction map where the average of the MS with VRF lesion map has been subtracted from the average of non-MS with VRF group lesion map was obtained to allow a direct statistical comparison of the lesion distributions, in transversal sections at different Z MNI coordinate levels in the upper half of the panel, and in a sagittal section at the level of the corpus callosum in the lower half of the panel. Red to yellow represents lesions more are more likely to be from the MS group with VRF, a light blue to dark blue where lesions are more likely to be in the non-MS group with VRF.

8.4. Summary of main findings

1. MS does not seem to associate with an increased burden of the studied cSVD imaging markers
2. Overall, lesion distribution between MS with VRF was similar to that of non-MS with VRF. Lesions in the corpus callosum seem to be more likely in MS with VRF than non-MS with VRF

8.5. Discussion

Specific cSVD imaging markers were compared between MS with VRF and non-MS with VRF, to the determine the influence of MS on these markers. Contrary to my

hypothesis MS did not seem to influence the presence of lacunae, central pons lesions or microbleeds. However, there are important limitations to this study. The MS with VRF was not age-matched with the whole non-MS group and the matched Amsterdam non-MS with VRF was quite small. The MS cohort was a relatively young cohort, thus possibly with a shorter exposure to the VRF compared to the whole non-MS with VRF cohort and this may have led to an underestimation of cSVD markers in the MS with VRF group. Also, the small number of individual cSVD outcomes may introduce biases to the regression models, which aimed to compare the two groups considering age. Another important confounder is that individual VRF, especially diabetes and smoking, were not matched between the two groups. It is also possible that treatments also differed and this information was not available. Finally, SWI was only available for a small number of cases.

It is challenging to integrate the present results with my pathology study where a much older group with end-stage disease was included. However, this *post mortem* study did not find a higher burden of lacunae, in MS, even in the young at death group, taking SysVasc burden into account.

There is a significant overlap between WML in both MS with VRF and non-MS without VRF, that is difficult to tear apart. MS does not seem to associate with an excess of WML in "vascular" locations, but the corpus callosum seems to be more likely affected, though this was not statistically significant in the voxel-wise analysis. Limitations to probabilistic map analysis have been discussed in Chapter 6 and these findings need to be confirmed in a larger study with better age and VRF matching between the groups.

Although they may not be present in excess in MS with VRF, compared the non-MS with VRF, cSVD lesions, as an add-on lesion burden, may still contribute to increased disability in MS.

9 Key findings, implications for clinical practice and for future research

The work presented in this thesis, enhanced the understanding of the interaction between VRF and whole-body vascular disease and MS pathology and imaging outcomes and furthermore identified markers of an MS-related vasculopathy.

My main research questions were:

1. Does MS associate with worse systemic and cerebrovascular disease?
2. Does the presence of VRF/vascular disease associate with a higher burden of MS lesions?

To respond to these questions, I took two complementary approaches. An internationally unique *post mortem* cohort, where detailed data on whole body cardiovascular disease and brain tissue were available, was studied for the first time, to obtain objective measures of end stage cardiovascular burden and cSVD in MS and age and sex-matched non-MS cases. Secondly, a novel multicentre brain imaging study compared MS only, VRF only and MS with VRF cohorts. The role of several imaging features in discriminating MS from cSVD was herein tested for the first time, as was the effect of VRF of MS-specific imaging markers.

Key findings to respond to the research questions, using these two approaches are (**Figure 9.1**):

1. Cardiovascular disease, in particular atherosclerosis, is not increased in MS but has a steeper increase with age at death compared with non-MS. Signs of cardiac hypertensive disease are seen less frequently in MS.
2. cSVD burden is seen in excess in those who die at young ages in MS with highly active disease, independent of cardiovascular burden.

3. Periarteriolar space dilatation, hemosiderin deposition and inflammation are key features of MS pathology and are seen outside of the classical MS plaque
4. The relationship between cardiovascular burden and cSVD is stronger in MS compared with non-MS.
5. Worse cardiovascular disease is associated with a lower burden of MS active demyelinating lesions in MS
6. Some imaging markers show excellent (U- S- shaped juxtacortical lesions, peripheral pons lesions) and good (non- U- S- shaped juxtacortical lesions, Dawson fingers) specificity for MS and others for cSVD (BG lacunae, central pons lesions, microbleeds).
7. The effect of VRF on MS-specific lesions differs between VRF: smoking and dyslipidaemia associate with a higher burden of these lesions but hypertension and diabetes seem to have no effect or an opposite effect, respectively.
8. MS does not seem to influence cSVD imaging markers

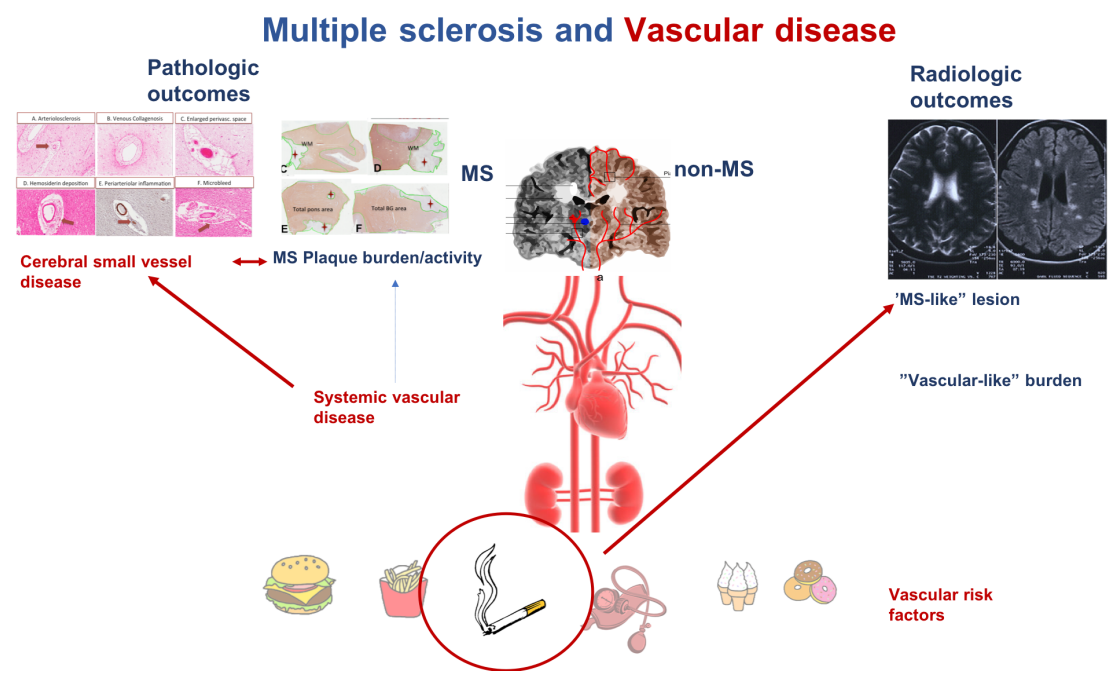

Figure 9.1. Summary of key findings

SysVasc was not increase in MS compared with non-MS and associated with a lower burden of active plaques (blue arrow), but was a stronger driver of cSVD in MS compared with non-MS (left red-arrow). MS cases that died before the age of 60 had a higher burden of cSVD and this associated with higher active lesion load. Periarteriolar pathology was seen in excess in MS, especially PSD, hemosiderin deposition and inflammation. From all the studied VRF, smoking was shown to influence MS imaging surrogate markers (Dawson fingers and juxtacortical lesions). MS did not seem to impact cSVD specific imaging markers.

These findings have the following implications for clinical practice:

1. When present vascular comorbidities seem to potentiate cSVD in MS and careful VRF data collection and treatment should be part of MS management. This is particularly relevant since more MS patients will reach an older age (Solaro *et al.*, 2015) and are thus susceptible to the accumulation of vascular comorbidities (Marrie, 2017).

2. This data supports a direct impact of smoking on MS lesions. MS patients should be actively advised to stop smoking.
3. This work supports that the identification of U-S shaped juxtacortical lesions and peripheral pons lesions indicate MS, whereas the presence of basal ganglia lacunae and microbleeds suggest cSVD. These features may be used to standardize the exclusion of "other diagnosis" and improve diagnostic criteria specificity, especially in cases with less typical MS presentations (Geraldes *et al.*, 2018). On the other hand, the more common Dawson fingers and juxtacortical lesions, may very occasionally be found in "pure VRF" cases.

Although the present work has advanced the understanding of the interaction of MS and vascular disease, it has also opened many other questions that warrant future investigation:

1. Cardiovascular disease in MS and its negative correlation with MS lesion activity needs to be confirmed *in vivo*. Assessment of *in vivo* atherosclerosis burden has improved with new imaging techniques (Ibrahimi *et al.*, 2013; Singh *et al.*, 2016) and can be applied longitudinally. Only a prospective study may provide information on the dynamic nature of the relationship of the two disorders.
2. The reason why MS patients have lower heart weights and lower burden of LVH needs to be explored. Physical deconditioning is a possible explanation but underlying cardiac microvascular changes should be excluded, on pathology examination.
3. Pathological markers of an outside MS plaque arteriolopathy were identified and these markers need to be tested *in vivo*. It is possible that periarteriolar

inflammation precedes MS plaque formation or that it represents a still unexplored component of MS pathology. High field MRI with SWI has shown to be useful in detecting veins inside the MS plaque (Sati *et al.*, 2016). Small arterioles have been difficult to assess *in vivo* but advances in high field MRI angiography (Park *et al.*, 2018), associated with SWI may make them more accessible for study in the near future.

4. Acknowledging that cerebral small vessel damage is associated with MS is the first step to consider vascular protective treatments to halt secondary neuronal loss in MS. For example, statin therapy is an effective and safe treatment for prevention of atherosclerotic cardiovascular disease (Kazi *et al.*, 2017) and may prevent neuronal damage in SPMS (Chataway *et al.*, 2014). Contrariwise, unfolding the relationship between MS inflammation and cerebral arteriolosclerosis and other cSVD pathologies may help find new therapeutic targets for these common causes of brain damage in the general population. An improved characterization of the molecular changes around the arteriole at the different stages of CNS inflammation in human post-mortem material and/or animal models (Kipp *et al.*, 2017; Horsburgh *et al.*, 2018), and how different drugs impact these changes, needs to be further explored.

5. No effect of MS on cSVD imaging markers was documented. This needs to be confirmed in a prospective study with well-matched age- and VRF- cohorts in MS with VRF and non-MS with VRF.

6. Brain MRI lesions are often used as surrogate markers for disease progression in MS. The obtained data indicate that the different VRF influence '*MS-like*'

lesions. Although a higher rate of increase in WML burden was not associated with VRF in a young MS cohort (Pichler *et al.*, 2019), we have provided enough evidence to support a longitudinal study to determine the effect on '*MS-like*' lesions progression rate, in a larger cohort with wider range of ages.

In summary, this thesis enhanced the understanding on how vascular disease and VRF contribute to MS heterogeneity and, by improving patient characterisation, to guide MS diagnosis, monitoring and new treatment development.

10 Bibliography

Aarli JA, Abramsky O, Browne P, Chandraratna D, Angood C, Helen Tremlett M, et al. Atlas of Multiple Sclerosis 2013: a growing global problema with widespread inequity. Neurology 2014; 83: 1022–1024.

Adams CW. Perivascular iron deposition and other vascular damage in multiple sclerosis. J Neurol Neurosurg Psychiatry 1988; 51: 260–5.

Adams CW, Abdulla YH, Torres EM, Poston RN. Periventricular lesions in multiple sclerosis: their perivenous origin and relationship to granular ependymitis. Neuropathol Appl Neurobiol 1987; 13: 141–52.

Adams CWM, Poston RN, Buk SJ, Sidhu YS, Vipond H. Inflammatory vasculitis in multiple sclerosis. J Neurol Sci 1985; 69: 269–283.

Agrawal SM, Williamson J, Sharma R, Kebir H, Patel K, Prat A, et al. Extracellular matrix metalloproteinase inducer shows active perivascular cuffs in multiple sclerosis. Brain 2013; 136: 1760–1777.

Ahmed O, Geraldes R, DeLuca GC, Palace J. Multiple sclerosis and the risk of systemic venous thrombosis: A systematic review. Mult Scler Relat Disord 2019; 27: 424–430.

Akashi T, Takahashi S, Mugikura S, Sato S, Murata T, Umetsu A, et al. Ischemic White Matter Lesions Associated With Medullary Arteries: Classification of MRI Findings Based on the Anatomic Arterial Distributions. Am J Roentgenol 2017; 209: W160–W168.

Alexander JS, Zivadinov R, Maghzi A-H, Ganta VC, Harris MK, Minagar A. Multiple sclerosis and cerebral endothelial dysfunction: Mechanisms. Pathophysiology 2011; 18: 3–12.

Aliaga ES, Barkhof F, E.S. A, F. B. MRI mimics of multiple sclerosis. Handb Clin Neurol 2014; 122: 291–316.

Alwahaibi, NY, Al-Himali S. Capability of Hematoxylin and Eosin Stain to Demonstrate Hemosiderin in Bone Marrow Trephine Biopsy. J Cytol Histol 2012; 03: 1–3.

Angelovich TA, Hearps AC, Jaworowski A. Inflammation-induced foam cell formation in chronic inflammatory disease. Immunol Cell Biol 2015; 93: 683–93.

Aono J, Ikeda S, Katsumata Y, Higashi H, Ohshima K, Ishibashi K, et al. Correlation between plaque vulnerability of aorta and coronary artery: an evaluation of plaque activity by direct visualization with angioscopy. Int J Cardiovasc Imaging 2015; 31: 1107–1114.

Arun T, Tomassini V, Sbardella E, de Ruiter MB, Matthews L, Leite MI, et al. Targeting ASIC1 in primary progressive multiple sclerosis: evidence of neuroprotection with amiloride. Brain 2013; 136: 106–15.

Ascherio A, Munger KL, White R, Köchert K, Simon KC, Polman CH, et al. Vitamin D as an early predictor of multiple sclerosis activity and progression. JAMA Neurol 2014; 71: 306–14.

Auriel E, Charidimou A, Gurol ME, Ni J, Van Etten ES, Martinez-Ramirez S, et al. Validation of Clinicoradiological Criteria for the Diagnosis of Cerebral Amyloid Angiopathy-Related Inflammation. JAMA Neurol 2016; 73: 197–202.

Baezner H, Blahak C, Poggesi a., Pantoni L, Inzitari D, Chabriat H, et al. Association of gait and balance disorders with age-related white matter changes: The LADIS Study. Neurology 2008; 70: 935–942.

Bagnato F, Hametner S, Boyd E, Endmayr V, Shi Y, Ikonomidou V, et al. Untangling the R2* contrast in multiple sclerosis: A combined MRI-histology study at 7.0 Tesla. PLoS One 2018; 13: 1–19.

Bagnato F, Hametner S, Yao B, Van Gelderen P, Merkle H, Cantor FK, et al. Tracking iron in multiple sclerosis: A combined imaging and histopathological study at 7 Tesla. Brain 2011; 134: 3599–3612.

Bardehle S, Rafalski VA, Akassoglou K. Breaking boundaries—coagulation and fibrinolysis at the neurovascular interface. Front Cell Neurosci 2015; 9: 354.

Barker R, Wellington D, Esiri MM, Love S. Assessing white matter ischemic damage in dementia patients by measurement of myelin proteins. J Cereb Blood Flow Metab 2013; 33: 1050–1057.

Barkhof F, Scheltens P. Imaging of white matter lesions. Cerebrovasc Dis 2002; 13 Suppl 2: 21–30.

Beauchet O, Celle S, Roche F, Bartha R, Montero-Odasso M, Allali G, et al. Blood pressure levels and brain volume reduction. J Hypertens 2013; 31: 1502–1516.

Beggs CB. Venous hemodynamics in neurological disorders: an analytical review with hydrodynamic analysis. BMC Med 2013; 11: 1–17.

Belbasis L, Bellou V, Evangelou E, Ioannidis JP a, Tzoulaki I. Environmental risk factors and multiple sclerosis: an umbrella review of systematic reviews and meta-analyses. Lancet Neurol 2015; 14: 263–273.

Bell JS, DeLuca GC. Genes, smoking, and organic solvent exposure. Neurology 2018; 91: 199–200.

Bell JS, Spencer JI, Yates RL, Yee SA, Jacobs BM, DeLuca GC. From Nose to Gut - The Role of the Microbiome in Neurological Disease. Neuropathol Appl Neurobiol 2018: 1–21.

Bennett M, Heard R. Hyperbaric Oxygen Therapy for Multiple Sclerosis. CNS Neurosci Ther 2010; 16: 115–124.

Bermel R, Bakshi R. The measurement and clinical relevance of brain atrophy in multiple sclerosis. Lancet Neurol 2006; 5: 158–70.

Blinder P, Tsai PS, Kaufhold JP, Knutsen PM, Suhl H, Kleinfeld D. The cortical angiome: an interconnected vascular network with noncolumnar patterns of blood flow. Nat Neurosci 2013; 16: 889–897.

Bogie JFJ, Stinissen P, Hendriks JJA. Macrophage subsets and microglia in multiple sclerosis. Acta Neuropathol 2014; 128: 191–213.

Bot JCJ, Barkhof F, Lycklama à Nijeholt G, van Schaardenburg D, Voskuyl AE, Ader HJ, et al. Differentiation of multiple sclerosis from other inflammatory disorders and cerebrovascular disease: value of spinal MR imaging. Radiology 2002; 223: 46–56.

Brainin M, Reisner T, Neuhold A, Omasits M, Wicke L. Topological characteristics of brainstem lesions in clinically definite and clinically probable cases of multiple sclerosis: an MRI-study. Neuroradiology 1987; 29: 530–4.

Brändle SM, Obermeier B, Senel M, Bruder J, Mentele R, Khademi M, et al. Distinct oligoclonal band antibodies in multiple sclerosis recognize ubiquitous self-proteins. Proc Natl Acad Sci U S A 2016; 113: 7864–9.

Breteler MM, van Swieten JC, Bots ML, Grobbee DE, Claus JJ, van den Hout JH, et al. Cerebral white matter lesions, vascular risk factors, and cognitive function in a population-based study: the Rotterdam Study. Neurology 1994; 44: 1246–52.

Brewer LC, Michos ED, Reis JP. Vitamin D in atherosclerosis, vascular disease, and endothelial function. Curr Drug Targets 2011; 12: 54–60.

Bridges LR, Andoh J, Lawrence AJ, Khoong CHL, Poon WW, Esiri MM, et al. Blood-brain barrier dysfunction and cerebral small vessel disease (arteriolosclerosis) in brains of older people. J Neuropathol Exp Neurol 2014; 73: 1026–33.

Brown R, Benveniste H, Black SE, Charpak S, Dichgans M, Joutel A, et al. Understanding the role of the perivascular space in cerebral small vessel disease. Cardiovasc Res 2018; 44: 1462–1473.

Brown WR, Moody DM, Challa VR, Thore CR, Anstrom JA. Venous collagenosis and arteriolar tortuosity in leukoaraiosis. J Neurol Sci 2002; 203–204: 159–163.

Brown WR, Thore CR. Letter To the Editor. Brain Pathol 2011; 21: 355–355.

Brown WR, Thore CR. Review: cerebral microvascular pathology in ageing and neurodegeneration. Neuropathol Appl Neurobiol 2011; 37: 56–74.

Brownell B, Hughes JT. The distribution of plaques in the cerebrum in multiple sclerosis. J Neurol Neurosurg Psychiatry 1962; 25: 315–20.

Brownlee WJ, Hardy TA, Fazekas F, Miller DH. Diagnosis of multiple sclerosis: progress and challenges. Lancet 2017; 389: 1336–1346.

Del Brutto OH, Mera RM. Enlarged perivascular spaces in the basal ganglia are independently associated with intracranial atherosclerosis in the elderly. Atherosclerosis 2017; 267: 34–38.

Bryan RN, Cai J, Burke G, Hutchinson RG, Liao D, Toole JF, et al. Prevalence and anatomic characteristics of infarct-like lesions on MR images of middle-aged adults: The atherosclerosis risk in communities study. Am J Neuroradiol 1999; 20: 1273–1280.

Cacciaguerra L, Meani A, Mesaros S, Radaelli M, Palace J, Dujmovic-Basuroski I, et al. Brain and cord imaging features in neuromyelitis optica spectrum disorders. Ann Neurol 2019; 85: 371–384.

Calabrese M, Oh MS, Favaretto A, Rinaldi F, Poretto V, Alessio S, et al. No MRI evidence of cortical lesions in neuromyelitis optica. Neurology 2012; 79: 1671–1676.

Calabrese M, Poretto V, Favaretto A, Alessio S, Bernardi V, Romualdi C, et al. Cortical lesion load associates with progression of disability in multiple sclerosis. Brain 2012; 135: 2952–61.

Capkun G, Dahlke F, Lahoz R, Nordstrom B, Tilson HH, Cutter G, et al. Mortality and comorbidities in patients with multiple sclerosis compared with a population without multiple sclerosis: An observational study using the US Department of Defense administrative claims database. Mult Scler Relat Disord 2015; 4: 546–554.

Caplan LR. Lacunar infarction and small vessel disease: pathology and pathophysiology. J Stroke 2015; 17: 2–6.

Catapano AL, Graham I, De Backer G, Wiklund O, Chapman MJ, Drexel H, et al. 2016 ESC/EAS Guidelines for the Management of Dyslipidaemias. Eur Heart J 2016; 37: 2999–3058.

Charidimou A, Boulouis G, Pasi M, Auriel E, van Etten ES, Haley K, et al. MRI-visible perivascular spaces in cerebral amyloid angiopathy and hypertensive arteriopathy. Neurology 2017; 88: 1157–1164.

Charil A, Yousry T a, Rovaris M, Barkhof F, De Stefano N, Fazekas F, et al. MRI and the diagnosis of multiple sclerosis: expanding the concept of 'no better explanation'. Lancet Neurol 2006; 5: 841–52.

Chataway J, Schuerer N, Alsanousi A, Chan D, MacManus D, Hunter K, et al. Effect of high-dose simvastatin on brain atrophy and disability in secondary progressive multiple sclerosis (MS-STAT): a randomised, placebo-controlled, phase 2 trial. Lancet 2014; 383: 2213–21.

Chen JJ, Carletti F, Young V, Mckean D, Quaghebeur G. MRI differential diagnosis of suspected multiple sclerosis. Clin Radiol 2016; 71: 815–827.

Chen R-L, Balami JS, Esiri MM, Chen L-K, Buchan AM. Ischemic stroke in the elderly: an

overview of evidence. Nat Rev Neurol 2010; 6: 256–65.

Christiansen CF. Risk of vascular disease in patients with multiple sclerosis: a review. Neurol Res 2012; 34: 746–53.

Christiansen CF, Christensen S, Farkas DK, Miret M, Sørensen HT, Pedersen L. Risk of arterial cardiovascular diseases in patients with multiple sclerosis: a population-based cohort study. Neuroepidemiology 2010; 35: 267–74.

Cifelli A, Arridge M, Jezzard P, Esiri MM, Palace J, Matthews PM. Thalamic neurodegeneration in multiple sclerosis. Ann Neurol 2002; 52: 650–3.

Compston A, Coles A. Multiple sclerosis. Lancet 2002; 359: 1221–1231.

Compston A, Coles A. Multiple sclerosis. Lancet 2008; 372: 1502–1517.

Confavreux C, Vukusic S. Age at disability milestones in multiple sclerosis. Brain 2006; 129: 595–605.

Confavreux C, Vukusic S. The clinical course of multiple sclerosis. Handb Clin Neurol 2014; 122: 343–369.

Conway DS, Thompson NR, Cohen JA. Influence of hypertension, diabetes, hyperlipidemia, and obstructive lung disease on multiple sclerosis disease course. Mult Scler 2017; 23: 277–285.

Cordonnier C, Al-Shahi Salman R, Wardlaw J. Spontaneous brain microbleeds: Systematic review, subgroup analyses and standards for study design and reporting. Brain 2007; 130: 1988–2003.

Correale J, Gaitán MI, Ysrraelit MC, Fiol MP. Progressive multiple sclerosis: from pathogenic mechanisms to treatment. Brain 2017; 140: 527–546.

Cortese M, Riise T, Bjørnevik K, Holmøy T, Kampman MT, Magalhaes S, et al. Timing of use of cod liver oil, a vitamin D source, and multiple sclerosis risk: The EnvIMS study. Mult Scler J 2015; 21: 1856–1864.

Craggs LJL, Yamamoto Y, Deramecourt V, Kalaria RN. Microvascular pathology and morphometrics of sporadic and hereditary small vessel diseases of the brain. Brain Pathol 2014; 24: 495–509.

Cruz PMR, Matthews L, Boggild M, Cavey A, Constantinescu CS, Evangelou N, et al. Time-and region-specific season of birth effects in multiple sclerosis in the United Kingdom. JAMA Neurol 2016; 73: 954–960.

Currais A. Ageing and inflammation – A central role for mitochondria in brain health and disease. Ageing Res Rev 2015; 21: 30–42.

D'haeseleer M, Cambron M, Vanopdenbosch L, De Keyser J. Vascular aspects of multiple

sclerosis. Lancet Neurol 2011; 10: 657–666.

D'haeseleer M, Hostenbach S, Peeters I, Sankari S El, Nagels G, De Keyser J, et al. Cerebral hypoperfusion: a new pathophysiologic concept in multiple sclerosis? J Cereb Blood Flow Metab 2015; 35: 1406–1410.

Dagan A, Gringouz I, Kliers I, Segal G. Disability Progression in Multiple Sclerosis Is Affected by the Emergence of Comorbid Arterial Hypertension. J Clin Neurol 2016; 12: 345–50.

Dal-Bianco A, Hametner S, Grabner G, Schernthaner M, Kronnerwetter C, Reitner A, et al. Veins in plaques of multiple sclerosis patients - a longitudinal magnetic resonance imaging study at 7 Tesla. Eur Radiol 2015; 25: 2913–20.

van Dalen JW, Scuric EEM, van Veluw SJ, Caan MWA, Nederveen AJ, Biessels GJ, et al. Cortical Microinfarcts Detected In Vivo on 3 Tesla MRI: Clinical and Radiological Correlates. Stroke 2015; 46: 255–257.

Daugherty AM, Raz N. Incident risk and progression of cerebral microbleeds in healthy adults: a multi-occasion longitudinal study. Neurobiol Aging 2017; 59: 22–29.

Davies AL, Desai RA, Bloomfield PS, McIntosh PR, Chapple KJ, Linington C, et al. Neurological deficits caused by tissue hypoxia in neuroinflammatory disease. Ann Neurol 2013; 74: 815–825.

Dawson JW. XVIII.—The Histology of Disseminated Sclerosis. Trans R Soc Edinburgh 1916; 50: 517–740.

Debernard L, Melzer TR, Van Stockum S, Graham C, Wheeler-Kingshott CA, Dalrymple-Alford JC, et al. Reduced grey matter perfusion without volume loss in early relapsing-remitting multiple sclerosis. J Neurol Neurosurg Psychiatry 2014; 85: 544–551.

DeLuca GC, Kimball SM, Kolasinski J, Ramagopalan S V., Ebers GC. Review: The role of vitamin D in nervous system health and disease. Neuropathol Appl Neurobiol 2013; 39: 458–484.

DeLuca GC, Yates RL, Beale H, Morrow SA. Cognitive impairment in multiple sclerosis: clinical, radiologic and pathologic insights. Brain Pathol 2015; 25: 79–98.

Dendrou CA, Fugger L, Friese MA. Immunopathology of multiple sclerosis. Nat Rev Immunol 2015; 15: 545–558.

Deramecourt V, Slade JY, Oakley AE, Perry RH, Ince PG, Maurage C-A, et al. Staging and natural history of cerebrovascular pathology in dementia. Neurology 2012; 78: 1043–50.

Desai RA, Davies AL, Tachrount M, Kasti M, Laulund F, Golay X, et al. Cause and prevention of demyelination in a model multiple sclerosis lesion. Ann Neurol 2016; 79: 591–604.

Diamantopoulos E, Andreadis E, Vassilopoulos C, Vlachonikolis I, Tarassi K, Chatzis N, et al. HLA phenotypes as promoters of cardiovascular remodelling in subjects with arterial

hypertension. J Hum Hypertens 2003; 17: 63–68.

Ding L, Hong Y, Peng B. Association between large artery atherosclerosis and cerebral microbleeds: A systematic review and meta-analysis. Stroke Vasc Neurol 2017; 2: 7–14.

Disanto G, Zecca C, MacLachlan S, Sacco R, Handunnetthi L, Meier UC, et al. Prodromal symptoms of multiple sclerosis in primary care. Ann Neurol 2018; 83: 1162–1173.

Dossi DE, Chaves H, Heck ES, Rodriguez Murúa S, Ventrice F, Bakshi R, et al. Effects of Systolic Blood Pressure on Brain Integrity in Multiple Sclerosis. Front Neurol 2018; 9: 487.

Drake C, Iadecola C. The role of neuronal signaling in controlling cerebral blood flow. Brain Lang 2007; 102: 141–152.

Duering M, Csanadi E, Gesierich B, Jouvent E, Herve D, Seiler S, et al. Incident lacunes preferentially localize to the edge of white matter hyperintensities: insights into the pathophysiology of cerebral small vessel disease. Brain 2013; 136: 2717–2726.

East E, Baker D, Pryce G, Lijnen HR, Cuzner ML, Gverić D. A role for the plasminogen activator system in inflammation and neurodegeneration in the central nervous system during experimental allergic encephalomyelitis. Am J Pathol 2005; 167: 545–54.

Eisele P, Alonso A, Griebe M, Szabo K, Hennerici MG, Gass A. Investigation of cerebral microbleeds in multiple sclerosis as a potential marker of blood-brain barrier dysfunction. Mult Scler Relat Disord 2016; 7: 61–4.

Elsankari S, Balédent O, van Pesch V, Sindic C, de Broqueville Q, Duprez T. Concomitant analysis of arterial, venous, and CSF flows using phase-contrast MRI: a quantitative comparison between MS patients and healthy controls. J Cereb Blood Flow Metab 2013; 33: 1314–1321.

Endo A. A historical perspective on the discovery of statins. Proc Jpn Acad Ser B Phys Biol Sci 2010; 86: 484–93.

Esiri MM, Chance S, Joachim C, Warden D, Smallwood A, Sloan C, et al. Cerebral Amyloid Angiopathy, Subcortical White Matter Disease and Dementia: Literature Review and Study in OPTIMA. Brain Pathol 2015; 25: 51–62.

Esiri MM, Gay D. Immunological and neuropathological significance of the Virchow-Robin space. J Neurol Sci 1990; 100: 3–8.

Esiri MM, Wilcock GK, Morris JH. Neuropathological assessment of the lesions of significance in vascular dementia. J Neurol Neurosurg Psychiatry 1997: 749–753.

Farez MF, Fiol MP, Gaitán MI, Quintana FJ, Correale J. Sodium intake is associated with increased disease activity in multiple sclerosis. 2015; 86: 26–31.

Farkas E, de Vos R a I, Donka G, Jansen Steur EN, Mihály A, Luiten PGM. Age-related

microvascular degeneration in the human cerebral periventricular white matter. Acta Neuropathol 2006; 111: 150–157.

Farrall AJ, Wardlaw JM. Blood-brain barrier: Ageing and microvascular disease - systematic review and meta-analysis. Neurobiol Aging 2009; 30: 337–352.

Fazekas F, Kleinert R, Offenbacher H, Schmidt R, Kleinert G, Payer F, et al. Pathologic correlates of incidental MRI white matter signal hyperintensities. Neurology 1993; 43: 1683–9.

Fazekas F, Schmidt R, Kleinert R, Kapeller P, Roob G, Flooh E. The spectrum of age-associated brain abnormalities: their measurement and histopathological correlates. J Neural Transm Suppl 1998; 53: 31–9.

Fernando MS, Simpson JE, Matthews F, Brayne C, Lewis CE, Barber R, et al. White matter lesions in an unselected cohort of the elderly: molecular pathology suggests origin from chronic hypoperfusion injury. Stroke 2006; 37: 1391–8.

Fierz W. Multiple sclerosis: an example of pathogenic viral interaction? Virol J 2017; 14: 42.

Filippi M, Bar-Or A, Piehl F, Preziosa P, Solari A, Vukusic S, et al. Multiple sclerosis. Nat Rev Dis Prim 2018; 4: 43.

Filippi M, Brück W, Chard D, Fazekas F, Geurts JJG, Enzinger C, et al. Association between pathological and MRI findings in multiple sclerosis. Lancet Neurol 2019; 18: 198–210.

Filippi M, Rocca MA, Ciccarelli O, De Stefano N, Evangelou N, Kappos L, et al. MRI criteria for the diagnosis of multiple sclerosis: MAGNIMS consensus guidelines. Lancet Neurol 2016; 15: 292–303.

Fisher E, Chang A, Fox RJ, Tkach JA, Svarovsky T, Nakamura K, et al. Imaging correlates of axonal swelling in chronic multiple sclerosis brains. Ann Neurol 2007; 62: 219–228.

Fisher E, Rudick RA, Cutter G, Baier M, Miller D, Weinstock-Guttman B, et al. Relationship between brain atrophy and disability: an 8-year follow-up study of multiple sclerosis patients. Mult Scler 2000; 6: 373–7.

Forsberg KME, Zhang Y, Reiners J, Ander M, Niedermayer A, Fang L, et al. Endothelial damage, vascular bagging and remodeling of the microvascular bed in human microangiopathy with deep white matter lesions. Acta Neuropathol Commun 2018; 6: 128.

Frischer JM, Bramow S, Dal-Bianco A, Lucchinetti CF, Rauschka H, Schmidbauer M, et al. The relation between inflammation and neurodegeneration in multiple sclerosis brains. Brain 2009; 132: 1175–1189.

Frischer JM, Weigand SD, Guo Y, Kale N, Parisi JE, Pirko I, et al. Clinical and pathological insights into the dynamic nature of the white matter multiple sclerosis plaque. Ann Neurol 2015; 78: 710–721.

Van Gaal LF, Mertens IL, De Block CE. Mechanisms linking obesity with cardiovascular disease. Nature 2006; 444: 875–880.

Gay D, Esiri M. Blood-brain barrier damage in acute multiple sclerosis plaques. An immunocytological study. Brain 1991; 114: 557–72.

Geraldes R, Ciccarelli O, Barkhof F, De Stefano N, Enzinger C, Filippi M, et al. The current role of MRI in differentiating multiple sclerosis from its imaging mimics. Nat Rev Neurol 2018; 14: 199–213.

Geraldes R, Esiri MM, DeLuca GC, Palace J. Age-related small vessel disease: a potential contributor to neurodegeneration in multiple sclerosis. Brain Pathol 2017; 27: 707–722.

Geurts JJG, Roosendaal SD, Calabrese M, Ciccarelli O, Agosta F, Chard DT, et al. Consensus recommendations for MS cortical lesion scoring using double inversion recovery MRI. Neurology 2011; 76: 418–424.

Giles JT. Cardiovascular disease in rheumatoid arthritis: Current perspectives on assessing and mitigating risk in clinical practice. Best Pract Res Clin Rheumatol 2015; 29: 597–613.

Giovannoni G, Handunnetthi L, Disanto G, Williamson AJ, Ramagopalan S V, Handel AE. An Updated Meta-Analysis of Risk of Multiple Sclerosis following Infectious Mononucleosis. PLoS One 2010; 5: e12496.

Girolamo F, Coppola C, Ribatti D, Trojano M. Angiogenesis in multiple sclerosis and experimental autoimmune encephalomyelitis. Acta Neuropathol Commun 2014; 2: 84.

Gisterå A, Hansson GK. The immunology of atherosclerosis. Nat Rev Nephrol 2017; 13: 368–380.

Golden LC, Voskuhl R. The importance of studying sex differences in disease: The example of multiple sclerosis. J Neurosci Res 2017; 95: 633–643.

Goodin DS, Corwin M, Kaufman D, Golub H, Reshef S, Rametta MJ, et al. Causes of Death among Commercially Insured Multiple Sclerosis Patients in the United States. PLoS One 2014; 9: e105207.

Gosse P. Left ventricular hypertrophy as a predictor of cardiovascular risk. J Hypertens 2005; 23: S27–S33.

Gouw A a, Seewann A, van der Flier WM, Barkhof F, Rozemuller AM, Scheltens P, et al. Heterogeneity of small vessel disease: a systematic review of MRI and histopathology correlations. J Neurol Neurosurg Psychiatry 2011; 82: 126–35.

Gouw AA, Seewann A, Vrenken H, van der Flier WM, Rozemuller JM, Barkhof F, et al. Heterogeneity of white matter hyperintensities in Alzheimer's disease: post-mortem quantitative MRI and neuropathology. Brain 2008; 131: 3286–3298.

Grajek S, Lesiak M, Pyda M, Zajac M, Paradowski S, Kaczmarek E. Hypertrophy or hyperplasia in cardiac muscle. Post-mortem human morphometric study. Eur Heart J 1993; 14: 40–7.

Gregoire SM, Chaudhary UJ, Brown MM, Yousry T a., Kallis C, Jäger HR, et al. The Microbleed Anatomical Rating Scale (MARS): Reliability of a tool to map brain microbleeds. Neurology 2009; 73: 1759–1766.

Groenewegen KA, Den Ruijter HM, Pasterkamp G, Polak JF, Bots ML, Peters SAE. Vascular age to determine cardiovascular disease risk: A systematic review of its concepts, definitions, and clinical applications. Eur J Prev Cardiol 2016; 23: 264–274.

Gustavsen S, Søndergaard HB, Oturai DB, Laursen B, Laursen JH, Magyari M, et al. Shift work at young age is associated with increased risk of multiple sclerosis in a Danish population. Mult Scler Relat Disord 2016; 9: 104–109.

Haglund M, Englund E. Cerebral amyloid angiopathy, white matter lesions and Alzheimer encephalopathy - a histopathological assessment. Dement Geriatr Cogn Disord 2002; 14: 161–6.

Haider L, Zrzavy T, Hametner S, Höftberger R, Bagnato F, Grabner G, et al. The topograpy of demyelination and neurodegeneration in the multiple sclerosis brain. Brain 2016; 139: 807–15.

Hall CN, Reynell C, Gesslein B, Hamilton NB, Mishra A, Sutherland B a, et al. Capillary pericytes regulate cerebral blood flow in health and disease. Nature 2014; 508: 55–60.

Hametner S, Wimmer I, Haider L, Pfeifenbring S, Brück W, Lassmann H. Iron and neurodegeneration in the multiple sclerosis brain. Ann Neurol 2013; 74: 848–61.

Handel AE, Williamson AJ, Disanto G, Dobson R, Giovannoni G, Ramagopalan S V. Smoking and Multiple Sclerosis : An Updated Meta- Analysis. 2011; 6: 2–7.

Hanlon P, Nicholl BI, Jani BD, Lee D, McQueenie R, Mair FS. Frailty and pre-frailty in middle-aged and older adults and its association with multimorbidity and mortality: a prospective analysis of 493 737 UK Biobank participants. Lancet Public Heal 2018; 3: e323–e332.

Hansen TP, Cain J, Thomas O, Jackson A. Dilated perivascular spaces in the Basal Ganglia are a biomarker of small-vessel disease in a very elderly population with dementia. AJNR Am J Neuroradiol 2015; 36: 893–898.

Hartmann DA, Hyacinth HI, Liao FF, Shih AY. Does pathology of small venules contribute to cerebral microinfarcts and dementia? J Neurochem 2018; 144: 517–526.

Hase Y, Horsburgh K, Ihara M, Kalaria RN. White matter degeneration in vascular and other ageing-related dementias. J Neurochem 2018; 144: 617–633.

Head T, Daunert S, Goldschmidt-Clermont PJ. The aging risk and atherosclerosis: A fresh look at arterial homeostasis. Front Genet 2017; 8: 1–11.

Healy BC, Ali EN, Guttmann CRG, Chitnis T, Glanz BI, Buckle G, et al. Smoking and Disease Progression in Multiple Sclerosis. Arch Neurol 2009; 66: 858–64.

Hedström AK, Alfredsson L, Lima Bomfim I, Hillert J, Olsson T. Obesity interacts with infectious mononucleosis in risk of multiple sclerosis. Eur J Neurol 2014; 22: 578-e38.

Hedström AK, Bäärnhielm M, Olsson T, Alfredsson L. Exposure to environmental tobacco smoke is associated with increased risk for multiple sclerosis. Mult Scler J 2011; 17: 788–793.

Hedström AK, Bomfim IL, Barcellos L, Gianfrancesco M, Schaefer C, Kockum I, et al. Interaction between adolescent obesity and HLA risk genes in the etiology of multiple sclerosis. Neurology 2014; 82: 865–872.

Hedström AK, Hillert J, Olsson T, Alfredsson L. Nicotine might have a protective effect in the etiology of multiple sclerosis. Mult Scler J 2013; 19: 1009–1013.

Hedström AK, Hössjer O, Katsoulis M, Kockum I, Olsson T, Alfredsson L. Organic solvents and MS susceptibility. Neurology 2018; 91: e455–e462.

den Heijer T, Launer LJ, Prins ND, van Dijk EJ, Vermeer SE, Hofman A, et al. Association between blood pressure, white matter lesions, and atrophy of the medial temporal lobe. Neurology 2005; 64: 263–7.

Hernán M, Jick SS, Logroscino G, Olek MJ, Ascherio A, Jick H. Cigarette smoking and the progression of multiple sclerosis. Brain 2005; 128: 1461–1465.

Heydarpour P, Manouchehrinia A, Beiki O, Mousavi SE, Abdolalizadeh A, -Lakeh MM, et al. Smoking and worsening disability in multiple sclerosis: A meta-analysis. Acta Neurol Scand 2018; 138: 62–69.

Hilal S, Sikking E, Shaik MA, Chan QL, van Veluw SJ, Vrooman H, et al. Cortical cerebral microinfarcts on 3T MRI: A novel marker of cerebrovascular disease. Neurology 2016; 87: 1583–1590.

Holland CM, Charil A, Csapo I, Liptak Z, Ichise M, Khoury SJ, et al. The relationship between normal cerebral perfusion patterns and white matter lesion distribution in 1,249 patients with multiple sclerosis. J Neuroimaging 2012; 22: 129–36.

Horowitz AL, Kaplan RD, Grewe G, White RT, Salberg LM. The ovoid lesion: a new MR observation in patients with multiple sclerosis. AJNR Am J Neuroradiol 1989; 10: 303–5.

Horsburgh K, Wardlaw JM, van Agtmael T, Allan SM, Ashford MLJ, Bath PM, et al. Small vessels, dementia and chronic diseases - molecular mechanisms and pathophysiology. Clin Sci 2018; 132: 851–868.

van Horssen J, Bö L, Vos CMP, Virtanen I, de Vries HE. Basement membrane proteins in multiple sclerosis-associated inflammatory cuffs: potential role in influx and transport of

leukocytes. J Neuropathol Exp Neurol 2005; 64: 722–729.

Howell OW, Reeves CA, Nicholas R, Carassiti D, Radotra B, Gentleman SM, et al. Meningeal inflammation is widespread and linked to cortical pathology in multiple sclerosis. Brain 2011; 134: 2755–71.

Huang T, Huang W, Zhang Z, Yu L, Xie C, Zhu D, et al. Hypoxia-inducible factor-1α upregulation in microglia following hypoxia protects against ischemia-induced cerebral infarction. Neuroreport 2014; 25: 1122–1128.

Huang YH, Zhang WW, Lin L, Feng J, Zhao XX, Guo WH, et al. Could changes in arterioles impede the perivascular drainage of interstitial fluid from the cerebral white matter in leukoaraiosis? Neuropathol Appl Neurobiol 2010; 36: 237–47.

Huitema MJD, Schenk GJ. Insights into the Mechanisms That May Clarify Obesity as a Risk Factor for Multiple Sclerosis. Curr Neurol Neurosci Rep 2018; 18

Iacobaeus E, Sugars R V., Törnqvist Andrén A, Alm JJ, Qian H, Frantzen J, et al. Dynamic Changes in Brain Mesenchymal Perivascular Cells Associate with Multiple Sclerosis Disease Duration, Active Inflammation, and Demyelination. Stem Cells Transl Med 2017; 6: 1840–1851.

Iadecola C. The pathobiology of vascular dementia. Neuron 2013; 80: 844–66.

Iadecola C, Anrather J. The immunology of stroke: from mechanisms to translation. Nat Med 2011; 17: 796–808.

Ibrahim TS, Laurienti PJ, Aizenstein HJ, MacCloud RL, Shaaban CE, Guralnik J, et al. In Vivo Imaging of Venous Side Cerebral Small-Vessel Disease in Older Adults: An MRI Method at 7T. Am J Neuroradiol 2017; 38: 1923–1928.

Ibrahimi P, Jashari F, Nicoll R, Bajraktari G, Wester P, Henein MY. Coronary and carotid atherosclerosis: How useful is the imaging? Atherosclerosis 2013; 231: 323–333.

Jacobsen C, Hagemeier J, Myhr K-M, Nyland H, Lode K, Bergsland N, et al. Brain atrophy and disability progression in multiple sclerosis patients: a 10-year follow-up study. J Neurol Neurosurg Psychiatry 2014; 85: 1109–1115.

Jain S, Ribbens A, Sima DM, Cambron M, De Keyser J, Wang C, et al. Two Time Point MS Lesion Segmentation in Brain MRI: An Expectation-Maximization Framework. Front Neurosci 2016; 10: 576.

Jain S, Sima DM, Ribbens A, Cambron M, Maertens A, Van Hecke W, et al. Automatic segmentation and volumetry of multiple sclerosis brain lesions from MR images. NeuroImage Clin 2015; 8: 367–375.

Janaway BM, Simpson JE, Hoggard N, Highley JR, Forster G, Drew D, et al. Brain haemosiderin in older people: Pathological evidence for an ischaemic origin of magnetic resonance imaging

(MRI) microbleeds. Neuropathol Appl Neurobiol 2014; 40: 258–269.

Jenkinson M, Bannister P, Brady M, Smith S. Improved optimization for the robust and accurate linear registration and motion correction of brain images. Neuroimage 2002; 17: 825–841.

Jiang T, Cadenas E. Astrocytic metabolic and inflammatory changes as a function of age. Aging Cell 2014; 13: 1059–67.

Jick SS, Li L, Falcone GJ, Vassilev ZP, Wallander M-A. Mortality of patients with multiple sclerosis: a cohort study in UK primary care. J Neurol 2014; 261: 1508–17.

Johnson MW, Kerfoot C, Bushnell T, Li M, Vinters H V. Hamartin and tuberin expression in human tissues. Mod Pathol 2001; 14: 202–210.

Jones EG. On the mode of entry of blood vessels into the cerebral cortex. J Anat 1970; 106: 507–520.

de Jong LW, Forsberg LE, Vidal J-S, Sigurdsson S, Zijdenbos AP, Garcia M, et al. Different susceptibility of medial temporal lobe and basal ganglia atrophy rates to vascular risk factors. Neurobiol Aging 2014; 35: 72–78.

Joseph P, Leong D, McKee M, Anand SS, Schwalm JD, Teo K, et al. Reducing the global burden of cardiovascular disease, part 1: The epidemiology and risk factors. Circ Res 2017; 121: 677–694.

Juryńczyk M, Geraldes R, Probert F, Woodhall MR, Waters P, Tackley G, et al. Distinct brain imaging characteristics of autoantibody-mediated CNS conditions and multiple sclerosis. Brain 2017; 140: 617–627.

Juryńczyk M, Tackley G, Kong Y, Geraldes R, Matthews L, Woodhall M, et al. Brain lesion distribution criteria distinguish MS from AQP4-antibody NMOSD and MOG-antibody disease. J Neurol Neurosurg Psychiatry 2017; 88: 132–136.

Kalaria RN. Cerebral vessels in ageing and Alzheimer's disease. Pharmacol Ther 1996; 72: 193–214.

Kapeller P, Ropele S, Enzinger C, Lahousen T, Strasser-Fuchs S, Schmidt R, et al. Discrimination of white matter lesions and multiple sclerosis plaques by short echo quantitative 1H-magnetic resonance spectroscopy. J Neurol 2005; 252: 1229–34.

Kappus N, Weinstock-Guttman B, Hagemeier J, Kennedy C, Melia R, Carl E, et al. Cardiovascular risk factors are associated with increased lesion burden and brain atrophy in multiple sclerosis. J Neurol Neurosurg Psychiatry 2015; 87: 181–187.

Kazi DS, Penko JM, Bibbins-Domingo K. Statins for Primary Prevention of Cardiovascular Disease. Med Clin North Am 2017; 101: 689–699.

Keith J, Gao FQ, Noor R, Kiss A, Balasubramaniam G, Au K, et al. Collagenosis of the Deep Medullary Veins: An Underrecognized Pathologic Correlate of White Matter Hyperintensities and Periventricular Infarction? J Neuropathol Exp Neurol 2017; 76: 299–312.

Ketelhuth DFJ, Hansson GK. Adaptive Response of T and B Cells in Atherosclerosis. Circ Res 2016; 118: 668–678.

De Keyser J, Steen C, Mostert JP, Koch MW. Hypoperfusion of the cerebral white matter in multiple sclerosis: possible mechanisms and pathophysiological significance. J Cereb Blood Flow Metab 2008; 28: 1645–1651.

Kiliç T, Akakin A. Anatomy of cerebral veins and sinuses. Front Neurol Neurosci 2008; 23: 4–15.

Kilsdonk I, Steenwijk M, Pouwels P, Zwanenburg J, Visser F, Luijten P, et al. Perivascular spaces in MS patients at 7 Tesla MRI: A marker of neurodegeneration? Mult Scler 2015; 21: 155–162.

Kim SH, Yun C-H, Lee S-Y, Choi K, Kim MB, Park H-K. Age-dependent association between cigarette smoking on white matter hyperintensities. Neurol Sci 2012; 33: 45–51.

Kincses ZT, Ropele S, Jenkinson M, Khalil M, Petrovic K, Loitfelder M, et al. Lesion probability mapping to explain clinical deficits and cognitive performance in multiple sclerosis. Mult Scler 2011; 17: 681–689.

Kingwell E, Marriott JJ, Jetté N, Pringsheim T, Makhani N, Morrow S a, et al. Incidence and prevalence of multiple sclerosis in Europe: a systematic review. BMC Neurol 2013; 13: 128.

Kipp M, Nyamoya S, Hochstrasser T, Amor S. Multiple sclerosis animal models: a clinical and histopathological perspective. Brain Pathol 2017; 27: 123–137.

Klawiter EC. Current and new directions in MRI in multiple sclerosis. Contin Lifelong Learn Neurol 2013; 19: 1058–1073.

Kobelt G, Eriksson J, Phillips G, Berg J. The burden of multiple sclerosis 2015: Methods of data collection, assessment and analysis of costs, quality of life and symptoms. Mult Scler 2017; 23: 4–16.

Koch-Henriksen N, Brønnum-Hansen H, Stenager E. Underlying cause of death in Danish patients with multiple sclerosis: results from the Danish Multiple Sclerosis Registry. J Neurol Neurosurg Psychiatry 1998; 65: 56–9.

Koch-Henriksen N, Sørensen PS. The changing demographic pattern of multiple sclerosis epidemiology. Lancet Neurol 2010; 9: 520–532.

Koch M, Mostert J, Heersema D, De Keyser J. Progression in multiple sclerosis: further evidence of an age dependent process. J Neurol Sci 2007; 255: 35–41.

Kowalec K, McKay KA, Patten SB, Fisk JD, Evans C, Tremlett H, et al. Comorbidity increases the risk of relapse in multiple sclerosis. Neurology 2017; 89: 2455–2461.

Kowara M, Kasarełło K, Czarzasta K, Opolski G, Cudnoch-Jędrzejewska A. Early-life inflammation pathways trigger a cascade leading to development of atherosclerotic plaque through the 'butterfly effect' - An hypothesis. Med Hypotheses 2019; 122: 106–110.

Kozinska D, Holland CM, Krissian K, Westin C-F, Guttmann CRG. A method for the analysis of the geometrical relationship between white matter pathology and the vascular architecture of the brain. Neuroimage 2004; 22: 1671–8.

Kugler N, Patel PJ, Lee CJ. Chronic Cerebrospinal Venous Insufficiency in Multiple Sclerosis: A Failed Concept. Vasc Spec Int 2015; 31: 11–4.

Kuhlmann T, Ludwin S, Prat A, Antel J, Brück W, Lassmann H. An updated histological classification system for multiple sclerosis lesions. Acta Neuropathol 2017; 133: 13–24.

Kulik T, Kusano Y, Aronhime S, Sandler AL, Winn HR. Regulation of cerebral vasculature in normal and ischemic brain. Neuropharmacology 2008; 55: 281–288.

Landis JR, Koch GG. The measurement of observer agreement for categorical data. Biometrics 1977; 33: 159–74.

Lao Y, Nguyen B, Tsao S, Gajawelli N, Law M, Chui H, et al. A T1 and DTI fused 3D corpus callosum analysis in MCI subjects with high and low cardiovascular risk profile. NeuroImage Clin 2017; 14: 298–307.

Lapointe E, Li DKB, Traboulsee AL, Rauscher A. What have we learned from perfusion MRI in multiple sclerosis? Am J Neuroradiol 2018; 39: 994–1000.

Lassmann H. Hypoxia-like tissue injury as a component of multiple sclerosis lesions. J Neurol Sci 2003; 206: 187–191.

Lassmann H. Review: The architecture of inflammatory demyelinating lesions: Implications for studies on pathogenesis. Neuropathol Appl Neurobiol 2011; 37: 698–710.

Lassmann H, Brück W, Lucchinetti CF. The Immunopathology of Multiple Sclerosis: An Overview. Brain Pathol 2007; 17: 210–218.

Lau KK, Pego P, Mazzucco S, Li L, Howard DP, Küker W, et al. Age and sex-specific associations of carotid pulsatility with small vessel disease burden in transient ischemic attack and ischemic stroke. Int J Stroke 2018; 13: 832–839.

Lau LW, Cua R, Keough MB, Haylock-Jacobs S, Yong VW. Pathophysiology of the brain extracellular matrix: a new target for remyelination. Nat Rev Neurosci 2013; 14: 722–9.

Laule C, Pavlova V, Leung E, Zhao G, MacKay AL, Kozlowski P, et al. Diffusely abnormal white matter in multiple sclerosis: further histologic studies provide evidence for a primary lipid

abnormality with neurodegeneration. J Neuropathol Exp Neurol 2013; 72: 42–52.

Laule C, Vavasour IM, Leung E, Li DKB, Kozlowski P, Traboulsee AL, et al. Pathological basis of diffusely abnormal white matter: insights from magnetic resonance imaging and histology. Mult Scler 2011; 17: 144–150.

Launer LJ, Lewis CE, Schreiner PJ, Sidney S, Battapady H, Jacobs DR, et al. Vascular factors and multiple measures of early brain health: CARDIA brain MRI study. PLoS One 2015; 10: e0122138.

Lauretani F, Meschi T, Ticinesi A, Maggio M. "Brain-muscle loop" in the fragility of older persons: from pathophysiology to new organizing models. Aging Clin Exp Res 2017; 29: 1305–1311.

Law M, Saindane AM, Ge Y, Babb JS, Johnson G, Mannon LJ, et al. Microvascular abnormality in relapsing-remitting multiple sclerosis: perfusion MR imaging findings in normal-appearing white matter. Radiology 2004; 231: 645–52.

Lee M a., Smith S, Palace J, Narayanan S, Silver N, Minicucci L, et al. Spatial mapping of T2 and gadolinium-enhancing T1 lesion volumes in multiple sclerosis: Evidence for distinct mechanisms of lesion genesis? Brain 1999; 122: 1261–1270.

Lee S-H, Kwon S-J, Kim KS, Yoon B-W, Roh J-K. Cerebral microbleeds in patients with hypertensive stroke. Topographical distribution in the supratentorial area. J Neurol 2004; 251: 1183–9.

Lemus HN, Warrington AE, Rodriguez M. Multiple Sclerosis: Mechanisms of Disease and Strategies for Myelin and Axonal Repair. Neurol Clin 2018; 36: 1–11.

Lengfeld J, Cutforth T, Agalliu D. The role of angiogenesis in the pathology of multiple sclerosis. Vasc Cell 2014; 6: 23.

Li M, Cima MJ, Milner DA, Jr. If It's Not One Thing, It's Another: An Inverse Relationship of Malignancy and Atherosclerotic Disease. PLoS One 2015; 10: e0126855.

Li X, Harrison DM, Liu H, Jones CK, Oh J, Calabresi PA, et al. Magnetic susceptibility contrast variations in multiple sclerosis lesions. J Magn Reson Imaging 2016; 43: 463–473.

Liu X. A Meta-Analysis of Association between Cerebral Microbleeds and Cognitive Impairment. Med Sci Monit 2014; 20: 2189–2198.

Liu Z, Pardini M, Yaldizli O, Sethi V, Muhlert N, Wheeler-Kingshott C a. M, et al. Magnetization transfer ratio measures in normal-appearing white matter show periventricular gradient abnormalities in multiple sclerosis. Brain 2015; 138: 1239–1246.

Loos CMJ, Klarenbeek P, van Oostenbrugge RJ, Staals J. Association between Perivascular Spaces and Progression of White Matter Hyperintensities in Lacunar Stroke Patients. PLoS One 2015; 10: e0137323.

López-Otín C, Blasco MA, Partridge L, Serrano M, Kroemer G. The hallmarks of aging. Cell 2013; 153: 1194–217.

Lotti CB de C, Oliveira ASB, Bichuetti DB, Castro I de, Oliveira EML. Late onset multiple sclerosis: concerns in aging patients. Arq Neuropsiquiatr 2017; 75: 451–456.

Lourenço CF, Ledo A, Dias C, Barbosa RM, Laranjinha J. Neurovascular and neurometabolic derailment in aging and Alzheimer's disease. Front Aging Neurosci 2015; 7: 103.

Love S, Chalmers K, Ince P, Esiri M, Attems J, Jellinger K, et al. Development, appraisal, validation and implementation of a consensus protocol for the assessment of cerebral amyloid angiopathy in post-mortem brain tissue. Am J Neurodegener Dis 2014; 3: 19–32.

Lublin FD. New multiple sclerosis phenotypic classification. Eur Neurol 2014; 72 Suppl 1: 1–5.

Lublin FD, Reingold SC, Cohen J a., Cutter GR, Sørensen PS, Thompson AJ, et al. Defining the clinical course of multiple sclerosis: The 2013 revisions. Neurology 2014; 83: 278–286.

Lycklama à Nijeholt GJ, Uitdehaag BM, Bergers E, Castelijns JA, Polman CH, Barkhof F. Spinal cord magnetic resonance imaging in suspected multiple sclerosis. Eur Radiol 2000; 10: 368–376.

Mahad DH, Trapp BD, Lassmann H. Pathological mechanisms in progressive multiple sclerosis. Lancet Neurol 2015; 14: 183–193.

Mahad DJ, Ziabreva I, Campbell G, Lax N, White K, Hanson PS, et al. Mitochondrial changes within axons in multiple sclerosis. Brain 2009; 132: 1161–74.

Maillard P, Carmichael OT, Reed B, Mungas D, DeCarli C. Cooccurrence of vascular risk factors and late-life white-matter integrity changes. Neurobiol Aging 2015; 36: 1670–1677.

Maki T, Liang AC, Miyamoto N, Lo EH, Arai K. Mechanisms of oligodendrocyte regeneration from ventricular-subventricular zone-derived progenitor cells in white matter diseases. Front Cell Neurosci 2013; 7: 275.

Mallucci G, Peruzzotti-Jametti L, Bernstock JD, Pluchino S. The role of immune cells, glia and neurons in white and gray matter pathology in multiple sclerosis. Prog Neurobiol 2015; 127–128: 1–22.

Mancia G, De Backer G, Dominiczak A, Cifkova R, Fagard R, Germano G, et al. 2007 Guidelines for the Management of Arterial Hypertension. J Hypertens 2007; 25: 1105–1187.

Marck CH, Neate SL, Taylor KL, Weiland TJ, Jelinek GA. Prevalence of Comorbidities, Overweight and Obesity in an International Sample of People with Multiple Sclerosis and Associations with Modifiable Lifestyle Factors. PLoS One 2016; 11: e0148573.

Marrie R a, Rudick R, Horwitz R, Cutter G, Tyry T, Campagnolo D, et al. Vascular comorbidity

is associated with more rapid disability progression in multiple sclerosis. Neurology 2010; 74: 1041–7.

Marrie RA. Comorbidity in multiple sclerosis: implications for patient care. Nat Rev Neurol 2017; 13: 375–382.

Marrie RA, Cohen J, Stuve O, Trojano M, Sørensen PS, Reingold S, et al. A systematic review of the incidence and prevalence of comorbidity in multiple sclerosis: Overview. Mult Scler 2015; 21: 1–19.

Marrie RA, Garland A, Schaffer SA, Fransoo R, Leung S, Yogendran M, et al. Traditional risk factors may not explain increased incidence of myocardial infarction in MS. Neurology 2019; 92: e1624–e1633.

Marrie RA, Reider N, Cohen J, Stuve O, Trojano M, Cutter G, et al. A systematic review of the incidence and prevalence of cardiac, cerebrovascular, and peripheral vascular disease in multiple sclerosis. Mult Scler 2014; 21: 318–331.

Marrie RA, Tremlett H. The epidemiology of multiple sclerosis. In: Multiple Sclerosis Therapeutics, Fourth Edition. 2011. p. 46–55

Marshall O, Lu H, Brisset J-C, Xu F, Liu P, Herbert J, et al. Impaired cerebrovascular reactivity in multiple sclerosis. JAMA Neurol 2014; 71: 1275–81.

Martinez Sosa S, Smith KJJ. Understanding a role for hypoxia in lesion formation and location in the deep and periventricular white matter in small vessel disease and multiple sclerosis. Clin Sci 2017; 131: 2503–2524.

Matthews L, Marasco R, Jenkinson M, Küker W, Luppe S, Leite MI, et al. Distinction of seropositive NMO spectrum disorder and MS brain lesion distribution. Neurology 2013; 80: 1330–1337.

Mehta LS, Beckie TM, DeVon HA, Grines CL, Krumholz HM, Johnson MN, et al. Acute Myocardial Infarction in Women: A Scientific Statement From the American Heart Association. Circulation 2016; 133: 916–47.

Meng R, Asmaro K, Meng L, Liu Y, Ma C, Xi C, et al. Upper limb ischemic preconditioning prevents recurrent stroke in intracranial arterial stenosis. Neurology 2012; 79: 1853–61.

Meng R, Ding Y, Asmaro K, Brogan D, Meng L, Sui M, et al. Ischemic Conditioning Is Safe and Effective for Octo- and Nonagenarians in Stroke Prevention and Treatment. Neurotherapeutics 2015; 12: 667–677.

Messner B, Bernhard D. Smoking and cardiovascular disease: Mechanisms of endothelial dysfunction and early atherogenesis. Arterioscler Thromb Vasc Biol 2014; 34: 509–515.

Miki Y, Grossman RI, Udupa JK, Wei L, Kolson DL, Mannon LJ, et al. Isolated U-fiber involvement in MS: preliminary observations. Neurology 1998; 50: 1301–6.

Mistry N, Abdel-Fahim R, Samaraweera A, Mougin O, Tallantyre E, Tench C, et al. Imaging central veins in brain lesions with 3-T T2*-weighted magnetic resonance imaging differentiates multiple sclerosis from microangiopathic brain lesions. Mult Scler J 2016; 22: 1289–1296.

Mitrovič M, Patsopoulos NA, Beecham AH, Dankowski T, Goris A, Dubois B, et al. Low-Frequency and Rare-Coding Variation Contributes to Multiple Sclerosis Risk. Cell 2018; 175: 1679-1687.e7.

Miwa K, Okazaki S, Sakaguchi M, Mochizuki H, Kitagawa K. Interleukin-6, interleukin-6 receptor gene variant, small-vessel disease and incident dementia. Eur J Neurol 2016; 23: 656–63.

Modat M, Ridgway GR, Taylor ZA, Lehmann M, Barnes J, Hawkes DJ, et al. Fast free-form deformation using graphics processing units. Comput Methods Programs Biomed 2010; 98: 278–284.

Mohan H, Krumbholz M, Sharma R, Eisele S, Junker A, Sixt M, et al. Extracellular matrix in multiple sclerosis lesions: Fibrillar collagens, biglycan and decorin are upregulated and associated with infiltrating immune cells. Brain Pathol 2010; 20: 966–75.

Montagne A, Barnes SR, Sweeney MD, Halliday MR, Sagare AP, Zhao Z, et al. Blood-Brain Barrier Breakdown in the Aging Human Hippocampus. Neuron 2015; 85: 296–302.

Moody DM, Brown WR, Challa VR, Anderson RL. Periventricular venous collagenosis: association with leukoaraiosis. Radiology 1995; 194: 469–76.

Moore GRW, Laule C, MacKay A, Leung E, Li DKB, Zhao G, et al. Dirty-appearing white matter in multiple sclerosis. J Neurol 2008; 255: 1802–1811.

Mora JR, Iwata M, von Andrian UH. Vitamin effects on the immune system: vitamins A and D take centre stage. Nat Rev Immunol 2008; 8: 685–98.

Moulton CD, Costafreda SG, Horton P, Ismail K, Fu CHY. Meta-analyses of structural regional cerebral effects in type 1 and type 2 diabetes. Brain Imaging Behav 2015; 9: 651–62.

Munger KL, Levin LI, Hollis BW, Howard NS, Ascherio A. Serum 25-hydroxyvitamin D levels and risk of multiple sclerosis. J Am Med Assoc 2006; 296: 2832–2838.

Murtonen A, Kurki S, Hänninen K, Soilu-Hänninen M, Sumelahti ML. Common comorbidities and survival in MS: Risk for stroke, type 1 diabetes and infections. Mult Scler Relat Disord 2018; 19: 109–114.

Nakashima I, Fujihara K, Kimpara T, Okita N, Takase S, Itoyama Y. Linear Pontine Trigeminal Root Lesions in Multiple Sclerosis. Arch Neurol 2001; 58: 101–104.

Narayana P a, Zhou Y, Hasan KM, Datta S, Sun X, Wolinsky JS. Hypoperfusion and T1-hypointense lesions in white matter in multiple sclerosis. Mult Scler 2014; 20: 365–73.

Negrotto L, Farez MF, Correale J. Immunologic effects of metformin and pioglitazone treatment on metabolic syndrome and multiple sclerosis. JAMA Neurol 2016; 73: 520–528.

Ni R, Chu L, Xu D, Li Y, Li Y, Zhang Y, et al. Risk factors of cerebral microbleeds in young and middle-aged patients with hypertension. Neurol Res 2018; 40: 413–418.

Nielsen NM, Munger KL, Koch-Henriksen N, Hougaard DM, Magyari M, Jørgensen KT, et al. Neonatal vitamin D status and risk of multiple sclerosis. Neurology 2017; 88: 44–51.

Nitkunan A, Lanfranconi S, Charlton R a., Barrick TR, Markus HS. Brain atrophy and cerebral small vessel disease a prospective follow-up study. Stroke 2011; 42: 133–138.

Norrving B. Lacunar infarcts: no black holes in the brain are benign. Pract Neurol 2008; 8: 222–8.

O'Gorman C, Lucas R, Taylor B. Environmental risk factors for multiple sclerosis: a review with a focus on molecular mechanisms. Int J Mol Sci 2012; 13: 11718–52.

Oakley R, Tharakan B. Vascular Hyperpermeability and Aging. Aging Dis 2014; 5: 114–125.

Okuda DT, Winkler MD, Pinho MC, Newton BD, Wright K, Dimitrov IE, et al. Three-Dimensional Shape and Surface Features Distinguish Multiple Sclerosis Lesions from Nonspecific White Matter Disease. J Neuroimaging 2017; 27: 613–619.

Olsson T, Barcellos LF, Alfredsson L. Interactions between genetic, lifestyle and environmental risk factors for multiple sclerosis. Nat Rev Neurol 2017; 13: 25–36.

Orton S-M, Herrera BM, Yee IM, Valdar W, Ramagopalan S V, Sadovnick AD, et al. Sex ratio of multiple sclerosis in Canada: a longitudinal study. Lancet Neurol 2006; 5: 932–936.

Ourselin S, Stefanescu R, Pennec X. Robust Registration of Multi-modal Images: Towards Real-Time Clinical Applications. In: Lecture Notes in Computer Science. Springer, Berlin, Heidelberg; 2002. p. 140–147

Öztoprak B, Öztoprak İ, Topalkara K, Erkoç MF, Şalk İ, Oztoprak B, et al. Role of thalamic diffusion for disease differentiation between multiple sclerosis and ischemic cerebral small vessel disease. Neuroradiology 2014; 57: 339–347.

Paling D, Thade Petersen E, Tozer DJ, Altmann DR, Wheeler-Kingshott C a M, Kapoor R, et al. Cerebral arterial bolus arrival time is prolonged in multiple sclerosis and associated with disability. J Cereb Blood Flow Metab 2014; 34: 34–42.

Pantoni L. Cerebral small vessel disease : from pathogenesis and clinical characteristics to therapeutic challenges. Lancet Neurol 2010; 9: 689–701.

Papandreou D, Hamid Z-T-N. The Role of Vitamin D in Diabetes and Cardiovascular Disease: An Updated Review of the Literature. Dis Markers 2015; 2015: 1–15.

Park CA, Kang C-K, Kim Y-B, Cho Z-H. Advances in MR angiography with 7T MRI: From

microvascular imaging to functional angiography. Neuroimage 2018; 168: 269–278.

Patenaude B, Smith SM, Kennedy DN, Jenkinson M. A Bayesian model of shape and appearance for subcortical brain segmentation. Neuroimage 2011; 56: 907–922.

Patzold U, Pocklington PR. Course of multiple sclerosis. First results of a prospective study carried out of 102 MS patients from 1976-1980. Acta Neurol Scand 1982; 65: 248–66.

Di Pauli F, Reindl M, Ehling R, Schautzer F, Gneiss C, Lutterotti A, et al. Smoking is a risk factor for early conversion to clinically definite multiple sclerosis. Mult Scler 2008; 14: 1026–30.

Perricone C, Versini M, Ben-Ami D, Gertel S, Watad A, Segel MJ, et al. Smoke and autoimmunity: The fire behind the disease. Autoimmun Rev 2016; 15: 354–374.

Pfefferbaum A, Mathalon DH, Sullivan E V, Rawles JM, Zipursky RB, Lim KO. A Quantitative Magnetic Resonance Imaging From Infancy to Late Adulthood. Arch Neurol 2012; 51: 874–887.

Pichler A, Khalil M, Langkammer C, Pinter D, Ropele S, Fuchs S, et al. The impact of vascular risk factors on brain volume and lesion load in patients with early multiple sclerosis. Mult Scler 2019; 25: 48–54.

Poggesi A, Pracucci G, Chabriat H, Erkinjuntti T, Fazekas F, Verdelho A, et al. Urinary complaints in nondisabled elderly people with age-related white matter changes: The Leukoaraiosis And DISability (LADIS) Study. J Am Geriatr Soc 2008; 56: 1638–1643.

Ponsonby A-L, Lucas RM, van der Mei IA, Dear K, Valery PC, Pender MP, et al. Offspring number, pregnancy, and risk of a first clinical demyelinating event: the AusImmune Study. Neurology 2012; 78: 867–74.

Prakash R, Carmichael ST. Blood–brain barrier breakdown and neovascularization processes after stroke and traumatic brain injury. Curr Opin Neurol 2015; 28: 556–564.

Pryce G, Baker D. Oligoclonal bands in multiple sclerosis; Functional significance and therapeutic implications. Does the specificity matter? Mult Scler Relat Disord 2018; 25: 131–137.

Pullicino P, Ostrow P, Miller L, Snyder W, Munschauer F. Pontine ischemic rarefaction. Ann Neurol 1995; 37: 460–466.

Putman T, Adler A. Vascular architecture of the lesions of multiple sclerosis. Arch Neurol Psychiatry 1937; 38: 1–15.

Putman TJ, Chiavacci L V. Results of treatment of multiple sclerosis with dicoumarin. Arch Neurol Psychiatry 1947; 57: 1–13.

Qiu C, Fratiglioni L. A major role for cardiovascular burden in age-related cognitive decline.

Nat Rev Cardiol 2015; 12: 267–277.

Rae-grant AD, Wong C, Bernatowicz R, Fox RJ. Observations on the brain vasculature in multiple sclerosis : A historical perspective. Mult Scler Relat Disord 2014; 3: 156–162.

Ramanujam R, Hedström AK, Manouchehrinia A, Alfredsson L, Olsson T, Bottai M, et al. Effect of smoking cessation on multiple sclerosis prognosis. JAMA Neurol 2015; 72: 1117–1123.

Ranadive SM, Yan H, Weikert M, Lane AD, Linden MA, Baynard T, et al. Vascular dysfunction and physical activity in multiple sclerosis. Med Sci Sports Exerc 2012; 44: 238–243.

Randolph JJ. Free-Marginal Multirater Kappa (multirater K[free]): An Alternative to Fleiss' Fixed-Marginal Multirater Kappa. Joensuu Learn Instr Symp 2005: Retrieved from http://eric.ed.gov/?id=ED490661.

Rashid W, Parkes LM, Ingle GT, Chard DT, Toosy a T, Altmann DR, et al. Abnormalities of cerebral perfusion in multiple sclerosis. J Neurol Neurosurg Psychiatry 2004; 75: 1288–93.

Reich DS, White R, Cortese IC, Vuolo L, Shea CD, Collins TL, et al. Sample-size calculations for short-term proof-of-concept studies of tissue protection and repair in multiple sclerosis lesions via conventional clinical imaging. Mult Scler 2015; 21: 1693–1704.

Reidel MA, Stippich C, Heiland S, Storch-Hagenlocher B, Jansen O, Hahnel S, et al. Differentiation of multiple sclerosis plaques, subacute cerebral ischaemic infarcts, focal vasogenic oedema and lesions of subcortical arteriosclerotic encephalopathy using magnetisation transfer measurements. Neuroradiology 2003; 45: 289–294.

Renard D, Castelnovo G, Bousquet PJ, de Champfleur N, de Seze J, Vermersch P, et al. Brain MRI findings in long-standing and disabling multiple sclerosis in 84 patients. Clin Neurol Neurosurg 2010; 112: 286–290.

Rindfleisch E. Histologisches Detail zu der grauen Degeneration von Gehirn und Rückenmark. (Zugleich ein Beitrag zu der Lehre von der Entstehung und Verwandlung der Zelle.). Arch für Pathol Anat und Physiol und für Klin Med 1863; 26: 474–483.

Ritz M-F, Grond-Ginsbach C, Kloss M, Tolnay M, Fluri F, Bonati LH, et al. Identification of inflammatory, metabolic, and cell survival pathways contributing to cerebral small vessel disease by postmortem gene expression microarray. Curr Neurovasc Res 2015; 13: 58–67.

Riva M, Ikonomidou VN, Ostuni JJ, Van Gelderen P, Auh S, Ohayon JM, et al. Tissue-specific imaging is a robust methodology to differentiate in vivo T1 black holes with advanced multiple sclerosis-induced damage. Am J Neuroradiol 2009; 30: 1394–1401.

Roberts JC, Wilkins RH, Moses C. Autopsy Studies in Atherosclerosis II: Distribution and Severity of Atherosclerosis in Patients Dying with Morphoogic Evidence of Atherosclerotic Catasrophy. Circulation 1959; 20: 520–526.

Rodríguez-Iturbe B, Pons H, Quiroz Y, Lanaspa MA, Johnson RJ. Autoimmunity in the

pathogenesis of hypertension. Nat Rev Nephrol 2014; 10: 56–62.

Rosand J, Muzikansky A, Kumar A, Wisco JJ, Smith EE, Betensky RA, et al. Spatial clustering of hemorrhages in probable cerebral amyloid angiopathy. Ann Neurol 2005; 58: 459–462.

Rosenberg GA, Wallin A, Wardlaw JM, Markus HS, Montaner J, Wolfson L, et al. Consensus statement for diagnosis of subcortical small vessel disease. J Cereb Blood Flow Metab 2016; 36: 6–25.

Roshanisefat H, Bahmanyar S, Hillert J, Olsson T, Montgomery S. Multiple sclerosis clinical course and cardiovascular disease risk - Swedish cohort study. Eur J Neurol 2014; 21: 1353-e88.

Rostrup E, Gouw a. a., Vrenken H, Van Straaten ECW, Ropele S, Pantoni L, et al. The spatial distribution of age-related white matter changes as a function of vascular risk factors-Results from the LADIS study. Neuroimage 2012; 60: 1597–1607.

Sacks DB, Arnold M, Bakris GL, Bruns DE, Horvath AR, Kirkman MS, et al. Position statement executive summary: Guidelines and recommendations for laboratory analysis in the diagnosis and management of diabetes mellitus. Diabetes Care 2011; 34: 1419–1423.

Saindane a. M, Law M, Ge Y, Johnson G, Babb JS, Grossman RI. Correlation of diffusion tensor and dynamic perfusion MR imaging metrics in normal-appearing corpus callosum: Support for primary hypoperfusion in multiple sclerosis. Am J Neuroradiol 2007; 28: 767–772.

Salvadó G, Brugulat-Serrat A, Sudre CH, Grau-Rivera O, Suárez-Calvet M, Falcon C, et al. Spatial patterns of white matter hyperintensities associated with Alzheimer's disease risk factors in a cognitively healthy middle-aged cohort. Alzheimers Res Ther 2019; 11: 12.

Salvetti M, Landsman D, Schwarz-Lam P, Comi G, Thompson AJ, Fox RJ. Progressive MS: from pathophysiology to drug discovery. Mult Scler 2015; 21: 1376–1384.

Salzer J, Sundstrom P. Timing of cigarette smoking as a risk factor for multiple sclerosis. Ther Adv Neurol Disord 2013; 6: 205.

Samaraweera APR, Clarke MA, Whitehead A, Falah Y, Driver ID, Dineen RA, et al. The Central Vein Sign in Multiple Sclerosis Lesions Is Present Irrespective of the T2* Sequence at 3 T. J Neuroimaging 2017; 27: 114–121.

Samaraweera APR, Falah Y, Pitiot A, Dineen RA, Morgan PS, Evangelou N. The MRI central vein marker; differentiating PPMS from RRMS and ischemic SVD. Neurol - Neuroimmunol Neuroinflammation 2018; 5: e496.

Sandberg K, Ji H, Hay M. Sex-specific immune modulation of primary hypertension. Cell Immunol 2015; 294: 95–101.

Santovito D, Weber C. Atherosclerosis revisited from a clinical perspective: Still an inflammatory disease? Thromb Haemost 2017; 117: 231–237.

Von Sarnowski B, Putaala J, Grittner U, Gaertner B, Schminke U, Curtze S, et al. Lifestyle risk factors for ischemic stroke and transient ischemic attack in young adults in the stroke in young Fabry patients study. Stroke 2013; 44: 119–125.

Sati P, Oh J, Constable RT, Evangelou N, Guttmann CRG, Henry RG, et al. The central vein sign and its clinical evaluation for the diagnosis of multiple sclerosis: a consensus statement from the North American Imaging in Multiple Sclerosis Cooperative. Nat Rev Neurol 2016; 12: 714–722.

Sawcer S, Hellenthal G, Pirinen M, Spencer CCA, Patsopoulos NA, Moutsianas L, et al. Genetic risk and a primary role for cell-mediated immune mechanisms in multiple sclerosis. Nature 2011; 476: 214–219.

Scalfari A, Neuhaus A, Daumer M, Muraro PA, Ebers GC. Onset of secondary progressive phase and long-term evolution of multiple sclerosis. J Neurol Neurosurg Psychiatry 2014; 85: 67–75.

Schmidt R, Enzinger C, Ropele S, Schmidt H, Fazekas F. Subcortical vascular cognitive impairment: similarities and differences with multiple sclerosis. J Neurol Sci 2006; 245: 3–7.

Schutzer WE, Xue H, Reed J, Oyama T, Beard DR, Anderson S, et al. Age-related β-adrenergic receptor-mediated vasorelaxation is changed by altering G protein receptor kinase 2 expression. Vascul Pharmacol; 55: 178–88.

Segarra M, Kirchmaier BC, Acker-Palmer A. A vascular perspective on neuronal migration. Mech Dev 2015; 138: 17–25.

Shi Y, Wardlaw JM. Update on cerebral small vessel disease: A dynamic whole-brain disease. Stroke Vasc Neurol 2016; 1: 83–92.

Shirani A, Tremlett H. The effect of smoking on the symptoms and progression of multiple sclerosis: A review. J Inflamm Res 2010; 3: 115–126.

Simpson RJ, McLean G, Guthrie B, Mair F, Mercer SW. Physical and mental health comorbidity is common in people with multiple sclerosis: nationally representative cross-sectional population database analysis. BMC Neurol 2014; 14: 128.

Singh N, Moody AR, Roifman I, Bluemke DA, Zavodni AEH. Advanced MRI for carotid plaque imaging. Int J Cardiovasc Imaging 2016; 32: 83–89.

de Sitter A, Steenwijk MD, Ruet A, Versteeg A, Liu Y, van Schijndel RA, et al. Performance of five research-domain automated WM lesion segmentation methods in a multi-center MS study. Neuroimage 2017; 163: 106–114.

Skrobot OA, Attems J, Esiri M, Hortobágyi T, Ironside JW, Kalaria RN, et al. Vascular cognitive impairment neuropathology guidelines (VCING): the contribution of cerebrovascular pathology to cognitive impairment. Brain 2016; 139: 2957–2969.

Smallwood A, Oulhaj A, Joachim C, Christie S, Sloan C, Smith AD, et al. Cerebral subcortical small vessel disease and its relation to cognition in elderly subjects: a pathological study in the Oxford Project to Investigate Memory and Ageing (OPTIMA) cohort. Neuropathol Appl Neurobiol 2012; 38: 337–43.

Smith SM, Jenkinson M, Woolrich MW, Beckmann CF, Behrens TEJ, Johansen-Berg H, et al. Advances in functional and structural MR image analysis and implementation as FSL. Neuroimage 2004; 23: 208–219.

Smith SM, Zhang Y, Jenkinson M, Chen J, Matthews PM, Federico A, et al. Accurate, robust, and automated longitudinal and cross-sectional brain change analysis. Neuroimage 2002; 17: 479–89.

Smyth LCD, Rustenhoven J, Scotter EL, Schweder P, Faull RLM, Park TIH, et al. Markers for human brain pericytes and smooth muscle cells. J Chem Neuroanat 2018; 92: 48–60.

Solaro C, Ponzio M, Moran E, Tanganelli P, Pizio R, Ribizzi G, et al. The changing face of multiple sclerosis: Prevalence and incidence in an aging population. Mult Scler 2015; 21: 1244–50.

Song M, Lin F, Ward SE, Fine JP. Composite variables: when and how. Nurs Res 2017; 62: 45–9.

Song TJ, Kim YD, Yoo J, Kim J, Chang HJ, Hong GR, et al. Association between Aortic Atheroma and Cerebral Small Vessel Disease in Patients with Ischemic Stroke. J Stroke 2016; 18: 312–320.

Sowa P, Bjørnerud A, Nygaard GO, Damangir S, Spulber G, Celius EG, et al. Reduced perfusion in white matter lesions in multiple sclerosis. Eur J Radiol 2015; 84: 2605–2612.

Spence JD, Pilote L. Importance of sex and gender in atherosclerosis and cardiovascular disease. Atherosclerosis 2015; 241: 208–210.

Spencer JI, Bell JS, DeLuca GC. Vascular pathology in multiple sclerosis: Reframing pathogenesis around the blood-brain barrier. J Neurol Neurosurg Psychiatry 2018; 89: 42–52.

Staals J, Booth T, Morris Z, Bastin ME, Gow AJ, Corley J, et al. Total MRI load of cerebral small vessel disease and cognitive ability in older people. Neurobiol Aging 2015; 36: 2806–2811.

Staessen JA, Wang J, Bianchi G, Birkenhäger WH. Essential hypertension. Lancet 2003; 361: 1629–41.

De Stefano N, Giorgio A, Tintoré M, Pia Amato M, Kappos L, Palace J, et al. Radiologically isolated syndrome or subclinical multiple sclerosis: MAGNIMS consensus recommendations. Mult Scler 2018; 24: 214–221.

Sumbria RK, Grigoryan MM, Vasilevko V, Krasieva TB, Scadeng M, Dvornikova AK, et al. A

murine model of inflammation-induced cerebral microbleeds. J Neuroinflammation 2016; 13: 1–12.

Taki Y, Thyreau B, Kinomura S, Sato K, Goto R, Wu K, et al. A longitudinal study of age- and gender-related annual rate of volume changes in regional gray matter in healthy adults. Hum Brain Mapp 2013; 34: 2292–2301.

Tashjian RS, Williams RR, Vinters H V., Yong WH. Autopsy biobanking: Biospecimen procurement, integrity, storage, and utilization. In: Methods in Molecular Biology. Humana Press, New York, NY; 2019. p. 77–87

Tettey P, Simpson S, Taylor B V, van der Mei IAF. Vascular comorbidities in the onset and progression of multiple sclerosis. J Neurol Sci 2014; 347: 23–33.

Thej MJ, Kalyani R, Kiran J. Atherosclerosis in coronary artery and aorta in a semi-urban population by applying modified American Heart Association classification of atherosclerosis: An autopsy study. J Cardiovasc Dis Res 2012; 3: 265–271.

Theocharakis P, Glotsos D, Kalatzis I, Kostopoulos S, Georgiadis P, Sifaki K, et al. Pattern recognition system for the discrimination of multiple sclerosis from cerebral microangiopathy lesions based on texture analysis of magnetic resonance images. Magn Reson Imaging 2009; 27: 417–422.

Thomas T, Miners S, Love S. Post-mortem assessment of hypoperfusion of cerebral cortex in Alzheimer's disease and vascular dementia. Brain 2015; 138: 1059–1069.

Thorn LM, Shams S, Gordin D, Liebkind R, Forsblom C, Summanen P, et al. Clinical and MRI Features of Cerebral Small-Vessel Disease in Type 1 Diabetes. Diabetes Care 2019; 42: 327–330.

Thorpe JW, Kidd D, Kendall BE, Tofts PS, Barker GJ, Thompson AJ, et al. Spinal cord MRI using multi-array coils and fast spin echo. I. Technical aspects and findings in healthy adults. Neurology 1993; 43: 2625–31.

Tortorella C, Bellacosa A, Paolicelli D, Fuiani A, Di Monte E, Simone IL, et al. Age-related gadolinium-enhancement of MRI brain lesions in multiple sclerosis. J Neurol Sci 2005; 239: 95–99.

Tremlett H, Zhu F, Ascherio A, Munger KL. Sun exposure over the life course and associations with multiple sclerosis. Neurology 2018; 90: e1191–e1199.

Tuladhar AM, Reid AT, Shumskaya E. Relationship Between White Matter Hyperintensities, Cortical Thickness, and Cognition. Stroke 2015; 46: 425–432.

Tutuncu M, Tang J, Zeid NA, Kale N, Crusan DJ, Atkinson EJ, et al. Onset of progressive phase is an age-dependent clinical milestone in multiple sclerosis. Mult Scler 2013; 19: 188–98.

Valgimigli M. The remarkable story of a wonder drug, which now comes to an end in the

primary prevention setting: say bye-bye to aspirin! Eur Heart J 2019; 40: 618–620.

Vis JC, de Bruin-Bon RH, Bouma BJ, Backx AP, Huisman SA, Imschoot L, et al. 'The sedentary heart': Physical inactivity is associated with cardiac atrophy in adults with an intellectual disability. Int J Cardiol 2012; 158: 387–393.

Voskuhl RR, Gold SM. Sex-related factors in multiple sclerosis susceptibility and progression. Nat Rev Neurol 2012; 8: 255–63.

Vukusic S, Confavreux C. Natural history of multiple sclerosis: risk factors and prognostic indicators. Curr Opin Neurol 2007; 20: 269–274.

Wagley S, Bokori-Brown M, Morcrette H, Malaspina A, D'Arcy C, Gnanapavan S, et al. Evidence of Clostridium perfringens epsilon toxin associated with multiple sclerosis. Mult Scler J 2018: 135245851876732.

Wakefield AJ, More LJ, Difford J, McLaughlin JE. Immunohistochemical study of vascular injury in acute multiple sclerosis. J Clin Pathol 1994; 47: 129–133.

Waldman A, Ness J, Pohl D, Simone IL, Anlar B, Amato MP, et al. Pediatric multiple sclerosis. Neurology 2016; 87: S74–S81.

Wang Y, Bos SD, Harbo HF, Thompson WK, Schork AJ, Bettella F, et al. Genetic overlap between multiple sclerosis and several cardiovascular disease risk factors. Mult Scler 2016; 22: 1783–1793.

Wang Y, Meng R, Song H, Liu G, Hua Y, Cui D, et al. Remote ischemic conditioning may improve outcomes of patients with cerebral small-vessel disease. Stroke 2017; 48: 3064–3072.

Ward RJ, Zucca F a, Duyn JH, Crichton RR, Zecca L. The role of iron in brain ageing and neurodegenerative disorders. Lancet Neurol 2014; 13: 1045–1060.

Wardlaw J., Smith C, Dichgans M. Mechanisms of sporadic cerebral small vessel disease: insights from neuroimaging. Lancet Neurol 2013; 12: 483–97.

Wardlaw J., Smith E., Biessels GJ, Cordonnier C, Fazekas F, Frayne R, et al. Neuroimaging standards for research into small vessel disease and its contribution to ageing and neurodegeneration. Lancet Neurol 2013; 12: 822–838.

Wardlaw JM. Journal of the Neurological Sciences Blood-brain barrier and cerebral small vessel disease ☆. J Neurol Sci 2010; 299: 66–71.

Wardlaw JM, Allerhand M, Doubal FN, Valdes Hernandez M, Morris Z, Gow AJ, et al. Vascular risk factors, large-artery atheroma, and brain white matter hyperintensities. Neurology 2014; 82: 1331–8.

Webber BJ, Seguin PG, Burnett DG, Clark LL, Otto JL. Prevalence of and risk factors for

autopsy-determined atherosclerosis among US service members, 2001-2011. JAMA 2012; 308: 2577–83.

Weinstock-Guttman B, Zivadinov R, Horakova D, Havrdova E, Qu J, Shyh G, et al. Lipid profiles are associated with lesion formation over 24 months in interferon-β treated patients following the first demyelinating event. J Neurol Neurosurg Psychiatry 2013; 84: 1186–91.

Weinstock-Guttman B, Zivadinov R, Mahfooz N, Carl E, Drake A, Schneider J, et al. Serum lipid profiles are associated with disability and MRI outcomes in multiple sclerosis. J Neuroinflammation 2011; 8: 127.

Welser J V., Halder SK, Kant R, Boroujerdi A, Milner R. Endothelial α6β4 integrin protects during experimental autoimmune encephalomyelitis-induced neuroinflammation by maintaining vascular integrity and tight junction protein expression. J Neuroinflammation 2017; 14: 217.

Westerlind H, Ramanujam R, Uvehag D, Kuja-Halkola R, Boman M, Bottai M, et al. Modest familial risks for multiple sclerosis: A registry-based study of the population of Sweden. Brain 2014; 137: 770–778.

Wijnands JMA, Kingwell E, Zhu F, Zhao Y, Högg T, Stadnyk K, et al. Health-care use before a first demyelinating event suggestive of a multiple sclerosis prodrome: a matched cohort study. Lancet Neurol 2017; 16: 445–451.

Wingerchuk DM. Smoking: Effects on multiple sclerosis susceptibility and disease progression. Ther Adv Neurol Disord 2012; 5: 13–22.

Winkler AM, Ridgway GR, Webster MA, Smith SM, Nichols TE. Permutation inference for the general linear model. Neuroimage 2014; 92: 381–97.

Wiseman SJ, Bastin ME, Jardine CL, Barclay G, Hamilton IF, Sandeman E, et al. Cerebral small vessel disease burden is increased in systemic lupus erythematosus. Stroke 2016; 47: 2722–2728.

Wu G-C, Liu H-R, Leng R-X, Li X-P, Li X-M, Pan H-F, et al. Subclinical atherosclerosis in patients with systemic lupus erythematosus: A systemic review and meta-analysis. Autoimmun Rev 2016; 15: 22–37.

Wu H, Roks AJM. Genomic instability and vascular aging: a focus on nucleotide excision repair. Trends Cardiovasc Med 2014; 24: 61–8.

Wuerfel J, Haertle M, Waiczies H, Tysiak E, Bechmann I, Wernecke KD, et al. Perivascular spaces--MRI marker of inflammatory activity in the brain? Brain 2008; 131: 2332–2340.

Xu W-H. Large artery: an important target for cerebral small vessel diseases. Ann Transl Med 2014; 2: 78.

Yakushiji Y, Wilson D, Ambler G, Charidimou A, Beiser A, van Buchem MA, et al. Distribution

of cerebral microbleeds in the East and West: Individual participant meta-analysis. Neurology 2019; 92: e1086–e1097.

Yates AJ, Thelmo W, Pappius HM. Postmortem Changes in the Chemistry and Histology of Normal and Edematous Brains. Am J Pathol 1975; 79: 555–564.

Yates RL, Esiri MM, Palace J, Jacobs B, Perera R, DeLuca GC. Fibrin(ogen) and neurodegeneration in the progressive multiple sclerosis cortex. Ann Neurol 2017; 82: 259–270.

Yates RL, Esiri MM, Palace J, Mittal A, DeLuca GC. The influence of HLA-DRB1*15 on motor cortical pathology in multiple sclerosis. Neuropathol Appl Neurobiol 2015; 41: 371–84.

Yeshokumar AK, Narula S, Banwell B. Pediatric multiple sclerosis. Curr Opin Neurol 2017; 30: 216–221.

Zamboni P, Galeotti R, Menegatti E, Malagoni a M, Tacconi G, Dall'Ara S, et al. Chronic cerebrospinal venous insufficiency in patients with multiple sclerosis. J Neurol Neurosurg Psychiatry 2008; 80: 392–399.

Zeydan B, Kantarci OH. Progressive Forms of Multiple Sclerosis. Neurol Clin 2018; 36: 163–171.

Zhang T, Tremlett H, Zhu F, Kingwell E, Fisk JD, Bhan V, et al. Effects of physical comorbidities on disability progression in multiple sclerosis. Neurology 2018; 90: e419–e427.

Zhang Y, Brady M, Smith S. Segmentation of brain MR images through a hidden Markov random field model and the expectation-maximization algorithm. IEEE Trans Med Imaging 2001; 20: 45–57.

Zhao Z, Nelson AR, Betsholtz C, Zlokovic BV. Establishment and Dysfunction of the Blood-Brain Barrier. Cell 2015; 163: 1064–1078.

Zivadinov R, Ramasamy DP, Benedict RRH, Polak P, Hagemeier J, Magnano C, et al. Cerebral Microbleeds in Multiple Sclerosis Evaluated on Susceptibility-weighted Images and Quantitative Susceptibility Maps: A Case-Control Study. Radiology 2016; 281: 884–895.

Zivadinov R, Weinstock-Guttman B, Hashmi K, Abdelrahman N, Stosic M, Dwyer M, et al. Smoking is associated with increased lesion volumes and brain atrophy in multiple sclerosis. Neurology 2009; 73: 504–510.

Zlokovic B V. Neurovascular pathways to neurodegeneration in Alzheimer's disease and other disorders. Nat Rev Neurosci 2011; 12: 723–739.